

UNIVERSIDADE FEDERAL DE PERNAMBUCO
Programa de Pós-Graduação em Inovação Terapêutica

MARINA GALDINO DA ROCHA PITTA

Novos Agentes Tiazacridínicos com Propriedades Anticâncer

RECIFE

2012

MARINA GALDINO DA ROCHA PITTA

Novos Agentes Tiazacridínicos com Propriedades Anticâncer

Tese de Doutorado apresentada ao Programa de Pós-Graduação em Inovação Terapêutica da Universidade Federal de Pernambuco, para a obtenção do Título de Doutor em Inovação Terapêutica

Orientadora: Profa. Dr. Maria do Carmo Alves de Lima
Co-orientador: Prof. Dr. César Augusto Souza de Andrade

RECIFE

2012

Catálogo na Fonte:
Bibliotecário Bruno Márcio Gouveia, CRB-4/1788

P688n Pitta, Marina Galdino da Rocha
Novos agentes tiazacridínicos com propriedades anticâncer / Marina Galdino da Rocha Pitta. – Recife: O Autor, 2012.

190 folhas: fig., tab.

Orientadora: Maria do Carmo Alves de Lima

Coorientador: César Augusto Souza de Andrade

Tese (doutorado) – Universidade Federal de Pernambuco. Centro de Ciências Biológicas. Pós-graduação em Inovação Terapêutica, 2012.

Inclui referências, anexos e apêndices

1. Farmacologia 2. Câncer – Tratamento I. Lima, Maria do Carmo Alves de (orientadora) II. Andrade, César Augusto Souza de (coorientador) III. Título.

615.3

CDD (22.ed.)

UFPE/CCB-2013-012

UNIVERSIDADE FEDERAL DE PERNAMBUCO
Programa de Pós-Graduação em Inovação Terapêutica

REITOR

Prof. Dr. Anísio Brasileiro de Freitas Dourado

VICE-REITOR

Prof. Dr. Sílvio Romero de Barros Marques

PRÓ-REITOR PARA ASSUNTOS DE PESQUISA E PÓS-GRADUAÇÃO

Prof. Dr. Francisco de Sousa Ramos

DIRETORA DO CENTRO DE CIÊNCIAS BIOLÓGICAS

Profa. Dr. Maria Eduarda Lacerda de Larrazabal

VICE-DIRETORA DO CENTRO DE CIÊNCIAS BIOLÓGICAS

Profa. Dr. Oliane Maria Correia Magalhães

COORDENADORA DO PROGRAMA DE PÓS-GRADUAÇÃO EM INOVAÇÃO TERAPÊUTICA

Profa. Dr. Suely Lins Galdino

VICE-COORDENADOR DO PROGRAMA DE PÓS-GRADUAÇÃO EM INOVAÇÃO TERAPÊUTICA

Prof. Dr. César Augusto Souza de Andrade

FOLHA DE APROVAÇÃO

Nome: PITTA, Marina Galdino da Rocha

Título: Novos Agentes Tiazacridínicos com Propriedades Anticâncer

Tese apresentada à Universidade Federal de Pernambuco, para obtenção do Título de
Doutor em Inovação Terapêutica

Aprovada em: ___/___/___

Banca Examinadora

Profa. Dr. Maria do Carmo Alves de Lima

Departamento de Antibióticos, Universidade Federal de Pernambuco

Assinatura: _____

Profa. Dr. Paloma Lys de Medeiros

Departamento de Histologia e Embriologia, Universidade Federal de Pernambuco

Assinatura: _____

Prof. Dr. Luiz Alberto Lira Soares

Departamento de Farmácia, Universidade Federal de Pernambuco

Assinatura: _____

Profa. Dr. Janaina de Albuquerque Couto

Departamento de Morfologia e Fisiologia Animal, Universidade Federal Rural de
Pernambuco

Assinatura: _____

Profa. Dr. Maria Danielly Lima de Oliveira

Departamento de Bioquímica, Universidade Federal de Pernambuco

Assinatura: _____

DEDICATÓRIA

*Aos meus amados, incríveis e encantadores pais Suely Lins Galdino e Ivan da Rocha Pitta,
que sempre estão ao meu lado e que são meus exemplos de vida.*

A Diego Cravo pelo carinho, apoio e incentivo.

*Aos meus irmãos Maira, Ivan, Luis, Tania, Maoro, Nadia,
pelo imenso amor, carinho e alegrias compartilhadas.*

Aos meus avós Felix, Gertrudes, Walter, Joanna, que construíram uma linda família.

*Aos meus queridos primos Lilia, Alice, Mariana, Bruno, Cauet, Lorena,
Talita, Daniel, Jane, Edoardo, Ivo, Lorena, Igor, Luciana, Walter, Evelise, Tatiana.*

Aos meus lindos sobrinhos Victor, Fernande, Salomé, Raissa, Miguel, Sofia, Lara.

Aos meus queridos tios Sérgio, Célia, Sandra, Paulo, Fátima, Antônio, Ivo, Walter.

AGRADECIMENTOS

A minha orientadora Profa. Dr. Maria do Carmo Alves de Lima, pesquisadora do Laboratório de Planejamento e Síntese de Fármacos, do Departamento de Antibióticos da Universidade Federal de Pernambuco, pelo incentivo e apoio constantes durante a condução da tese e em momentos decisivos da minha vida.

Ao Prof. Dr. César Augusto Souza de Andrade, pesquisador do Laboratório de Polímeros não Convencionais, do Departamento de Bioquímica da Universidade Federal de Pernambuco, pela co-orientação e compromissos a pesquisa, o ensino e, sobretudo, com a instituição, representada pelo Programa de Pós-Graduação em Inovação Terapêutica.

A Profa. Dr. Suely Lins Galdino e ao Prof. Dr. Ivan da Rocha Pitta do Departamento de Antibióticos da Universidade Federal de Pernambuco, pela imensurável amizade, confiança, incentivo e, sobretudo, pela inestimável contribuição à minha formação acadêmico-científica e pessoal.

A Profa. Dr. Maira Galdino da Rocha Pitta e equipe, do Laboratório de Imunomodulação e Novas Abordagens Terapêuticas, do Departamento de Bioquímica da Universidade Federal de Pernambuco, pela inestimável colaboração científica na realização da avaliação da atividade anticâncer *in vitro*.

A Universidade Federal de Pernambuco pela importante contribuição para o desenvolvimento do país quando, cumprindo sua missão, busca capacitar técnica, científica e culturalmente alunos de graduação e de pós-graduação.

A Fundação de Amparo à Ciência e Tecnologia do Estado de Pernambuco, pela concessão da bolsa de pós-graduação.

Em nome de Breno Caldas de Araujo, Douglas Carvalho Francisco Viana, Leidiane Carla Lira de Oliveira e Maria Juliana Dantas de Paula, agradeço aos colegas e professores do Programa de Pós-Graduação em Inovação Terapêutica pela oportunidade de um convívio “intelectualmente refrescante”.

A Paulo Germano Moreira de Brito, Secretário do Programa de Pós-Graduação em Inovação Terapêutica, pela imprescindível colaboração demonstrada durante todo o curso.

Aos amigos e amigas do Laboratório de Planejamento e Síntese de Fármacos, bem como do Núcleo de Pesquisa em Inovação Terapêutica, pelos agradáveis momentos e pela colaboração direta ou indireta na realização de todas as etapas deste trabalho.

A todos aqueles não mencionados que, de alguma maneira, contribuíram na realização deste trabalho.

HÁ MOMENTOS

*Há momentos na vida em que sentimos tanto
a falta de alguém que o que mais queremos
é tirar esta pessoa de nossos sonhos
e abraçá-la.*

*Sonhe com aquilo que você quiser.
Seja o que você quer ser,
porque você possui apenas uma vida
e nela só se tem uma chance
de fazer aquilo que se quer.*

*Tenha felicidade bastante para fazê-la doce.
Dificuldades para fazê-la forte.
Tristeza para fazê-la humana.
E esperança suficiente para fazê-la feliz.*

*As pessoas mais felizes
não têm as melhores coisas.
Elas sabem fazer o melhor
das oportunidades que aparecem
em seus caminhos.*

*A felicidade aparece para aqueles que choram.
Para aqueles que se machucam.
Para aqueles que buscam e tentam sempre.
E para aqueles que reconhecem
a importância das pessoas que passam por suas
vidas.*

*O futuro mais brilhante
é baseado num passado intensamente vivido.
Você só terá sucesso na vida
quando perdoar os erros
e as decepções do passado.*

*A vida é curta, mas as emoções que podemos
deixar
duram uma eternidade.
A vida não é de se brincar
porque um belo dia se morre.*

Clarice Lispector

RESUMO

O câncer é uma das principais causas de morte no mundo e recebe crescentes investimentos em pesquisa oriundos dos setores público e privado. Mais da metade de todos os casos de câncer ocorrem na América do Sul e na Ásia. A busca de novos medicamentos para o tratamento do câncer tem sido intensa. O Laboratório de Planejamento e Síntese de Fármacos (LPSF) da Universidade Federal de Pernambuco tem envidado esforços em pesquisas, desenvolvimento e inovação para a concepção de novos fármacos anticâncer. Entre as classes químicas bioativas exploradas pelo LPSF estão as tiazacridinas intercaladoras de DNA, compostos resultantes da hibridização molecular dos heterocíclicos tiazolidina e acridina. Neste sentido, com a finalidade de minimizar o impacto dessa doença global, foram sintetizadas dezesseis moléculas inéditas potencialmente ativas para o tratamento do câncer. Os compostos codificados LPSF AA-10, LPSF AA-13, LPSF AA-16, LPSF AA-17, LPSF AA-19 e LPSF AA-23 tiveram suas bioatividades avaliadas *in vitro* na linhagem celular maligna de Linfoma de Burkitt (RAJI) e os compostos LPSF AA-14, LPSF AA-15, LPSF AA-18 e LPSF AA-19 foram avaliados na linhagem celular maligna de Leucemia Aguda de Células T (JUKART). Para a realização das sínteses, foram aplicadas reações de N-alquilação, condensação, ciclização e adição de Michael. As moléculas obtidas foram comprovadas através de métodos espectroscópicos no infravermelho e ressonância magnética nuclear de hidrogênio. Os resultados revelam que na linhagem de células RAJI o composto LPSF AA-17 (3,4,5-OCH₃) foi o mais ativo, enquanto na linhagem de células JUKART o LPSF AA-19 (2,4-Cl) foi o mais ativo. Em trabalhos realizados anteriormente no LPSF, tiazacridinas diferentes das apresentadas nesta tese foram testadas nas linhagens neoplásicas de células SF-295 (Sistema Nervoso Central), MDA-MB435 (melanoma) e HCT-8 (carcinoma de cólon). Os resultados revelam que os compostos LPSF AA-2 (*bis*-acridina), LPSF AA-3 (4-OCH₃) e LPSF AA-6 (4-Br) destacaram-se entre os mais ativos da série, pois apresentaram, respectivamente, 92,4%, 86,7% e 96,6% de inibição da proliferação celular contra a linhagem HCT-8; enquanto que a doxorubicina, fármaco de referência, apresentou 95,2% de inibição contra a mesma linhagem de células. Estes resultados confirmam a importância de derivados tiazacridínicos no combate do câncer.

Palavras-chave: Acridina. Tiazolidina. Câncer. Intercaladores de DNA.

ABSTRACT

Cancer is the main cause of death in the world and receives increasing research investment from the public and private sectors. More than half of all cancer cases occur in South America and Asia. The search for new drugs for the treatment of cancer has been intense. The Laboratory of Planning and Drug Synthesis (LPSF) in Federal University of Pernambuco has worked in research, development and radical innovation for the design of new anticancer drugs. Among the chemical classes operated by the LPSF are thiazacridines DNA intercalators compounds resulting from hybridization of molecular thiazolidine heterocyclic and acridine. In this sense, in order to minimize the overall impact of this disease, we synthesized new potentially active molecules for the treatment of cancer. The molecules codified LPSF AA-10, LPSF AA-13, LPSF AA-16, LPSF AA-17, LPSF AA-19 and LPSF AA-23 had their bioactivity evaluated *in vitro* in the malignant cell lines Burkitt's Lymphoma (RAJI) and the compounds LPSF AA-14, LPSF AA-15, LPSF AA-18 e LPSF AA-19 were evaluated in T-cell acute leukemia (JUKART). The syntheses were carried out with N-alkylation, condensation, cyclization and Michael addition reactions. The obtained molecules were analysed by spectroscopic methods, such as infrared and nuclear magnetic resonance of hydrogen. The results indicate that in cancer cell line RAJI the compound LPSF AA-17 (3,4,5-OCH₃) was the most active, while in cancer cell line JURKAT the compound LPSF AA-19 (4-NO₂) was the most active. On previously work done in LPSF, different thiazacridines of the ones presented in this thesis were tested in cancer cell lines HL-60 (promyelocytic leukemia), MDA-MB435 (breast carcinoma) and HCT-8 (colon carcinoma). The compounds LPSF AA-2 (*bis*-acridine), LPSF AA-3 (4-OCH₃) and LPSF AA-6 (4-Br) were the most active of the series, and presented, respectively, 92.4%, 86.7% and 96.6% of inhibition of cell proliferation against HCT-8, whereas doxorubicin, the reference drug, presented 95.2% of inhibition against same cell line. These results confirm the importance of thiazacridine derivatives in combat of cancer.

Keywords: Acridine. Thiazolidine. Cancer. DNA intercalators.

LISTA DE ILUSTRAÇÕES

Figura 1 - Prevalência dos principais tipos de câncer no mundo, em 2008	25
Figura 2 - Representação espacial das taxas de mortalidade por câncer no mundo, por 100.000 homens, em 2008	26
Figura 3 - Representação espacial das taxas de mortalidade por câncer no mundo, por 100.000 mulheres, em 2008	27
Figura 4 - Distribuição percentual da mortalidade por tipo de câncer e faixa etária no Brasil, 2001-2005	28
Figura 5 - Inibidores da enzima tirosina quinase	34
Figura 6 - Fármacos derivados de tiazolidinas	37
Figura 7 - Topoisomerase I humana complexada com o DNA	44
Figura 8 - Clivagem do DNA (rosa) via topoisomerase (preta)	45
Figura 9 - Inibidores de topo II	46
Figura 10 - Reativação da telomerase e inibição de células cancerosas	47
Figura 11 - Acridinas dissubstituídas inibidoras de telomerase sintetizadas por HARRISON (1999) e FU (2009)	48
Figura 12 - Indutores da atividade transcripcional do gene p53	50
Figura 13 - Acridina e tiazolidina	51
Figura 14 - Núcleos da tiazolidina-2,4-diona e da acridina	62
Figura 15 - Células de linfoma de Burkitt, com destaque a presença de vacúolos lipídicos e paracromatina clara	85
Figura 16 - Células da linhagem JUKART	85
Figura 17 - Aspectos morfológicos de células de leucemia de células T. Imagens de células em mitose podem estar presentes	86
Figura 18 - LPSF AA-19 e controle positivo	89
Figura 19 - Viabilidade celular (%) da linhagem RAJI, em função da dose do LPSF AA-19, e da amsacrina	90
Figura 20 - Tiazacridinas testadas na linhagem de células neoplásicas RAJI	91
Figura 21 - Viabilidade celular (%) da linhagem RAJI, em função das doses do LPSF AA-16, do LPSF AA-17 e da amsacrina	92

Figura 22 - Tiazacridinas testadas na linhagem de células neoplásicas JUKART	93
Figura 23 - Viabilidade celular (%) da linhagem JUKART, em função da dose dos LPSF AA-14, LPSF AA-15, LPSF AA-18, LPSF AA-19, e amsacrina	95
Figura 24 - Espectro de NMR ¹ H (400 MHz, δ ppm, DMSO-d ₆) do LPSF AA-1A	157
Figura 25 - Espectro de IR do LPSF AA-1A	158
Figura 26 - Espectro de NMR ¹ H do LPSF AA-10	159
Figura 27 - Espectro de IR do LPSF AA-10. Deformação axial normal de C=O, 1744 cm ⁻¹ , 1689 cm ⁻¹ . Deformação axial das ligações C=C do anel, 1599 cm ⁻¹ . Deformação axial de C-N, 1375 cm ⁻¹ . Deformação axial simétrica de C-O-C, 1258 cm ⁻¹ . Deformação angular fora do plano de C-H de aromático, 751 cm ⁻¹	160
Figura 28 - Espectro de NMR ¹ H do LPSF AA-11	161
Figura 29 - Espectro de IR do LPSF AA-11. Deformação axial normal de C=O, 1739 cm ⁻¹ , 1682 cm ⁻¹ . Deformação axial das ligações C=C do anel, 1593 cm ⁻¹ . Deformação axial de C-N, 1382 cm ⁻¹ . Deformação angular fora do plano de C-H de aromático, 755 cm ⁻¹ . Deformação angular de C=C, 707 cm ⁻¹	162
Figura 30 - Espectro de NMR ¹ H do LPSF AA-12	163
Figura 31 - Espectro de IR do LPSF AA-12. Deformação axial normal de C=O, 1738 cm ⁻¹ , 1685 cm ⁻¹ . Deformação axial das ligações C=C do anel, 1606 cm ⁻¹ . Deformação axial de C-N, 1372 cm ⁻¹ . Deformação axial simétrica de C-O-C, 1300 cm ⁻¹ . Deformação angular fora do plano de C-H de aromático, 754 cm ⁻¹ . Deformação angular de C=C, 707 cm ⁻¹	164
Figura 32 - Espectro de NMR ¹ H do LPSF AA-13	165
Figura 33 - Espectro de IR do LPSF AA-13. Deformação axial normal de C=O, 1748 cm ⁻¹ , 1693 cm ⁻¹ . Deformação axial das ligações C=C do anel, 1604 cm ⁻¹ . Deformação axial de C-N, 1374 cm ⁻¹ . Deformação angular fora do plano de C-H de aromático, 746 cm ⁻¹ . Deformação angular de C=C, 740 cm ⁻¹	166
Figura 34 - Espectro de NMR ¹ H do LPSF AA-14	167
Figura 35 - Espectro de IR do LPSF AA-14. Deformação axial normal de C=O, 1746 cm ⁻¹ , 1689 cm ⁻¹ . Deformação axial das ligações C=C do anel, 1609 cm ⁻¹ . Deformação axial de C-N, 1374 cm ⁻¹ . Deformação angular fora do plano de C-H de aromático, 752 cm ⁻¹ . Deformação angular de C=C, 678 cm ⁻¹	168
Figura 36 - Espectro de NMR ¹ H do LPSF AA-15	169
Figura 37 - Espectro de IR do LPSF AA-15. Deformação axial de N-H, 3376 cm ⁻¹ . Deformação axial normal de C=O, 1728 cm ⁻¹ , 1672 cm ⁻¹ . Deformação angular de N-H, 1598 cm ⁻¹ . Deformação axial de C-N, 1376 cm ⁻¹ . Deformação angular fora do plano de C-H de aromático, 739 cm ⁻¹	170

Figura 38 - Espectro de NMR ¹ H do LPSF AA-16	171
Figura 39 - Espectro de IR do LPSF AA-16. Deformação axial normal de C=O, 1733 cm ⁻¹ , 1676 cm ⁻¹ . Deformação axial das ligações C=C do anel, 1596 cm ⁻¹ . Deformação axial de C-N, 1380 cm ⁻¹ . Deformação angular fora do plano de C-H de aromático, 766 cm ⁻¹	172
Figura 40 - Espectro de NMR ¹ H do LPSF AA-17	173
Figura 41 - Espectro de IR do LPSF AA-17. Deformação axial normal de C=O, 1738 cm ⁻¹ , 1687 cm ⁻¹ . Deformação axial das ligações C=C do anel, 1605 cm ⁻¹ . Deformação axial de C-N, 1382 cm ⁻¹ . Deformação axial assimétrica C-O-C, 1130 cm ⁻¹ . Deformação angular fora do plano de C-H de aromático, 754 cm ⁻¹ . Deformação angular de C=C, 707 cm ⁻¹	174
Figura 42 - Espectro de NMR ¹ H do LPSF AA-18	175
Figura 43 - Espectro de IR do LPSF AA-18. Deformação axial normal de C=O, 1744 cm ⁻¹ , 1687 cm ⁻¹ . Deformação axial das ligações C=C do anel, 1611 cm ⁻¹ . Deformação axial de C-N, 1380 cm ⁻¹ . Deformação angular fora do plano de C-H de aromático, 756 cm ⁻¹	176
Figura 44 - Espectro de NMR ¹ H do LPSF AA-19	177
Figura 45 - Espectro de IR do LPSF AA-19. Deformação axial normal de C=O, 1742 cm ⁻¹ , 1689 cm ⁻¹ . Deformação axial de C-N, 1375 cm ⁻¹ . Deformação angular fora do plano de C-H de aromático, 759 cm ⁻¹	178
Figura 46 - Espectro de NMR ¹ H do LPSF AA-20	179
Figura 47 - Espectro de IR do LPSF AA-20. Deformação axial normal de C=O, 1748 cm ⁻¹ , 1683 cm ⁻¹ . Deformação axial das ligações C=C do anel, 1606 cm ⁻¹ . Deformação axial simétrica de N=O, 1523 cm ⁻¹ . Deformação axial de C-N, 1345 cm ⁻¹ . Deformação angular fora do plano de C-H de aromático, 765 cm ⁻¹	180
Figura 48 - Espectro de NMR ¹ H do LPSF AA-22	181
Figura 49 - Espectro de IR do LPSF AA-22. Deformação axial normal de C=O, 1737 cm ⁻¹ , 1676 cm ⁻¹ . Deformação axial das ligações C=C do anel, 1593 cm ⁻¹ . Deformação axial de C-N, 1378 cm ⁻¹ . Deformação angular fora do plano de C-H de aromático, 749 cm ⁻¹	182
Figura 50 - Espectro de NMR ¹ H do LPSF AA-23	183
Figura 51 - Espectro de IR do LPSF AA-23. Deformação axial normal de C=O, 1741 cm ⁻¹ , 1685 cm ⁻¹ . Deformação axial assimétrica de N=O, 1519 cm ⁻¹ . Deformação axial simétrica de N=O, 1345 cm ⁻¹ . Deformação angular fora do plano de C-H de aromático, 764 cm ⁻¹	184
Figura 52 - Espectro de NMR ¹ H do LPSF AA-26	185

- Figura 53 - Espectro de IR do LPSF AA-26. Deformação axial normal de C=O, 1740 cm^{-1} , 1684 cm^{-1} . Deformação axial das ligações C=C do anel, 1593 cm^{-1} . Deformação axial de C-N, 1382 cm^{-1} . Deformação angular fora do plano de C-H de aromático, 754 cm^{-1} 186
- Figura 54 - Espectro de NMR¹H do LPSF AA-30 187
- Figura 55 - Espectro de IR do LPSF AA-30. Deformação axial normal de C=O, 1744 cm^{-1} , 1693 cm^{-1} . Deformação axial das ligações C=C do anel, 1608 cm^{-1} . Deformação axial de C-N, 1378 cm^{-1} . Deformação angular fora do plano de C-H de aromático, 753 cm^{-1} 188
- Figura 56 - Espectro de NMR¹H do LPSF AA-31 189
- Figura 57 - Espectro de IR do LPSF AA-31. Deformação axial de O-H, larga, 3300-2500 cm^{-1} . Deformação axial normal de C=O, 1732 cm^{-1} , 1673 cm^{-1} . Deformação angular fora do plano de C-H de aromático, 756 cm^{-1} 190

LISTA DE TABELAS

Tabela 1 - Mortalidade por câncer, brutas e ajustadas por idade, pelas populações mundial e brasileira, por 100.000 homens e mulheres, Brasil, 2000-2010	29
Tabela 2 - Medicamentos moduladores da autofagia e da angiogênese utilizados na terapia contra o câncer	30
Tabela 3 - Fármacos relevantes que modulam a autofagia	32
Tabela 4 - Anticorpos monoclonais e inibidores da enzima tirosina quinase utilizados no tratamento do câncer	34
Tabela 5 - Agentes citotóxicos convencionais subdivididos de acordo com o mecanismo de ação	35
Tabela 6 - Derivados da acridina	38
Tabela 7 - Ésteres de Cope sintetizados	53
Tabela 8 - Tiazacridinas sintetizadas	54
Tabela 9 - Características físico-químicas de tiazacridinas sintetizadas no LPSF	60
Tabela 10 - Absorções características no IR de alguns grupos funcionais característicos das tiazacridinas	64
Tabela 11 - Inibição da proliferação (%) realizado em duplicata pelo método do MTT para as células SF-295 (SNC), HCT-8 (carcinoma de cólon) e MDA-MB435 (melanoma); doxorubicina foi usada como controle positivo	82
Tabela 12 - Valores de IC ₅₀ (concentração inibitória de 50%) e intervalo de confiança de 95% (IC 95%) realizado pelo método do MTT para as células HL-60 (leucemia promielocítica), CEM (leucemia linfocítica), MDA-MB435 (melanoma), HCT-8 (carcinoma de cólon) e SF-295 (SNC) obtidos por regressão não-linear através do programa GraphPad Prism	83
Tabela 13 - Linhagens de células neoplásicas humanas utilizadas	84
Tabela 14 - LPSF AA-19 e Amsacrina: viabilidade celular (%) da linhagem RAJI em função da dose	89
Tabela 15 - Viabilidade celular (%) da linhagem RAJI em função da dose do LPSF AA-10, LPSF AA-13, LPSF AA-16, LPSF AA-17, LPSF AA-23 e Amsacrina	91
Tabela 16 - Viabilidade celular (%) da linhagem JUKART, em função da dose do LPSF AA-19, e da amsacrina	94

LISTA DE ESQUEMAS

Esquema 1 - Mecanismo de ativação transcricional pelo PPAR: Requer a liberação do complexo co-repressor (atividade Histona Deacetilase), feito por um ligante, e o recrutamento de complexo co-ativador (atividade acetiltransferase). O complexo PPAR:RXR ativado liga-se ao PPRE, produzindo alteração na estrutura da cromatina, originando uma estrutura transcricionalmente competente	40
Esquema 2 - Representação esquemática do mecanismo citotóxico de um intercalador de DNA	42
Esquema 3 - Rota geral de síntese de tiazacridinas	56
Esquema 4 - Mecanismo da reação hipotético de ciclização para obtenção de tiazolidina-2,4-diona	57
Esquema 5 - Mecanismo reacional hipotético de <i>N</i> -alquilação da tiazolidina-2,4-diona	58
Esquema 6 - Mecanismo da reação hipotético de condensação de Knoevenagel para obtenção dos intermediários LPSF IPs	59
Esquema 7 - Mecanismo da reação hipotético de adição de Michael para obtenção de derivados tiazacridínicos	59
Esquema 8 - Possíveis estruturas do nitro-benzeno	63
Esquema 9 - Representação do método MTT	87
Esquema 10 - Metodologia utilizada no estudo para ensaio de citotoxicidade em células neoplásicas	88

LISTA DE ABREVIATURAS E SIGLAS

AcrH	Hidrogênios pertencentes ao núcleo acridínico
AINEs	Antiinflamatórios Não Estereoidais
ARF	“Frame” de Leitura Alternativo, “Alternative Reading Frame”
ArH	Hidrogênios pertencentes ao anel fenílico
ATM	Ataxia Telangiectasia Mutada, “Ataxia Telangiectasia Mutated”
bFGF	Fator de Crescimento Fibroblástico Básico
BL	Linfoma de Burkitt, “Burkitt's Lymphoma”
COX-2	Ciclo-Oxigenase 2
DMSO	Dimetilsulfóxido, “Dimethyl sulfoxide”
DNA	Ácido desoxirribonucléico, “Deoxyribonucleic Acid”
EBV	Vírus Epstein-Barr, “Epstein Barr vírus”
Ex	Exemplo
FACEPE	Fundação de Amparo à Ciência e Tecnologia do Estado de Pernambuco
FM	Fórmula molecular
HBV	Hepatite B, “Hepatitis B Virus”
HCV	Hepatite C, “Hepatitis C Virus”
HPV	Papiloma Vírus Humano, “Human Papillomavirus”
IR	Infravermelho, “Infrared”
JUKART	Leucemia Aguda de Células T, “T-cell acute leucemia”
LINAT	Laboratório de Imunomodulação e Novas Abordagens Terapêuticas
LPSF	Laboratório de Planejamento e Síntese de Fármacos
MDM 2	Minuto Duplo Murino 2, “Murine Double Minute 2”
MDR	Resistência a Múltiplas Drogas, “Multi-Drug Resistance”
mTORC1	‘Alvo da Rapacimina’ Complexo 1 de Mamíferos, “Mammalian Target Of Rapamycin Complex 1”
MTT	3-(4,5-Dimetil-2-tiazol)-2,5-difenil-2-H-brometo de tetrazolium, “3-(4,5-Dimethylthiazol-2-yl)-2,5-diphenyltetrazolium bromide”
NCI	National Cancer Institute
N-CoR	Co-repressor Núcleo Receptor
NMR ¹ H	Ressonância Magnética Nuclear de Hidrogênio, “Proton Nuclear Magnetic Resonance”
NUPIT SG	Núcleo de Pesquisa em Inovação Terapêutica Suely Galdino
p53	Proteína de 53 kDa

PF	Ponto de Fusão
PM	Peso Molecular, “Molecular Weight”
PPAR	Receptor Ativador da Proliferação de Peroxissomos, “Peroxisome Proliferator-Activated Receptors”
PPER	Elementos Responsivos aos Proliferadores de Peroxissoma, “Peroxisome Proliferator Response Element”
PPGIT	Programa de Pós-Graduação em Inovação Terapêutica
RAJI	Linfoma de Burkitt, “Burkitt's Lymphoma”
Rdt	Rendimento
RENAME	Relação Nacional de Medicamentos Essenciais
Rf	Fator de Retenção
RXR	Receptor do ácido 9-cis Retinóico, “Retinoid X Receptor”
SN ₂	Substituição Nucleofílica de Segunda Ordem, “Bimolecular Nucleophilic Substitution”
SNC	Sistema Nervoso Central
SRC-1	Co-ativador 1 do Receptor de Esteróides
TEM	Taxa Específica de Mortalidade
TK	Tirosina Quinase, “Tyrosine Kinase”
Topo	Topoisomerase
TZDs	Tiazolidinas, “Thiazolidine”
UFPE	Universidade Federal de Pernambuco
VEGF	Fator de Crescimento do Endotélio Vascular Humano, “Vascular Endothelial Growth Factor”

SUMÁRIO

1	Introdução	20
2	Objetivos	22
2.1	Geral	22
2.2	Específicos	22
3	Revisão da Literatura	23
3.1	Gênese do câncer	23
3.2	Epidemiologia do câncer	24
3.3	Controle e diagnóstico	29
3.4	Abordagens terapêuticas para o tratamento do câncer	30
3.4.1	Moduladores da autofagia	30
3.4.2	Inibidores da angiogênese	32
3.4.3	Agentes citotóxicos clássicos	35
3.5	Alvos moleculares selecionados de tiazolidinas e acridinas e seus inibidores anticâncer	37
3.5.1	Receptor ativador da proliferação de peroxissomos - PPAR	39
3.5.2	Ácido desoxiribonucléico - DNA	41
3.5.3	Enzimas topoisomerase I e II	43
3.5.4	Enzima telomerase	47
3.5.5	Gene supressor tumoral p53	48
4	Obtenção de Derivados Tiazacridínicos	51
4.1	Material	52
4.2	Metodologias de síntese	53
4.2.1	Tiazolidina-2,4-diona	53
4.2.2	Ésteres de Cope (LPSF IPs)	53
4.2.3	3-Acridin-9-il-metil-tiazolidina-2,4-diona (LPSF AA-1A)	54
4.2.4	Derivados tiazacridínicos (LPSF AAs)	54
4.3	Rotas de síntese	55
4.4	Mecanismos reacionais	57
4.5	Características físico-químicas & identificação estrutural	60
4.5.1	Ressonância magnética nuclear de hidrogênio	61
4.5.2	Espectrofotometria de absorção no infravermelho	63
4.5.3	3-Acridin-9-il-metil-tiazolidina-2,4-diona (LPSF AA-1A)	65
4.5.4	3-Acridin-9-ilmetil-5-(5-bromo-2-metoxi-benzilideno)-tiazolidina-2,4-diona (LPSF AA-10)	66
4.5.5	3-Acridin-9-ilmetil-5-bifenil-4-ilmetileno-tiazolidina-2,4-diona (LPSF AA-11)	67
4.5.6	3-Acridin-9-ilmetil-5-(3,5-dimetoxi-benzilideno)-tiazolidina-2,4-diona (LPSF AA-12)	68
4.5.7	3-Acridin-9-ilmetil-5-(2,3-dicloro-benzilideno)-tiazolidina-2,4-diona (LPSF AA-13)	69
4.5.8	3-Acridin-9-ilmetil-5-(3-bromo-benzilideno)-tiazolidina-2,4-diona (LPSF AA-14)	70

4.5.9	3-Acridin-9-ilmetil-5-(1H-indol-3-ilmetileno)-tiazolidina-2,4-diona (LPSF AA-15)	71
4.5.10	3-Acridin-9-ilmetil-5-(4-fluoro-benzilideno)-tiazolidina-2,4-diona (LPSF AA-16)	72
4.5.11	3-Acridin-9-ilmetil-5-(3,4,5-trimetoxi-benzilideno)-tiazolidina-2,4-diona (LPSF AA-17)	73
4.5.12	3-Acridin-9-ilmetil-5-(3,4-dicloro-benzilideno)-tiazolidina-2,4-diona (LPSF AA-18)	74
4.5.13	3-Acridin-9-ilmetil-5-(2,4-dicloro-benzilideno)-tiazolidina-2,4-diona (LPSF AA-19)	75
4.5.14	3-Acridin-9-ilmetil-5-(2-cloro-5-nitro-benzilideno)-tiazolidina-2,4-diona (LPSF AA-20)	76
4.5.15	3-Acridin-9-ilmetil-5-(4-benziloxi-benzilideno)-tiazolidina-2,4-diona (LPSF AA-22)	77
4.5.16	3-Acridin-9-ilmetil-5-(4-nitro-benzilideno)-tiazolidina-2,4-diona (LPSF AA-23)	78
4.5.17	3-Acridin-9-ilmetil-5-(9H-fluoren-3-ilmetileno)-tiazolidina-2,4-diona (LPSF AA-26)	79
4.5.18	3-Acridin-9-ilmetil-5-(3-cloro-benzilideno)-tiazolidina-2,4-diona (LPSF AA-30)	80
4.5.19	3-Acridin-9-ilmetil-5-(4-hidroxi-benzilideno)-tiazolidina-2,4-diona (LPSF AA-31)	81
5	Atividade Anticâncer	82
5.1	Linhagens de células neoplásicas	84
5.2	Manutenção das células neoplásicas em cultura	86
5.3	Ensaio de citotoxicidade em células neoplásicas	86
5.4	Análise de dados	88
5.5	Resultados	89
5.5.1	Avaliação da atividade citotóxica na linhagem de células neoplásicas RAJI	89
5.5.2	Avaliação da atividade citotóxica na linhagem de células neoplásicas JUKART	93
4	Conclusões	96
5	Perspectivas	97
6	Referências	98
	APÊNDICE A - Artigo Publicado. Synthesis and cytotoxic activity of new acridine-thiazolidine derivatives	105
	APÊNDICE B - Artigo publicado. Niche for Acridine Derivatives in Anticancer Therapy	113
	APÊNDICE C - Artigo publicado. Synthesis and in vitro anticancer activity of novel thiazacridine derivatives	130
	APÊNDICE D - Artigo Publicado. Inhibition of DNA topoisomerase I activity and induction of apoptosis by thiazacridine derivatives	140
	APÊNDICE E - Patente depositada. Tiazacridinas utilizadas na terapia anticâncer	151
	APÊNDICE F - Espectros de NMR¹H e IR de tiazacridinas	157



1 Introdução

Dentre todas as patologias que acometem os humanos, o câncer é uma das mais devastadoras, estando atrás apenas das doenças cardiovasculares (WHO, 2012). Apesar do avanço científico, vários tipos de cânceres ainda não têm cura, ou ainda, as células tumorais se tornam resistentes aos fármacos disponíveis na clínica. Dessa forma, o tratamento para o câncer continua sendo um desafio em todo o mundo.

Os avanços científicos possibilitaram demonstrar diferenças moleculares significantes entre as linhagens celulares malignas e as normais. Em função dessas diferenças, novas tecnologias têm permitido a identificação de características genéticas únicas em tumores específicos que podem ser usadas como ferramentas de diagnóstico, prevenção e tratamento, marcadores de prognóstico e preditores de resposta à terapia, como a detecção de mutação no gene KRAS (GOETSCH, 2011).

A busca de novos medicamentos para o tratamento do câncer tem se mostrado intensa. O Laboratório de Planejamento e Síntese de Fármacos da Universidade Federal de Pernambuco (LPSF) vem investigando novos fármacos para o tratamento do câncer. Uma das classes químicas exploradas pelo LPSF pertence à série tiazacridina, que têm como característica principal a presença dos núcleos tiazolidínico e acridínico em uma mesma molécula. A combinação de núcleos farmacofóricos distintos em uma entidade química, o que denominamos hibridização molecular, constitui uma das importantes estratégias utilizadas pela Química Medicinal para obtenção de medicamentos mais potentes, eficazes, seguros e confiáveis.

No decorrer do desenvolvimento desta tese foram elaborados três artigos e uma patente, os quais se encontram nos anexos. Estas publicações descreveram as sínteses e as propriedades anticâncer de tiazacridinas. O primeiro artigo, publicado neste ano, intitulado “Synthesis and cytotoxic activity of new acridine-thiazolidine derivatives” foi um trabalho realizado em colaboração com a Universidade Federal do Ceará e apresenta

Introdução

moléculas obtidas anteriormente no LPSF, semelhantes em estrutura aos compostos obtidos nesta tese. O segundo artigo, submetido no mestrado e aceito para publicação no doutorado “Synthesis and in vitro anticancer activity of novel thiazacridine derivatives”, e a patente “Tiazacridinas utilizadas na terapia anticâncer”, contém tiazacridinas sintetizadas durante a dissertação de mestrado: “Novos agentes anticâncer e tiazacridínicos substituídos: Síntese, estrutura e efeitos biológicos” (PITTA, 2010). Um trabalho que gerou bons resultados de atividade citotóxica e que justificou a contínua busca de agentes anticâncer mais potentes, eficazes, seguros e confiáveis. O terceiro artigo é uma revisão da literatura intitulada “Niche for Acridine Derivatives in Anticancer Therapy”. Este trabalho descreve propriedades químicas e biológica de acridinas e detalha 13 classes de acridinas sintéticas e naturais.

Nesse sentido, os objetivos deste trabalho foram desenhar e sintetizar novos derivados tiazacridínicos, otimizar a síntese de tiazacridinas, determinar propriedades e caracterizar estruturalmente as tiazacridinas e avaliar a atividade anticâncer in vitro de tiazacridinas nas linhagens de células neoplásicas RAJI (Linfoma de Burkitt) e JUKART (Leucemia Aguda de Células T).

Introdução



2 Objetivos

2.1 Geral

Desenvolver novas alternativas terapêuticas para o tratamento do câncer através da síntese orgânica e avaliação da atividade biológica *in vitro* de moléculas tiazacridínicas intercaladoras de DNA.

2.2 Específicos

- ✓ Desenhar e sintetizar novos derivados tiazacridínicos;
- ✓ Otimizar a síntese de tiazacridinas;
- ✓ Determinar propriedades e caracterizar estruturalmente as tiazacridinas;
- ✓ Avaliar a atividade anticâncer *in vitro* de tiazacridinas nas linhagens de células neoplásicas RAJI (Linfoma de Burkitt) e JUKART (Leucemia Aguda de Células T).



3 Revisão da Literatura

3.1 Gênese do câncer

O câncer é definido pela Organização Mundial da Saúde (WHO, 2012) como crescimento e propagação descontrolado de células. O câncer pode afetar qualquer parte do corpo, e o crescimento pode invadir tecidos adjacentes e metastizar para locais distantes do ponto focal. Muitos tipos de câncer, aproximadamente 40% deles, podem ser evitados pela supressão à exposição aos fatores de risco comuns, tais como o tabagismo, e cerca de 70% ocorrem em países em desenvolvimento, o que demonstra a necessidade de adoção de medidas sistemáticas de saúde pública (WHO, 2007).

O câncer surge a partir de uma única célula normal que sofre uma transformação. Essa transformação se dá através de múltiplos estágios, consistindo basicamente na progressão de uma lesão pré-cancerosa para tumores malignos. Essas modificações são o resultado da interação de fatores genéticos com agentes externos, tais como (INCA, O que é o câncer? 2012):

- Radiação ultravioleta e ionizante; agentes químicos, como amianto, álcool, substâncias tóxicas presentes no tabaco, aflotoxinas (contaminante de alimentos), arsênio (contaminante de água);
- Agentes biológicos, como vírus da hepatite B (HBV) e da hepatite C (HCV), papiloma vírus humano (HPV), bactérias e parasitas;
- Estilo de vida, como a falta de atividade física, alimentação precária, obesidade, poluição urbana entre outros.

O envelhecimento é outro fator importante para o desenvolvimento dessa doença. A incidência do câncer aumenta drasticamente com a idade, provavelmente devido a elevação dos riscos de câncer específicos associada à menor eficácia dos mecanismos de reparação celular (INCA, O que é o câncer? 2012).

A maioria dos cânceres humanos surge a partir de tecidos epiteliais cujas células são submetidas à replicação contínua para manutenção de uma camada protetora de células que estão em contato com o ambiente. Exemplos incluem as estruturas normais que se renovam constantemente, como a medula óssea, os pêlos e a mucosa do tubo digestivo (INCA, Quimioterapia, 2012).

Uma mudança essencial necessária para o desenvolvimento de todos os cânceres é a mutação em genes apropriados. Normalmente, existem várias alterações genéticas que envolvem, por exemplo, proto-oncogenes, genes supressores de tumor e genes que regulam eventos de ciclo celular. Uma vez que, uma célula perdeu o controle do seu crescimento e divisão, ela se expande e se multiplica para formar o tumor primário inicial. Nesta fase, o tumor é alimentado por difusão a partir de vasos sanguíneos próximos, no entanto, como as células tumorais aumentam em número, eventualmente tornam-se carentes de nutrientes, tais como oxigênio e glicose (BERGERS, 2003).

A análise minuciosa do perfil e das características de um tumor para predizer o prognóstico e tratamento ideal tem sido o objetivo principal da oncologia. Pesquisas científicas estão focadas na mecânica de controle de células a nível molecular e genético. Proteínas, os produtos finais da expressão gênica, estão frequentemente alteradas em células malignas. A presença, ausência ou abundância relativa de certas proteínas representam informações de prognóstico que podem ajudar no tratamento. Genes que codificam para tais proteínas podem estar com defeitos ou sua expressão pode estar desregulada (silenciado, “up-regulado”, ou modulada) por outros fatores genéticos e epigenéticos (GOETSCH, 2011).

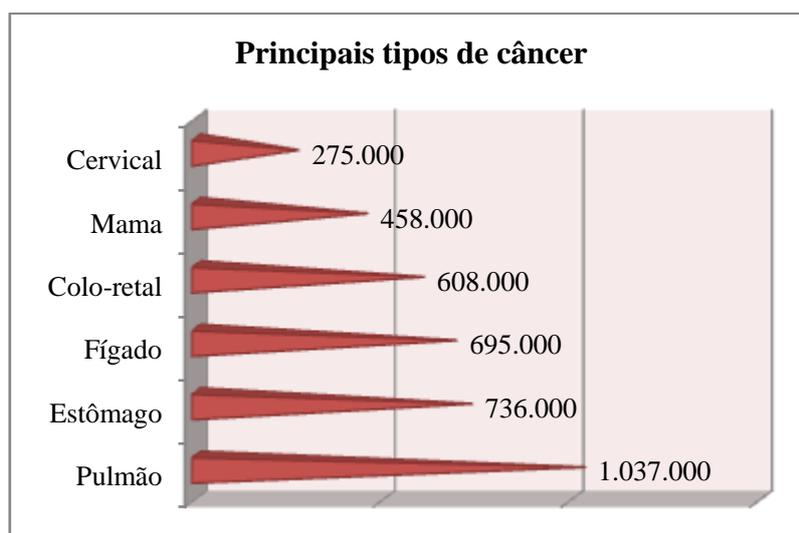
3.2 Epidemiologia do câncer

O câncer é um dos líderes mundiais em causas de morte, contando com 7,6 milhões de mortes (13% do total), em 2008. Mais da metade de todos os casos de câncer ocorrem na América do Sul e na Ásia.

O número de mortes provocado por câncer no mundo deve aumentar 45% entre os anos de 2007 e 2030, passando de 7,9 para 11 milhões. Esse fato está principalmente relacionado com o crescimento e envelhecimento da população. Ainda, estima-se que os novos casos de câncer saltem, no mesmo período, de 11,3 para 15,5 milhões (WHO, 2012).

Na maioria dos países, o câncer ocupa o segundo lugar em mortalidade, estando atrás das doenças cardiovasculares. O câncer de pulmão é o que acomete o maior número de pessoas, responsável por 1.8 milhões de mortes por ano, uma tendência que deve ser reduzida com a intensificação de campanhas para o controle do tabagismo (WHO, 2012). A Figura 1 apresenta dados da Organização Mundial de Saúde que indicam os principais tipos de câncer que acometem a população mundial, em 2008.

Figura 1 - Prevalência dos principais tipos de câncer no mundo, em 2008



Fonte: Adaptado de WHO, 2012

O câncer de mama é o segundo tipo mais frequente no mundo, e é o mais comum entre as mulheres, respondendo por 22% dos casos novos a cada ano. Se diagnosticado e tratado oportunamente, o prognóstico é relativamente bom. No Brasil, as taxas de mortalidade por câncer de mama continuam elevadas, muito provavelmente porque a doença ainda é diagnosticada em estádios avançados. Na população mundial, a sobrevivência média após cinco anos é de 61%. Relativamente raro antes dos 35 anos, acima desta faixa etária sua incidência cresce rápida e progressivamente. Estatísticas indicam

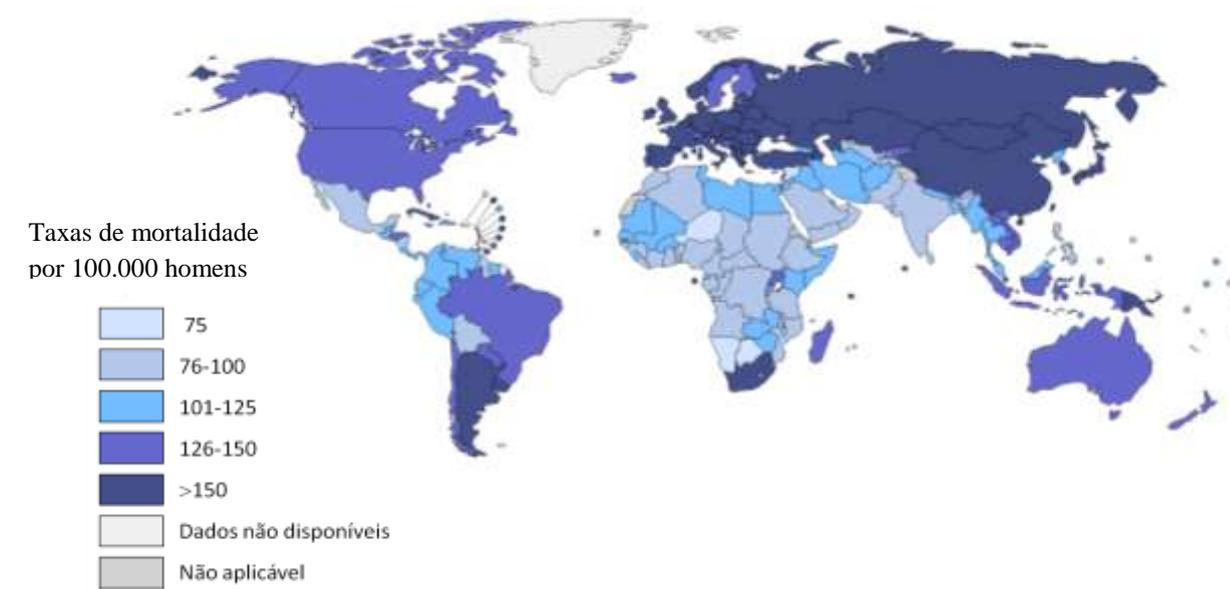
Revisão da Literatura

aumento da incidência do câncer de mama tanto nos países desenvolvidos quanto nos em desenvolvimento (INCA, Mama, 2012).

- Estimativa de novos casos de câncer de mama em 2012: 52.680
- Número de mortes provocado pelo câncer de mama em 2010: 12.852, sendo 147 homens e 12.705 mulheres

O mapa ilustrado na Figura 2 mostra os países mais afetados pela doença no ano de 2008, por 100.000 homens. O Brasil registrou uma média de 136 óbitos do sexo masculino a cada 100.000 habitantes provocados pelo câncer e ocupou a posição nº 119 de 193 dos países que participaram do estudo (WHO, 2011).

Figura 2 - Representação espacial das taxas de mortalidade por câncer no mundo, por 100.000 homens, em 2008



Fonte: WHO, 2011

Em relação ao sexo feminino, obteve-se uma proporção de 95 óbitos a cada 100.000 habitantes, e o Brasil ocupou a posição nº 95 (Figura 3) (WHO, 2011).

Revisão da Literatura

Figura 3 - Representação espacial das taxas de mortalidade por câncer no mundo, por 100.000 mulheres, em 2008



Fonte: WHO, 2011

O câncer infantil não pode ser considerado uma simples doença, mas sim como uma gama de diferentes malignidades. Este tipo de câncer varia de acordo com o tipo histológico, localização primária do tumor, etnia, sexo e idade (INCA, 2008).

O câncer infanto-juvenil deve ser estudado separadamente do câncer do adulto por apresentar diferenças nos locais primários, diferentes origens histológicas e diferentes comportamentos clínicos. Tende a apresentar menores períodos de latência, costuma crescer rapidamente e torna-se bastante invasivo, porém responde melhor à quimioterapia. A maioria dos tumores pediátricos apresenta achados histológicos que se assemelham a tecidos fetais nos diferentes estágios de desenvolvimento, sendo considerados embrionários. Essa semelhança a estruturas embrionárias gera grande diversidade morfológica resultante das constantes transformações celulares, podendo haver um grau variado de diferenciação celular (INCA, 2008).

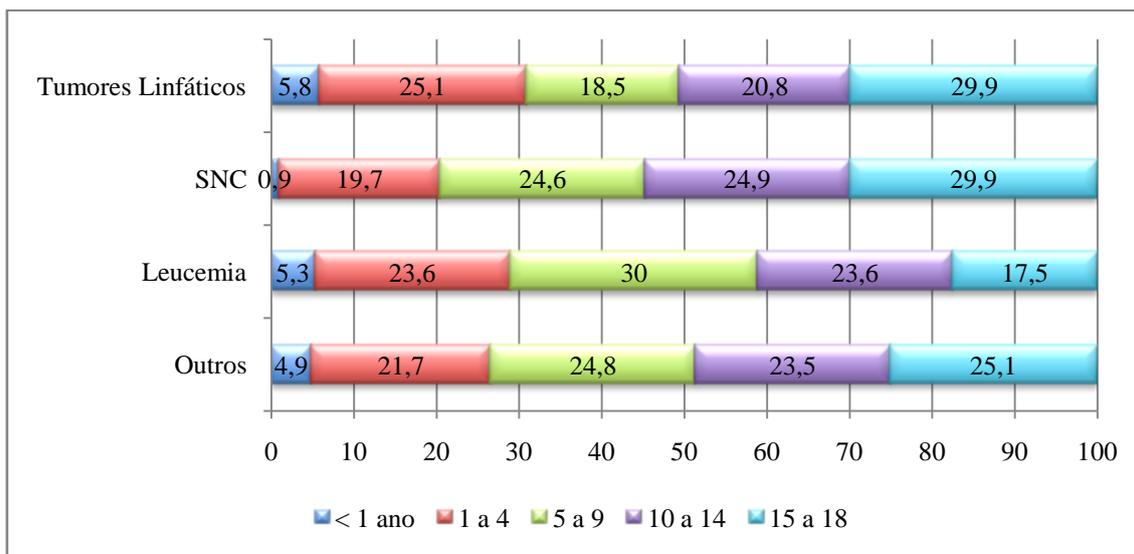
Diversos fatores podem interferir na probabilidade de sobrevivência no câncer pediátrico. Um dos principais é o atraso do diagnóstico. A demora na procura de cuidados médicos pode ser consequência da precariedade dos serviços de saúde, falta de percepção da possibilidade de cura tanto do leigo como da classe médica e até mesmo barreiras religiosas. Os sinais e sintomas são muito inespecíficos, confundindo-se com moléstias frequentes da infância (INCA, 2008).

Para uma visão panorâmica, a Figura 4 mostra a distribuição percentual da mortalidade pelos principais tipos de tumores malignos, por idade, para ambos os sexos.

Revisão da Literatura

Percebe-se que para os tumores linfáticos, as maiores ocorrências de óbitos foram observadas nas faixas etárias iniciais (1-4 anos) e finais (15-18 anos). Nas leucemias, o predomínio foi observado na faixa etária de 5-9 anos. Os óbitos para os tumores de SNC, à exceção dos menores de um ano, distribuíram-se de forma semelhante (INCA, 2008).

Figura 4 - Distribuição percentual da mortalidade por tipo de câncer e faixa etária no Brasil, 2001-2005



Fontes: Adaptado de dados do MS/SVS/DASIS/CGIAE/Sistema de Informação sobre Mortalidade (SIM), MP/Fundação Instituto Brasileiro de Geografia e Estatística (IBGE), MS/INCA/Conprev/Divisão de Informação

A Tabela 1 apresenta dados sobre a mortalidade por câncer relacionados à faixa etária no Brasil, no período entre 2000 e 2010. A taxa específica de mortalidade (TEM) se refere ao risco de morte em cada grupo etário. E, na referida Tabela 1, o valor da TEM aumenta com o avançar da idade, nos homens e nas mulheres. A faixa etária responsável pelo maior número dos óbitos nos homens e nas mulheres foi a de 70 a 79 anos, contando com 221.326 e 163.872, respectivamente, óbitos por 100.000 habitantes. A TEM nas mulheres é menor quando comparado os homens em praticamente todas as idades, com exceção a faixa de 30 a 49 anos. O câncer de mama é um fator importante a ser considerando para explicar esse fato, pois, além de ser o tipo de câncer mais comum nas mulheres, prevalece principalmente nessa faixa etária (INCA, Atlas de Mortalidade por Câncer, 2012).

Revisão da Literatura

Tabela 1 - Mortalidade por câncer, brutas e ajustadas por idade, pelas populações mundial e brasileira, por 100.000 homens e mulheres, Brasil, 2000-2010

Faixa Etária	Homens		Mulheres	
	Número de Óbitos	Taxa Específica de Mortalidade	Número de Óbitos	Taxa Específica de Mortalidade
00 a 04	4.358,00	4,70	3.657,00	4,09
05 a 09	3.950,00	4,15	3.053,00	3,32
10 a 14	3.880,00	3,95	3.143,00	3,29
15 a 19	5.789,00	5,76	4.011,00	4,05
20 a 29	13.606,00	7,61	12.916,00	7,13
30 a 39	23.248,00	15,84	35.157,00	22,82
40 a 49	72.445,00	63,05	85.102,00	69,26
50 a 59	152.221,00	198,09	132.980,00	158,35
60 a 69	212.326,00	449,83	158.498,00	290,07
70 a 79	221.326,00	885,23	163.872,00	516,89
80 ou mais	137.640,00	1.421,36	123.019,00	844,47
Idade Ignorada	446,00	-	272,00	-
Total	851.004,00	-	725.680,00	-
Taxa Bruta	-	86,32	-	71,21
Taxa Padrão Mundial (1)	-	102,62	-	72,18
Taxa Padrão Brasil (2)	-	87,90	-	62,52

Fonte: Adaptado de dados do INCA, 2012

3.3 Controle e diagnóstico

A detecção precoce de células cancerosas no organismo é crucial para ter um início rápido de tratamento e, conseqüentemente, aumento das chances de cura e sobrevida do paciente. O tratamento do câncer requer uma ou mais intervenções, tais como cirurgia, radioterapia, hormonoterapia e quimioterapia. O conhecimento do mecanismo molecular da doença e das formas de intervenção que a previnem e controlam é essencial para a identificação de estratégias de controle e diagnóstico.

O objetivo do tratamento é curar ou prolongar a sobrevida, com melhoria na qualidade de vida do paciente. Os casos de câncer podem ser reduzidos através de campanhas e da implementação de estratégias de prevenção, detecção precoce e tratamento, como por exemplo: diminuição da exposição a fatores de risco; vacinação contra o vírus HPV, HBV e HCV; controle de riscos ocupacionais; redução da exposição à luz solar.

Revisão da Literatura

3.4 Abordagens terapêuticas para o tratamento do câncer

A quimioterapia e radioterapia são as terapias mais utilizadas para os casos de câncer sem indicação de intervenção cirúrgica. Mesmo com os recentes avanços e aumento da sobrevivência dos pacientes resultantes do desenvolvimento de agentes citotóxicos, o prognóstico geral de pacientes portadores de tipos comuns de câncer continua aquém do desejável. Além disso, a escassez na melhoria das terapias convencionais impulsiona a busca de novas abordagens terapêuticas para o tratamento do câncer (BICKNEL, 2005).

As abordagens terapêuticas têm evoluído a partir de uma maior compreensão das vias que regulam a proliferação celular e metástase. Estes estudos identificaram alvos novos de fármacos e possibilitaram o desenvolvimento de terapêuticas específicas. A grande maioria dos medicamentos utilizados na clínica envolve moduladores da autofagia, como o bevacizumab, um anticorpo monoclonal se liga e neutraliza seletivamente a atividade biológica do fator de crescimento do endotélio vascular humano - VEGF; os moduladores da angiogênese, como o tamoxifeno, um antiestrogênio (Tabela 2); e os agentes anticâncer clássicos, como os agentes intercalantes de DNA, agentes túbulo-afins, antimetabólitos, alquilantes, inibidores da topoisomerase I e II, agentes cinidores de DNA e análogos da purina e pirimidina (BICKNEL, 2005).

Tabela 2 - Medicamentos moduladores da autofagia e da angiogênese utilizados na terapia contra o câncer

Fármaco	Efeito biológico	Mecanismo de ação	Indicações
Bevacizumab (Avastint®)	Inibição da angiogênese	Anti-VEGF	Câncer colorretal metastático, câncer de pulmão, câncer metastático de rim, câncer de mama
Tamoxifeno (Nolvadex®)	Indução da autofagia e da apoptose	Bloqueio dos receptores estrogênicos (RE)	Câncer de mama

Fonte: Autora, 2012

3.4.1 Moduladores da autofagia

O ambiente tumoral é caracterizado por uma redução nos níveis de oxigênio e nutrientes. Isso sugere que as células cancerosas, além do aumento da glicólise

Revisão da Literatura

(MORENO-SÁNCHEZ et al., 2007), induzem o processo autofágico para a produção de energia.

A autofagia é uma via catabólica lisossomal pela qual as células reciclam macromoléculas e organelas. A capacidade de autofagia melhora a sobrevivência das células tanto pela capacidade de manter o metabolismo celular em condições de hipóxia ou de privação de nutrientes, quanto pelo fato de remover organelas danificadas sob condições de estresse (HØYER-HANSEN, JÄÄTTELÄ, 2008).

No câncer, o processo de autofagia está geralmente alterado nos níveis de regulação, indução e degradação lisossomal, e talvez seja uma via alternativa para a identificação de novos alvos terapêuticos para o tratamento do câncer pelos seguintes fatores: 1) no ambiente tumoral os baixos níveis de oxigênio e nutrientes melhoram a sinalização de autofagia em tecidos cancerígenos (MATHEW et al., 2007), 2) vários tumores estão associadas alterações genéticas em genes que regulam autofagia, como o ‘Alvo da Rapamicina’ Complexo 1 de Mamíferos (mTORC1), através da indução da mesma (MATHEW et al., 2007; GOZUACIK, KIMCHI, 2004), e por fim, 3) o término do processo de autofagia requer lisossomas cuja atividade está muito alterada durante a tumorigênese (KROEMER, JAATTELA, 2005).

Nas células tumorais com defeitos na apoptose, a autofagia permite sobrevivência prolongada. Paradoxalmente, defeitos no processo autofágico estão associados com aumento da tumorigênese. A perda monoalélica do gene essencial da autofagia Beclin1 causa susceptibilidade ao estresse metabólico e também promove a tumorigênese. No entanto, o mecanismo envolvido ainda não foi determinado. Evidências recentes sugerem que a autofagia fornece uma função protetora para limitar necrose tumoral e inflamação, e para atenuar os danos do genoma nas células tumorais em resposta ao estresse metabólico (MATHEW, KARANTZA-WADSWORTH, WHITE, 2007). Por outro lado, mesmo que a autofagia atue como uma resposta de pró-sobrevivência na homeostase de células normais, ela pode ser capaz de sinalizar a morte celular nas células tumorais. No entanto, várias questões importantes relativas às consequências da modulação da autofagia *in vivo* permanecem sem resposta, e ainda é especulativo se autofagia é um alvo adequado para tratamento do câncer.

A questão de induzir ou inibir a autofagia no tratamento do câncer não é simples e a resposta é difícil de prever antes de serem testados moduladores de autofagia específicos em ensaios clínicos. No entanto, vários compostos, inclusive alguns

Revisão da Literatura

desenvolvidos para outros fins, podem contribuir com importantes informações sobre o emprego de moduladores de autofagia no tratamento do câncer (Tabela 3).

Tabela 3 - Fármacos relevantes que modulam a autofagia

Fármaco	Alvo molecular	Nível de modulação da autofagia^I	Efeito na autofagia	Indicação	Referências
Tamoxifeno	Receptor de estrogênio	Indução	Aumento	Câncer de mama	GONZALEZ-MALERVA et al., 2012
Kringle 5 (inibidor de angiogênese)	Receptor de angiogênese	Indução	Aumento	Cânceres de várias origens	NGUYEN et al., 2007
Imatinib (inibidor de tirosina quinase)	Tirosina quinase	Indução	Aumento	Leucemia mieloide crônica	ERTMER et al., 2007
Temozolomida (agente alquilante)	DNA	Indução	Aumento	Ensaio clínico fase II, glioblastoma	NCT01102595*
Hidrocloroquina	Agente lisossomotrópico	Inibição	Diminuição	Ensaio clínico fase II, câncer de mama	NCT01292408*
Omeprazol	Bomba de prótons	Fusão/Degradação	Diminuição	Úlcera péptica	UDELNOW et al., 2011

Fonte: Adaptado de HØYER-HANSEN, 2008

^IA indução da autofagia pode promover morte celular (morte autofágica), e sua inibição pode levar à apoptose, resultando em um maior grau de morte de células de câncer do que é possível com terapias atualmente disponíveis

*Número de identificação no Clinicaltrials.gov

3.4.2 Inibidores da angiogênese

Os grandes avanços ocorridos na área da biologia molecular têm possibilitado uma melhor compreensão dos mecanismos de carcinogênese. Dentre estes, destaca-se a angiogênese como o processo através do qual as células tumorais estimulam a formação de novos vasos sanguíneos necessários para o fornecimento dos nutrientes essenciais para seu crescimento acelerado. Sabe-se hoje que a angiogênese resulta da liberação local pelo tumor de algumas proteínas com ação estimuladora para o desenvolvimento vascular, como o fator de crescimento fibroblástico básico (bFGF), a ciclo-oxigenase 2 (COX-2) e o fator de crescimento endotelial vascular (VEGF). Sucessivos estudos têm demonstrado uma significativa correlação entre os níveis séricos e teciduais destas

Revisão da Literatura

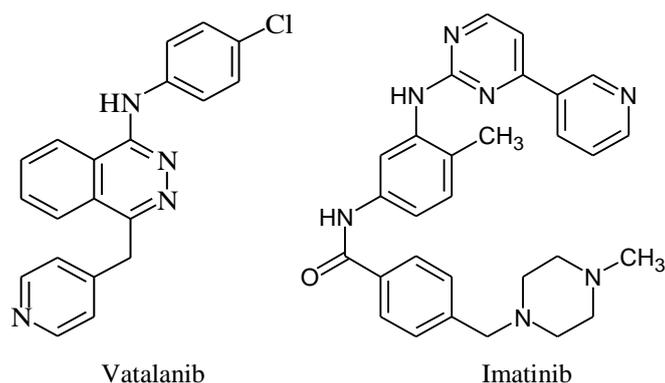
proteínas e as características clínico-patológicas de diversos tumores, incluindo o câncer colorretal. Como consequência direta destes achados, a terapia anti-angiogênica, baseada na inibição destas moléculas, representa hoje uma promissora linha de estudo em oncologia (PINHO, 2005).

A ativação da angiogênese no microambiente tumoral em desenvolvimento ocorre quando o saldo de inibidores de angiogênese endógenos e os ativadores de angiogênese mudam em favor do processo angiogênico. Embora existam evidências de que essa mudança possa envolver alterações irreversíveis na célula do carcinoma, um fator importante é a resposta da célula à carência de oxigênio (hipóxia) e outros nutrientes. Por exemplo, muitas células normais, assim como as células neoplásicas, irão liberar o Fator de Crescimento do Endotélio Vascular Humano (VEGF) e outros fatores pró-angiogênicos quando expostas à hipóxia. Uma vez que um ambiente pró-angiogênico é alcançado, novos vasos sanguíneos no tumor emergem e sustentam o crescimento e desenvolvimento do tumor. Além disso, as características desorganizadas e imaturas da neovascularização tumoral fornecem pontos de saída de fácil acesso para a propagação das células cancerosas pelo sangue, aumentando as chances de metástase (BICKNEL, 2005).

A maioria dos medicamentos inibidores de angiogênese aprovados ou em fase de avaliação clínica pode ser classificada em duas categorias principais: anticorpos monoclonais e inibidores da tirosina kinase (TK) (Figura 5) (Tabela 4). A terapia com anticorpos monoclonais neutraliza os ligantes ou receptores que são super expressos em certos tipos de câncer (HARRIS, 2004). O bevacizumabe, por exemplo, é um anticorpo monoclonal humanizado recombinante que reduz a vascularização de tumores através da inibição do VEGF, reduzindo assim a velocidade de crescimento de células neoplásicas de câncer de mama (Bula do Avastint®, 2012).

Receptores transmembranares com atividade TK intrínseca foram identificados como reguladores de tumor ou crescimento de vasos tumorais (DREVS et al., 2003).

Figura 5 - Inibidores da enzima tirosina quinase



Fonte: Autora, 2012

Tabela 4 - Anticorpos monoclonais e inibidores da enzima tirosina quinase utilizados no tratamento do câncer

Fármaco	Alvo molecular	Indicações	Reações adversas
Anticorpos monoclonais			
Bevacizumab (Avastint [®])	VEGF	Câncer colorretal metastático, câncer de mama metastático, câncer de pulmão, câncer de células renais metastático	Perfurações intestinais, aumento da pressão arterial, problemas de cicatrização de feridas e de cortes cirúrgicos, derrame cerebral e infarto agudo do miocárdio, hemorragias entre outras
Trastuzumab (Herceptin [®])	Fator de crescimento epidérmico humano tipo 2 (HER-2)	Câncer de mama metastático	Dispnéia, hipotensão, sibilância, broncoespasmo, taquicardia entre outras
Cetuximab (Erbix [®])	Receptor do factor de crescimento epidérmico (EGFR)	Câncer colorretal metastático	Doenças respiratórias, reações cutâneas, perturbações eletrolíticas, neutropenia entre outras
Inibidores da tirosina quinase			
Vatalanib (PTK787)	Enzima tirosina quinase	Câncer colorretal	Aumento da pressão arterial, desarranjos intestinais (diarréia, náuseas e vômito), cansaço, tontura entre outras
Imatinib (Gefitinib [®])	Enzima tirosina quinase	Leucemia mielóide crônica	Náuseas leves, vômitos, diarréia, mialgia, câibras musculares, rash (erupção cutânea), edemas superficiais entre outras

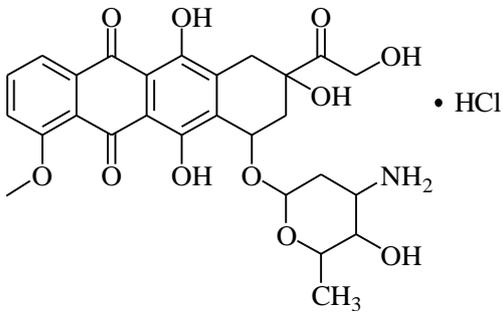
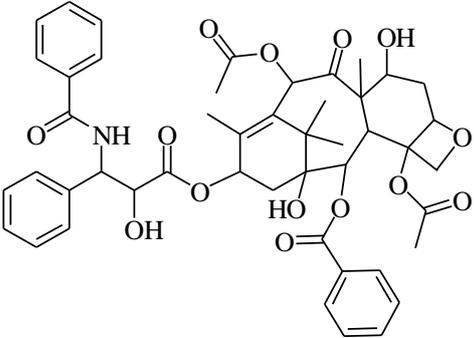
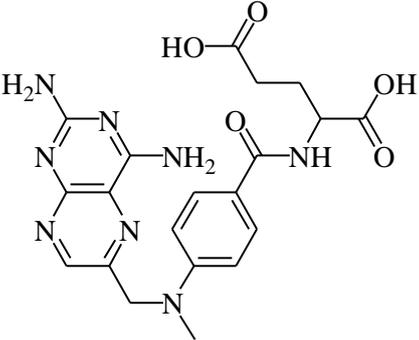
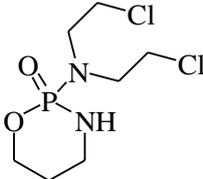
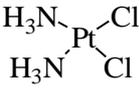
Fonte: Adaptado de Bicknell, 2005

Revisão da Literatura

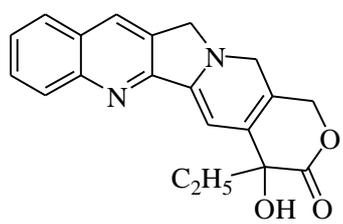
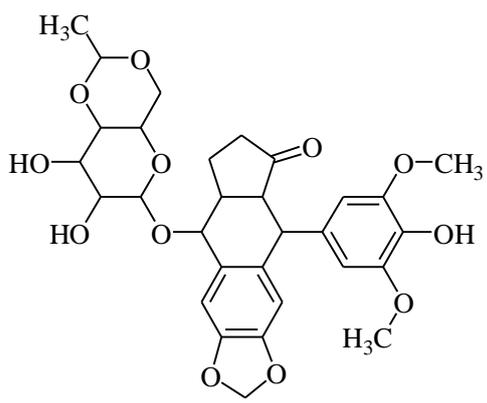
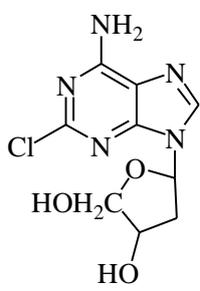
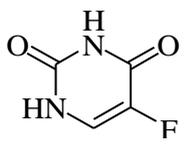
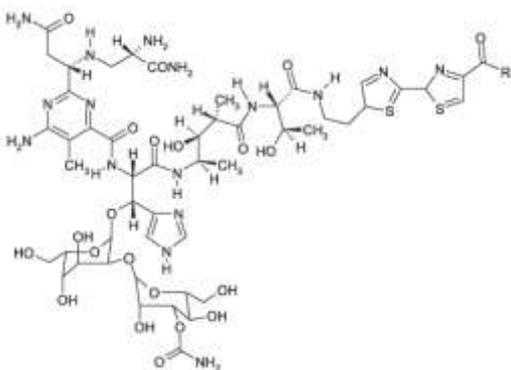
3.4.3 Agentes citotóxicos clássicos

Os agentes citotóxicos clássicos podem ser subdivididos de acordo com o mecanismo de ação: agentes intercalantes de DNA, agentes túbulo-afins, agentes antimetabólitos, agentes alquilantes, agentes inibidores da topoisomerase I e II, agentes cinidores de DNA e análogos da purina e pirimidina. Alguns exemplos de medicamentos que agem de acordo com estes mecanismos de ação encontram-se na Tabela 5.

Tabela 5 - Agentes citotóxicos convencionais subdivididos de acordo com o mecanismo de ação

<p style="text-align: center;">Agente intercalador de DNA</p>  <p style="text-align: center;">Cloridrato de doxorrubicina Inibe a síntese de ácidos nucleicos</p>	<p style="text-align: center;">Agente túbulo-afim</p>  <p style="text-align: center;">Paclitaxel Estabiliza microtúbulos</p>
<p style="text-align: center;">Agente Antimetabólito</p>  <p style="text-align: center;">Metotrexato Inibe a biossíntese da enzima diidrofolato redutase</p>	<p style="text-align: center;">Agentes alquilantes</p>  <p style="text-align: center;">Ciclofosfamida Formaligações covalentes com o DNA</p>  <p style="text-align: center;">Cisplatina Forma complexo inorgânico de Pt⁺⁺ com o DNA</p>

Revisão da Literatura

<p>Agente inibidor da topoisomerase I</p>  <p>Camptotecina Inibe a enzima topoisomerase I</p>	<p>Agente inibidor da topoisomerase II</p>  <p>Etoposida Inibe a enzima topoisomerase II</p>
<p>Análogo da purina</p>  <p>Cladribina Análogo clorado do nucleotídeo purínico adenina</p>	<p>Análogos de Pirimidina</p>  <p>Fluoracil Inibe a timidilato sintase</p>
<p>Agente cinidor</p>  <p>Bleomicina Provoca fragmentação dos filamentos de DNA após a formação de radicais livres</p>	

Fonte: Autora, 2012

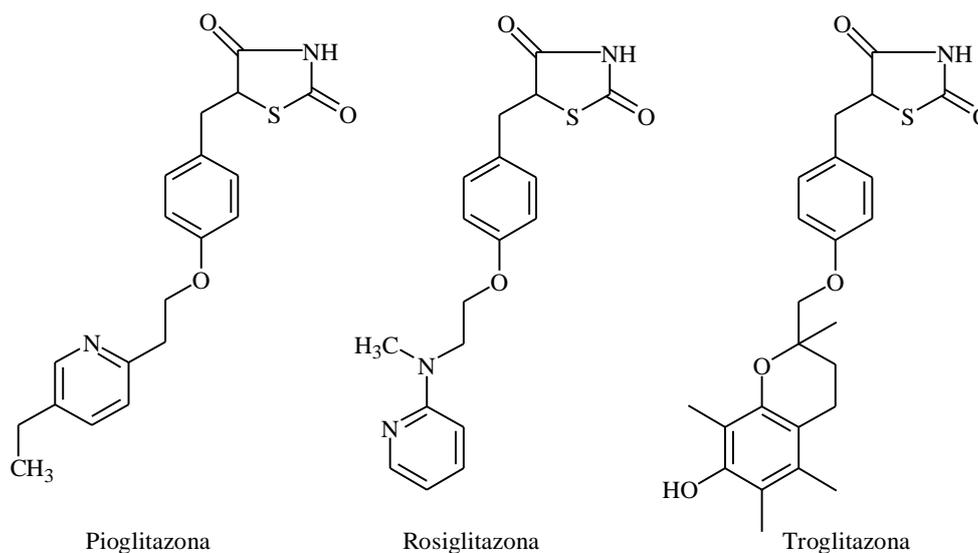
Revisão da Literatura

3.5 Alvos moleculares selecionados de tiazolidinas e acridinas e seus inibidores anticâncer

As tiazolidinas (TZDs) possuem propriedades antidiabética, anticâncer, antibacteriana (BONDE, GAIKWAD, 2004), antifúngica (CESUR et al., 1994), antiviral (RAO et al., 2003) e antituberculose (SAMADHIYA et al., 2012).

As TZDs são ligantes sintéticos do Receptor Ativador da Proliferação de Peroxissomos γ (PPAR γ) e agem como agonistas do PPAR γ (Figura 5). Sua descoberta durante a última década revelou novas vias envolvidas no controle da diferenciação celular, proliferação e apoptose, que têm sido implicadas na regulação de processos biológicos importantes, tais como inflamação, remodelação do tecido e biologia vascular (ELANGBAM et al., 2001).

Figura 6 - Fármacos derivados de tiazolidinas



Fonte: Autora, 2012

Os derivados da acridina foram inicialmente desenvolvidos como pigmentos e corantes no final do Século XIX e, durante a Primeira Guerra Mundial, suas propriedades farmacológicas foram avaliadas. O pioneiro interesse medicinal desses compostos data de 1888, mas apenas em 1913 começaram a ser usados na prática médica quando Browning descobriu a ação bactericida da proflavina e da acriflavina (Tabela 6) (DEMEUNYNCK et al., 2001). Em 1930, a mepacrina (Tabela 6) foi

Revisão da Literatura

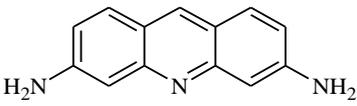
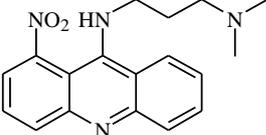
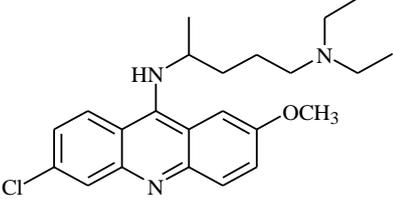
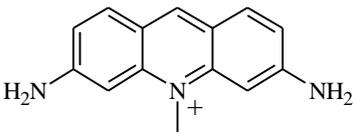
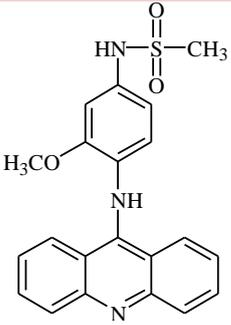
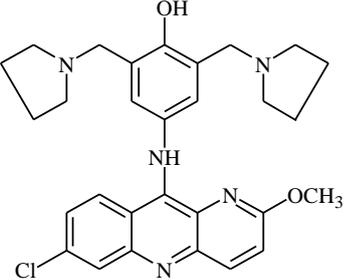
descoberta, o primeiro antimalárico sintético concorrente da quinina em atividade, fato que impulsionou o ritmo das investigações científicas (Tabela 6) (DENNY, 2001).

Os derivados acridínicos são conhecidos por apresentarem um amplo espectro de atividades biológicas, como, além da atividade anticâncer, atividades antimicrobiana, antimalárica, antialzheimer, antitripanossômica (BONSE et al., 1999), leishmanicida (GIRAULT et al., 2000).

A atividade anticâncer das acridinas foi considerada pela primeira vez em 1920. A partir de então, vários compostos, alcalóides naturais ou moléculas sintéticas, foram testados como agentes antitumorais (DEMEUNYNCK et al., 2001).

A amsacrina (Tabela 6) é um derivado da aminoacridina. É um potente agente intercalante antineoplásico, é efetiva no tratamento de leucemia aguda e de linfomas malignos, mas é pouco ativa contra tumores sólidos (GRAZIANO et al., 1996).

Tabela 6 - Derivados da acridina

Atividade antibacteriana	Atividade anticâncer	Atividade antimalárica
		
Proflavina	Nitracrina	Mepacrina
		
Acriflavina	Amsacrina	Pironaridina

Fonte: Autora, 2012

O mecanismo de ação de derivados de acridina envolve ligação ao DNA pela inserção do esqueleto da molécula entre bases nitrogenadas, causando o desenrolamento da hélice e, finalmente, resultando na interrupção da função do DNA (CHOW et al., 2009). Outros mecanismos de ação incluem:

Revisão da Literatura

- Inibição das enzimas topoisomerase I e II (topo I e II);
- Inibição da enzima telomerase;
- Regulação da proteína p53.

3.5.1 Receptor ativador da proliferação de peroxissomos - PPAR

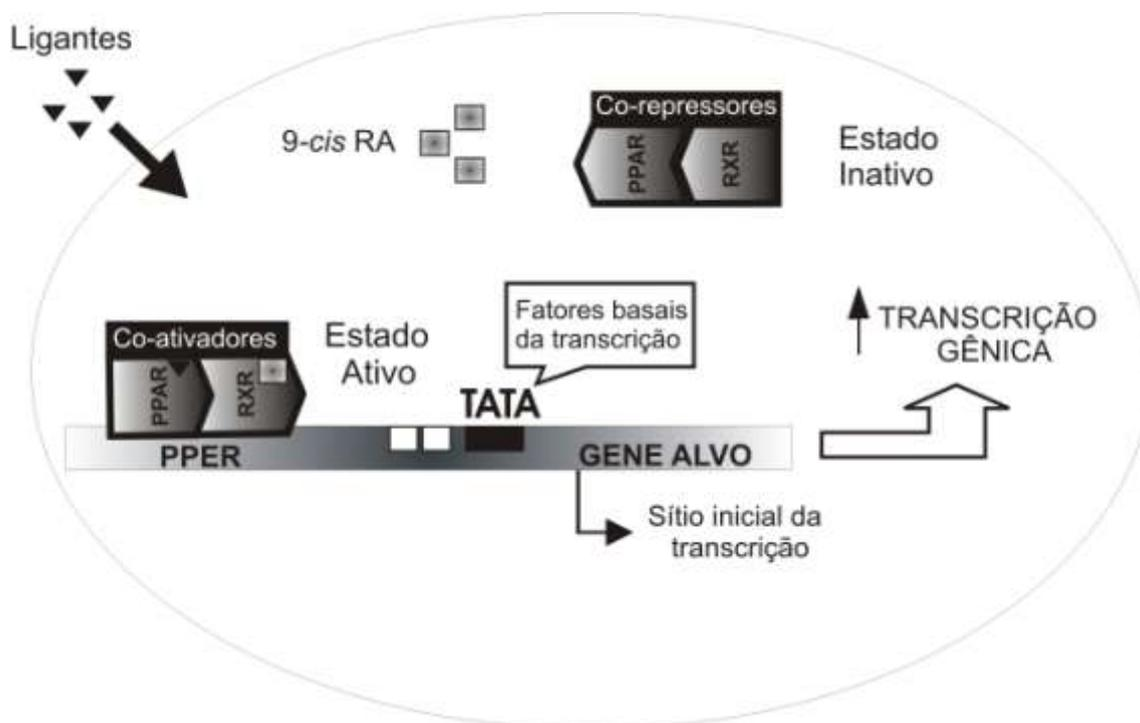
O PPAR é membro de uma família de receptores nucleares estereoidais. Três isótipos codificados por genes distintos foram identificados até o presente: PPAR α , PPAR β e PPAR γ . Os PPARs são fatores de transcrição ligante-dependentes que regulam a expressão do gene-alvo pela ligação a específicos PPREs (Elementos Responsivos aos Proliferadores de Peroxissoma) situados em sítios regulatórios de cada gene. O PPAR liga-se ao PPRE como um heterodímero, juntamente com um fator protéico adicional, o receptor do ácido 9-cis retinóico (RXR). Assim como os PPARs, foram identificadas três isoformas distintas de RXR: RXR α , β e γ , apresentando distribuição distinta nos tecidos. O RXR pode ser ativado pelo ácido 9-cis retinóico e por ligantes sintéticos (BERGER, MOLLER, 2002).

Sob atuação de agonistas naturais ou sintéticos, a conformação do PPAR é alterada e estabilizada, criando um sítio de ligação, com posterior recrutamento de coativadores transcricionais, resultando em aumento na transcrição gênica. Um exemplo de co-ativador é o SRC-1 (Co-ativador 1 do Receptor de Esteróides). Ele possui atividade histona acetilase e pode remodelar a estrutura da cromatina, deixando-a mais frouxa e facilitando a atividade transcricional (Esquema 1). Por sua vez, o co-repressor N-CoR (Co-repressor Núcleo Receptor) é uma proteína que interage com o receptor nuclear livre, mediando um sinal repressivo para o promotor no qual o complexo está ligado (TAVARES et al., 2007).

Derivados de ácidos graxos e eicosanóides são ligantes naturais do PPAR γ . Eles se ligam e ativam o PPAR γ em concentrações micromolares. Exemplos de ácidos graxos que ativam o PPAR γ são: ácido linoléico, ácido araquidônico e ácido eicosapentaenóico. Os seus níveis de concentração intracelular são desconhecidos (BERGER, MOLLER, 2002).

As tiazolidinonas são ligantes sintéticos e agonistas do PPAR γ . Além destes potentes ligantes, um grupo de antiinflamatórios não estereoidais (AINEs) apresentam fraca atividade com o PPAR γ e PPAR α : indometacina, fenoprofeno e ibuprofeno (BERGER, MOLLER, 2002).

Esquema 1 - Mecanismo de ativação transcricional pelo PPAR: Requer a liberação do complexo co-repressor (atividade Histona Deacetilase), feito por um ligante, e o recrutamento de complexo co-ativador (atividade acetiltransferase). O complexo PPAR:RXR ativado liga-se ao PPRE, produzindo alteração na estrutura da cromatina, originando uma estrutura transcricionalmente competente



Fonte: Adaptado de TAVARES et al., 2007

O PPAR γ está envolvido com o metabolismo dos lipídeos, com a sensibilização de células periféricas à insulina, com a inflamação e com a diferenciação e proliferação de células tumorais (SUH et al., 1999). As TZDs são utilizadas no tratamento de diabetes mellitus tipo II dado seu efeito de sensibilização à insulina.

Três drogas pertencentes ao grupo das tiazolidinas, pioglitazona, rosiglitazona e troglitazona, são potentes e altamente seletivas para o PPAR γ (Figura 6). Elas têm sido utilizadas na prática clínica, embora o emprego da rosiglitazona e da troglitazona tenha

Revisão da Literatura

sido descontinuado, haja vista o aparecimento de casos de toxicidade cardiovascular e de hepatotoxicidade (TAVARES et al., 2007).

O efeito das TZDs no crescimento de células tumorais vem sendo estudado extensivamente. As TZDs inibem a proliferação celular e intensificam a apoptose (PANIGRAHY et al., 2003). Esse efeito é dependente do nível de expressão de PPAR γ . A troglitazona, por exemplo, mostrou inibir a proliferação celular por meio da interação com inibidores de ciclinas e quinases dependente de ciclinas, tais como p21waf1 e p27kip1, induzindo a parada do ciclo celular e diferenciação terminal (KOGA et al., 2001, 2003). A troglitazona também induziu a apoptose em linhagens de células de câncer de fígado *in vitro* via ativação da caspase 3 (TOYODA, 2002).

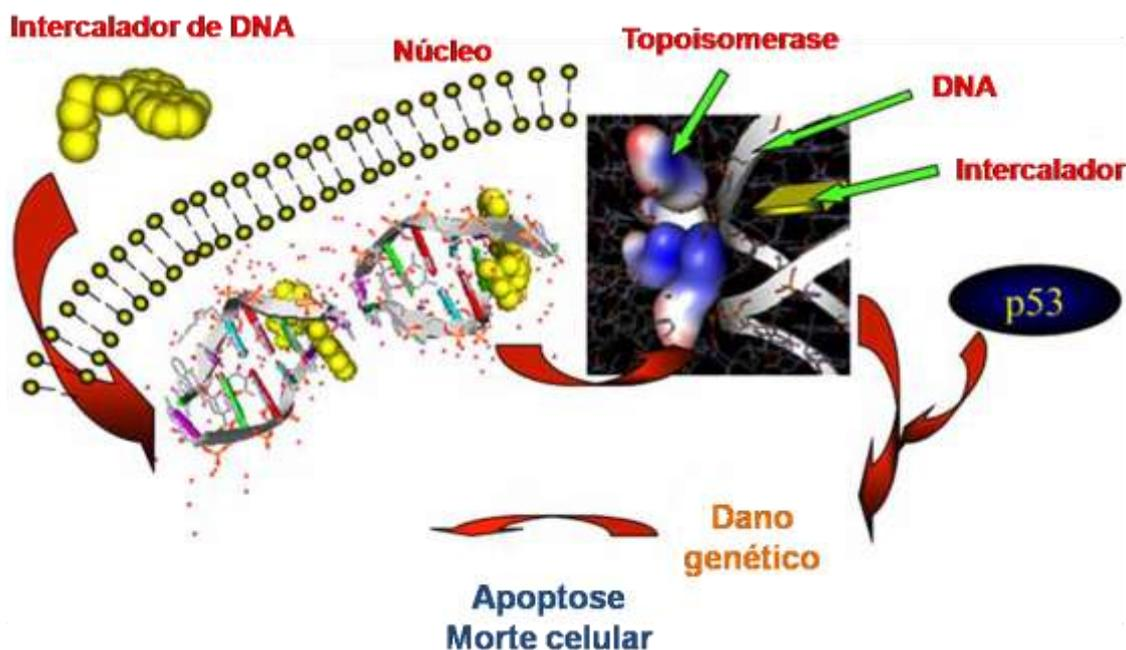
A pioglitazona, outro derivado das TZDs, foi capaz de reduzir a sobrevivência e proliferação de células pré-neoplásicas *in vitro* e em modelos animais *in vivo* (KAWAGUCHI et al., 2002). Além disso, a pioglitazona preveniu a síntese de colágeno e a ativação de células estreladas hepáticas em modelos de fibrose hepática em animais, sugerindo um benefício adicional de agonistas de PPAR γ no tratamento de cirrose hepática (GALLI et al., 2002). Esse fato pode ter um efeito indireto sobre a prevenção de câncer de fígado primário.

3.5.2 Ácido desoxiribonucléico - DNA

A descoberta de novos compostos com atividade antitumoral tornou-se um dos objetivos mais importantes da química medicinal. Um interessante grupo de agentes quimioterápicos utilizados no tratamento do câncer compreende moléculas que interagem com o DNA. Investigação nesta área tem revelado uma série de moléculas que reconhecem o DNA e que atuam como agentes antitumorais, incluindo ligantes do tipo “groove”, agentes alquilantes e intercalantes. Os intercalantes de DNA (moléculas que se intercalam entre os pares de base) (Esquema 2) têm atraído uma atenção particular devido à sua atividade antitumoral. Por exemplo, derivados de acridina e de antraciclina são excelentes intercaladores de DNA que estão agora no mercado como agentes quimioterápicos. Os derivados de acridinas e antraciclina disponíveis na clínica têm sido amplamente estudados a partir de uma variedade de pontos de vista, tais como as propriedades físico-químicas, características estruturais, síntese e atividade

biológica. No entanto, a aplicação clínica destes compostos, e de outros da mesma classe, apresentou certas dificuldades, tais como a resistência a múltiplas drogas (MDR) e efeitos secundários e/ou colaterais. Estas dificuldades têm motivado a pesquisa direcionada à busca de novos compostos para substituir os existentes ou para serem usados como terapia adjuvante (MARTÍNEZ, CHACON-GARCIA, 2005).

Esquema 2 - Representação esquemática do mecanismo citotóxico de um intercalador de DNA



Fonte: Adaptado de MARTÍNEZ, CHACON-GARCIA, 2005

O DNA tem uma forte afinidade para vários compostos aromáticos heterocíclicos tais como acridina e seus derivados. Lerman em 1961 propôs pela primeira vez a intercalação como fonte desta afinidade e, desde então, esse modo de interação foi alvo de bastante estudo. No modelo proposto, moléculas aromáticas planares possuindo 2 ou 3 anéis de 6 membros são inseridas entre os pares de bases adjacentes da dupla fita do DNA. O cromóforo aromático intercalado se orienta paralelamente aos pares de bases nucleotídicos e perpendicularmente ao eixo da dupla hélice formando um complexo que é então estabilizado por ligações não covalentes, como interações hidrofóbicas, ligações de van der Waals e por ligações de hidrogênio. Estas interações são consideradas as mais importantes na intercalação. A intercalação gera deformações estruturais e alterações das características físico-químicas dos ácidos

Revisão da Literatura

nucléicos. A dupla hélice se torna rígida e se estica, fazendo com que haja perda de funcionalidade do DNA (LERMAN, 1961, 1963).

Intercaladores orgânicos podem inibir a síntese de ácidos nucleicos *in vivo*, e são agora fármacos anticâncer comuns aplicados na terapia clínica (LIU, SADLER, 2011).

3.5.3 Enzimas topoisomerase I e II

A maioria das moléculas de DNA de ocorrência natural tem super-hélices negativas. A super-hélice negativa surge de desenrolamento ou subelicoidização do DNA. Em essência, a super-hélice negativa prepara o DNA para processos que resultam na separação dos filamentos de DNA, tais como a replicação. A super-hélice positiva condensa o DNA com eficiência, mas dificulta a separação dos filamentos (BERG et al., 2008).

A presença de super hélices na área imediata à deselicoidização dificultaria, entretanto, o desenrolamento do DNA. Portanto, as super-hélices negativas têm de ser continuamente removidas, e o DNA relaxado, à medida que a dupla hélice se desenrola (BERG et al., 2008).

Enzimas específicas, chamadas topoisomerasas, introduzem ou eliminam as super-hélices. A topoisomerase tipo I catalisa o relaxamento do DNA em super-hélice, um processo termodinamicamente favorável. A topoisomerase tipo II usa energia livre de hidrólise de ATP para adicionar super-hélices negativas ao DNA (BERG et al., 2008).

Estas enzimas alteram o número de ligação do DNA, catalizando um processo de três etapas: (1) a *clivagem* de um ou ambos os filamentos do DNA, (2) a *passagem* de um segmento do DNA por esta quebra, e (3) a *ressoldagem* da quebra do DNA. Os dois tipos de enzimas têm várias características comuns, incluindo o uso de tirosinas importantes para formar ligações covalentes no arcabouço polinucleotídico que é temporariamente quebrado (BERG et al., 2008).

As estruturas tridimensionais de vários tipos de topo I já foram determinadas (Figura 7). Estas estruturas revelam muitas características do mecanismo de ação. A topo I humana compreende quatro domínios, que são dispostos ao redor de uma cavidade central que tem o tamanho correto para acomodar uma molécula bifilamentar

Revisão da Literatura

de DNA. Essa cavidade também contém uma tirosina (Tir 723), que atua como um nucleófilo, cortando o arcabouço de DNA no curso da catálise (BERG et al., 2008).

Figura 7 - Topoisomerase I humana complexada com o DNA

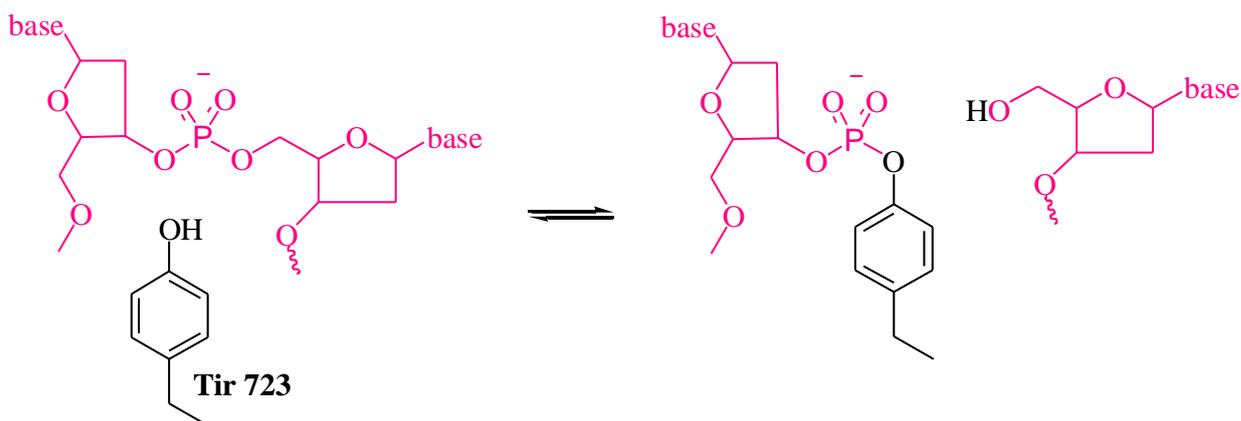


Fonte: PDB 1EJ9.pdb

Pelas análises destas estruturas e por resultados de outros estudos, sabe-se que o relaxamento das moléculas de DNA em super-hélice negativa ocorre do seguinte modo (Figura 8). Primeiro, a molécula de DNA liga-se dentro da cavidade da topo. A hidroxila da tirosina 723 ataca um fosfato em um dos filamentos do DNA, cortando-o e liberando uma hidroxila 5' (BERG et al., 2008).

Revisão da Literatura

Figura 8 - Clivagem do DNA (rosa) via topoisomerase (preta)



Fonte: Adaptado de BERG et al., 2008

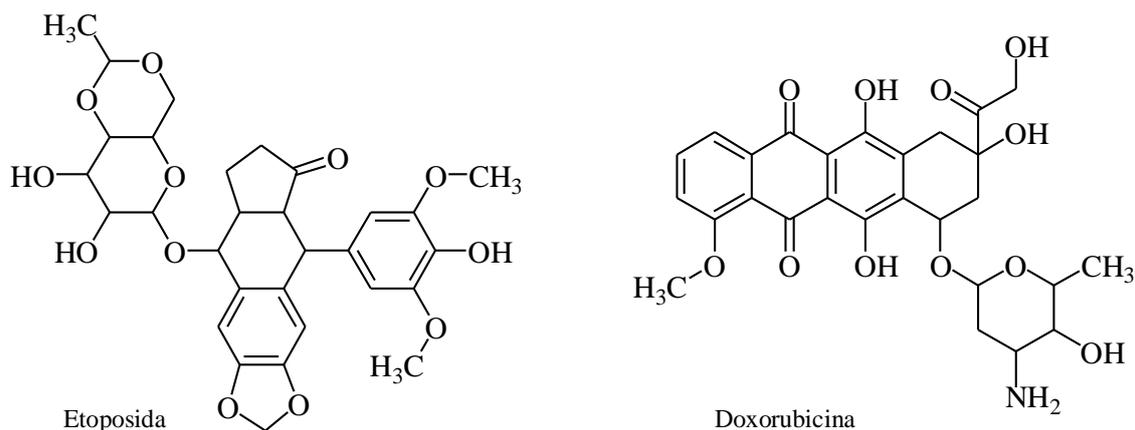
A topo I humana altera o número de ligações através da quebra de uma fita da dupla hélice do DNA, seguida da liberação da fita quebrada. Já enzima topo II humana (formas α e β) altera o número de ligações através da quebra das duas fitas do DNA (OPPEGARD, 2009).

As enzimas DNA topo são responsáveis pelo controle das formas topológicas do DNA e desempenham papéis cruciais no metabolismo do DNA. Suas funções são essenciais, e desempenham um papel crítico em células ativas replicantes, gerando mudanças na topologia do DNA e assim permitindo a replicação, transcrição, recombinação e remodelação da cromatina através da quebra temporária de uma ou duas fitas do DNA. As enzimas topoisomerase a tipo I e tipo II quebram e ligam as cadeias de DNA através da formação de ligação covalente entre a enzima e o DNA no local da quebra das hélices. Além disso, elas regulam o nível de enovelamento do DNA, tanto para facilitar a interação do DNA com proteínas, quanto para impedir o super enovelamento do DNA, que é deletério (CHAMPOUX, 2001). Se o equilíbrio é deslocado por um inibidor de topo, para estimular a clivagem ou inibir a ligação das fitas, o complexo de clivagem pode persistir no DNA, como se a enzima estivesse presa em um complexo terciário topo-fármaco-DNA (OPPEGARD, 2009).

A maioria dos derivados de acridina que atuam como fármacos anticâncer agem inibindo a enzima topo II, incluindo etoposida, amsacrina e doxorubicina (Figura 9).

Revisão da Literatura

Figura 9 - Inibidores de topo II



Fonte: Autora, 2012

Os atuais inibidores de topo II são classificados como inibidores de topo II ou venenos catalíticos de topo II, sendo a maioria dos inibidores atuais venenos catalíticos. Os venenos de topo II agem estabilizando o complexo clivável, resultando na formação de uma ligação covalente entre a enzima e o DNA, levando a quebra irreversível de filamentos do DNA. Os inibidores catalíticos agem em qualquer estágio do ciclo catalítico de sete etapas, sendo a associação enzima/DNA a primeira etapa (GOODEL et al., 2008).

Estudos anteriores indicaram que os venenos de topo II podem causar danos irreversíveis durante a fase S (quando os níveis de topo II α estão altos), levando a um acúmulo de células na fase G2 (LARSEN et al., 2003).

A citotoxicidade dos “venenos” de topo está associada com a inibição da replicação do DNA e geração de quebras das fitas do DNA, o que leva à geração de rearranjos cromossômicos (AZAROVA et al., 2007). Assim, inibidores de topo II são inerentemente citotóxicos e mutagênicos. Os inibidores de topo II humana agem tanto nas formas α e β (CORNAROTTI et al., 1996). No entanto, ambas as subformas são reguladas de modos diferentes. Os níveis da subforma α de topo II são maiores em tecidos em que se replicam rapidamente, como a medula óssea e o baço, em células de câncer de pulmão, linfomas e uma variedade de leucemias (CAPRANICO et al., 1992; GOODEL, 2008).

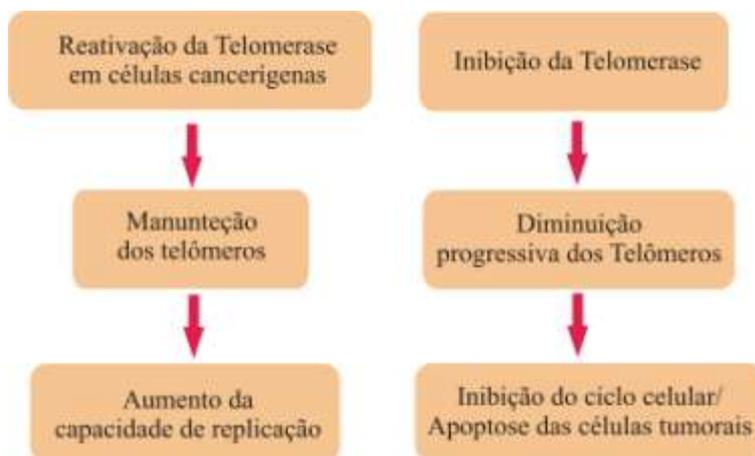
Revisão da Literatura

3.5.4 Enzima telomerase

Os telômeros consistem em repetições das bases TTAGGG que protegem as extremidades dos cromossomos prevenindo a degradação do DNA, fusão das extremidades, rearranjos e perda de cromossomos. Os telômeros perdem cerca de 50-200 pares de bases a cada divisão celular, resultado da incompleta replicação do DNA ou de outros eventos que ocorrem na última etapa da replicação. Entretanto, esta redução pode ser superada pela super expressão da enzima telomerase (SHAY, WRIGHT, 2002).

Os telômeros das células cancerosas apresentam um comportamento diferente, seu comprimento é extritamente regulado. Eles não diminuem de comprimento durante a replicação. As extremidades dos cromossomos são mantidas no decurso de sucessivas replicações do DNA. A explicação para essas observações veio em 1994, com a descoberta de uma enzima que alonga telômeros, ativada apenas por células neoplásicas (NEIDLE, PARKINSON, 2002). A enzima telomerase é uma enzima transcriptase reversa e um complexo ribonucleoprotéico que é ativa em 80-90% de todas as células tumorais humanas (Figura 9) (ZAMBRE, 2009).

Figura 10 - Reativação da telomerase e inibição de células cancerosas



Fonte: Adaptado de Gellert, 2005

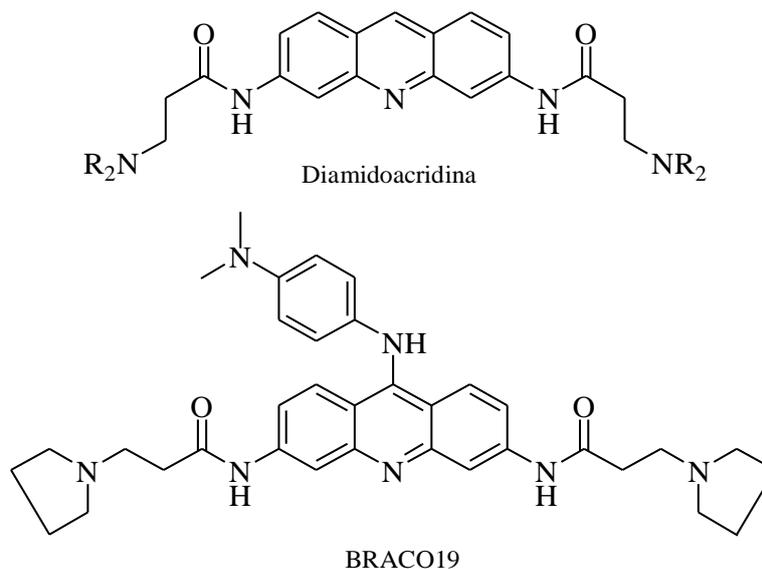
Essa atividade altamente seletiva sugere sua aplicação como marcador molecular para o diagnóstico de câncer, visto que em células somáticas normais não há atividade mensurável da telomerase. Os níveis de telomerase foram correlacionados com a

Revisão da Literatura

progressão e estados metastáticos de uma grande variedade de câncer, tais como câncer de próstata, câncer cervical, câncer de mama e gliomas (NEIDLE, PARKINSON, 2002).

A ativação da telomerase é o evento genético chave que conduz à imortalidade das células tumorais. Logo, as substâncias que agem inibindo esta enzima, como a diamidoacridina e a BRACO19 (Figura 11) são promissores fármacos anticâncer.

Figura 11 - Acridinas dissustituídas inibidoras de telomerase sintetizadas por HARRISON (1999) e FU (2009)



Fonte: Autora, 2012

3.5.5 Gene supressor tumoral p53

O p53 é um gene supressor tumoral, que codifica uma fosfoproteína nuclear que desempenha um papel importante no controle do ciclo celular, no reparo do DNA e na indução da apoptose. Em condições de stress, particularmente por indução de dano no DNA, a proteína p53 bloqueia o ciclo celular, permitindo dessa forma o reparo do DNA ou promovendo a apoptose. Estas funções são efetuadas pela capacidade transcricional da proteína p53 que ativa uma série de genes envolvidos na regulação do ciclo celular. A forma mutada da p53 é incapaz de controlar a proliferação celular, resultando em reparo ineficiente do DNA e na emergência de células geneticamente instáveis. As

Revisão da Literatura

alterações mais comuns nas neoplasias são mutações pontuais dentro das seqüências codificantes deste gene (CAVALCANTI JUNIOR et al., 2002).

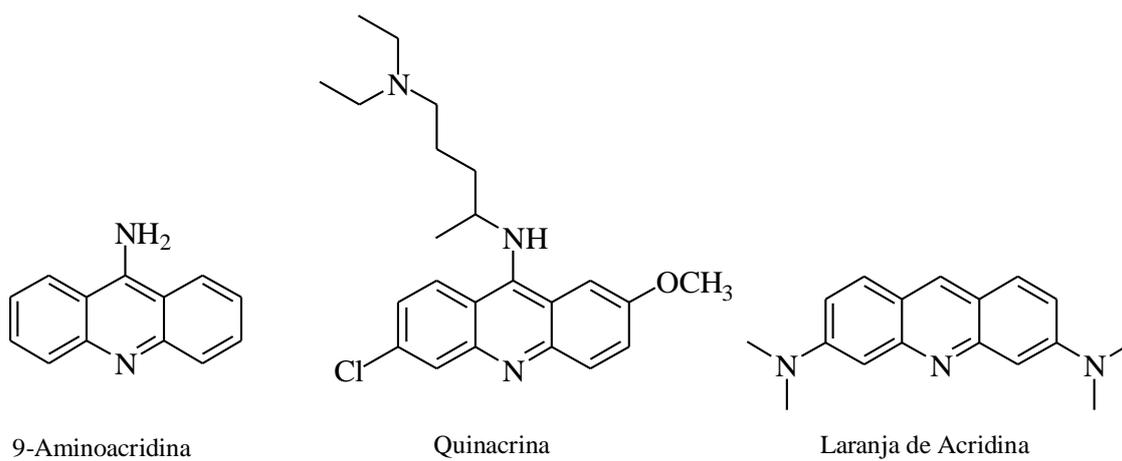
No caso de lesão no DNA por agentes físicos tais como radiação ultravioleta, raios gama ou ainda, por produtos químicos mutagênicos, o gene p53 é ativado, levando à transcrição da proteína p53. O acúmulo dessa proteína no núcleo da célula inibe o ciclo mitótico no início da fase G1 e ativa a transcrição de genes de reparo do DNA, impedindo desta forma a propagação do erro genético para as células filhas. No entanto, se o reparo do DNA não for efetuado de forma satisfatória, a proteína p53 dispara o mecanismo de morte celular programada denominada apoptose. A capacidade regulatória da transcrição de genes envolvidos na apoptose pode resultar na ativação do gene bax cujo produto de transcrição, a proteína bax, irá inibir a ação antiapoptótica do gene bcl-2 (CAVALCANTI JUNIOR et al., 2002).

A proteína supressora de tumor p53 tem um papel importante na tumorigênese e na terapia do câncer. Dados epidemiológicos indicaram que em mais da metade dos casos de câncer o gene da proteína p53 sofreu mutação. Na outra metade dos casos, apesar do gene p53 selvagem estar expresso, o bloqueio do ciclo celular ou o mecanismo de apoptose estão ineficazes devido à infecção por vírus, super expressão do Minuto Duplo Murino 2 (MDM 2, um protooncogene, que quando amplificado ou superexpresso, pode inativar funções da p53, iniciando e conduzindo à progressão tumoral), deficiência de “Frame” de Leitura Alternativo (ARF) ou Ataxia Telangiectasia Mutada (ATM, mutações no gene ATM produzem grande instabilidade cromossômica e impedem a expressão de p53). Na clínica, houve relação entre o estado funcional do p53 e o prognóstico, progressão e resposta terapêutica de tumores. Todas estas características fazem do p53 um importante alvo molecular para a supressão de tumores e o desenvolvimento de fármacos (WANG et al., 2005).

As acridinas ativam o gene p53. A 9-aminoacridina, amsacrina, quinacrina e laranja de acridina (Figura 12) induzem a atividade transcripcional do gene p53. Estes derivados estabilizam a proteína p53 através do bloqueio de sua ubiquitinação, não permitindo que haja fosforilação da ser15 e da ser20 do p53. Além disso, as acridinas induzem a morte celular por um caminho dependente da proteína p53 (WANG et al., 2005).

Revisão da Literatura

Figura 12 - Indutores da atividade transcripcional do gene p53



Fonte: Autora, 2012



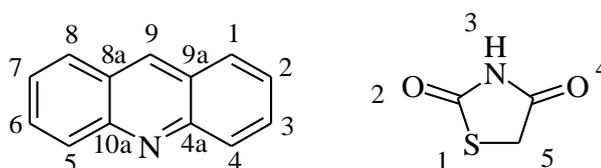
4 Obtenção de Derivados Tiazacridínicos

Diversas substâncias sintéticas são obtidas a partir de derivações de anéis heterocíclicos, dentre as quais, destaca-se a acridina (Figura 13) devido à sua potencialidade como protótipo para o desenvolvimento de novos fármacos. A reatividade de acridinas foi revisada por Albert (1966), Acheson (1973) e Chiron (2004).

O nitrogênio do anel central da acridina é a posição mais nucleofílica da molécula, o que facilita as reações de *N*-alquilação. A *N*-alquilação mais descrita é a *N*-metilação, que pode ser realizada por vários agentes metilantes, como iodeto de metila e dimetilsulfato, resultando nos sais *N*-metilados correspondentes. Outros derivados halogenoalquilados também alquilam os derivados de acridina em seu nitrogênio. Além disso, a acridina é uma base fraca (pKa 5,74 à 25 °C) podendo ser facilmente protonada resultando no sal acridinium em meio extremamente ácido (CHIRON, 2004).

Skonieczny, em 1977, observou que a posição 9 da acridina é particularmente eletrofílica devido à presença do nitrogênio na posição *para* do anel central. Dessa forma, agentes nucleofílicos reagem facilmente nesta posição, conduzindo à formação da acridana ou à rearomatização da acridina dependendo da estabilidade da acridana e das condições experimentais

Figura 13 - Acridina e tiazolidina



Fonte: Autora, 2012

Obtenção de derivados tiazacridínicos

A tiazolidina 2,4-diona se comporta de forma característica na presença de determinados reagentes. O nitrogênio do anel tiazolidínico (Figura 13) age como um ácido fraco em meio básico, e isto facilita a ocorrência de reações de *N*-alquilação com cloretos ou brometos de alquila. Além disso, a tiazolidina também pode reagir na posição 5 com ésteres de Cope substituídos em reação de adição de Michael.

As metodologias de síntese da tiazolina-2,4-diona, de ésteres de Cope, da tiazolina-2,4-diona *N*-alquilada e de tiazacridinas encontram-se descritas na seção 4.2.

4.1 Material

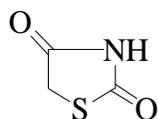
A cromatografia em camada delgada foi realizada em placas Merck silicagel 60 F254, de 0,25 mm de espessura, reveladas em luz ultravioleta (254 ou 366 nm) e a cromatografia “flash” (sob pressão) em sílica gel 60 Merck (230-400 Mesh). Todos os reagentes e solventes que foram utilizados na síntese dos compostos e para suas análises pertencem as marcas Sigma/Aldrich, Acros, Merck, Vetec ou Quimis.

Os reagentes, solventes e intermediários utilizados para a realização das etapas de síntese foram: morfolina, tiouréia, ácido monocloroacético, água destilada, hidróxido de sódio, álcool etílico, 9-bromo-metil-acridina, 2-ciano-3-(2-metoxi-5-bromo-fenil)-acrilato de etila (LPSF IP-23), 2-ciano-3-(4-fenil-fenil)-acrilato de etila (LPSF IP-48), 2-ciano-3-(3,5-dimetoxi-fenil)-acrilato de etila (LPSF IP-67), 2-ciano-3-(2,3-dicloro-fenil)-acrilato de etila (LPSF IP-64), 2-ciano-3-(3-bromo-fenil)-acrilato de etila (LPSF IP-25), 2-ciano-3-(indol-3il-fenil)-acrilato de etila (LPSF IP-19), 2-ciano-3-(3-flúor-fenil)-acrilato de etila (LPSF IP-24), 2-ciano-3-(3,4,5-trimetoxi-fenil)-acrilato de etila (LPSF IP-26), 2-ciano-3-(3,4-dicloro-fenil)-acrilato de etila (LPSF IP-27), 2-ciano-3-(2,4-dicloro-fenil)-acrilato de etila (LPSF IP-28), 2-ciano-3-(2-cloro-5-nitro-fenil)-acrilato de etila (LPSF IP-66), 2-ciano-3-(4-benziloxi-fenil)-acrilato de etila (LPSF IP-20), 2-ciano-3-(4-nitro-fenil)-acrilato de etila (LPSF IP-13), 2-ciano-3-(fluoreno-2il-fenil)-acrilato de etila (LPSF IP-54), 2-ciano-3-(3-cloro-fenil)-acrilato de etila (LPSF IP-10), 2-ciano-3-(4-hidroxi-fenil)-acrilato de etila (LPSF IP-11).

Obtenção de derivados tiazacridínicos

4.2 Metodologias de síntese

4.2.1 Tiazolidina-2,4-diona



Em balão de fundo redondo foram adicionadas quantidades equimolares de tiouréia e ácido monocloroacético, previamente dissolvidos em 16 mL de água destilada. A mistura reacional foi aquecida e mantida sob refluxo a uma temperatura de 80°C por 18 horas e, em seguida, mantida sob refrigeração durante 24h. Os cristais formados foram isolados por filtração e purificados através de lavagens sucessivas com água destilada.

4.2.2 Ésteres de Cope (LPSF IPs)

Tabela 7 - Ésteres de Cope sintetizados

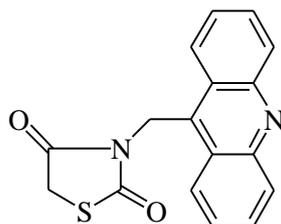
	R	Código LPSF	R	Código LPSF
	5-Br,2-OCH ₃	AA-10	3,4-Cl	AA-18
	4-bifenil	AA-11	2,4-Cl	AA-19
	3,5-OCH ₃	AA-12	2-Cl,5-NO ₂	AA-20
	2,3-Cl	AA-13	4-OCH ₂ C ₆ H ₅	AA-22
	3-Br	AA-14	4-NO ₂	AA-23
	1H-indol-3-ilmetileno	AA-15	9H-fluoren-3ilmetileno	AA-26
	4-F	AA-16	3-Cl	AA-30
	3,4,5-OCH ₃	AA-17	4-OH	AA-31

Fonte: Autora, 2012

Em balão de fundo redondo foram adicionadas quantidades equimolares de aldeído aromático substituído e de cianoacetato de etila na presença de morfolina como catalisador e benzeno como solvente. A mistura reacional foi aquecida e mantida sob refluxo a uma temperatura de 110°C por 4 horas. Passado esse tempo, o produto precipitado foi lavado com água destilada, filtrado e purificado por cristalização com álcool etílico.

Obtenção de derivados tiazacridínicos

4.2.3 3-Acridin-9-il-metil-tiazolidina-2,4-diona (LPSF AA-1A)



Em balão de fundo redondo foram adicionadas a tiazolidina-2,4-diona e hidróxido de sódio previamente dissolvido em álcool etílico. A mistura reacional foi agitada durante 10 minutos. Passado esse tempo, foi adicionado a 9-bromo-metil-acridina em quantidades equimolares e a mistura foi aquecida e mantida sob refluxo a uma temperatura de 60°C durante 7 horas. O produto foi lavado com água destilada e, depois, purificado com álcool etílico.

4.2.4 Derivados tiazacridínicos (LPSF AAs)

Tabela 8 - Tiazacridinas sintetizadas

	R	Código LPSF	R	Código LPSF
	5-Br,2-OCH ₃	AA-10	3,4-Cl	AA-18
	4-bifenil	AA-11	2,4-Cl	AA-19
	3,5-OCH ₃	AA-12	2-Cl,5-NO ₂	AA-20
	2,3-Cl	AA-13	4-OCH ₂ C ₆ H ₅	AA-22
	3-Br	AA-14	4-NO ₂	AA-23
	1H-indol-3-ilmetileno	AA-15	9H-fluoren-3ilmetileno	AA-26
	4-F	AA-16	3-Cl	AA-30
	3,4,5-OCH ₃	AA-17	4-OH	AA-31

Fonte: Autora, 2012

Em balão de fundo redondo foram adicionadas quantidades equimolares de 3-acridin-9-il-metil-tiazolidina-2,4-diona (LPSF AA-1A) e de derivados 2-ciano-3-fenil-acrilatos de etila (série LPSF IP) substituídos previamente dissolvidos em álcool etílico, na presença de morfolina como catalisador. A mistura reacional foi aquecida e mantida sob refluxo a 50°C por 4 horas levando à formação dos novos derivados tiazacridínicos. A purificação ocorreu através de sucessivas lavagens com água destilada e, posteriormente, álcool etílico.

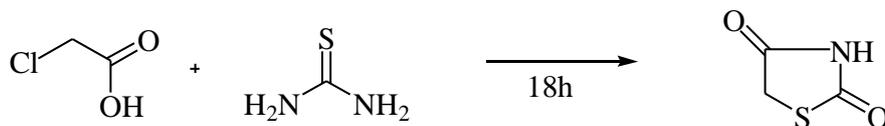
Obtenção de derivados tiazacridínicos

4.3 Rotas de síntese

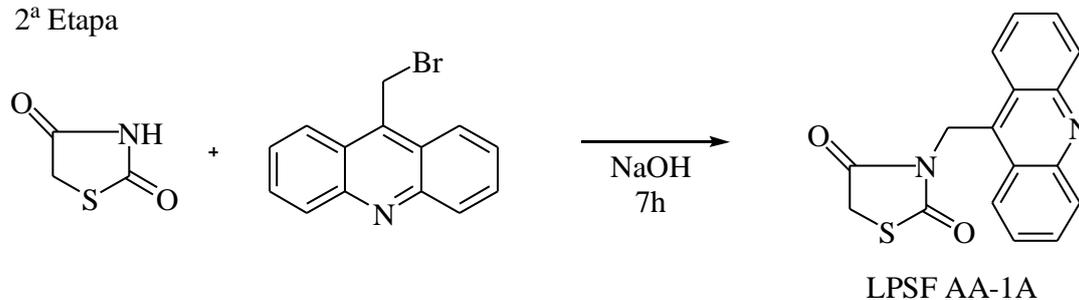
Os derivados tiazacridínicos foram obtidos através de 4 etapas reacionais. A primeira reação consistiu em uma reação de ciclização partindo da tiouréia com o ácido monocloroacético para a obtenção do anel da tiazolidina-2,4-diona. Na segunda etapa, a tiazolidina-2,4-diona foi N-alkilada na presença de 9-bromo-metil-acridina dando origem ao intermediário 3-acridin-9-il-metil-tiazolidina-2,4-diono (LPSF AA-1A). Na terceira etapa houve a formação do éster cianoacetato de etila, que na etapa final reage para formar os compostos finais através de uma reação de adição de Michael (Esquema 3) (PCT/BR2012/000421).

Esquema 3 - Rota geral de síntese de tiazacridinas

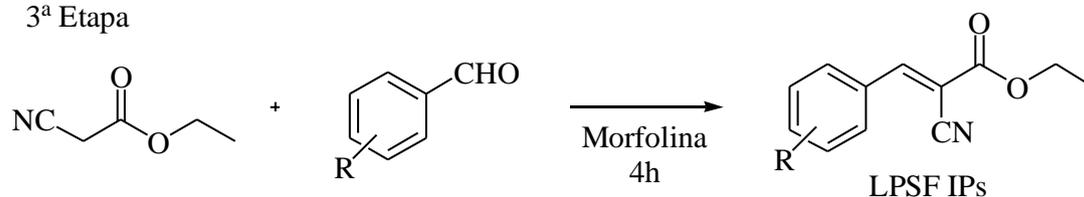
1ª Etapa



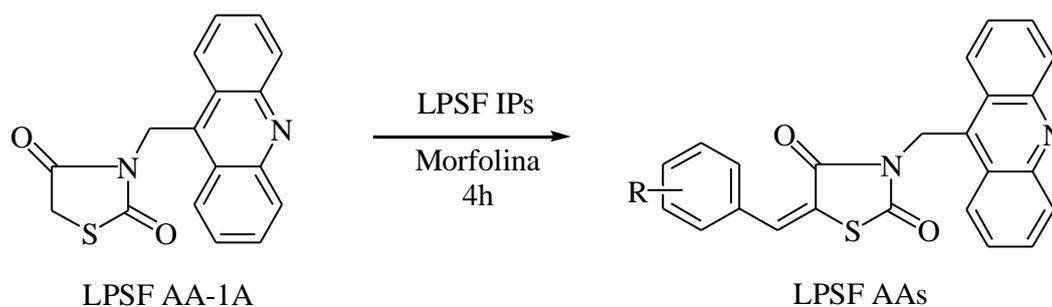
2ª Etapa



3ª Etapa



Etapa Final



Fonte: Autora, 2012

R	Código LPSF	R	Código LPSF
5-Br,2-OCH ₃	AA-10	3,4-Cl	AA-18
4-bifenil	AA-11	2,4-Cl	AA-19
3,5-OCH ₃	AA-12	2-Cl,5-NO ₂	AA-20
2,3-Cl	AA-13	4-OCH ₂ C ₆ H ₅	AA-22
3-Br	AA-14	4-NO ₂	AA-23
1H-indol-3-ilmetileno	AA-15	9H-fluoren-3ilmetileno	AA-26
4-F	AA-16	3-Cl	AA-30
3,4,5-OCH ₃	AA-17	4-OH	AA-31

Fonte: Autora, 2012

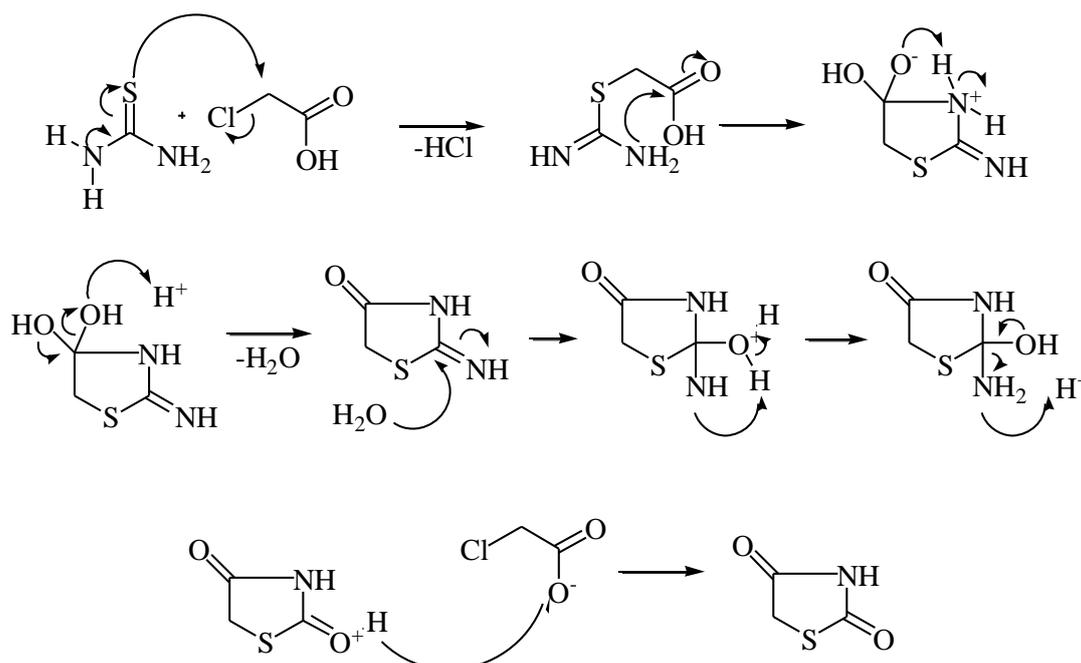
Obtenção de derivados tiazacridínicos

Novos Agentes Tiazacridínicos com Propriedades Anticâncer
Marina G R Pitta

4.4 Mecanismos reacionais

O núcleo tiazolidínico foi obtido através da reação da tiouréia com o ácido α -cloroacético em meio ácido (LIBERMANN, 1948). No Esquema 4 detalhamos o hipotético mecanismo da reação de ciclização anteriormente descrita.

Esquema 4 - Mecanismo da reação hipotético de ciclização para obtenção de tiazolidina-2,4-diona



Fonte: Autora, 2012

A reação se inicia quando o átomo de enxofre da tiouréia ataca o carbono α do ácido monocloroacético, liberando um próton e o ânion cloreto, através de uma reação de substituição nucleofílica de segunda ordem (S_N2). Em seguida, o par de elétrons livre do nitrogênio da amina primária ataca o carbono parcialmente positivo da carbonila (ataque intramolecular) levando a ciclização do anel, que para se estabilizar, transfere o próton do nitrogênio carregado positivamente para o oxigênio com carga negativa, formando uma hidroxila. O meio ácido facilita que o oxigênio da hidroxila seja protonado levando a perda de uma molécula de água e a formação de uma carbonila na posição 4. A posição 2 tiazolidina reage com uma molécula de água e através de um

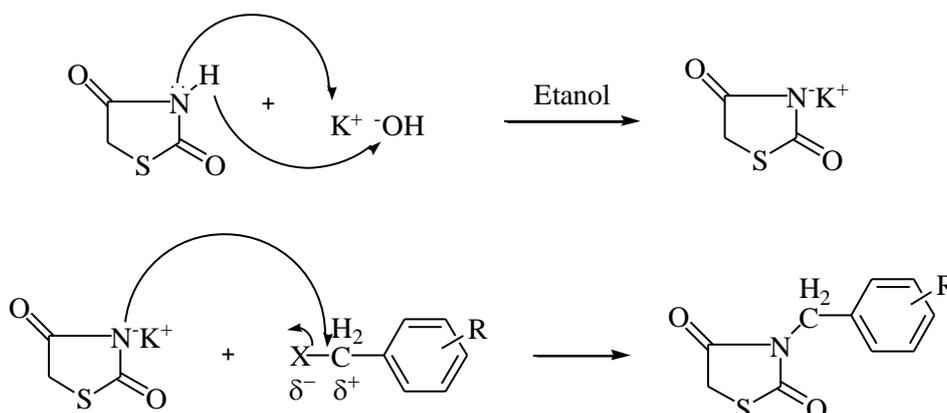
Obtenção de derivados tiazacridínicos

rearranjo molecular uma molécula de amônia é liberada. A formação da tiazolidina-2,4-diona se dá quando a base $\text{ClCH}_2\text{COO}^-$ desprotona o oxigênio positivo da posição 2.

A tiazolidina-2,4-diona comporta-se como um ácido fraco quando não apresenta substituições no átomo de nitrogênio e reage com haletos de alquila, substituídos ou não, em soluções alcalinas conduzindo à formação de sais.

As reações de *N*-alquilação ocorrem através de SN_2 , onde o hidrogênio ligado ao átomo de nitrogênio é suficientemente ácido para ser suprimido por ação de uma base, conduzindo à formação de um sal. O sal obtido atua como um agente nucleofílico atacando o haleto de alquila para formar a tiazolidina-2,4-diona substituída em posição 3 (Esquema 5).

Esquema 5 - Mecanismo reacional hipotético de *N*-alquilação da tiazolidina-2,4-diona



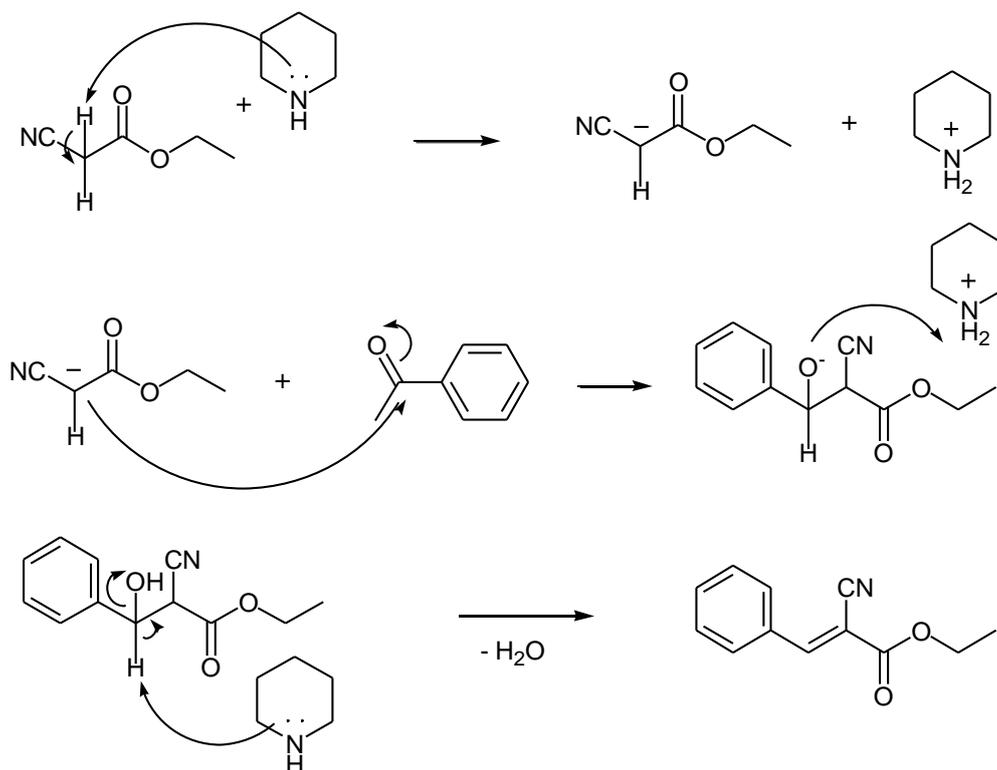
Fonte: Autora, 2012

Derivados de aldeídos aromáticos, tais como os ésteres de Cope, são obtidos através da reação de condensação do tipo Knoevenagel entre aldeídos aromáticos substituídos e cianoacetato de etila, em presença de uma base, normalmente a morfolina. O éster cianocinâmico atua como um intermediário para as reações de adição de Michael em posição 5 da tiazolidina-2,4-diona *N*-alquilada (Esquema 6).

No Esquema 7 encontra-se o hipotético mecanismo da reação de adição de Michael para obtenção de derivados tiazolidínicos utilizando-se morfolina como catalizador.

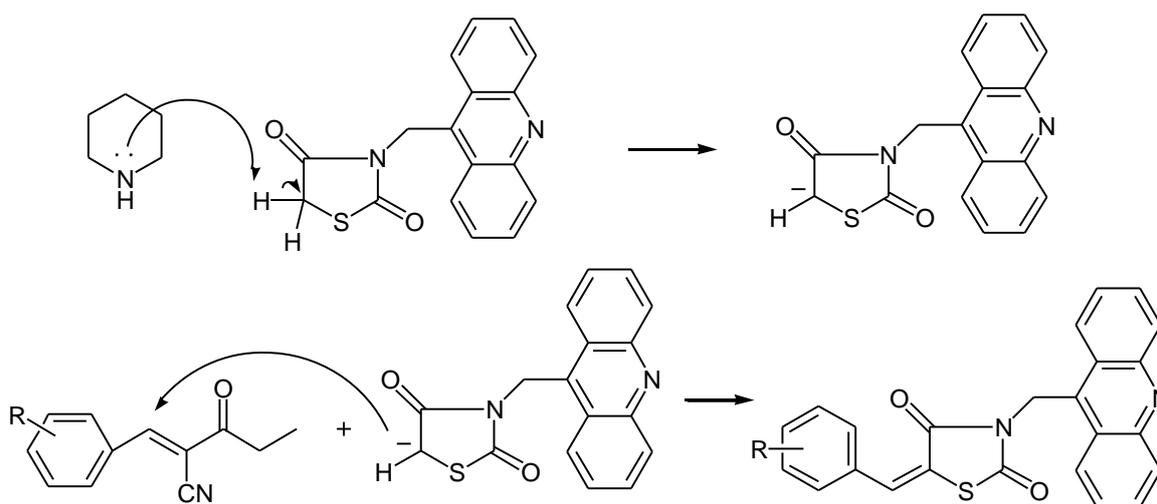
Obtenção de derivados tiazacridínicos

Esquema 6 - Mecanismo da reação hipotético de condensação de Knoevenagel para obtenção dos intermediários LPSF IPs



Fonte: Autora, 2012

Esquema 7 - Mecanismo da reação hipotético de adição de Michael para obtenção de derivados tiazacridínicos



Fonte: Autora, 2012

Obtenção de derivados tiazacridínicos

Novos Agentes Tiazacridínicos com Propriedades Anticâncer
Marina G R Pitta

O grupo metilênico da posição 5 da tiazolidina-2,4-diona apresenta uma reatividade característica frente a vários reagentes. Este carbono metilênico comporta-se como um nucleófilo, e as reações ocorrem normalmente em presença de uma base, onde a tiazolidina-2,4-diona comporta-se como um ânion. A formação do ânion da tiazolidina é facilitada pela presença dos grupamentos carbonílicos nas posições 2 e 4, que através da ressonância deixa o intermediário mais estável.

A formação da dupla exocíclica no núcleo tiazolidinônico a partir do éster de Cope ocorre através da seguinte forma: observa-se a formação de um carbânion na posição 5 da tiazolidina-2,4-diona *N*-alquilada e subsequente ataque ao carbono α do éster cianocinâmico através de uma reação de adição de Michael, conduzindo aos novos derivados tiazacridínicos substituídos.

4.5 Características físico-químicas & identificação estrutural

As características físico-químicas da tiazolidina-2,4-diona e dos derivados tiazacridínicos sintetizados no LPSF encontram-se listados na Tabela 9.

Tabela 9 - Características físico-químicas de tiazacridinas sintetizadas no LPSF

Produto	F.M.	P.M.	Rdt. (%)	P.F. (°C)	Rf
Tiazolidina	C ₃ H ₃ NO ₂ S	117,00	84,0	121-122	0,51 (Triclorometano/MeOH 96:4)
LPSFAA-1A	C ₁₇ H ₁₂ N ₂ O ₂ S	308,06	51,0	196-197	0,24 (<i>n</i> -Hexano/AcOEt 7:3)
LPSF AA-10	C ₂₅ H ₁₇ BrN ₂ O ₃ S	504,01	68,3	120	0,63 (<i>n</i> -Hexano/AcOEt 7:3)
LPSF AA-11	C ₃₀ H ₂₀ N ₂ O ₂ S	472,12	78,0	240	0,48 (<i>n</i> -Hexano/AcOEt 7:3)
LPSF AA-12	C ₂₆ H ₂₀ N ₂ O ₄ S	456,11	34,0	188-89	0,70 (<i>n</i> -Hexano/AcOEt 7:3)
LPSF AA-13	C ₂₄ H ₁₄ Cl ₂ N ₂ O ₂ S	464,02	85,4	213	0,53 (<i>n</i> -Hexano/AcOEt 7:3)
LPSF AA-14	C ₂₄ H ₁₅ BrN ₂ O ₂ S	474,00	52,0	214-15	0,40 (<i>n</i> -Hexano/AcOEt 7:3)
LPSF AA-15	C ₂₆ H ₁₇ N ₃ O ₂ S	435,10	14,6	270	0,34 (<i>n</i> -Hexano/AcOEt 7:3)
LPSF AA-16	C ₂₄ H ₁₅ FN ₂ O ₂ S	414,08	74,0	245	0,56 (<i>n</i> -Hexano/AcOEt 7:3)
LPSF AA-17	C ₂₇ H ₂₂ N ₂ O ₅ S	486,12	76,0	220	0,46 (<i>n</i> -Hexano/AcOEt 7:3)
LPSF AA-18	C ₂₄ H ₁₄ Cl ₂ N ₂ O ₂ S	464,02	50,0	210	0,47 (<i>n</i> -Hexano/AcOEt 7:3)
LPSF AA-19	C ₂₄ H ₁₄ Cl ₂ N ₂ O ₂ S	464,02	50,0	246-48	0,59 (<i>n</i> -Hexano/AcOEt 7:3)
LPSF AA-20	C ₂₄ H ₁₄ ClN ₃ O ₄ S	475,04	49,0	218-20	0,45 (<i>n</i> -Hexano/AcOEt 7:3)
LPSF AA-22	C ₃₁ H ₂₂ N ₂ O ₃ S	502,14	20,3	221-23	0,60 (<i>n</i> -Hexano/AcOEt 7:3)
LPSF AA-23	C ₂₄ H ₁₅ N ₃ O ₄ S	441,08	41,0	255	0,67 (<i>n</i> -Hexano/AcOEt 7:3)
LPSF AA-26	C ₃₁ H ₂₀ N ₂ O ₂ S	484,12	63,8	247-50	0,67 (<i>n</i> -Hexano/AcOEt 7:3)
LPSF AA-30	C ₂₄ H ₁₅ ClN ₂ O ₂ S	430,05	50,0	210-13	0,68 (<i>n</i> -Hexano/AcOEt 7:3)
LPSF AA-31	C ₂₄ H ₁₆ N ₂ O ₃ S	412,09	36,6	270	0,2 (<i>n</i> -Hexano/AcOEt 7:3)

Fonte: Autora, 2012

Obtenção de derivados tiazacridínicos

Os compostos sintetizados tiveram suas estruturas comprovadas através da técnica espectroscópica de ressonância magnética nuclear de hidrogênio (NMR^1H) e espectrofotometria de absorção no IR.

- Espectrometria de NMR^1H : espectrômetro Varian Modelo Plus 300 MHz e 400 MHz. O solvente utilizado para análise foi o DMSO à temperatura ambiente. Os principais picos de absorção encontrados nos espectros foram oriundos de hidrogênios de alcanos, alcenos e de anéis aromáticos.
- Espectrofotometria de Absorção no Infravermelho: aparelho FTIR Bruker Modelo IFS 66. Para análise, foram utilizadas pastilhas de KBr a 1%. As principais bandas observadas foram: C=O, C=C, C-N e C-H de aromáticos.

4.5.1 Ressonância magnética nuclear de hidrogênio

Para a realização da espectrometria de NMR^1H o composto de referência utilizado foi o tetrametil-silano (TMS). Este padrão tem a vantagem de ser quimicamente inerte, simétrico, volátil (ponto de ebulição 27°C) e solúvel na maior parte dos solventes orgânicos. O composto possui um único sinal de absorção, agudo e intenso, e seus hidrogênios são mais “blindados” do que quase todos os hidrogênios dos compostos orgânicos. O pico de TMS é colocado no extremo direito do espectro e corresponde a zero na escala em Hz ou δ (SILVERSTEIN, 2010).

No espectro, valores positivos em Hz ou δ aumentam para a esquerda, valores negativo aumentam para a direita. O termo “blindado” significa para a direita, e o termo “desblindado” significa para a esquerda da escala. Isso significa que os hidrogênios fortemente desblindados do dimetil-éter, por exemplo, estão mais expostos do que os do TMS em relação ao campo aplicado, e a ressonância ocorre em frequência mais alta, isto é, à esquerda, da ressonância dos hidrogênios de TMS. Assim, tanto a escala em Hz como a escala em δ refletem o aumento da frequência aplicada, em campo constante, para a esquerda e a diminuição da frequência aplicada para a direita da frequência de ressonância do TMS (SILVERSTEIN, 2010).

Os deslocamentos químicos foram reportados em ppm; as constantes de acoplamento foram indicadas em Hz e as multiplicidades dos sinais foram designadas

Obtenção de derivados tiazacridínicos

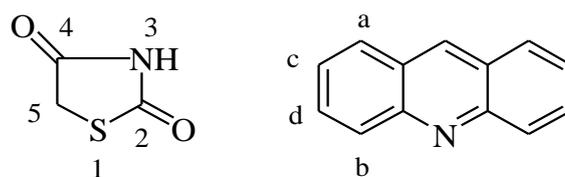
da seguinte forma: s - singlete, d - dubleto, dd - duplo dubleto, t - tripleto, m - multiplete.

O singlete do grupo CH₂ ligado ao átomo de Nitrogênio da tiazolidina foi detectado no espectro em 5,7 ppm no intermediário LPSF AA-1A e na faixa de 5,9 ppm para os produtos finais LPSF AAs.

No espectro do LPSF AA-1A, pudemos observar um singlete na faixa de 4,2 ppm com 2 hidrogênios representando os hidrogênios da posição 5 do anel da tiazolidina. Este singlete não apareceu em nenhum dos espectros dos compostos finais, o que comprovou que a última etapa reacional (adição de Michael) aconteceu.

Alguns picos foram característicos de todos os espectros de NMR¹H, como os hidrogênios aromáticos e os hidrogênios do anel benzilideno. Com relação ao anel acridínico, os hidrogênios da posição c (tripleto de 2H na faixa de 7,6 - 7,7 ppm) são os mais blindados. Em campo mais baixo, na sequência, encontramos os H¹ da posição “d”, “a” e “b” (Figura 14). Os H¹ da posição b (dubleto de 2H na faixa de 8,5 - 8,4 ppm) foram encontrados em campo mais alto provavelmente devido à proximidade do nitrogênio do anel central da acridina. Os hidrogênios da posição “a” (dubleto de 2H na faixa de 8,1- 8,2 ppm) também estão mais desprotegidos que os H¹ da posição “c” e , e este fato pode ser explicado pela presença da carbonila que se aproxima do H¹ graças a livre rotação da ligação entre o anel da tiazolidina e da acridina.

Figura 14 - Núcleos da tiazolidina-2,4-diona e da acridina



Fonte: Autora, 2012

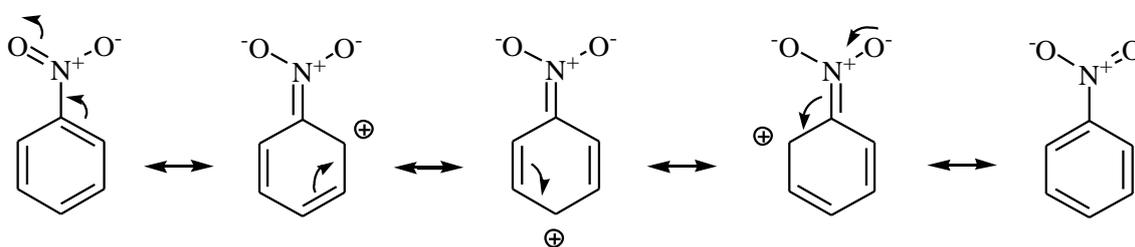
Nos produtos finais (LPSFAA-10 o LPSF AA-31) um singlete de intensidade moderada foi encontrado na região dos H¹ acridínicos, na faixa de 7,9-7,8 ppm representando o hidrogênio vinílico –HC=. Alguns picos também foram encontrados provenientes de substituições no anel benzílico, como os H¹ do grupo metoxila (singlete de 3H na faixa de 4,0 - 3,7 ppm), metila (singlete de 3H na faixa de 2,34 ppm) e metanosulfonila (singlete de 3H na faixa de 3,25 ppm).

Obtenção de derivados tiazacridínicos

Os prótons do anel benzílico não foram detectados em faixas específicas por causa da influência das diferentes substituições no anel, variando de 8,0 a 6,3 ppm.

No composto LPSF AA-20, os H^1 do anel benzílico foram encontrados em campo mais baixo do que o habitual. Isso pode ser explicado pela presença dos substituintes Cloro e Nitro no anel benzílico. O Cl e o NO_2 são substituintes que exercem um efeito indutivo negativo (I) forte. O grupo nitro, por sua vez, é um grupo desativante forte, pois além do efeito I, ele é um sacador de elétrons via ressonância (Esquema 8).

Esquema 8 - Possíveis estruturas do nitro-benzeno



Fonte: Adaptado de McMURRY, 2006

4.5.2 Espectrofotometria de absorção no infravermelho

As duas regiões mais importantes para o exame preliminar dos espectros de IV são as regiões de 4000 a 1300 cm^{-1} e de 900 a 650 cm^{-1} . A região de mais alta frequência é chamada região dos grupos funcionais. Nessa região, ocorrem as absorções que correspondem aos grupos funcionais mais importantes, como O-H, N-H e C=O (SILVERSTEIN, 2010).

A maioria das bandas de absorção características no IR não muda de um composto para outro, por exemplo, a absorção C=C de um alceno está sempre na faixa de 1640 a 1680 cm^{-1} . A presença da carbonila é evidenciada na região de 1850 a 1540 cm^{-1} . As aminas secundárias (Ex. LPSF AA-15) mostram uma única banda, fraca, entre 3350 cm^{-1} e 3310 cm^{-1} . Bandas fortes características de do esqueleto aromático e de heteroaromáticos aparecem na região de 1600 a 1300 cm^{-1} (SILVERSTEIN, 2010).

As bandas dos anéis aromáticos são encontradas na região de 900 a 650 cm^{-1} . Nessa região, os compostos aromáticos e heteroaromáticos produzem bandas intensas,

Obtenção de derivados tiazacridínicos

originadas nas deformações angulares fora do plano de C-H e dos anéis, que podem ser correlacionadas com o modo de substituição do anel aromático (SILVERSTEIN, 2010).

No espectro de IR dos produtos finais LPSF AAs, encontramos bandas representativas do estiramento C=C, o que comprovou a reação de adição de Michael entre o intermediário LPSF AA-1A e os ésteres de Cope.

A Tabela 10 lista as bandas de IR características dos principais grupos funcionais encontrados nos espectros deste trabalho.

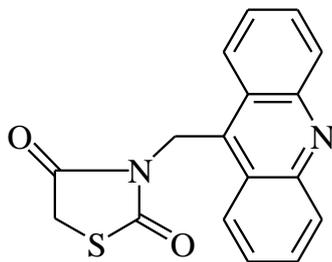
Tabela 10 - Absorções características no IR de alguns grupos funcionais característicos das tiazacridinas

Classe dos grupos funcionais	Posição da banda (cm ⁻¹)	Intensidade de absorção
Alcanos, grupos alquila C-H	2850 – 2960	Médio a forte
Alcenos =C-H C=C	3020 – 3100 1640 – 1680	Médio Médio
Haleto de alquila C-Cl C-Br	600 – 800 500 – 600	Forte Forte
Aromáticos C-H -C=C-	3030 1660 – 2000 1450 – 1600	Fraco Fraco Médio
Compostos carbonílicos C=O	1540 – 1850	Forte

Fontes: McMURRY, 2006; SILVERSTEIN, 2010

Obtenção de derivados tiazacridínicos

4.5.3 3-Acridin-9-il-metil-tiazolidina-2,4-diona (LPSF AA-1A)

FM: C₁₇H₁₂N₂O₂S

PM: 308,06

PF: 196-7°C

Rdt: 51,0%

Rf: 0,24 (*n*-Hexano/AcOEt 7:3)

Cor: Amarela

NMR¹H

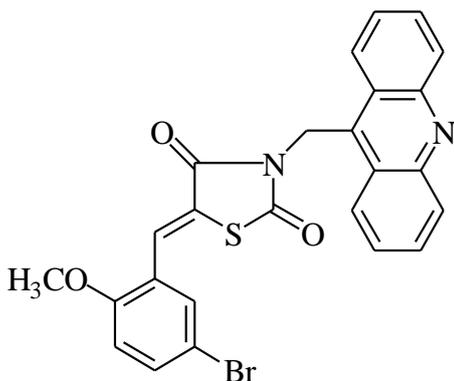
NMR¹H (400 MHz, DMSO-d₆): δ 4,22 (s, 2H, -CH₂-S) (f), 5,75 (s, 2H, -CH₂) (e), 7,67 (t, 2H, J=19,6 Hz, j=9,2 Hz, AcrH) (c), 7,85 (t, 2H, J=19,6 Hz, j=9,2 Hz, AcrH) (d), 8,17 (d, 2H, J=8,4 Hz, AcrH) (a), 8,42 (d, 2H, J=8,7 Hz, AcrH) (b).

IR

IR (KBr, cm⁻¹) 2889, 1750, 1694, 750.

Obtenção de derivados tiazacridínicos

4.5.4 3-Acridin-9-ilmetil-5-(5-bromo-2-metoxi-benzilideno)-tiazolidina-2,4-diona
(LPSF AA-10)



FM: C₂₅H₁₇BrN₂O₃S

PM: 504,01

PF: 120°C

Rdt: 68,3%

Rf: 0,63 (*n*-Hexano/AcOEt 7:3)

Cor: Amarela

NMR¹H (400 MHz, δ ppm, DMSO-d₆)

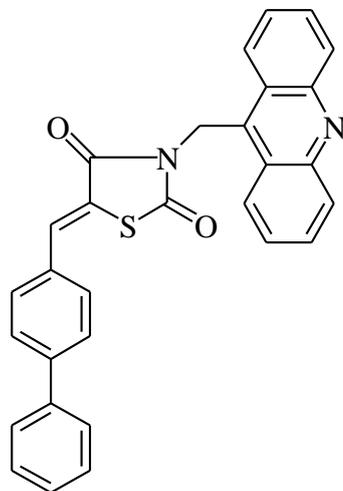
NMR¹H (400 MHz, DMSO-d₆): δ 3,85 (s, 3H, -OCH₃) (j), 5,90 (s, 2H, -CH₂) (e), 7,09 (d, 1H, J=8,4 Hz, ArH) (h), 7,46 (d, 1H, J=2,4 Hz, ArH) (g), 7,61 (dd, 1H, J=9,2 Hz, j=2,4 Hz, ArH) (i), 7,68 (t, 2H, J=15,2 Hz, j=8,0 Hz, AcrH) (c), 7,85 (t, 2H, J=15,2 Hz e j=8,0 Hz, AcrH) (d), 7,89 (s, 1H, =CH) (f), 8,18 (d, 2H, J=8,4 Hz, AcrH) (a), 8,45 (d, 2H, J=8,8 Hz, AcrH) (b).

IR

IR (KBr, cm⁻¹): 1744, 1689, 1599, 1480, 1375, 1312, 1258, 1149, 751, 494.

Obtenção de derivados tiazacridínicos

4.5.5 3-Acridin-9-ilmetil-5-bifenil-4-ilmetileno-tiazolidina-2,4-diona (LPSF AA-11)

FM: C₃₀H₂₀N₂O₂S

PM: 472,12

PF: 240°C

Rdt: 78,0%

Rf: 0,48 (n-Hexano/AcOEt 7:3)

Cor: Bege claro

NMR¹H (400 MHz, δ ppm, DMSO-d₆)

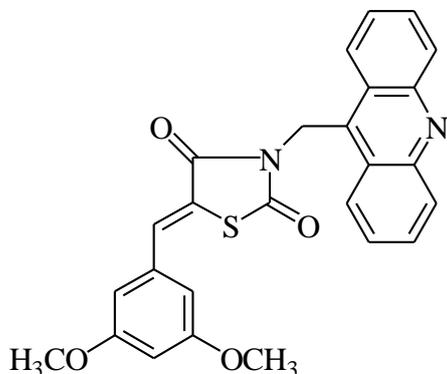
NMR¹H (400 MHz, DMSO-d₆): δ 5,95 (s, 2H, -CH₂) (e), 7,92-7,47 (m, 13H, ArH, AcrH) (d,c,g,h,i,j,k), 7,97 (s,1H, =CH₂) (f), 8,18 (d, 2H, AcrH) (a), 8,45 (d, 2H, J=16 Hz, AcrH) (b).

IR

IR (KBr, cm⁻¹): 1739, 1682, 1593, 1382, 1327, 1149, 1079, 755, 504.

Obtenção de derivados tiazacridínicos

4.5.6 3-Acridin-9-ilmetil-5-(3,5-dimetoxi-benzilideno)-tiazolidina-2,4-diona (LPSF AA-12)



FM: C₂₆H₂₀N₂O₄S

PM: 456,11

PF: 188-89°C

Rdt: 34,0%

Rf: 0,70 (*n*-Hexano/AcOEt 7:3)

Cor: Bege

NMR¹H (400 MHz, δ ppm, DMSO-d₆)

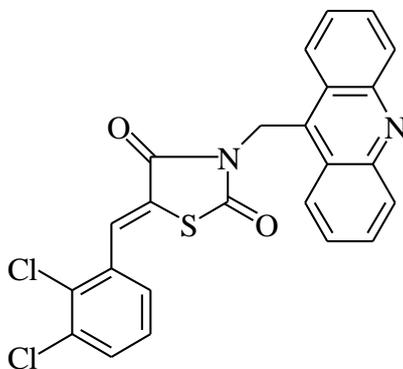
NMR¹H (400 MHz, DMSO-d₆): δ 3,77 (s, 6H, -CH₃) (i), 5,92 (s, 2H, -CH₂) (e), 6,62 (s, 1H, ArH) (h), 6,70 (s, 1H, ArH) (g), 7,68 (t, 2H, J=16,8 Hz, j=8,0 Hz, AcrH) (c), 7,87-7,83 (m, 3H, =CH, AcrH) (d,f), 8,18 (d, 2H, J=8,8 Hz, AcrH) (a), 8,46 (d, 2H, J=8,8 Hz, AcrH) (b).

IR

IR (KBr, cm⁻¹): 1738, 1685, 1606, 1579, 1372, 1300, 754, 497.

Obtenção de derivados tiazacridínicos

4.5.7 3-Acridin-9-ilmetil-5-(2,3-dicloro-benzilideno)-tiazolidina-2,4-diona (LPSF AA-13)



FM: C₂₄H₁₄Cl₂N₂O₂S

PM: 464,02

PF: 213°C

Rdt: 85,4%

Rf: 0,53 (*n*-Hexano/AcOEt 7:3)

Cor: Marrom

NMR¹H (400 MHz, δ ppm, DMSO-d₆)

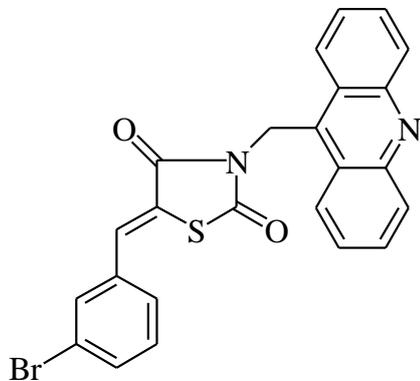
NMR¹H (400 MHz, DMSO-d₆): δ 5,92 (s, 2H, -CH₂) (e), 7,52-7,47 (m, 2H, ArH) (g,h), 7,74-7,67 (m, 3H, AcrH e ArH) (c,i), 7,86 (t, 2H, J=16,4 Hz, j=7,6 Hz, AcrH) (d), 7,98 (s, 1H, =CH) (f), 8,19 (d, 2H, J=8,8 Hz, AcrH) (a), 8,46 (d, 2H, J=8,8 Hz, AcrH) (b).

IR

IR (KBr, cm⁻¹): 1748, 1693, 1604, 1449, 1407, 1374, 1325, 1149, 1080, 746, 597, 537, 505.

Obtenção de derivados tiazacridínicos

4.5.8 3-Acridin-9-ilmetil-5-(3-bromo-benzilideno)-tiazolidina-2,4-diona (LPSF AA-14)



FM: C₂₄H₁₅BrN₂O₂S

PM: 474,00

PF: 214-15°C

Rdt: 52,0%

Rf: 0,40 (*n*-Hexano/AcOEt 7:3)

Cor: Bege claro

NMR¹H (400 MHz, δ ppm, DMSO-d₆)

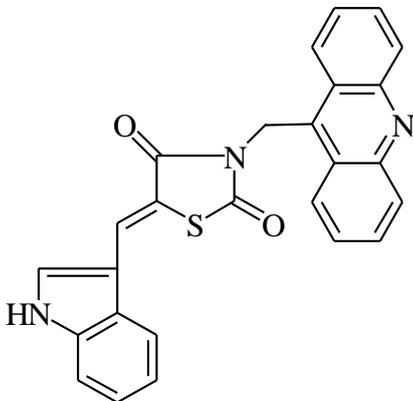
NMR¹H (400 MHz, DMSO-d₆): δ 5,93 (s, 2H, -CH₂) (e), 7,47 (t, 1H, J=16,0 Hz, j=8,0 Hz, ArH) (i), 7,55 (d, 1H, J=7,6 Hz, ArH) (j) 7,70-7,65 (m, 3H, ArH e AcrH) (h,c), 7,78 (s, 1H, ArH) (g), 7,85 (t, 2H, J=15,6 Hz, j=6,8 Hz, AcrH) (d), 7,90 (s, 1H, =CH) (f), 8,19 (d, 2H, J=8,0 Hz, AcrH) (a), 8,46 (d, 2H, J=8,4 Hz, AcrH) (b).

IR

IR (KBr, cm⁻¹): 1746, 1689, 1609, 1556, 1518, 1446, 1374, 1128, 1076, 752, 678.

Obtenção de derivados tiazacridínicos

4.5.9 3-Acridin-9-ilmetil-5-(1H-indol-3-ilmetileno)-tiazolidina-2,4-diona (LPSF AA-15)



FM: C₂₆H₁₇N₃O₂S

PM: 435,10

PF: 270°C

Rdt: 14,6%

Rf: 0,34 (*n*-Hexano/AcOEt 7:3)

Cor: Bege

NMR¹H (400 MHz, δ ppm, DMSO-d₆)

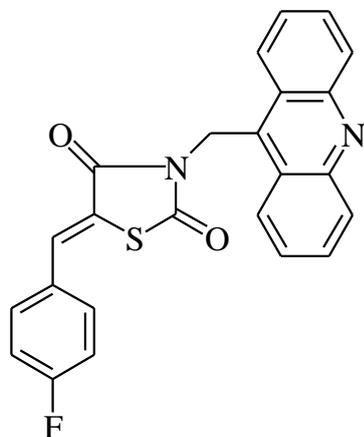
NMR¹H (400 MHz, DMSO-d₆): δ 5,92 (s, 2H, -CH₂) (e), 7,26-7,16 (m, 2H, ArH) (j,k), 7,48 (d, 1H, J=8,0 Hz, ArH) (i), 7,68 (t, 2H, J=16,4 Hz, j=8,8 Hz, AcrH) (c), 7,77 (s, 1H, ArH) (g), 7,85 (t, 2H, J=13,2 Hz, j=8,4 Hz, AcrH) (d), 7,89 (s, 1H, =CH) (f), 8,20-8,17 (m, 3H, AcrH, ArH) (a,l), 8,50 (d, 2H, J=8,8 Hz, AcrH) (b).

IR

IR (KBr, cm⁻¹): 3376, 1728, 1598, 1519, 1444, 1376, 1310, 1226, 1134, 739, 502.

Obtenção de derivados tiazacridínicos

4.5.10 3-Acridin-9-ilmetil-5-(4-fluoro-benzilideno)-tiazolidina-2,4-diona (LPSF AA-16)



FM: C₂₄H₁₅FN₂O₂S

PM: 414,08

PF: 245°C

Rdt: 74,0%

Rf: 0,56 (*n*-Hexano/AcOEt 7:3)

Cor: Amarela

NMR¹H (400 MHz, δ ppm, DMSO-d₆)

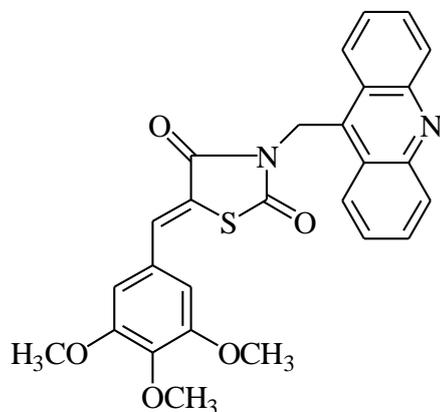
NMR¹H (400 MHz, DMSO-d₆): δ 5,93 (s, 2H, -CH₂) (e), 7,37 (t, 2H, J=7,37, ArH) (g), 7,71-7,64 (m, 4H, ArH e AcrH) (h,c), 7,86 (t, 2H, J=14,8 Hz, j=6,8 Hz, AcrH) (d), 7,95 (s, 1H, =CH) (f), 8,18 (d, 2H, J=8,4 Hz, AcrH) (a), 8,46 (d, 2H, J=8,8 Hz, AcrH) (b).

IR

IR (KBr, cm⁻¹): 1733, 1676, 1596, 1510, 1380, 1338, 1237, 1146, 831, 766, 486.

Obtenção de derivados tiazacridínicos

4.5.11 3-Acridin-9-ilmetil-5-(3,4,5-trimetoxi-benzilideno)-tiazolidina-2,4-diona (LPSF AA-17)



FM: C₂₇H₂₂N₂O₅S

PM: 486,12

PF: 220°C

Rdt: 76,0%

Rf: 0,46 (*n*-Hexano/AcOEt 7:3)

Cor: Bege

NMR¹H (400 MHz, δ ppm, DMSO-d₆)

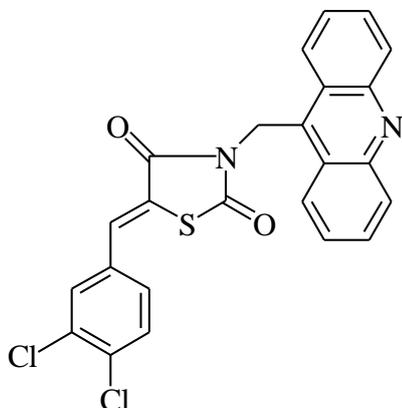
NMR¹H (400 MHz, DMSO-d₆): δ 3,71 (s, 3H, -CH₃) (i), 3,79 (s, 6H, -CH₃) (h), 5,93 (s, 2H, -CH₂) (e), 6,89 (s, 2H, ArH) (g), 7,68 (t, 2H, J=14,4 Hz, j=7,2 Hz, AcrH) (c), 7,86 (t, 2H, J=14,8 Hz, j=7,2 Hz, AcrH) (d), 7,89 (s, 1H, =CH) (f), 8,19 (d, 2H, J=8,8 Hz, AcrH) (a), 8,45 (d, 2H, J=8,8 Hz, AcrH) (b).

IR

IR (KBr, cm⁻¹): 1738, 1687, 1605, 1574, 1502, 1452, 1419, 1376, 1324, 1241, 1130, 1000, 754, 504.

Obtenção de derivados tiazacridínicos

4.5.12 3-Acridin-9-ilmetil-5-(3,4-dicloro-benzilideno)-tiazolidina-2,4-diona (LPSF AA-18)



FM: C₂₄H₁₄Cl₂N₂O₂S

PM: 464,02

PF: 210°C

Rdt: 50,0%

Rf: 0,47 (*n*-Hexano/AcOEt 7:3)

Cor: Bege

NMR¹H (400 MHz, δ ppm, DMSO-d₆)

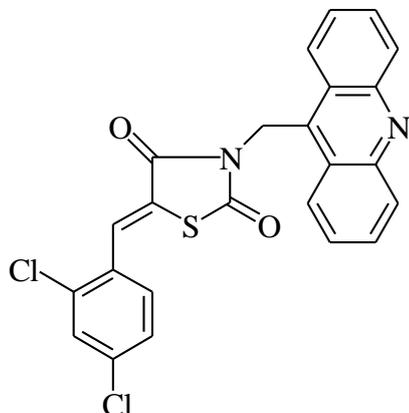
NMR¹H (400 MHz, DMSO-d₆): δ 5,93 (s, 2H, -CH₂) (e), 7,52 (d, 1H, J=5,1 Hz, ArH) (g), 7,69 (t, 2H, J=11,1 Hz, j=5,7 Hz, AcrH) (c), 7,77 (d, 1H, J=6,3 Hz, ArH) (h), 7,87-7,84 (m, 3H, ArH e AcrH) (d, i), 7,92 (s, 1H, =CH) (f), 8,19 (d, 2H, J=6,6 Hz, AcrH) (a), 8,45 (d, 2H, J=6,9 Hz, AcrH) (b).

IR

IR (KBr, cm⁻¹): 1744, 1687, 1611, 1470, 1380, 1329, 1131, 756, 546.

Obtenção de derivados tiazacridínicos

4.5.13 3-Acridin-9-ilmetil-5-(2,4-dicloro-benzilideno)-tiazolidina-2,4-diona (LPSF AA-19)



FM: C₂₄H₁₄Cl₂N₂O₂S

PM: 464,02

PF: 246-48°C

Rdt: 50,0%

Rf: 0,59 (*n*-Hexano/AcOEt 7:3)

Cor: Bege escuro

NMR¹H (300 MHz, δ ppm, DMSO-d₆)

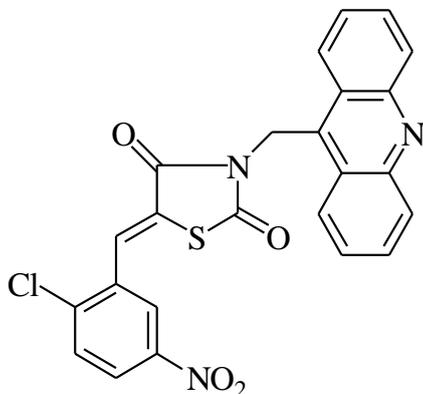
NMR¹H (400 MHz, DMSO-d₆): δ 5,93 (s, 2H, -CH₂) (e), 7,59-7,54 (m, 2H, ArH) (g,h), 7,70 (t, 2H, J=14,4 Hz e j=7,6 Hz, AcrH) (c), 7,89-7,83 (m, 3H, AcrH e ArH) (d,i), 7,93 (s, 1H, =CH) (f), 8,19 (d, 2H, J=8,4 Hz, AcrH) (a), 8,45 (d, 2H, J=8,8 Hz, AcrH) (b).

IR

IR (KBr, cm⁻¹): 1742, 1689, 1606, 1577, 1446, 1375, 1331, 1305, 1129, 1047, 759, 510.

Obtenção de derivados tiazacridínicos

4.5.14 3-Acridin-9-ilmetil-5-(2-cloro-5-nitro-benzilideno)-tiazolidina-2,4-diona (LPSF AA-20)



FM: C₂₄H₁₄ClN₃O₄S

PM: 475,04

PF: 218-20°C

Rdt: 49,0%

Rf: 0,45 (*n*-Hexano/AcOEt 7:3)

Cor: Amarela

NMR¹H (400 MHz, δ ppm, DMSO-d₆)

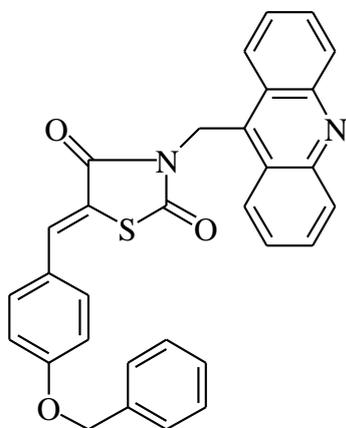
NMR¹H (400 MHz, DMSO-d₆): δ 5,94 (s, 2H, -CH₂) (e), 7,71 (t, 2H, J=15,2 Hz e j=7,2 Hz, AcrH) (c), 7,87 (t, 2H, J=15,2 Hz e j=7,6 Hz, AcrH) (d), 7,91 (d, 1H, J=6,4 Hz, ArH) (g), 7,94 (s, 1H, =CH) (f), 8,20 (d, 2H, J=8,4 Hz, AcrH) (a), 8,29-8,27 (m, 2H, ArH) (i,h), 8,46 (d, 2H, J=8,8 Hz, AcrH) (b).

IR

IR (KBr, cm⁻¹): 1748, 1683, 1606, 1523, 1445, 1378, 1345, 1266, 1148, 1127 1076, 765, 539, 503.

Obtenção de derivados tiazacridínicos

4.5.15 3-Acridin-9-ilmetil-5-(4-benziloxi-benzilideno)-tiazolidina-2,4-diona (LPSF AA-22)



FM: C₃₁H₂₂N₂O₃S

PM: 502,14

PF: 221-23°C

Rdt: 20,3%

Rf: 0,60 (*n*-Hexano/AcOEt 7:3)

Cor: Bege claro

NMR¹H (400 MHz, δ ppm, DMSO-d₆)

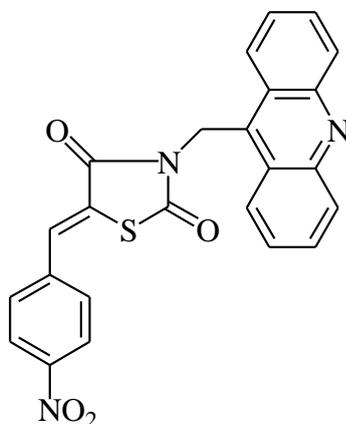
NMR¹H (400 MHz, DMSO-d₆): δ 5,18 (s, 2H, -OCH₂-) (i), 5,92 (s, 2H, -CH₂) (e), 7,16 (d, 2H, J=9,20 Hz, ArH) (h), 7,48-7,33 (m, 5H, ArH) (j, k, l), 7,54 (d, 2H, J=8,40 Hz, ArH) (g), 7,68 (t, 2H, J=15,60 Hz, j=7,60 Hz, AcrH) (c), 7,85 (t, 2H, J=15,20 Hz, j=7,20 Hz, AcrH) (d), 7,88 (s, 1H, =CH) (f), 8,18 (d, 2H, J=8,80 Hz, AcrH) (a), 8,47 (d, 2H, J=8,80 Hz, AcrH) (b).

IR

IR (KBr, cm⁻¹): 1737, 1676, 1593, 1512, 1378, 1260, 1182, 1129, 1022, 830, 749, 496.

Obtenção de derivados tiazacridínicos

4.5.16 3-Acridin-9-ilmetil-5-(4-nitro-benzilideno)-tiazolidina-2,4-diona (LPSF AA-23)

FM: C₂₄H₁₅N₃O₄S

PM: 441,08

PF: 255°C

Rdt: 41,0%

Rf: 0,67 (*n*-Hexano/AcOEt 7:3)

Cor: Amarela

NMR¹H (400 MHz, δ ppm, DMSO-d₆)

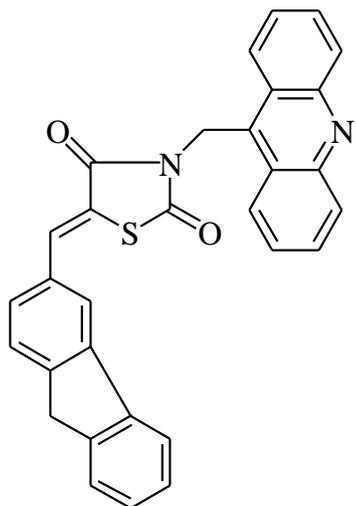
NMR¹H (400 MHz, DMSO-d₆): δ 5,94 (s, 2H, -CH₂) (e), 7,69 (t, 2H, J=15,20 Hz, j=8,80 Hz, AcrH) (c), 7,84 (t, 2H, J=18,40 Hz, j=8,80 Hz, AcrH) (d), 7,87 (d, 2H, J=6,80 Hz, ArH) (g), 8,02 (s, 1H, =CH₂) (f), 8,19 (d, 2H, J=8,40 Hz, AcrH) (a), 8,31 (d, 2H, J=8,80 Hz, AcrH) (h), 8,46 (d, 2H, J=8,80 Hz, AcrH) (b).

IR

IR (KBr, cm⁻¹): 1741, 1685, 1613, 1519, 1446, 1383, 1345, 1153, 1081, 848, 764, 526, 506.

Obtenção de derivados tiazacridínicos

4.5.17 3-Acridin-9-ilmetil-5-(9H-fluoren-3-ilmetileno)-tiazolidina-2,4-diona (LPSF AA-26)



FM: C₃₁H₂₀N₂O₂S

PM: 484,12

PF: 247-50°C

Rdt: 63,8%

Rf: 0,67 (*n*-Hexano/AcOEt 7:3)

Cor: Amarela

NMR¹H (400 MHz, δ ppm, DMSO-d₆)

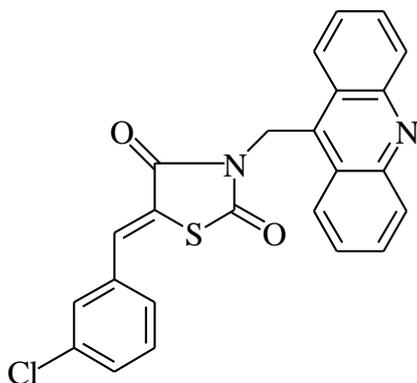
NMR¹H (400 MHz, DMSO-d₆): δ 4,05 (s, 2H, -CH₂) (j), 5,95 (s, 2H, -CH₂) (e), 8,12 (s, 1H, =CH₂) (f), 8,49-7,44 (m, 15H, H Aromáticos).

IR

IR (KBr, cm⁻¹): 1740, 1684, 1593, 1518, 1458, 1382, 1323, 1151, 1127, 1083, 754, 591, 548, 494.

Obtenção de derivados tiazacridínicos

4.5.18 3-Acridin-9-ilmetil-5-(3-cloro-benzilideno)-tiazolidina-2,4-diona (LPSF AA-30)

FM: C₂₄H₁₅ClN₂O₂S

PM: 430,05

PF: 210-13°C

Rdt: 50,0%

Rf: 0,68 (*n*-Hexano/AcOEt 7:3)

Cor: Branca

NMR¹H (400 MHz, δ ppm, DMSO-d₆)

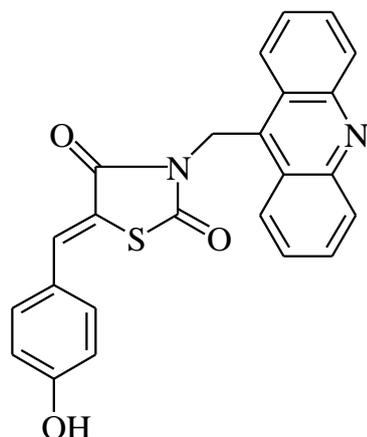
NMR¹H (400 MHz, DMSO-d₆): δ 5,93 (s, 2H, -CH₂) (e), 7,54 (s, 3H, ArH) (h, i, j), 7,65 (s, 2H, ArH) (g), 7,69 (t, 2H, J=15,2 Hz, j=8,0 Hz, AcrH) (c), 7,86 (t, 2H, J=15,2 Hz, j=7,6 Hz, AcrH) (d), 7,92 (s, 1H, =CH) (f), 8,19 (d, 2H, J=8,4 Hz, AcrH) (a), 8,46 (d, 2H, J=8,4 Hz, AcrH) (b).

IR

IR (KBr, cm⁻¹): 1744, 1693, 1608, 1449, 1378, 1316, 1129, 783, 753, 675, 532, 504.

Obtenção de derivados tiazacridínicos

4.5.19 3-Acridin-9-ilmetil-5-(4-hidroxi-benzilideno)-tiazolidina-2,4-diona (LPSF AA-31)



FM: C₂₄H₁₆N₂O₃S

PM: 412,09

PF: 270°C

Rdt: 36,6%

Rf: 0,2 (*n*-Hexano/AcOEt 7:3)

Cor: Amarelo claro

NMR¹H (400 MHz, δ ppm, DMSO-d₆)

NMR¹H (400 MHz, DMSO-d₆): δ 5,92 (s, 2H, -CH₂) (e), 6,89 (d, 2H, J=8,0 Hz, ArH) (h), 7,44 (d, 2H, J=8,4 Hz, ArH) (g), 7,68 (t, 2H, J=15,6 Hz, j=8,0 Hz, AcrH) (c), 7,83 (s, 1H, =CH₂) (f), 7,85 (t, 2H, J=16,0 Hz, j=8,4 Hz, AcrH) (d), 8,18 (d, 2H, J=8,4 Hz, AcrH) (a), 8,47 (d, 2H, J=8,8 Hz, AcrH) (b).

IR

IR (KBr, cm⁻¹): 1732, 1673, 1579, 1516, 1440, 1294, 1238, 1172, 1132, 1084, 756.

Obtenção de derivados tiazacridínicos



5 Atividade Anticâncer

Nos últimos anos, o nosso laboratório, o Laboratório de Planejamento e Síntese de Fármacos, vem sintetizando derivados tiazacridínicos em que o grupo acridínico está *N*-alquilado na posição 3 da tiazolidina e o grupo benzila está na posição 3. Vários derivados foram sintetizados com as seguintes substituições no anel benzilidênico: acridina, 4-OCH₃, 4-CH₃, 4-Cl, 4-Br, 4-SO₂CH₃, 3-Br,4-OCH₃. Estes foram diluídos em DMSO na concentração de 5mg/mL e foram testados na Universidade Federal do Ceará nas seguintes linhagens: SF-295 (câncer do SNC); HCT-8 (carcinoma de cólon) e MDA-MB435 (melanoma). Os resultados da atividade citotóxica estão apresentados na Tabela 11 (GALDINO-PITTA, 2012).

Tabela 11 - Inibição da proliferação (%) realizado em duplicata pelo método do MTT para as células SF-295 (SNC), HCT-8 (carcinoma de cólon) e MDA-MB435 (melanoma); doxorubicina foi usada como controle positivo

Composto	SF-295	HCT-8	MDA-MB435
Acridina	76,7 (MO)	92,4 (MA)	95,9 (MA)
4-OCH ₃	59,5 (MO)	86,7 (MA)	84,2 (MO)
4-CH ₃	29,9 (SA)	51,3 (PA)	31,2 (SA)
4-Cl	31,3 (PA)	37,8 (SA)	0,0 (SA)
4-Br	62,2 (PA)	96,6 (MA)	85,3 (MO)
4-SO ₂ CH ₃	44,3 (PA)	64,3 (MO)	12,9 (SA)
4-OCH ₃	48,0 (PA)	72,5 (MO)	53,0 (PA)
Doxorrubicina	91,1 (MA)	95,2 (MA)	93,6 (MA)

0 - 35% (SA) - Sem Atividade; 36 - 55% (PA) - Pouca Atividade; 56 - 85% (MO) - Moderada Atividade; 86 - 100% (MA) - Muita Atividade

Fonte: GALDINO-PITTA et al., 2012

Os compostos com as substituições no anel benzilidênico 4-OCH₃, 4-Br e acridina foram selecionados para a determinação do IC₅₀ (tabela 12), pois apresentaram

Atividade Anticâncer

percentual de inibição do crescimento tumoral maior que 80% nas linhagens celulares utilizadas.

Como podemos observar na Tabela 12, dos 3 compostos mais potentes, o bis-acridínico apresentou os melhores valores de IC₅₀: 4,4 µg/mL para MDA-MB435, 4,45 µg/mL para HCT-8, 7,01 µg/mL para SF-295 e valores maiores que 25 µg/mL para HL-60 e CEM, mas ainda assim estes valores estão muito altos quando comparados a doxorrubicina.

Tabela 12 - Valores de IC₅₀ (concentração inibitória de 50%) e intervalo de confiança de 95% (IC 95%) realizado pelo método do MTT para as células HL-60 (leucemia promielocítica), CEM (leucemia linfocítica), MDA-MB435 (melanoma), HCT-8 (carcinoma de cólon) e SF-295 (SNC) obtidos por regressão não-linear através do programa GraphPad Prism

Composto	HL-60 IC ₅₀ (µg/mL)	CEM IC ₅₀ (µg/mL)	MDA-MB435 IC ₅₀ (µg/mL)	HCT-8 IC ₅₀ (µg/mL)	SF-295 IC ₅₀ (µg/mL)
AA-2 (Acridina)	>25	>25	4,44 3,37 - 5,85	4,45 3,57 - 5,55	7,01 5,50 - 8,92
AA-3 (4-OCH3)	>25	>25	>25	19,26 15,11-24,53	>25
AA-6 (4-Br)	19,49 14,21 - 26,73	>25	>25	20,63 18,24-23,34	>25
Doxorrubicina	0,02 0,01 - 0,02	0,02 0,02 - 0,03	0,48 0,34 - 0,66	0,01 0,01 - 0,02	0,24 0,17 - 0,36

Fonte: GALDINO-PITTA et al., 2012

A molécula bis-acridínica foi a molécula mais ativa para as três linhagens de células neoplásicas testadas, SF-295, HCT-8 e MDA-MB435. Todos os compostos mostram um potencial citotóxico seletivo para a linhagem de células HCT-8, tendo o composto com a substituição 4-Br apresentado o maior potencial citotóxico para esta linhagem (GALDINO-PITTA, 2012). Estes promissores resultados estimularam a busca de novos derivados tiazacridínicos mais eficazes, potentes, seguros e confiáveis e justificam a execução deste trabalho de tese.

A avaliação da atividade biológica *in vitro* dos derivados tiazacridínicos sintetizados nesta tese foi realizada no Laboratório de Imunomodulação e Novas Abordagens Terapêuticas (LINAT) da Universidade Federal de Pernambuco e conduzido pela Profa. Dr. Maira Galdino da Rocha Pitta.

Os derivados de tiazacridinas foram dissolvidos em DMSO (Sigma Chemical) a 20mg/mL e armazenados na concentração estoque de 10 mM/mL e 50 mM/mL. As

Atividade Anticâncer

diluições mais baixas, com as quais os compostos foram testados (1, 10, 25, 50 e 100 μ M), foram realizadas diretamente no meio de cultura. A concentração final de DMSO, em todos os testes incluindo os controles, foi de 0,25%.

5.1 Linhagens de células neoplásicas

O estudo da atividade antitumoral foi realizado nas linhagens de células neoplásicas humanas RAJI e JUKART (Tabela 13), originadas do Banco de Células do Rio de Janeiro.

Tabela 13 - Linhagens de células neoplásicas humanas utilizadas

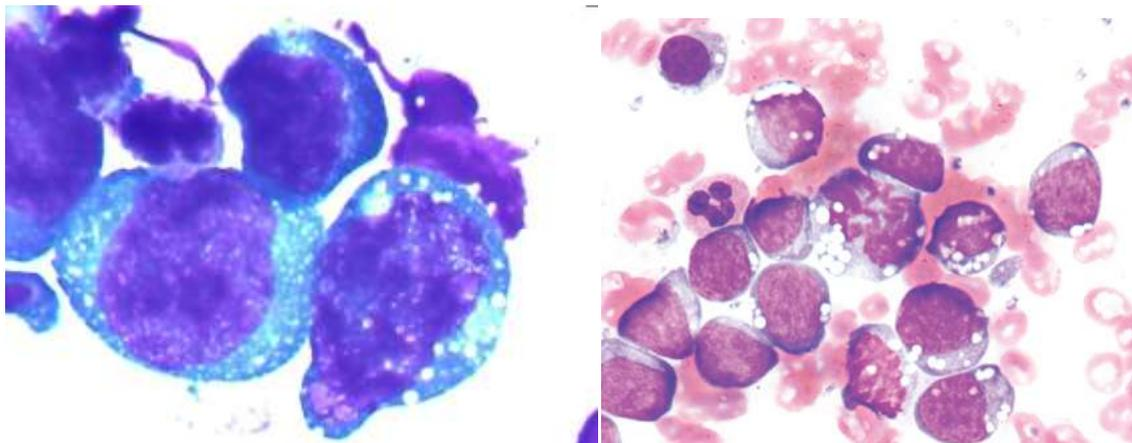
Linhagem	Doença	Tipo Celular
RAJI	Linfoma de Burkitt	Linfócitos B
JUKART	Leucemia Aguda de Células T	Linfócitos T

Fonte: ATCC, 2012

O linfoma de Burkitt (BL) é um câncer do sistema linfático (em particular, de linfócitos B). É um linfoma altamente agressivo, que geralmente é encontrado em sítios extranodais ou se apresentam como uma leucemia aguda. O vírus responsável pela doença de BL é o Epstein-Barr (EBV). O genoma do EBV é encontrado na maioria das células neoplásicas de BL. As anomalias genéticas (translocação do gene c-myc) desempenham um papel fundamental na patogênese do BL (Clinical Flow Wiki, 2012).

As células do linfoma de Burkitt são de tamanho médio, semelhantes em tamanho e morfologia, possuem altas atividades proliferativa e apoptótica. A aparência de “céu estrelado” vista à baixa potência é devida a presença de substâncias tingidas carregadas por macrófagos (macrófagos contendo resíduos de células apoptóticas tumorais) (Figura 15). As células tumorais apresentam uma pequena quantidade de citoplasma basófilo (Clinical Flow Wiki, 2012).

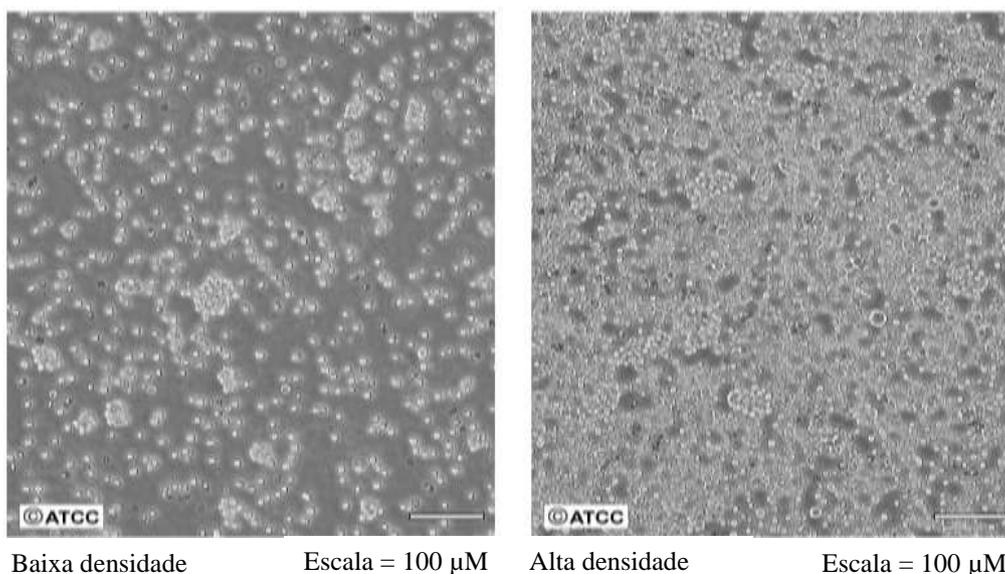
Figura 15 - Células de linfoma de Burkitt, com destaque a presença de vacúolos lipídicos e paracromatina clara



Fonte: Clinical Flow Wiki, 2012

As células de leucemia de células T são predominantemente de médio a grande porte e são caracterizadas por um acentuado pleomorfismo celular (ocorrência de duas ou mais formas estruturais durante o ciclo de vida), irregularidades nucleares e condensação da cromatina nuclear variável. O citoplasma é freqüentemente escasso e o núcleo irregular pode apresentar esboços de nucléolos. As células grandes são semelhantes à imunoblasto com citoplasma basofílico e cromatina nuclear delicada, com nucléolos proeminentes e aberrantes (Figuras 16 e 17) (SILVA et al., 2002).

Figura 16 - Células da linhagem JUKART, número ATCC: TIB-152

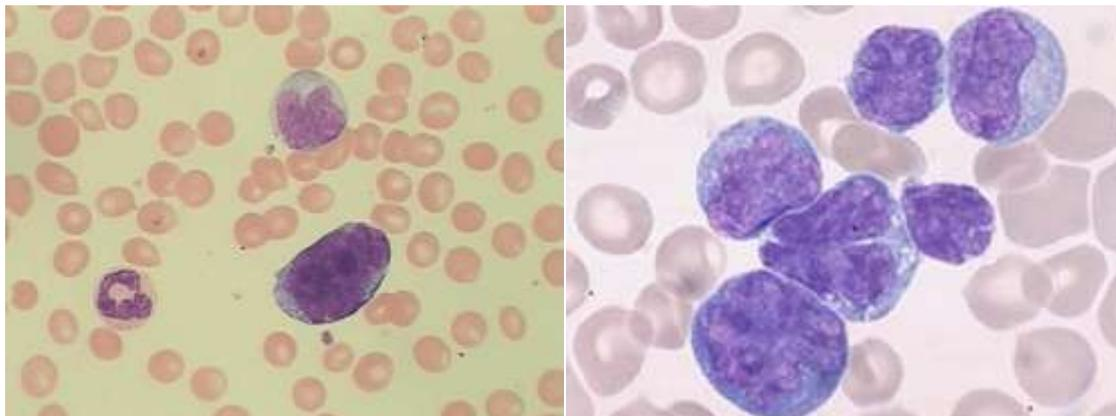


Fonte: ATCC, 2012

Atividade Anticâncer

Novos Agentes Tiazacridínicos com Propriedades Anticâncer
Marina G R Pitta

Figura 17 - Aspectos morfológicos de células de leucemia de células T. Imagens de células em mitose podem estar presentes



Fonte: Clinical Flow Wiki, 2012

5.2 Manutenção das células neoplásicas em cultura

As linhagens foram cultivadas em garrafa de cultura de células (75cm³, volume 250 mL) em meio RPMI 1640 (Gibco) suplementado com L-Glutamina, 10% de soro fetal bovino (Lonza), 10 mM de HEPES (ácido 4-(2-hidroxietil)-1-piperazinaetanosulfônico) (Gibco) e 200U/mL de penicilina/estreptomicina (Gibco). Estas células foram cultivadas em estufa de CO₂ 5% a 37 °C. O crescimento celular foi acompanhado diariamente com a utilização de microscópio invertido com contraste de fase e o meio de cultura trocado sempre que o crescimento atingia confluência necessária para a renovação dos nutrientes.

5.3 Ensaio de citotoxicidade em células neoplásicas

O teste de citotoxicidade foi realizado *in vitro* nas células neoplásicas listadas na Tabela 13, com diferentes concentrações dos derivados tiazacridínicos. A citotoxicidade celular foi quantificada pelo método 3-(4,5-dimetil-2-tiazol)-2,5-difenil-2-H-brometo de tetrazolium (MTT).

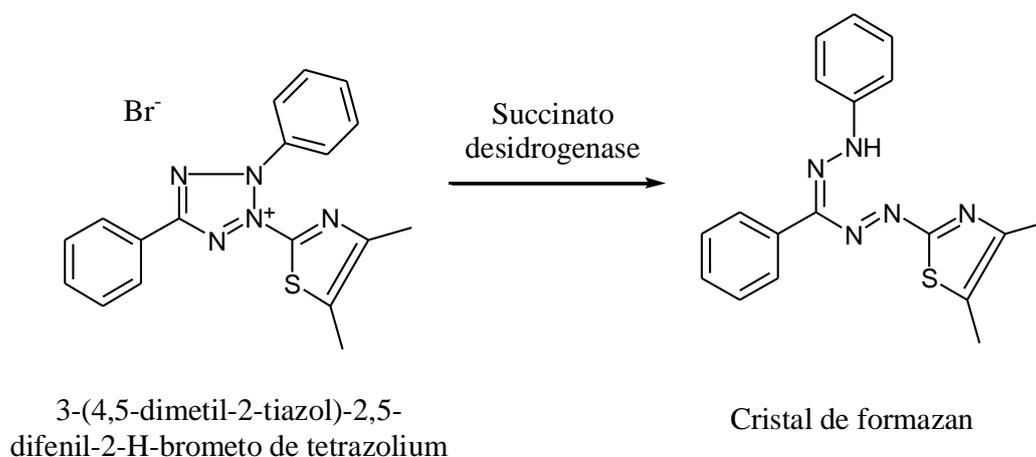
Descrita por Mosmann, em 1983, a análise de citotoxicidade pelo método do MTT, vem sendo utilizada no programa de *screening* do *National Cancer Institute*

Atividade Anticâncer

Novos Agentes Tiazacridínicos com Propriedades Anticâncer
Marina G R Pitta

(NCI) dos Estados Unidos, que testa mais de 10.000 amostras a cada ano. É um método rápido, sensível e barato que tem a capacidade de analisar a viabilidade e o estado metabólico da célula. É uma análise colorimétrica baseada na conversão do sal 3-(4,5-dimetil-2-tiazol)-2,5-difenil-2-H-brometo de tetrazolium (MTT) em azul de formazan, a partir de enzimas mitocondriais presentes somente nas células metabolicamente ativas (Esquema 9). O estudo citotóxico pelo método do MTT permite definir facilmente a citotoxicidade, mas não o mecanismo de ação (BERRIDGE et al., 1996).

Esquema 9 - Representação do método MTT

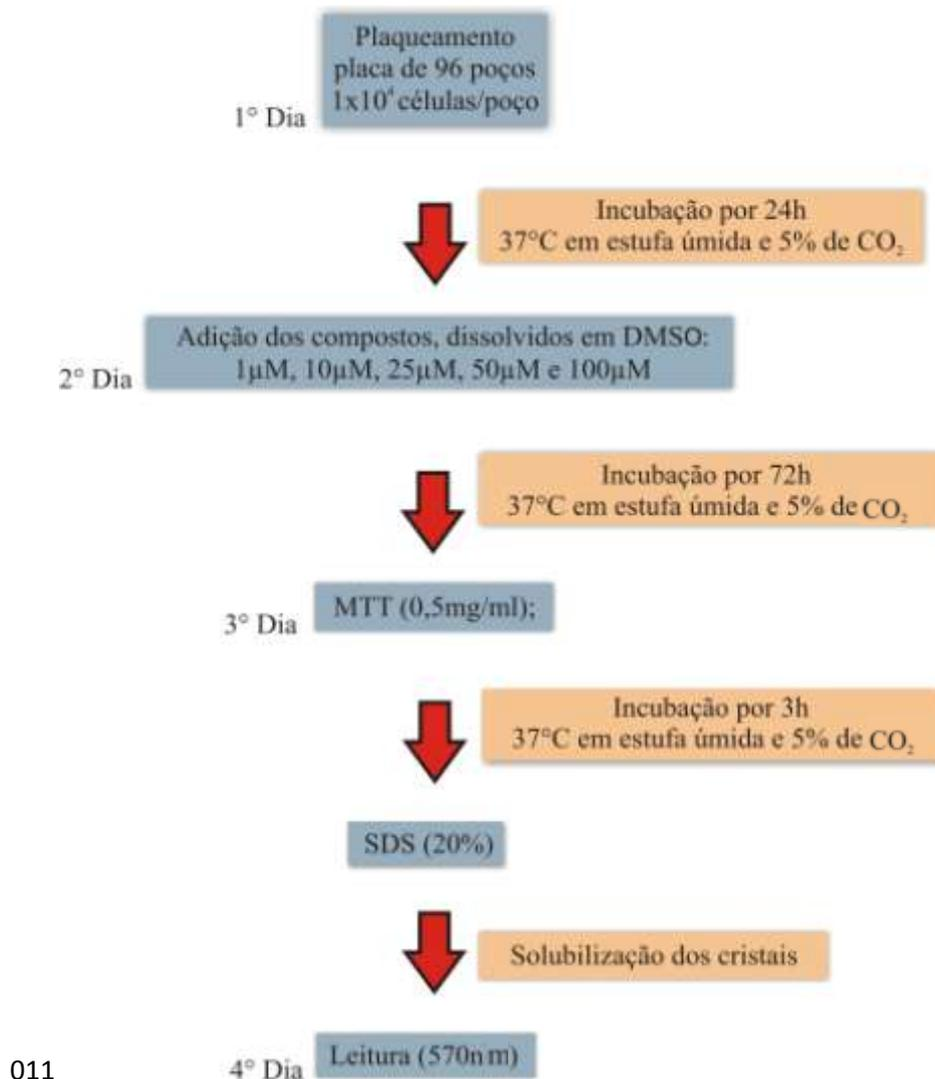


Fonte: Adaptado de MOSMANN, 1983

As células foram plaqueadas na concentração de 1×10^4 céls./100 mL e, posteriormente, as placas foram incubadas por 24 horas a 37°C em estufa úmida e 5% de CO₂. Após esse período, os compostos foram acrescidos em diferentes concentrações (1, 10, 25, 50 e 100 µM) e as placas, novamente incubadas por 72 horas. Em seguida, adicionou-se 20µL da solução de MTT (sal de tetrazolium) e as placas foram incubadas por 3h. Passado esse tempo, foram adicionados 130 µL de SDS 20% para dissolução do precipitado. A absorbância foi lida após 24h em espectrofotômetro de placa a 570 nm. No estudo, as amostras foram testadas em triplicata e a amsacrina foi utilizada como controle positivo (Esquema 10).

Atividade Anticâncer

Esquema 10 - Metodologia utilizada no estudo para ensaio de citotoxicidade em células neoplásicas



Fonte: Adaptado de MOURA, 2012

5.4 Análise de dados

O percentual de morte celular foi determinado de maneira relativa ao controle negativo e os dados foram analisados a partir da média de 3 experimentos independentes utilizando o software estatístico GraphPad Prism versão 5.

Atividade Anticâncer

Novos Agentes Tiazacridínicos com Propriedades Anticâncer
Marina G R Pitta

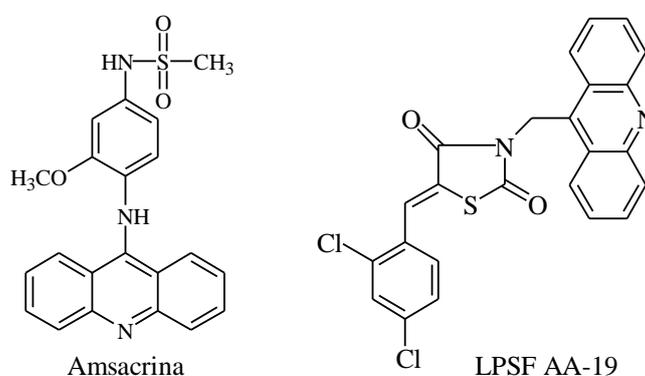
5.5 Resultados

5.5.1 Avaliação da atividade citotóxica na linhagem de células neoplásicas RAJI

O composto LPSF AA-19 foi testado nas concentrações de 1, 10, 25, 50 e 100 μM e a sua atividade citotóxica foi avaliada nas células neoplásicas RAJI. A amsacrina foi utilizada como controle positivo e o percentual de viabilidade das células foi determinado após o tratamento com o controle (Figura 18).

O percentual de viabilidade das células RAJI, após o tratamento com o LPSF AA-19, em relação às doses utilizadas pode ser observado na Tabela 14.

Figura 18 - LPSF AA-19 e controle positivo



Fonte: Autora, 2012

Tabela 14 - LPSF AA-19 e Amsacrina: viabilidade celular (%) da linhagem RAJI em função da dose

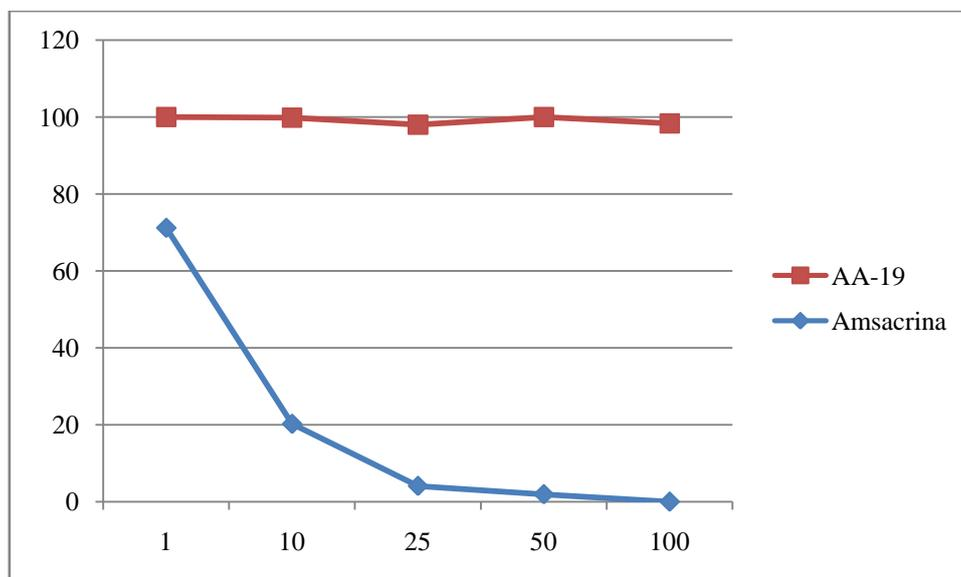
Composto	Dose (μM)	Exp. 1 (%)	Exp. 2 (%)	Exp. 3 (%)	Média (%)	DP
LPSF AA-19	1	100,00	100,00	100	100,00	0,00
	10	100,00	100,00	99,53	99,84	0,27
	25	100,00	100,00	93,97	97,99	3,48
	50	100,00	100,00	100,00	100,00	0,00
	100	100,00	100,00	94,99	98,33	2,89
Amsacrina	1	81,62	66,13	65,76	71,17	9,05
	10	25,40	18,92	16,39	20,23	4,65
	25	7,64	1,87	2,80	4,10	3,10
	50	5,81	0,00	0,00	1,94	3,35
	100	0,00	0,00	0,00	0,00	0,00

Experimento realizado em triplicata

Fonte: LINAT/UFPE

A Figura 19 apresenta o percentual de viabilidade das células neoplásicas da linhagem RAJI, após o tratamento com o LPSF AA-19, em relação às cinco doses utilizadas.

Figura 19 - Viabilidade celular (%) da linhagem RAJI, em função da dose do LPSF AA-19, e da amsacrina

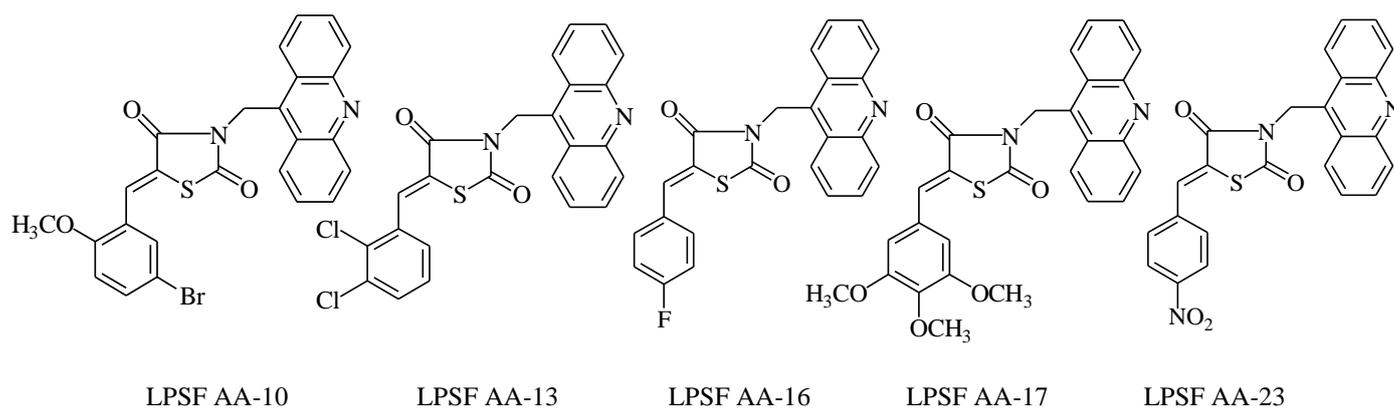


Fonte: Autora, 2012

A amsacrina teve uma resposta dose dependente na linhagem de células RAJI, apresentando um percentual de viabilidade celular de 0,00 % na dose de 100 μM . No entanto, o LPSF AA-19 foi muito pouco efetivo na mesma linhagem de células.

O composto LPSF AA-10 foi testado nas concentrações de 1, 5, 10, 25, 50 e 100 μM e os compostos LPSF AA-13 e LPSF AA-23 foram testados nas concentrações de 1, 10, 25, 50 e 75 μM (Figura 20) nas mesmas linhagens de células neoplásicas RAJI (Tabela 15). O percentual de viabilidade das células RAJI, após o tratamento com o LPSF AA-10, LPSF AA-13 e LPSF AA-23 foi de 100% em todas as doses utilizadas.

Figura 20 - Tiazacridinas testadas na linhagem de células neoplásicas RAJI



Fonte: Autora, 2012

Tabela 15 - Viabilidade celular (%) da linhagem RAJI em função da dose do LPSF AA-10, LPSF AA-13, LPSF AA-16, LPSF AA-17, LPSF AA-23 e Amsacrina

Composto	Dose (µM)	Exp. 1 (%)	Exp. 1 (%)	Exp. 2 (%)	Exp. 3 (%)	Média (%)	DP
LPSF AA-10	1	-	100,00	100,00	100,00	100,00	0,00
	5	-	100,00	100,00	100,00	100,00	0,00
	10	-	100,00	100,00	100,00	100,00	0,00
	25	-	100,00	100,00	100,00	100,00	0,00
	50	-	100,00	100,00	100,00	100,00	0,00
	100	-	100,00	100,00	100,00	100,00	0,00
LPSF AA-13	1	-	100,00	100,00	100,00	100,00	0,00
	10	-	100,00	100,00	100,00	100,00	0,00
	25	-	100,00	100,00	100,00	100,00	0,00
	50	-	100,00	100,00	100,00	100,00	0,00
	75	-	100,00	100,00	100,00	100,00	0,00
LPSF AA-16	1	100,00	75,85	85,29	100,00	90,28	11,86
	5	-	100,00	95,94	72,67	89,53	14,75
	10	100,00	59,33	70,97	73,96	76,06	17,16
	25	-	100,00	100,00	87,05	95,68	7,47
	50	100,00	100,00	100	66,47	91,62	16,76
LPSF AA-17	1	-	67,24	74,17	54,73	65,38	9,85
	10	-	50,80	73,09	79,69	67,86	15,14
	50	-	72,89	100,00	61,11	78,00	19,94
	100	-	72,89	101,26	61,11	78,42	20,64
	250	-	76,68	83,59	90,62	83,63	6,97
LPSF AA-23	1	-	100,00	100,00	100,00	100,00	0,00
	10	-	100,00	100,00	100,00	100,00	0,00
	25	-	100,00	100,00	100,00	100,00	0,00
	50	-	100,00	100,00	100,00	100,00	0,00
	75	-	100,00	100,00	100,00	100,00	0,00
Amsacrina	1	-	65,62	47,14	0,00	37,58	33,84
	5	-	37,30	23,38	0,00	20,23	18,85
	10	-	30,91	14,46	0,00	15,12	15,46
	25	-	-	9,03	0,00	4,51	6,38

Experimento realizado em triplicata

Fonte: LINAT/UFPE

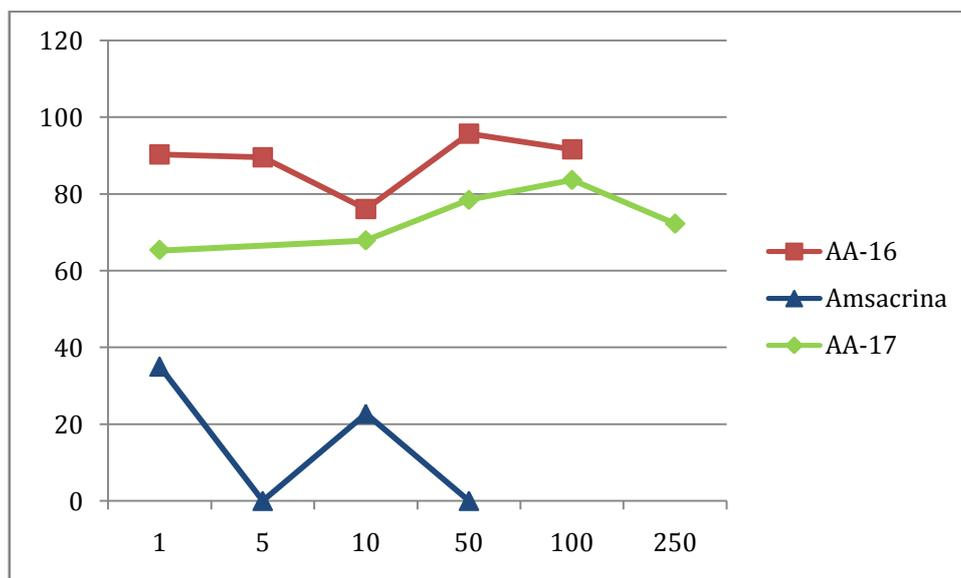
Atividade Anticâncer

Novos Agentes Tiazacridínicos com Propriedades Anticâncer
Marina G R Pitta

Por sua vez, o composto LPSF AA-16 foi testado nas concentrações de 1, 5, 10, 25 e 50 μM e o composto LPSF AA-17 foi testado nas concentrações de 1, 10, 25, 50 e 75 μM . Estas duas tiazacridinas, com as substituições 4-F e 3,4,5-OCH₃ respectivamente, foram mais ativas frente a linhagem de células RAJI, quando comparamos com os outros derivados testados. O LPSF AA-16 teve um menor percentual de viabilidade celular na dose de 10 μM (76,06 %) e o LPSF AA-17 foi mais ativo nas doses de 1 μM (65,38 %) e 10 μM (67,86 %) (Figura 21).

O derivado tiazacridínico com três grupamentos metóxi no anel benzilidênico, o LPSF AA-17, foi o mais ativo de todos os compostos testados na linhagem de células RAJI (Figura 21).

Figura 21 - Viabilidade celular (%) da linhagem RAJI, em função das doses do LPSF AA-16, do LPSF AA-17 e da amsacrina



Fonte: Autora, 2012

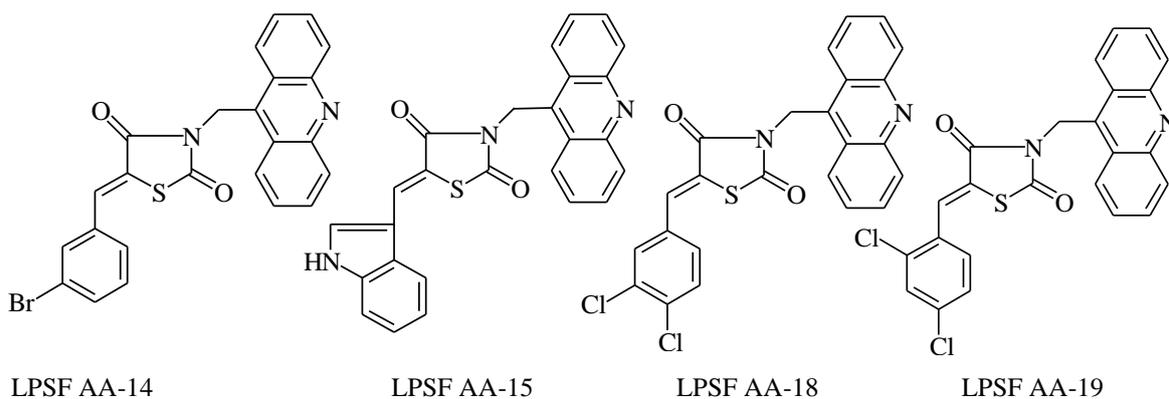
A determinação da IC₅₀ (concentração capaz de inibir 50% do crescimento celular) não pôde ser efetuada, pois os compostos testados LPSF AA-10, LPSF AA-13, LPSF AA-16, LPSF AA-17, LPSF AA-19 e LPSF AA-23 não apresentaram atividade capaz de inibir 50 % do crescimento celular nas duas linhagens de células testadas.

Atividade Anticâncer

5.5.2 Avaliação da atividade citotóxica na linhagem de células neoplásicas JUKART

O percentual de viabilidade das células neoplásicas da linhagem Jukart foi obtido após o tratamento dessas células com os derivados LPSF AA-14, LPSF AA-15, LPSF AA-18 e LPSF AA-19 (Figura 22) nas concentrações de 1, 10, 25, 50 e 100 μM . A amsacrina foi utilizada como controle positivo (Tabela 16).

Figura 22 - Tiazacridinas testadas na linhagem de células neoplásicas JUKART



Fonte: Autora, 2012

Tabela 16 - Viabilidade celular (%) da linhagem JUKART, em função da dose do LPSF AA-19, e da amsacrina

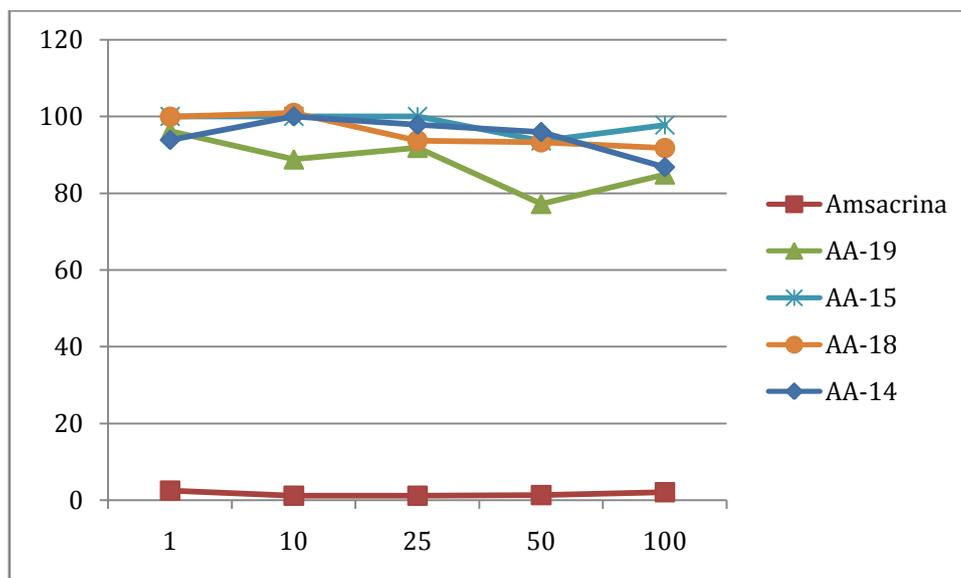
Composto	Dose (μM)	Exp. 1 (%)	Exp. 2 (%)	Exp. 3 (%)	Média (%)	DP
LPSF AA-14	1	97,29	89,43	94,91	93,87	4,03
	10	100,00	100,00	93,02	97,67	4,03
	25	93,02	100,00	100,00	97,67	4,03
	50	91,33	100,00	94,91	95,41	4,35
	100	82,75	79,95	97,68	86,79	9,53
LPSF AA-15	1	98,69	100,00	100,00	99,56	0,75
	10	99,95	100,00	100,00	99,98	0,02
	25	100,00	100,00	100,00	100,00	0,00
	50	90,49	90,46	99,87	93,61	5,42
	100	88,56	99,69	100,00	96,08	6,51
LPSF AA-18	1	99,08	97,28	98,55	98,30	0,92
	10	100,00	100,00	100,00	100,00	0,00
	25	85,56	94,75	100,00	93,44	7,30
	50	90,75	89,80	94,67	91,74	2,58
	100	92,36	92,02	98,07	94,15	3,39
LPSF AA-19	1	100,00	100,00	88,61	96,20	6,57
	10	86,00	96,48	84,07	88,85	6,67
	25	87,26	96,78	91,55	91,86	4,76
	50	71,91	78,37	81,43	77,24	4,86
	100	90,85	92,58	71,35	84,93	11,79
Amsacrina	1	3,05	2,62	1,85	2,50	0,60
	10	1,24	0,62	1,69	1,18	0,53
	25	0,00	0,00	3,54	1,18	2,04
	50	0,00	0,00	4,09	1,36	2,36
	100	0,00	0,00	6,28	2,09	3,62

Experimento realizado em triplicata

Fonte: LINAT/UFPE

A Figura 23 apresenta o percentual de viabilidade das células neoplásicas da linhagem JUKART, após o tratamento com o LPSF AA-19, em relação às doses utilizadas.

Figura 23 - Viabilidade celular (%) da linhagem JUKART, em função da dose dos LPSF AA-14, LPSF AA-15, LPSF AA-18, LPSF AA-19, e amsacrina



Fonte: Autora, 2012

Na linhagem de células JUKART, o controle positivo, a amsacrina, foi bastante efetiva já na concentração de 1 μM . O LPSF AA-19 foi o mais ativo das tiazacridinas testadas nesta linhagem de células. Ele apresentou o menor percentual de viabilidade celular na dose de 50 μM (77,24 %), e foi mais ativo nessa linhagem de células do que na linhagem celular maligna de Linfoma de Burkitt. Mas, mesmo assim, o percentual de inibição das células neoplásicas foi aquém do desejável.

A determinação da IC_{50} (concentração capaz de inibir 50% do crescimento celular) não pôde ser efetuada, pois os compostos LPSF AA-14, LPSF AA-15, LPSF AA-18 e LPSF AA-19 testado não apresentaram atividade capaz de inibir 50 % do crescimento celular nas duas linhagens de células testadas.



4 Conclusões

Considerando a vasta gama de efeitos adversos e o possível desenvolvimento de resistência aos fármacos anticâncer disponíveis atualmente na clínica, neste trabalho foi realizada a síntese de 16 novos compostos da série 3-(Acridin-9-il-metil)-tiazolidina-2,4-diona. Entre os compostos sintetizados, foi avaliada a atividade anticâncer *in vitro* pelo método 3-(4,5-dimetil-2-tiazol)-2,5-difenil-2-H-brometo de tetrazolium nas linhagens de células neoplásicas JUKART (derivados LPSF AA-14, LPSF AA-15, LPSF AA-18, LPSF AA-19) e RAJI (derivados LPSF AA-10, LPSF AA-13, LPSF AA-16 e LPSF AA-17).

Todas as 16 substâncias e seus respectivos intermediários tiveram suas estruturas confirmadas pelas técnicas de Ressonância Magnética Nuclear de Hidrogênio e Infravermelho. As metodologias de síntese orgânica mostraram ser eficientes e eficazes e levaram a rendimentos satisfatórios.

Os resultados revelam que na linhagem de células RAJI o composto LPSF AA-17, derivado com as substituições 3,4,5-OCH₃ no anel benzilidênico, foi o mais ativo, enquanto na linhagem de células JUKART o LPSF AA-19, dissubstituído com o cloro nas posições 2 e 4 do anel benzilidênico, foi o mais ativo.



5 Perspectivas

- ✓ Realizar o ensaio de atividade anticâncer *in vitro* pelo método MTT dos demais compostos sintetizados nas linhagens de células neoplásicas RAJI e JUKART;
- ✓ Testar as tiazacridinas em outras linhagens de células neoplásicas;
- ✓ Formular nanopartículas lipossomais com acridinas;
- ✓ Determinar o diâmetro e o potencial zeta dos sistemas lipossoma-acridina;
- ✓ Caracterizar estrutural e morfológicamente os sistemas lipossoma-acridina utilizando-se microscopia eletrônica de varredura, microscopia eletrônica de transmissão e microscopia de força atômica;
- ✓ Caracterizar as estruturas químicas através de espectrometria de massas;
- ✓ Realizar o ensaio de atividade anticâncer em combinação com outros agentes quimioterápicos.



6 Referências

ALBERT, "The Acridines", London 1966. In: DEMEUNYNCK, M.; CHARMANTRAY, F.; MARTELLI, A. Interest of acridine derivatives in the anticancer chemotherapy. **Current Pharmaceutical Design**, Grenoble, v. 7, p. 1703-24, nov. 2001.

ACHESON, A. Acridines, John Wiley & Sons: New York, 1973. In: CHIRON, J.; GALY, J. P. Reactivity of the Acridine Ring: A Review. **Synthesis**, France, n. 3, p. 313-25, apr. 2004.

ATCC. The essentials of life science research. Globally delivered. Disponível em: <<http://www.atcc.org/>>. Acesso em: 01 set. 2012.

AZAROVA, A. M. et al. Roles of DNA topoisomerase II isozymes in chemotherapy and secondary malignancies. **Proceedings of the National Academy of Sciences of the United States of America**, New Jersey, v. 104, n. 26, p. 11014-11019, jun. 2007.

Banco de Células do Rio de Janeiro. Disponível em: <<http://www.bcrj.hucff.ufrj.br/>>. Acesso em: 09 fev. 2011.

BERG, J. M.; TYMOCZKO, J. L.; STRYER, L. **Bioquímica**. 6^aed., Rio de Janeiro: Guanabara Koogan, 2008.

BERGER, J.; MOLLER, D. E. The mechanisms of action of PPARs. **Annual Review of Medicine**, New Jersey, v. 53, p. 409-435, 2002.

BERGERS, G.; BENJAMIN, L. E. Tumorigenesis and the angiogenic switch. **Nature Reviews Cancer**, California, v. 3, n. 6, p. 401-410, jun. 2003.

BERRIDGE, M. V. et al. The Biochemical and Cellular Basis of Cell Proliferation Assays That Use Tetrazolium Salts. **Biochemica**, Beijing, n. 4, p. 14-19, 1996.

BICKNELL, R. The realisation of targeted antitumour therapy. **British Journal of Cancer**, Oxford, v. 92, n. suppl. 1, p. S2-S5, jun. 2005.

Referências

BONDE, C. G. GAIKWAD, N. J. Synthesis and preliminary evaluation of some pyrazine containing thiazolines and thiazolidinones as antimicrobial agents. **Bioorganic & Medicinal Chemistry**, Nagpur, v. 12, n. 9, p. 2151-2161, may. 2004.

BONSE, S. et al. Inhibition of Trypanosoma cruzi trypanothione reductase by acridines: kinetic studies and structure-activity relationships. **Journal of Medicinal Chemistry**, Heidelberg, v. 42, n. 26, p. 5448-54, dec. 1999.

CAPRANICO, G. et al. Different patterns of gene expression of topoisomerase II isoforms in differentiated tissues during murine development. **Biochimica et Biophysica Acta**, Itália, v. 1132, n. 1, p. 43-48, aug. 1992.

CAVALCANTI JUNIOR, G. B. C.; KLUMB, C. E.; MAIA, R. C. p53 e as hemopatias malignas. **Revista Brasileira de Cancerologia**, Rio de Janeiro, v. 48, n. 3, p. 419-427, jul. 2002.

CESUR, N. et al. Synthesis and antifungal activity of some 2-aryl-3-substituted 4-thiazolidinones. **Archiv der Pharmazie (Weinheim, Germany)**, Turkey, v. 327, n. 4, p. 271-273, apr. 1994.

CHAMPOUX, J. J. DNA topoisomerases: structure, function, and mechanism. **Annual Review of Biochemistry**, Washington, v. 70, p. 369-413, jul. 2001.

CHIRON, J.; GALY, J-P. Reactivity of the Acridine Ring: A Review. **Synthesis**, France, n. 3, p. 313-25, apr. 2004.

CHOW, L.M.; CHAN, T.H. Novel Classes of Dimer Antitumour Drug Candidates. **Current Pharmaceutical Design**, Hong Kong, v. 15, n. 6, p. 659-674, feb. 2009.

Clinical Flow Wiki. Disponível em: <<http://wiki.clinicalflow.com/Cases>>. Acesso em: 04 set. 2012.

Clinical Trials. Autophagy Inhibition Using Hydrochloroquine in Breast Cancer Patients, 2012. Disponível em: <<http://clinicaltrials.gov/ct2/show/NCT01292408?term=autophagy&rank=1>>. Acesso em: 09 set. 2012.

Clinical Trials. Neo-adjuvant treatment with temozolomide and bevacizumab previous to temozolomide plus radiation plus bevacizumab therapy in unresectable glioblastoma, 2012. Disponível em: <http://clinicaltrials.gov/ct2/show/NCT01102595?term=temozolomide&recr=Open&no_unk=Y&rank=3>. Acesso em: 09 set. 2012.

CORNAROTTI, M. et al. Drug sensitivity and sequence specificity of human recombinant DNA topoisomerases I α (p170) and I β (p180). **Molecular Pharmacology**, Itália, v. 50, n. 6, p. 1463-1471, dec. 1996.

DEMEUNYNCK, M.; CHARMANTRAY F., MARTELLI, A. Interest of acridine derivatives in the anticancer chemotherapy. **Current Pharmaceutical Design**, Grenoble, v. 7, n. 17, p. 1703-1724, nov. 2001.

Referências

DENNY, W. A. Acridine derivatives as chemotherapeutic agents. **Current Medicinal Chemistry**, New Zealand, v. 9, n. 18, p. 1655-1665, sep. 2002.

DREVS, J. et al. Receptor tyrosine kinases: the main targets for new anticancer therapy. **Current Drug Targets**, Freiburg, v. 4, n. 2, p. 113-121, feb. 2003.

ELANGBAM, C. S.; TYLER, R. D.; LIGHTFOOT, R. M. Peroxisome proliferator-activated receptors in atherosclerosis and inflammation: an update. **Toxicologic Pathology**, North Carolina, v. 29, n. 2, p. 224-231, mar. 2001.

ERTMER, A. et al., The anticancer drug imatinib induces cellular autophagy. **Leukemia**, Munich, v. 21, n. 5, p. 936-942, may. 2007.

FU, Y. T. et al. BRACO19 analog dimers with improved inhibition of telomerase and hPot 1. **Bioorganic & Medicinal Chemistry**, North Carolina, v. 17, n. 5, p. 2030-2037, mar. 2009.

GALDINO-PITTA, M. R. et al., Synthesis and in vitro anticancer activity of novel thiazacridine derivatives. **Medicinal Chemistry Research**, Recife, v. 22, n. 5, p. 2421-2429, maio 2013.

GALLI, A. et al. Antidiabetic thiazolidinediones inhibit collagen synthesis and hepatic stellate cell activation in vivo and in vitro. **Gastroenterology**, Florence, v. 122, n. 7, p. 1924-1940, jun. 2002.

GELLERT, G. C. et al. Telomerase as a therapeutic target in cancer. **Drug Discovery Today: Disease Mechanisms**, Ankara, v. 2, n. 2, 2005.

GIRAULT, S. et al. Antimalarial, antitrypanosomal, and antileishmanial activities and cytotoxicity of bis(9-amino-6-chloro-2-methoxyacridines): influence of the linker. **Journal of Medicinal Chemistry**, Lille, v. 43, n. 14, p.2646-54, jul. 2000.

GOETSCH, C. M. Genetic tumor profiling and genetically targeted cancer therapy. **Seminars in Oncology Nursing**, Washington, v. 27, n. 1, p. 34-44, feb. 2011.

GONZALEZ-MALERVA, L. et al., Autophagy and Tamoxifen Resistance in Breast Cancer. **Cancer Research**, Massachusetts, v. 69, n. 24, s.6, dec. 2009.

GOODELL, J. R. et al. Acridine-Based Agents with Topoisomerase II Activity Inhibit Pancreatic Cancer Cell Proliferation and Induce Apoptosis. **Journal of Medicinal Chemistry**, Minnesota, v. 51, n. 2, p. 179-182, jan. 2008.

GOZUACIK, D.; KIMCHI, A. Autophagy as a cell death and tumor suppressor mechanism. **Oncogene**, Rehovot, v. 23, n. 16, p. 2891-2906, apr. 2004.

Referências

GRAZIANO, M. J.; et al. Carcinogenicity of the anticancer topoisomerase inhibitor, amsacrine, in Wistar rats. **Fundamental Applied Toxicology**, Michigan, v. 32, n. 1, p. 53-65, jul. 1996.

HARRIS, M. Monoclonal antibodies as therapeutic agents for cancer. **The Lancet Oncology**, Australia, v. 5, n. 5, p. 292-302, may. 2004.

HARRISON, R. J. et al. Human telomerase inhibition by substituted acridine derivatives. **Bioorganic & Medicinal Chemistry Letters**, v. 9, n. 17, p. 2463-2468, sep. 1999.

HØYER-HANSEN, M.; JÄÄTTELÄ, M. Autophagy: An emerging target for cancer therapy. **Autophagy**, Copenhagen, v. 4, n. 5, p. 574-80, jul. 2008.

Instituto Nacional do Câncer. **Atlas de Mortalidade por Câncer**. 2012. Disponível em: <<http://mortalidade.inca.gov.br/Mortalidade/prepararModelo02.action>>. Acesso em: 06 set. 2012.

Instituto Nacional do Câncer. **Câncer na criança e no adolescente no Brasil**. Rio de Janeiro – RJ, 2008. Disponível em: <http://www1.inca.gov.br/tumores_infantis/>. Acesso em: 11 abr. 2012.

Instituto Nacional do Câncer. **Mama**. 2012. Disponível em: <<http://www2.inca.gov.br/wps/wcm/connect/tiposdecancer/site/home/mama>>. Acesso em: 21 set. 2012.

Instituto Nacional do Câncer. **O que é o câncer?** 2012. Disponível em: <http://www1.inca.gov.br/conteudo_view.asp?id=322>. Acesso em: 16 set. 2012.

Instituto Nacional do Câncer. **Quimioterapia**. 2012. Disponível em: <http://www.inca.gov.br/conteudo_view.asp?ID=101>. Acesso em: 16 set. 2012.

KAWAGUCHI, K. et al. Pioglitazone prevents hepatic steatosis, fibrosis, and enzyme-altered lesions in rat liver cirrhosis induced by acholine-deficient L-amino acid-defined diet. **Biochemical and Biophysical Research Communications**, Japan, v. 315, n. 1, p. 187-195, feb. 2004.

KOGA, H. et al. Troglitazone induces 27Kip1-associated cell-cycle arrest through down-regulating Skp2 in human hepatoma cells. **Hepatology**, Japan, v. 37, n. 5, p. 1086-1096, may. 2003.

KOGA, H. et al. Involvement of p21 (WAF1/Cip1), p27 (Kip1), and p18 (INK4c) in troglitazone-induced cell-cycle arrest in human hepatoma cell lines. **Hepatology**, Japan, v. 33, n. 5, p. 1087-1097, may. 2001.

KROEMER, G. JAATTELA, M. Lysosomes and autophagy in cell death control. **Nature Reviews Cancer**, França, v. 5, n. 11, p. 886-897, nov. 2005.

Referências

- LARSEN, A. K. et al. Catalytic topoisomerase II inhibitors in cancer therapy. **Pharmacology & Therapeutics**, França, v. 99, n. 2, p. 167-181, aug. 2003.
- LERMAN, L. S. Structural considerations in the interaction of DNA and acridines. **Journal of Molecular Biology**, v. 3, n. 1, p. 18-30, feb. 1961.
- LERMAN, L. S. The structure of the DNA-acridine complex. **Proceedings of the National Academy of Sciences of the USA**, USA, v. 49, n. 1, p. 94-102, jan. 1963.
- LIBERMANN, D.; HIMBERT, J.; HENGL, L. Thiazolidinedione as starting material in a synthesis of substituted thiopyruvic and thioglyoxylic acids. **Bulletin de la Societe Chimique de France**, p. 1120-1124, 1948.
- LIU, H. K.; SADLER, P. J. Metal Complexes as DNA Intercalators. **Accounts of Chemical Research**, UK, v. 44, n. 5, p. 349-359, mar. 2011.
- MARTÍNEZ, R.; CHACÓN-GARCÍA, L. The Search of DNA-Intercalators as Antitumoral Drugs: What it Worked and What did not Work. **Current Medicinal Chemistry**, México, v. 12, n. 2, p. 127-151, jan. 2005.
- MATHEW, R.; KARANTZA-WADSWORTH, V.; WHITE, E. Role of autophagy in cancer. **Nature Reviews Cancer**, New Jersey, v. 7, n. 12, p. 961-967, dez. 2007.
- MATHEW, R. et al. Autophagy suppresses tumor progression by limiting chromosomal instability. **Genes & Development**, New Jersey, v. 21, n. 11, p. 1367-1381, jun. 2007.
- MCMURRY, J. **Química Orgânica**. Trad, técnica Ana Flavia Nogueira e Izilda Aparecida Bagatin. 6. ed. São Paulo: Thompson, vol 1, 2006.
- MORENO-SÁNCHEZ, R. et al. Energy metabolism in tumor cells. **The FEBS Journal**, Tlalpan, v. 274, n. 6, p. 1393-1418, mar. 2007.
- MOSMANN, T. Rapid colorimetric assay for cellular growth and survival: application to proliferation and cytotoxicity assays. **Journal of Immunological Methods**, v. 65, n. 1-2, p. 55-63, dez. 1983.
- MOURA, E. D. **Avaliação in vitro da atividade anticâncer de novos agentes tiazacridínicos**. 2012. Trabalho de conclusão de curso. Universidade Federal de Pernambuco, Recife, 2012.
- PINHO, M. S. L. Angiogênese: o gatilho proliferativo. Revista Brasileira de Coloproctologia. **Revista Brasileira de Coloproctologia**, Joinville, v. 25, n. 4, p. 396-402, dez. 2005.
- NEIDLE, S.; PARKINSON, G. Telomere maintenance as a target for anticancer drug discovery. **Nature Reviews Drug Discovery**, London, v. 1, n. 5, p. 383-393, may. 2002.

Referências

NGUYEN, T. M. et al., Kringle 5 of human plasminogen, an angiogenesis inhibitor, induces both autophagy and apoptotic death in endothelial cells. **Blood**, Minnesota, v. 109, n. 11, p. 4793-4802, jun. 2007.

OPPEGARD, L. M. et al. Novel acridine-based compounds that exhibit an anti-pancreatic cancer activity are catalytic inhibitors of human topoisomerase II. **European Journal of Pharmacology**, USA, v. 602, n. 2-3, p. 223-229, jan. 2009.

PANIGRAHY, D. et al. Therapeutic potential of thiazolidinediones as anticancer agents. **Expert Opinon Investigational Drugs**, USA, v. 12, n. 12, p. 1925-1937, dez. 2003.

PCT/BR2012/000421. Thiazacridines used in anti-cancer therapy. LINS GALDINO, Suely; DA ROCHA PITTA, Ivan; DO CARMO ALVES DE LIMA, Maria; GALDINO DA ROCHA PITTA, Marina; ARAUJO BARROS, Francisco Washington; DO Ó PESSOA, Claudia; DE MORAES FILHO, Manoel Odorico; DA ROCHA PITTA, Maira Galdino.

PDB. Protein Data Bank. Disponível em : <<http://www.rcsb.org/pdb/home/home.do>>. Acesso em: 05 set. 2012.

PITTA, Marina Galdino da Rocha. **Novos agentes anticâncer e tiazacridínicos substituídos**: Síntese, estrutura e efeitos biológicos. 2010. 184f. Dissertação (Mestrado em Inovação Terapêutica) - Universidade Federal de Pernambuco, Recife, 2010.

RAO, A. et al. Synthesis and anti-HIV activity of 2,3-diaryl-1,3-thiazolidin-4-ones. **Farmaco**, Italy, v. 58, n. 2, p. 115-20, fev. 2003.

SAMADHIYA, P. et al., Synthesis of 4-thiazolidine derivatives of 6-nitroindazole: pharmaceutical importance. **Journal of the Chilean Chemical Society**, Sagar, v. 57, n. 1, p. 1036-1043, mar. 2012.

SHAY, J. W.; WRIGHT, W.E. Telomerase: a target for cancer therapeutics. **Cancer Cell**, Texas, v. 2, n. 4, p. 257-265, oct. 2002.

SILVA, F. A. et al., Leucemia-linfoma de células T do adulto no Brasil: epidemiologia, tratamento e aspectos controversos. **Revista Brasileira de Cancerologia**, Rio de Janeiro, v. 48, n. 4, p. 585-595, set. 2002.

SILVERSTEIN, R. M.; WEBSTER, F. X.; KIEMLE, D. J. **Identificação espectrométrica de compostos orgânicos**. 7ª ed., Rio de Janeiro: LTC, 2010.

Sistema de Informação sobre Mortalidade (SIM) MS/SVS/DASIS/CGIAE/, MP/Fundação Instituto Brasileiro de Geografia e Estatística (IBGE), MS/INCA/Conprev/Divisão de Informação.

SKONIECZNY, S. *Heterocycles*, v. 6, p. 987, 1977. In: CHIRON, J.; GALY, J-P. Reactivity of the Acridine Ring: A Review. **Synthesis**, France, n. 3, p. 313-25, apr. 2004.

Referências

SUH, N. et al. A new ligand for the peroxisome proliferator-activated receptor-gamma (PPAR γ), GW7845, inhibits rat mammary carcinogenesis. **Cancer Research**, North Carolina, v. 59, n. 22, p. 5671–5673, nov. 1999.

TAVARES, V.; HIRATA, M. H.; HIRATA, R. D. C. Receptor ativado por proliferadores de peroxissoma gama (Pparg): estudo molecular na homeostase da glicose, metabolismo de lipídeos e abordagem terapêutica. **Arquivos Brasileiros de Endocrinologia & Metabologia**, Brasil, v. 51, n.4, jun. 2007.

TOYODA, M. et al. A ligand for peroxisome proliferator activated receptor gamma inhibits cell growth and induces apoptosis in human liver cancer cells. **Gut, An International Journal of Gastroenterology and Hepatology**, Japão, v. 50, n. 4, p. 563–567, abr. 2002.

UDELNOW, A. et al., Omeprazole inhibits proliferation and modulates autophagy in pancreatic cancer cells. **PLoS One**, Ulm, v. 6, n. 5, p. e20143, may. 2011.

WANG, W. et al. Acridine Derivatives Activate p53 and Induce Tumor Cell Death through Bax. **Cancer Biology & Therapy**, Pennsylvania, v. 4, n. 8, p. 893-898, aug. 2005.

World Health Organization, **Fight Against Cancer**. Suíça, 2007. Disponível em: <<http://www.who.int/cancer/publicat/WHOCancerBrochure2007.FINALweb.pdf>>. Acesso em: 11 abr. 2012.

World Health Organization. Suíça, 2012. Disponível em: <<http://www.who.int/topics/cancer/en/>>. Acesso em: 14 mar. 2012.

World Health Organization. Suíça, 2011. Disponível em: <http://gamapserv.who.int/mapLibrary/Files/Maps/Global_Deaths_Cancer_Females_2008.png>. Acesso em: 08 set. 2012.

World Health Organization. Suíça, 2011. Disponível em: <http://gamapserv.who.int/mapLibrary/Files/Maps/Global_Deaths_Cancer_Males_2008.png>. Acesso em: 14 mar. 2012.

ZAMBRE, V. P. et al. Structural investigations of acridine derivatives by CoMFA and CoMSIA reveal novel insight into their structures toward DNA G-quadruplex mediated telomerase inhibition and offer a highly predictive 3D-model for substituted acridines. **Journal of Chemical Information and Modeling**, India, v. 49, n. 5, p. 1298-1311, may. 2009.

Referências

APÊNDICE A - Artigo Publicado. Synthesis and cytotoxic activity of new acridine-thiazolidine derivatives

Journal: Bioorganic & Medicinal Chemistry, v. 10, p. 3533-3539, 2012.

Autors: Francisco W.A. Barros, Teresinha Gonçalves Silva, **Marina Galdino da Rocha Pitta**, Daniel P. Bezerra, Letícia V. Costa-Lotufo, Manoel Odorico de Moraes, Cláudia Pessoa, Maria Aline F.B. de Moura, Fabiane C. de Abreu, Maria do Carmo Alves de Lima, Suely Lins Galdino, Ivan da Rocha Pitta, Marília O.F. Goulart.



Synthesis and cytotoxic activity of new acridine-thiazolidine derivatives

Francisco W.A. Barros^a, Teresinha Gonçalves Silva^b, Marina Galdino da Rocha Pitta^b, Daniel P. Bezerra^c, Leticia V. Costa-Lotuf^a, Manoel Odorico de Moraes^a, Cláudia Pessoa^a, Maria Aline F.B. de Moura^d, Fabiane C. de Abreu^d, Maria do Carmo Alves de Lima^b, Suely Lins Galdino^b, Ivan da Rocha Pitta^{b,*}, Marília O.F. Goulart^{d,*}

^a Departamento de Fisiologia e Farmacologia, Faculdade de Medicina, Universidade Federal do Ceará, Fortaleza, Ceará, Brazil

^b Laboratório de Manejamento e Síntese de Fármacos – LPSF, Grupo de Pesquisa em Inovação Terapêutica – GPIT, Universidade Federal de Pernambuco, Avenida Moraes Rego 1235, Cidade Universitária, CEP 50670-901 Recife, Pernambuco, Brazil

^c Departamento de Fisiologia, Centro de Ciências Biológicas e da Saúde, Universidade Federal de Sergipe, São Cristóvão, Sergipe, Brazil

^d Instituto de Química e Biotecnologia, Universidade Federal de Alagoas, Maceió, Alagoas, Brazil

ARTICLE INFO

Article history:

Received 7 January 2012

Revised 27 March 2012

Accepted 4 April 2012

Available online 10 April 2012

Keywords:

Acridine
Thiazolidines
Cytotoxicity
DNA sensors

ABSTRACT

Although their exact role in controlling tumour growth and apoptosis in humans remains undefined, acridine and thiazolidine compounds have been shown to act as tumour suppressors in most cancers. Based on this finding, a series of novel hybrid 5-acridin-9-ylmethylene-3-benzyl-thiazolidine-2,4-diones were synthesised via N-alkylation and Michael reaction. The cell viability was analysed using a 3-(4,5-dimethylthiazol-2-yl)-2,5-diphenyltetrazolium bromide (MTT) assay, and DNA interaction assays were performed using electrochemical techniques.

© 2012 Elsevier Ltd. All rights reserved.

1. Introduction

Acridine derivatives have been used for commercial purposes for more than a century. They are capable of interacting with nuclear DNA in a sequence-specific manner and with biological targets, such as topoisomerase I and II (topo I and II) and telomerase. These compounds play an important role in a variety of diseases, and they have been used clinically in past decades as antiviral,^{1,2} antiprion,³ antiprotozoal,⁴ anti-inflammatory, antineoplastic⁵ and as analgesic compounds.⁶

The biological activity of acridines has been attributed to the planarity of these aromatic structures, which can intercalate within double-stranded DNA, thus interfering with cellular functions.⁷ Indeed, the mode of action of acridines has been the focus of continuous and exciting research.⁸ In cancer chemotherapy, the biological targets of acridines include DNA topoisomerases I and/or II, telomerase/telomeres and protein-kinases.^{9–15}

Amsacrine is the best-known acridine, and it exhibits potent cytotoxic activity and has been found to be clinically useful. It was also one of the first DNA-intercalating agents to be considered as a topoisomerase II inhibitor. Amsacrine is active in the treatment

of acute leukaemias and lymphomas but is ineffective in solid tumours. Widespread clinical use of this compound has been limited by problems, such as side effects, drug resistance and poor bioavailability, which have encouraged the further structural modification of this compound.¹⁶

In contrast, thiazolidine compounds have emerged as antineoplastic agents with a broad spectrum of antitumour activity against many human cancer cells.^{17–23} These molecules are agonists of peroxisome proliferator-activated receptor γ (PPAR γ), which is expressed in many human tumours, including lung, breast, colon, prostate and bladder,²⁴ and they modulate the proliferation and apoptosis of many cancer cell types. Arylidene-thiazolidine-2,4-diones were also synthesised and screened as anti-inflammatory compounds, showing considerable biological efficacy, when compared to rosiglitazone, agonist of PPAR γ and used as a reference drug.²⁵ As cytotoxic compounds, they were shown to be moderately active in a range higher than 30 μ M.²⁶ Troglitazone and derivatives were assayed as anticancer against PC-3 and androgen dependent LNCaP cells. The respective IC₅₀ values for troglitazone and its Δ^2 -dehydro derivative were 30 \pm 2 and 20 \pm 2 μ M in PC-3 cells and 22 \pm 3 and 14 \pm 1 μ M in LNCaP cells.²⁷

Considering these facts, our strategy was to couple acridine and thiazolidine nucleus to obtain a new class of compounds, the thiaz-acridine derivatives. By assaying their biological activities using diverse techniques based on various mechanisms of action, we found

* Corresponding authors.

E-mail address: mofg@qui.ufal.br (M.O.F. Goulart).

these derivatives to be a new class of drugs that are effective in cancer therapy.

It is clearly of fundamental importance to explore the factors that determine the affinity and selectivity of DNA-binding compounds to ascertain the nature and potency of such molecules, particularly with respect to their potential to cause DNA damage. In this context, the need for stable, low cost, and readily adaptable analytical tools for the detection of DNA damage has been the driving force in the development of DNA-biosensor technology.^{28,29} An electrochemical DNA-biosensor is a receptor-transducer that employs double-stranded DNA (dsDNA) immobilised onto the surface of an electrochemical transducer as a molecular recognition element through which specific DNA-binding processes may be assessed.^{28,30} The interaction of an analyte (i.e., a drug, pro-drug or in situ-generated intermediate) with dsDNA may lead to the rupture of hydrogen bonds and the consequential opening of the double helix, resulting in increased accessibility to the constituent bases. The extent of DNA damage may be determined by monitoring the oxidation of the exposed bases by voltammetric methods. The electrochemical characteristics of such dsDNA-biosensors have been evaluated, and it is clear that this approach can provide a greater understanding of the mechanism of interaction between drugs and DNA and can offer new insights in rational drug design.^{30,31}

Herein, we describe the synthesis of the following acridine-thiazolidine derivatives: 5-(acridin-9-ylmethylene)-3-(4-methyl-benzyl)-thiazolidine-2,4-dione (**9**), 5-(acridin-9-ylmethylene)-3-(4-bromo-benzyl)-thiazolidine-2,4-dione (**10**), 5-(acridin-9-ylmethylene)-3-(4-chloro-benzyl)-thiazolidine-2,4-dione (**11**), and 5-(acridin-9-ylmethylene)-3-(4-fluoro-benzyl)-thiazolidine-2,4-dione (**12**). Moreover, the cytotoxic properties of these derivatives and of some of their precursors were examined in different histotype cancer cell lines, and they were also tested for DNA interaction, using electrochemical methods and DNA biosensors.

2. Results and discussion

2.1. Chemistry

The thiazacridine derivatives **9–12** were synthesised by the nucleophilic addition of substituted 3-benzyl-thiazolidine-diones **5–8** on 3-acridin-9-yl-2-cyano-acrylic acid ethyl ester **3** (Scheme 1). Indeed, the direct condensation of 9-acridinaldehyde **2**, with the substituted thiazolidines **5–8**, did not lead to the expected acridinylidene-thiazolidines. 9-Methyl-acridine **1** was prepared

from diphenylamine with zinc dichloride in acetic acid according to Tsuge et al. (1963).³² Subsequently, the oxidation of **1** with pyridinium chlorochromate, according to Mosher and Natale (1995),³³ gave the 9-acridinaldehyde **2**. The synthetic pathways are illustrated in Scheme 1.

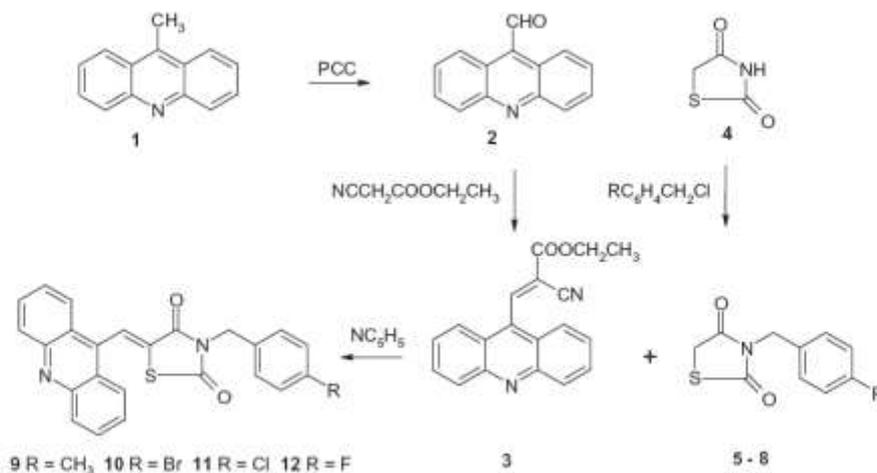
The acridinylidene-thiazolidine **9** was isolated as a single isomer. X-ray crystallographic studies and ¹³C NMR have demonstrated a preferred *Z* configuration for 5-benzylidene-thiazolidinones and 5-benzylidene-imidazolinones.^{34,35} The ³J_{CH}-coupling constant value between the ethylene hydrogen and the carbon atom located at the 4-position of the heterocyclic ring is of special interest in this structural elucidation.³⁶ In contrast, compounds **10** and **12** were isolated as isomeric mixtures. The *Z* isomer was the major stereoisomer formed, and the isomers were readily identified by ¹H NMR, as the ethylene hydrogen is more deshielded in the *Z* isomer than it is in the *E* isomer. The *Z* isomer was isolated for the derivative **11**.

2.2. Biological assays

2.2.1. Cytotoxicity assay

The cytotoxicity of the acridine-thiazolidine derivatives and of some of the precursors: **3** (3-acridin-9-yl-2-cyano-acrylic acid ethyl ester), **5** (3-(4-methyl-benzyl)-thiazolidine-2,4-dione) and **6** (3-(4-bromo-benzyl)-thiazolidine-2,4-dione) was evaluated against tumour cell lines of different histotypes using a previously described MTT assay.³⁷ Amsacrine was used as a positive control. Table 1 summarises the IC₅₀ data for cytotoxic activity. The results indicated that the precursor thiazolidine-2,4-diones **5** and **6** were inactive (IC₅₀ > 25 µg/mL) (not shown in Table 1) and that the 3-acridin-9-yl derivative was significantly active against HL-60 (4.07 µM). The thiazacridines exhibit relatively high cytotoxicity against colon carcinoma and glioblastoma tumour cell lines, possessing IC₅₀ values in the range of 7.4–46.4, 7.2–35.5, 5.8–29.0, and 5.6–58.0 µM for (**9**, **10**, **11**) and (**12**), respectively. However, amsacrine was most active showing IC₅₀ values ranging from 0.08 to 3.3 µM.

The cytotoxicity of the quimeric thiazacridines was also evaluated against normal cells (PBMC and V79). The results presented in Table 1 show that the cytotoxic effects of these acridine-thiazolidine derivatives were less pronounced in normal cells, with a selectivity index (SI) for glioblastoma (SF-295) of 3.7, 3.1, 3.1 and 5.9 for **9–12**, respectively. In addition, these compounds were not found to be active in leukaemia, breast carcinoma or normal lymphoblast cells.



Scheme 1. Synthetic route involved in the preparation of acridine-thiazolidine derivatives.

Apêndice A

Table 1
Cytotoxic activity of acridine-thiazolidine derivatives on cancer and normal cells, in $\mu\text{g/mL}$ (μM)

Cell line ^b	Histotype	Acridine derivatives ^a						Amsacrine ^c
		9	10	11	12	3	3	
Tumour cell								
HL-60	Promyelocytic leukaemia	>25 (60.9)	>25 (52.6)	>25 (58.0)	>25 (60.3)	1.23 (4.07)	0.98–1.55	0.03 (0.08) 0.01–0.09
K-562	Myeloblastoid leukaemia	>25 (60.9)	>25 (52.6)	>25 (58.0)	>25 (60.3)	Nd	Nd	Nd
CEM	Lymphoblastic leukaemia	>25 (60.9)	>25 (52.6)	>25 (58.0)	>25 (60.3)	Nd	Nd	Nd
HCT-8	Colon carcinoma	3.1 (7.4) 2.4–3.8	5.3 (11.2) 4.5–6.3	3.6 (8.3) 3.0–4.3	2.3 (5.6) 1.8–3.0	Nd	2.3 (5.6) 1.8–3.0	0.1 (0.3) 0.03–0.3
HCT-15	Colon carcinoma	11.9 (29.2) 7.5–19.0	9.4 (19.8) 4.9–18.0	9.3 (21.5) 6.6–13.1	24.0 (58.0) 13.4–43.2	Nd	24.0 (58.0) 13.4–43.2	0.1 (0.3) 0.1–1.7
SW-620	Colon carcinoma	11.0 (26.8) 6.7–18.1	16.9 (35.5) 11.2–23.3	8.7 (20.1) 5.8–13.1	12.9 (31.3) 7.8–19.4	Nd	12.9 (31.3) 7.8–19.4	0.1 (0.3) 0.1–0.2
COLO-205	Colon carcinoma	19.1 (46.4) 8.6–42.3	>25 (52.6)	2.7 (6.3) 1.8–4.1	9.5 (23.0) 5.5–16.4	Nd	9.5 (23.0) 5.5–16.4	0.4 (1.1) 0.4–2.0
MDA-MB-231	Breast carcinoma	>25 (60.9)	Nd	>25 (58.0)	Nd	Nd	Nd	Nd
HS-578-T	Breast carcinoma	>25 (60.9)	Nd	>25 (58.0)	Nd	Nd	Nd	Nd
MX-1	Breast carcinoma	>25 (60.9)	Nd	>25 (58.0)	Nd	Nd	Nd	Nd
PC-3	Prostate carcinoma	7.3 (17.7) 5.5–9.5	4.1 (8.6) 2.4–6.8	5.6 (13.0) 3.7–8.5	11.2 (27.1) 6.1–20.8	Nd	11.2 (27.1) 6.1–20.8	1.3 (3.3) 0.5–3.2
DU-145	Prostate carcinoma	>25 (60.9)	Nd	>25 (58.0)	Nd	Nd	Nd	Nd
SF-295	Glioblastoma	3.2 (7.8) 2.6–4.0	3.4 (7.2) 2.8–4.1	4.1 (9.5) 3.5–4.8	2.3 (5.6) 1.8–2.9	Nd	2.3 (5.6) 1.8–2.9	0.10 (0.3) 0.06–0.18
OVCAR-8	Ovarian carcinoma	8.1 (19.7) 5.6–11.7	17.7 (37.2) 13.4–23.4	2.5 (5.7) 1.8–3.5	3.9 (9.3) 2.6–5.8	Nd	7.04 (23.30) 5.73–8.66	0.18 (0.5) 0.08–0.43
UACC-62	Melanoma	8.6 (21.1) 5.3–14.11	24.1 (50.7) 17.8–32.6	12.5 (29.0) 8.4–18.7	3.9 (9.5) 2.7–5.6	Nd	3.9 (9.5) 2.7–5.6	0.5 (1.4) 0.3–0.9
MDA-MB-435	Melanoma	6.4 (15.6) 4.9–8.2	12.3 (25.9) 10.2–14.9	9.6 (22.2) 7.7–11.8	5.8 (14.1) 4.9–7.0	Nd	5.8 (14.1) 4.9–7.0	Nd
Normal cells								
PERMC ^d	Peripheral lymphoblast	>25 (60.9)	>25 (52.6)	>25 (58.0)	>25 (60.3)	Nd	>25 (60.3)	8.5 (21.7) 6.8–9.9
V79	Lung fibroblasts ^e	11.7 (28.5) 7.8–18.5	10.7 (22.6) 6.4–18.1	7.7 (17.9) 5.7–10.5	13.5 (32.7) 9.1–20.1	Nd	13.5 (32.7) 9.1–20.1	2.3 (5.8) 1.7–3.6

^a Data are presented as K_{50} values in $\mu\text{g/mL}$ (μM) and as the 95% confidence interval obtained by nonlinear regression for all of the cell lines from two independent experiments, performed in duplicate, after 72 h of incubation.

^b Cell survival was evaluated by the MTT assay, as reported in the Section 4.

^c Amsacrine was used as a positive control.

^d Cell survival was evaluated by the Alamar blue assay, as reported in the Section 4.

^e Chinese hamster cell line. Nd: not determined.

Apêndice A

The selectivity index of amsacrine to glioblastoma was of 11.6 showing a greater selectivity for tumour cells compared with thiazacridines. The SI was calculated with the following formula: $SI = IC_{50}(V79)/IC_{50}(SF-295)$.

Although the thiazacridines were shown to be less active and less selective than amsacrine, the selectivity for solid tumour cell lines is interesting and deserves attention as a target for study. In fact, some compounds, such as bisannulated acridines, have been shown to have solid tumour-selective cytotoxicity.³⁸ Some aminoderivatives of azapyranoxanthene have shown greater cytotoxic potential against colon tumour cells than against leukaemia cells.³⁹ However, the basis for this solid tumour selectivity remains unclear.

None of the compounds described here were able to cause haemolysis in mouse erythrocytes, even at the highest concentration (200 $\mu\text{g/mL}$) (data not shown). The absence of lytic effects suggests that the cytotoxicity of these compounds is not related to membrane disruption and is likely related to more specific cellular pathways. The target could be DNA, as has been observed for acridine compounds.^{40,41}

2.2.2. DNA interaction assay

Results from the dsDNA biosensor show positive interactions for all of the acridines, as represented by the appearance of guanosine ($E_p = 0.8 \text{ V}$) and adenosine ($E_p = 1.0 \text{ V}$) peaks (Figs. 1A–4A). This clearly demonstrates that damage from the compounds caused a distortion of the double helix and exposure of the bases to oxidation. In the experiments using ssDNA in solution, a decrease of the oxidation waves of the nucleobases, guanosine and adenosine, with eventual anodic potential shifts (mainly for **11**), were observed, confirming the interaction with DNA (Figs. 1B–4B).

3. Conclusion

The acridine-thiazolidines derivatives herein investigated showed promising cytotoxic activity. The synthesis of the quimeric compounds is worthy once there was an increase of cytotoxic activity compared to precursors. Although less active and selective than the positive control amsacrine, all of them exhibited relatively high cytotoxicity, predominantly on colon carcinoma and glioblastoma tumour cell lines, whereas no activity on leukaemia, breast carcinoma, or normal lymphoblast cells was observed. Taking into account the selectivity for cells of solid tumours, as well as, the positive interaction with the DNA shown in the electrochemical tests,

we propose that the modified acridine-thiazolidines could be promising key structures in anticancer drug development.

4. Experimental part

4.1. Chemistry

The melting points were measured in capillary tubes on a Buchi (or Quimis) apparatus. Thin layer chromatography was performed on silica gel plates from Merck (60_{F254}). The infrared spectra of 1% KBr pellets were recorded on a Bruker IFS66 spectrometer. ¹H NMR spectra were recorded on a Bruker AC 300 P spectrophotometer using DMSO-*d*₆ as the solvent, with tetramethylsilane as an internal standard. Electronic impact mass spectra were measured at 70 eV on a Finnigan GCQ Mat Quadrupole Ion-Trap. The MS data fully agreed with the proposed structures.

The chemical data on 5-acridin-9-ylmethylene-3-(4-methylbenzyl)-thiazolidine-2,4-dione **9**, 5-acridin-9-ylmethylene-3-(4-bromo-benzyl)-thiazolidine-2,4-dione **10**⁴² and 5-(acridin-9-ylmethylene)-3-(4-fluoro-benzyl)-1,3-thiazolidine-2,4-dione **12**⁴³ are reported elsewhere.^{42,43} Thiazolidine-2,4-dione was N-(3-alkylated) in the presence of potassium hydroxide, which enabled the thiazolidine potassium salt to react with substituted benzyl halide in a hot alcohol medium.

4.1.1. (5Z)-5-(Acridin-9-ylmethylene)-3-(4-chloro-benzyl)-1,3-thiazolidine-2,4-dione **11**

4-Chloro-benzylthiazolidine (0.9 mmol) and 3-acridin-9-yl-2-cyano-acrylic acid ethyl ester (0.9 mmol) were dissolved in absolute ethanol (8 mL). The solution was refluxed for 4 h in the presence of a small amount of piperidine as a catalyst. The precipitate obtained was filtered and washed with water. C₂₄H₁₅ClN₂O₂S. Yield 51%. Mp 204–206 °C. TLC *R*_f 0.73, (*n*-hexane/ethyl acetate 6:4). IR cm⁻¹ (KBr) ν 1748, 1695, 1624, 1379, 1334, 1149, and 760. ¹H NMR (δ ppm, DMSO-*d*₆) 4.88 (s, CH₂); 7.46 (s, 4H benzyl), 7.69 (dt, 2H 2,7-acridin, *J* = 7.8 and 1.2 Hz), 7.92 (dt, 2H 3,6-acridin, *J* = 7.8 and 1.2 Hz), 8.15 (d, 2H 1,8-acridin, *J* = 8.4 Hz), 8.24 (d, 2H 4,5-acridin, *J* = 8.4 Hz), 8.79 (s, 1H, ethylene). ¹³C NMR (DMSO-*d*₆, DEPT): δ 44(CH₂), 122.3(2C), 125.6 (2CH), 126.9 (2CH), 128.5 (2CH), 129 (C), 129.7 (C), 129.9 (2CH), 130.7 (2CH), 131.9 (C), 132.5 (C), 134.2 (C), 138.0 (2C), 148 (2CH), 164 (CO), 166.8 (CO). Ms EI 70 eV, *m/z* (%) 430 (M⁺ 2.5), 305(20.3), 235(100), 234(75.1), 231(80.1), 203(16.8), 190(16.9), and 125(28.8).

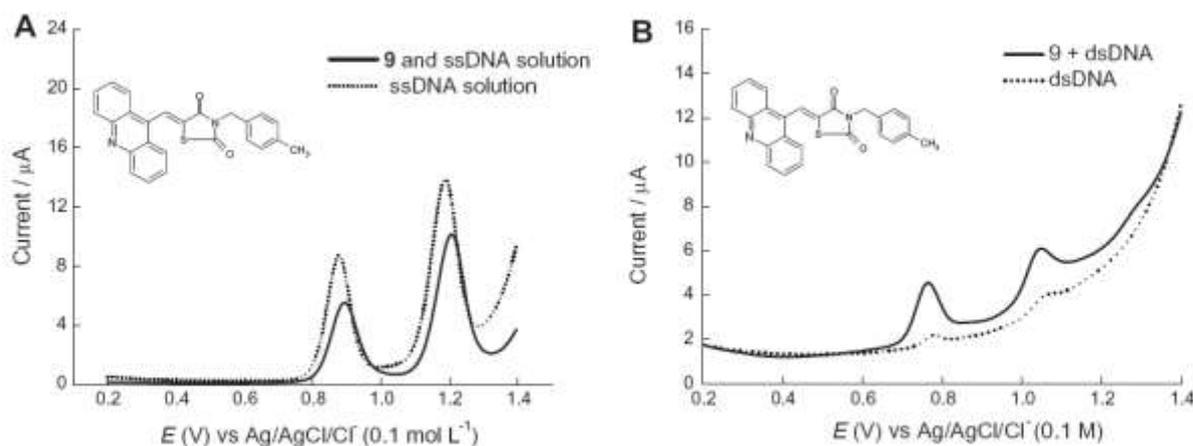


Figure 1. (A) Differential pulse voltammogram (DPV) at pH 4.5 for the oxidation of **9** attached to the surface of carbon paste electrode (CPE) in the presence of a ssDNA solution ($1.0 \times 10^{-4} \text{ M}$). (B) Differential pulse voltammogram, at pH 4.5, of the dsDNA biosensor in the absence and in the presence of **9** in solution ($1.0 \times 10^{-4} \text{ M}$). Equilibration time = 5 s, $\Delta E_s = 2 \text{ mV}$, $\Delta E_{\text{DPV}} = 50 \text{ mV}$, $\nu = 5 \text{ mV s}^{-1}$.

Apêndice A

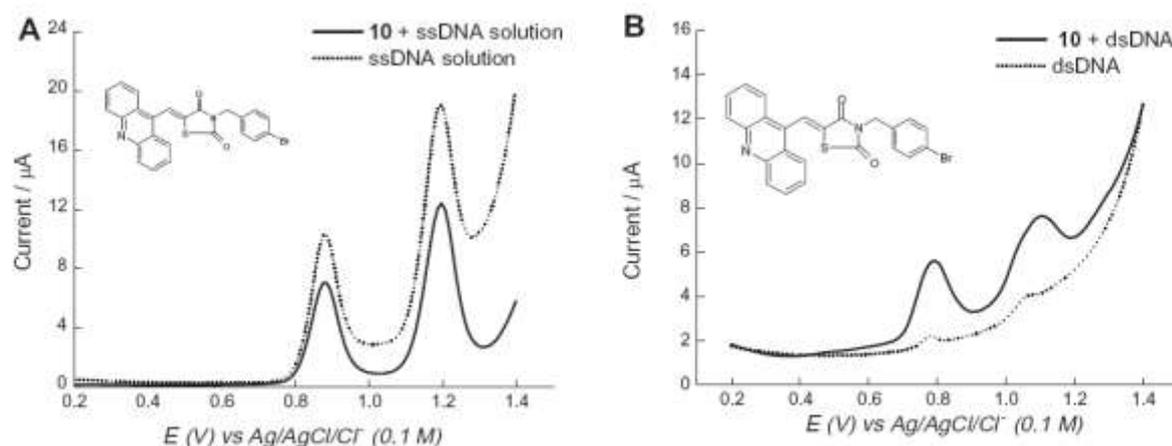


Figure 2. (A) Differential pulse voltammogram at pH 4.5 for the oxidation of **10** attached to the surface of CPE in the presence of a ssDNA solution (1.0×10^{-4} M). (B) Differential pulse voltammogram at pH 4.5 of the dsDNA biosensor in the absence and in the presence of **10** in solution (1.0×10^{-4} M). Equilibration time = 5 s, $\Delta E_s = 2$ mV, $\Delta E_{dpv} = 50$ mV, $v = 5$ mV s $^{-1}$.

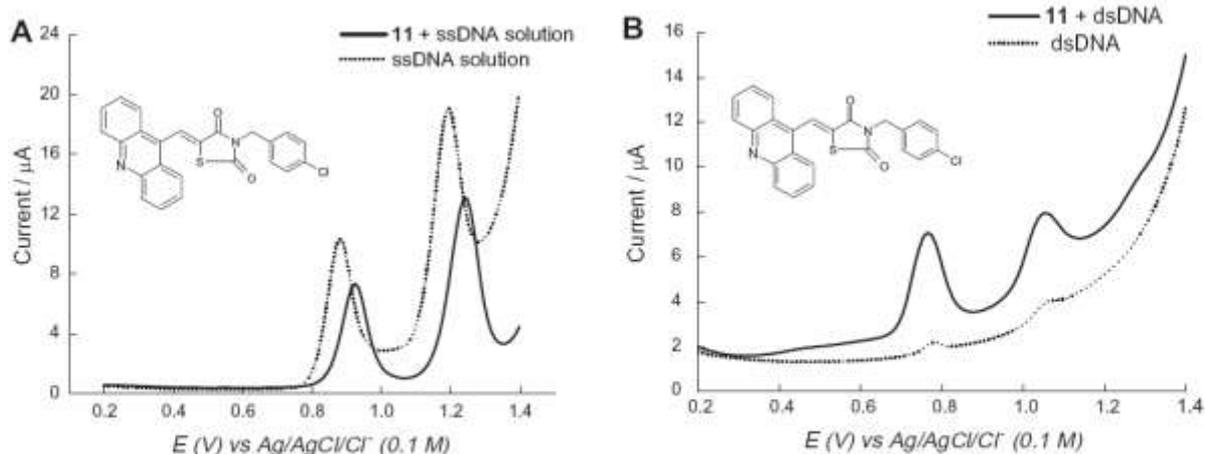


Figure 3. (A) Differential pulse voltammograms at pH 4.5 for the oxidation of **11** attached to the surface of CPE in the presence of a ssDNA solution (1.0×10^{-4} M). (B) Differential pulse voltammogram at pH 4.5 of the dsDNA biosensor in the absence and in the presence of **11** solution (1.0×10^{-4} M). Equilibration time = 5 s, $\Delta E_s = 2$ mV, $\Delta E_{dpv} = 50$ mV, $v = 5$ mV s $^{-1}$.

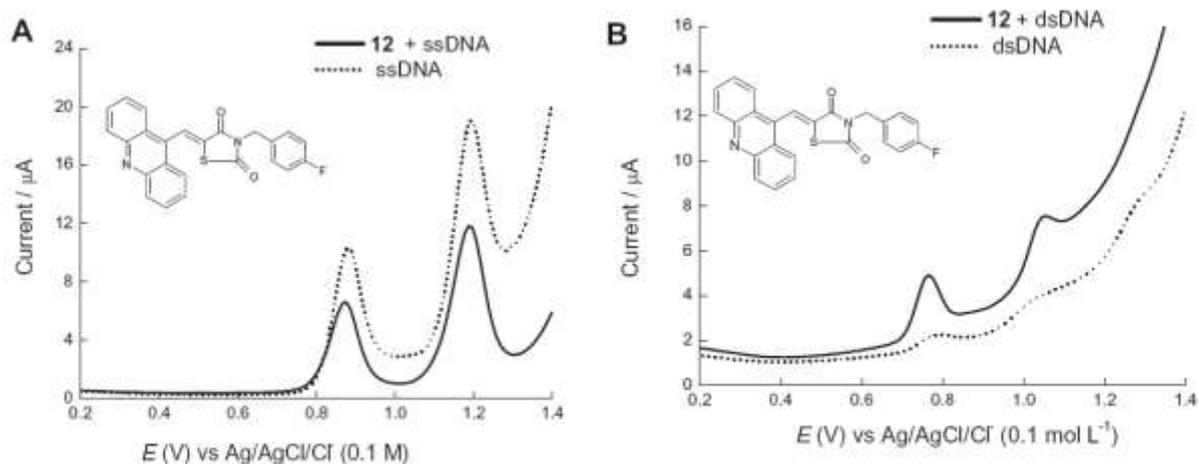


Figure 4. (A) Differential pulse voltammogram at pH 4.5 for the oxidation of **12** attached to the surface of CPE in the presence of a ssDNA solution (1.0×10^{-4} M). (B) Differential pulse voltammogram at pH 4.5 of the dsDNA biosensor in the absence and in the presence of **12** in solution (1.0×10^{-4} M). Equilibration time = 5 s, $\Delta E_s = 2$ mV, $\Delta E_{dpv} = 50$ mV, $v = 5$ mV s $^{-1}$.

Apêndice A

4.2. Biological

4.2.1. MTT assay

The cytotoxic effects of the synthesised compounds were evaluated against the following human cancer cell lines, all obtained from the National Cancer Institute, Bethesda, MD, USA: HL-60 (promyelocytic leukaemia), K-562 (myeloblastoid leukaemia), CEM (lymphoblastic leukaemia), HCT-8 (colon carcinoma), HCT-15 (colon carcinoma), SW-620 (colon carcinoma), COLO-205 (colon carcinoma), MDA-MB-231 (breast carcinoma), HS-578-T (breast carcinoma), MX-1 (breast carcinoma), PC-3 (prostate carcinoma), DU-145 (prostate carcinoma), SF-295 (glioblastoma), OVCAR-8 (ovarian carcinoma), UACC-62 (melanoma), and MDA-MB-435 (melanoma). Chinese hamster lung fibroblasts (V79 – normal cells), kindly provided by Dr. J.A.P. Henriques (Federal University of Rio Grande do Sul, Porto Alegre, Brazil), were also used. The cell lines were maintained in RPMI-1640 medium (cancer cells) or MEM with Earle's salts (V79 cells) supplemented with 10% foetal bovine serum, 2 mM glutamine, 100 U/mL penicillin and 100 µg/mL streptomycin at 37 °C with 5% CO₂.

Cell growth was quantified by the ability of living cells to reduce a yellow dye, 3-(4,5-dimethyl-2-thiazolyl)-2,5-diphenyl-2H-tetrazolium bromide (MTT), to a purple formazan product.³⁷ For all of the experiments, the cells were seeded in 96-well plates (0.7 × 10⁵ cells/well for adherent cells and 0.3 × 10⁶ cells/mL for suspended cells). After 24 h, the compounds (0.048–25 µg/mL), dissolved in DMSO, were added to each well (using an HTS (high-throughput screening) Biomek 3000, Beckman Coulter, Inc., Fullerton, California, USA) and incubated for 72 h. Amsacrine (Sigma Aldrich Co., St. Louis, MO, USA) was used as a positive control. At the end of the incubation, the plates were centrifuged, and the medium was replaced by fresh medium (150 µL) containing 0.5 mg/mL MTT. After 3 h, the formazan product was dissolved in 150 µL DMSO, and the absorbance was measured using a multiplate reader (DTX 880 Multimode Detector, Beckman Coulter, Inc., Fullerton, California, USA). The substance effect was quantified as the percentage of the control absorbance at 595 nm.

4.2.2. Alamar blue assay

The cytotoxic effects of the synthesised compounds were evaluated against PBMC (peripheral blood mononuclear cells) from healthy donors using the Alamar blue assay.⁴⁴ Heparinised blood (from healthy, non-smoker donors who had not taken any drug for at least 15 days prior to sampling) was collected, and the PBMC were isolated by a standard method of density-gradient centrifugation using Ficoll-Hypaque. PBMC were cultivated in RPMI-1640 medium supplemented with 20% foetal bovine serum, 2 mM glutamine, 100 U/mL penicillin, and 100 mg/mL streptomycin at 37 °C with 5% CO₂. Phytohaemagglutinin (2%) was added at the beginning of the culture period.

Briefly, the PBMC were plated in 96-well plates (3 × 10⁵ cells/mL in 100 µL of medium). After 24 h, the compounds (0.048–25 µg/mL), dissolved in DMSO, were added to each well (using an HTS Biomek 3000, Beckman Coulter, Inc., Fullerton, California, USA) and incubated for 72 h. Amsacrine (Sigma Aldrich Co., St. Louis, MO, USA) was used as a positive control. At 24 h before the end of the incubation, 10 µL of a stock solution (0.312 mg/mL) of Alamar blue (resazurin, Sigma Aldrich Co., St. Louis, MO, USA) was added to each well. The absorbance was measured using a multiplate reader (DTX 880 Multimode Detector, Beckman Coulter, Inc., Fullerton, California, USA), and the effect of the drug was quantified as the percentage of the control absorbance at 570 and 595 nm.

4.2.3. Haemolysis assay

The test was performed in 96-well plates using a 2% mouse erythrocyte suspension in 0.85% NaCl containing 10 mM CaCl₂ fol-

lowing the method described by Costa-Lotufo et al. (2002).⁴⁵ The diluted compounds were tested at concentrations ranging from 1.5 to 200 mg/mL. Triton X-100 (1%) was used as a positive control. After incubation at room temperature for 30 min followed by centrifugation, the supernatant was removed, and the liberated haemoglobin was measured spectrophotometrically at 540 nm.

4.3. DNA interaction assay

4.3.1. Electrochemical approaches

The following experiments were conducted to evaluate the interaction of acridine-thiazolidine derivatives with DNA by electrochemical methods. Electrochemical experiments including differential pulse voltammetry (DPV) were performed using an Autolab (Echo-Chemie, Utrecht, Netherlands) PGSTAT 20 or PGSTAT-30. The working electrodes were a BAS (Bioanalytical Systems, West Lafayette, IN, USA) GC electrode of 3-mm diameter or a carbon paste electrode and a carbon paste electrode modified with acridine-thiazolidine derivatives. The counter electrode was a platinum coil, and the reference electrode was Ag|AgCl, Cl⁻ (0.1 M); all electrodes were contained in a single-compartment electrochemical cell with a 10 mL capacity. The optimised differential pulse voltammetry parameters were as follows: pulse amplitude (ΔE_{sw}) of 50 mV, pulse width of 70 ms and a scan rate of 5 mV s⁻¹ (using a step potential [ΔE_s] of 2 mV). The glassy carbon electrode was polished with alumina on a polishing felt (BAS polishing kit). After mechanical cleaning, the electrochemical pretreatment of the glassy carbon electrode involved a sequence of five cyclic potential scans from 0 to +1.4 V in acetate buffer at pH 4.5. All of the experiments were carried out at room temperature (25 ± 1 °C).

4.3.1.1. Preparation of the dsDNA-GC biosensor and its interaction with acridine-thiazolidine derivatives.

The electrochemical procedure for the investigation of the acridine-thiazolidine derivatives and dsDNA interaction involved three steps: preparation of the electrode surface, immobilisation of the dsDNA gel and voltammetric transduction. The GC electrode was first polished with alumina, using a Metrohm felt-polishing pad, until the surface displayed a mirror-like appearance. The electrode was then electrochemically pretreated with a sequence of five cyclic potential scans from 0 to +1.4 V versus Ag|AgCl, Cl⁻ (0.1 M) in acetate buffer,²⁸ washed thoroughly with distilled/deionised water, dried and placed in an upright position in the cell.

To immobilise the dsDNA (calf thymus, type 1), the surface of the electrode was coated with 10 µL of calf thymus DNA solution (containing 12.0 mg of dsDNA in 1.0 mL of acetate buffer). The quantity (0.36 mg) of dsDNA employed was estimated to be sufficient to cover the entire surface of the GC electrode.²⁸ The dsDNA was allowed to dry at room temperature under a stream of nitrogen. Immediately after drying, 20 µL of an ethanolic solution of the acridine-thiazolidine derivatives (10⁻⁴ M) was added with sequential drying. The prepared biosensor was then put into the appropriate cell, covered with 5 mL of aqueous acetate buffer and analysed at $E = 0$ to 1.4 V.²⁸ For each series of experiments, an identical dsDNA-GC electrode was prepared as a reference blank as a control; this electrode was not treated with substrate but received the same pre- and post-treatments as the test electrode.

The procedure produced a thick-layer dsDNA-modified electrode. Because uniform coverage of the electrode surface had been achieved, any new peaks observed in the presence of the additive were due solely to the interaction of the analyte with the DNA film not from the diffusion process in solution.²⁹

4.3.1.2. Preparation of the carbon paste electrode modified with acridine-thiazolidine derivatives.

Analyses of the interaction between test substances and ssDNA are generally

Apêndice A

performed in solution. Due to the insolubility of acridines in aqueous solution, it was necessary to adapt a methodology to analyse them. This one consisted of incorporating acridine-thiazolidine derivatives in carbon paste.⁴⁶ Activated graphite (45 mg) was mixed with 1 mL of an ethanol solution of the acridine-thiazolidine samples (10^{-4} mol L⁻¹) and stirred for approximately 20 min until the solvent was completely evaporated. To ensure complete evaporation, the mixture was subjected to a nitrogen atmosphere. Next, 20 μ L of commercial mineral oil was added and mixed strongly to achieve a uniform texture. In this case, a blank (control) was also produced by the addition of ethanol only (no substance) to graphite and a subsequent mixture with mineral oil.

4.3.1.3. Preparation of ssDNA and its interaction with acridine-thiazolidine derivatives. Single-stranded DNA (ssDNA) was prepared by dissolving 3.0 mg of dsDNA in 1.0 mL of hydrochloric acid (1 M) and heating for 1 h until complete dissolution. This treatment was followed by neutralising the solution with 1.0 mL of sodium hydroxide (1 M) and 9 mL of acetate buffer was then added.^{28,29}

Freshly prepared ssDNA solution was added to the cell, and single-scan DPV experiments were conducted in the range of 0 to +1.4 V versus Ag/AgCl, Cl⁻ (0.1 M). Two peaks corresponding to the oxidation of the guanosine and adenosine bases appeared at potentials of +0.815 and +1.131 V, respectively. To ensure reproducibility, this assay format was repeated at least three times, and the oxidation current and potential of the bases were very similar (rsd of 5%). After this process, the carbon paste electrode modified with acridine-thiazolidine derivatives was inserted into the ssDNA solution, and the DPV experiment was performed. An unmodified carbon paste electrode was also employed in the DPV experiments involving the ssDNA solution and was used for comparison.

4.3.1.4. Statistical analysis. The IC₅₀ values and their 95% confidence intervals (CI 95%) were obtained by nonlinear regression using the GRAPHPAD program (Intuitive Software for Science, San Diego, CA, USA).

Acknowledgments

This study was supported by the Brazilian National Research Council and National Institute of Science and Technology for Pharmaceutical Innovation (CNPq/RENORBIO/INCT_IF), as well as the INCT-Bioanalítica. The authors wish to thank Professor José Dias de Souza Filho (Universidade Federal de Minas Gerais, Belo Horizonte, MG, Brazil) for the obtention of the ¹³C NMR.

Supplementary data

Supplementary data associated with this article can be found, in the online version, at <http://dx.doi.org/10.1016/j.bmc.2012.04.007>.

References and notes

1. Csuk, R.; Barthel, A.; Brezesinski, T.; Raschke, C. *Bioorg. Med. Chem. Lett.* **2004**, *14*, 4983.
2. Aly El-Moghazy, S. M.; Mikhael, A. N.; Eissa, A. A. H.; Ebeid, M. Y. *Egypt J. Pharm. Sci.* **1994**, *34*, 401.
3. Dollinger, S.; Loeber, S.; Klingenstein, S.; Korth, C.; Gmeiner, P. A. *J. Med. Chem.* **2006**, *49*, 6591.
4. Karolak-Wojciechowska, J.; Mrozek, A.; Amiel, P.; Brouant, P.; Barbe, J. *Acta Crystallogr., Sect. C* **1996**, *C52*, 2939.
5. Hartwell, J. L.; Shear, M. J.; Johnson, J. M.; Kornberg, S. R. *L. Cancer Res.* **1946**, *6*, 489.
6. Sondhi, S. M.; Bhattacharjee, G.; Jameel, R. K.; Shukla, R.; Raghuram, R.; Lozach, O.; Meijer, L. *Cent. Eur. J. Chem.* **2004**, *2*, 1.
7. Belmont, P.; Bosson, J.; Godet, T.; Tiano, M. *Anticancer Agents Med. Chem.* **2007**, *7*, 139.
8. Pigatto, M. C.; Lima, M. C. A.; Galdino, S. L.; Pitta, I. R.; Vessecchi, R.; Assis, M. D.; Santos, J. S.; Costa, T. D.; Lopes, N. P. *Eur. J. Med. Chem.* **2011**, *46*, 4245.
9. Goodell, J. R.; Ougolkov, A. V.; Hiasa, H.; Kaur, H.; Remmel, R.; Billadeau, D. D.; Ferguson, D. M. *J. Med. Chem.* **2008**, *51*, 179.
10. Rogojina, A. T.; Nitiss, J. L. *J. Biol. Chem.* **2008**, *283*, 29239.
11. Oppgard, L. M.; Ougolkov, A. V.; Luchini, D. N.; Schoon, R. A.; Goodell, J. R.; Kaur, H.; Billadeau, D. D.; Ferguson, D. M.; Hiasa, H. *Eur. J. Pharmacol.* **2009**, *602*, 223.
12. Kleideiter, E.; Piotrowska, K.; Klotz, U. *Methods Mol. Biol.* **2007**, *405*, 167.
13. Gunaratnam, M.; Greciano, O.; Martins, C.; Reszka, A. P.; Schultes, C. M.; Morjani, H.; Riou, J. F.; Neidle, S. *Biochem. Pharmacol.* **2007**, *74*, 679.
14. Castillo-González, D.; Cabrera-Pérez, M. A.; Pérez-González, M.; Helguera, A. M.; Durán-Martínez, A. *Eur. J. Med. Chem.* **2009**, *44*, 4826.
15. Guo, C.; Gasparian, A. V.; Zhuang, Z.; Bosykh, D. A.; Komar, A. A.; Gudkov, A. V.; Gurova, K. V. *Oncogene* **2009**, *28*, 1151.
16. Sánchez, I.; Rechtes, R.; Caignard, D. H.; Renard, P.; Pujol, M. D. *Eur. J. Med. Chem.* **2006**, *41*, 340.
17. Ban, J. O.; Kwak, D. H.; Oh, J. H.; Park, E. J.; Cho, M. C.; Song, H. S.; Song, M. J.; Han, S. B.; Moon, D. C.; Kang, K. W.; Hong, J. T. *Chem. Biol. Interact.* **2010**, *188*, 75.
18. El-Gaby, M. S. A.; Ismail, Z. H.; Abdel-Gawad, S. M.; Aly, H. M.; Ghorab, M. M. *Phosphorus, Sulfur Silicon Relat. Elem.* **2009**, *184*, 2645.
19. Beharry, Z.; Zemskova, M.; Mahajan, S.; Zhang, F.; Ma, J.; Xia, Z.; Lilly, M.; Smith, C. D.; Kraft, A. S. *Mol. Cancer Ther.* **2009**, *8*, 1473.
20. Chandrappa, S.; Benaka, P. S. B.; Vinaya, K.; Ananda, K. C. S.; Thimmegowda, N. R.; Rangappa, K. S. *Invest. New Drugs* **2008**, *26*, 437.
21. Li, W.; Lu, Y.; Wang, Z.; Dalton, J. T.; Miller, D. D. *Bioorg. Med. Chem. Lett.* **2007**, *17*, 4113.
22. Shiao, C. W.; Yang, C. C.; Kulp, S. K.; Chen, K. F.; Chen, C. S.; Huang, J. W.; Chen, C. S. *Cancer Res.* **2005**, *65*, 1561.
23. Ip, M. M.; Sylvestre, P. W.; Schenkel, L. *Cancer Res.* **1986**, *46*, 1735.
24. Han, S.; Roman, J. *Anti-Cancer Drugs* **2009**, *18*, 237.
25. Barros, C. D.; Amato, A. A.; de Oliveira, T. B.; Iannini, K. B.; Silva, A. L.; Silva, T. G.; Leite, E. S.; Hernandez, M. Z.; Alves de Lima, M. do C.; Galdino, S. L.; Neves, F. de A.; Pitta, R. *Bioorg. Med. Chem.* **2010**, *18*, 3805.
26. Alegaon, S. G.; Alagawadi, K. R. *Med. Chem. Res.* <http://dx.doi.org/10.1007/s00044-011-9876-x>.
27. Shiao, C.-W.; Yang, C.-C.; Kulp, S. K. *Cancer Res.* **2005**, *65*, 1561–1569.
28. Diclescu, V. C.; Paquim, A. M. C.; Brett, A. M. O. *Sensors* **2005**, *5*, 377.
29. De Abreu, F. C.; De Paula, F. S.; Ferreira, D. C. M.; Nascimento, V. B.; Santos, A. M. C.; Santoro, M. M.; Salas, C. E.; Lopes, J. C. D.; Goulart, M. O. F. *Sensors* **2008**, *8*, 1519.
30. Hillard, E. A.; De Abreu, F. C.; Ferreira, D. C. M.; Jaouen, G.; Goulart, M. O. F.; Amatore, C. *Chem. Commun.* **2008**, 2612.
31. Rauf, S.; Gooding, J. J.; Akhtar, K.; Ghauri, M. A.; Rahman, M.; Anwar, M. A.; Khalid, A. M. *J. Pharm. Biomed. Anal.* **2005**, *37*, 205.
32. Tsuge, O.; Nishinohara, M.; Tashiro, M. B. *Chem. Soc. Jpn.* **1963**, *36*, 1477.
33. Mosher, M. D.; Natale, N. R. *J. Heterocycl. Chem.* **1995**, *32*, 779.
34. Tan, F.; Ang, K. P.; Fong, Y. F. *J. Chem. Soc., Perkin Trans. II* **1941**, 1986, 12.
35. De Simone, C. A.; Zukerman-Schpector, J.; Pereira, M. A.; Luu-Duc, C.; Pitta, I. R.; Galdino, S. L.; Amorim, E. L. C. *Acta Cryst.* **1995**, *C51*, 2620.
36. Karabatsos, G. J.; Orzech, C. E. *J. Am. Chem. Soc.* **1965**, *87*, 560.
37. Mosmann, T. *J. Immunol. Methods* **1983**, *316*, 55.
38. Thale, Z.; Johnson, T.; Tenney, K.; Wenzel, P. J.; Lobkovsky, E.; Clardy, J.; Media, J.; Pietraszkiewicz, H.; Valeriote, F. A.; Crews, P. *J. Org. Chem.* **2002**, *67*, 9384.
39. Kolokythas, G.; Pouli, N.; Marakos, P.; Pratsinis, H.; Kletsas, D. *Eur. J. Med. Chem.* **2006**, *41*, 71.
40. Antonini, I. *Curr. Med. Chem.* **2002**, *9*, 1701.
41. Janovec, L.; Kořturková, M.; Sabolová, D.; Ungvárský, J.; Paulíková, H.; Pšáková, J.; Vantová, Z.; Imrich, J. *Bioorg. Med. Chem.* **2011**, *19*, 1790.
42. Silva, T. G.; Barbosa, F. S. V.; Brandão, S. S. F.; Lima, M. C. A.; Galdino, S. L.; Pitta, I. R.; Barbe, J. *Heter. Comm.* **2001**, *7*, 523.
43. Mourão, R. H.; Silva, T. G.; Soares, A. L.; Vieira, E. S.; Santos, J. N.; Lima, M. C.; Lima, V. L.; Galdino, S. L.; Barbe, J.; Pitta, I. R. *Eur. J. Med. Chem.* **2005**, *40*, 1129.
44. Ahmed, S. A.; Gogal, R. M.; Walsh, J. E. *J. Immunol. Meth.* **1994**, *170*, 211.
45. Costa-Lotufu, L. V.; Cunha, G. M. A.; Farias, P. A. M.; Viana, G. S. B.; Cunha, K. M. A.; Pessoa, C.; Moraes, M. O.; Silveira, E. R.; Gramosa, N. V.; Rao, V. S. N. *Toxicol.* **2002**, *40*, 1231.
46. Lima, P. R.; Miranda, P. R. B.; Oliveira, A. B.; Goulart, M. O. F.; Kubota, L. T. *Electroanalytical* **2009**, *21*, 2311.

Apêndice A

APÊNDICE B - Artigo publicado. Niche for Acridine Derivatives in Anticancer Therapy

Journal: Mini-reviews in Medicinal Chemistry, v. 13, n. 9, 2013.

Autores: **Marina Galdino da Rocha Pitta**, Maria do Carmo Alves de Lima, Suely Lins
Galdino, Ivan da Rocha Pitta



Niche for Acridine Derivatives in Anticancer Therapy

Galdino-Pitta, M.R.; Pitta, M.G.R.; Lima, M.C.A.; Galdino, S.L. and Pitta, I.R.*

Núcleo de Pesquisa em Inovação Terapêutica Sueli Galdino, Universidade Federal de Pernambuco

Abstract: During the last 4 decades, intensive research has focussed on the effect of small organic molecules with antitumour activity that are able to intercalate into DNA and inhibit topoisomerase and telomerase enzymes. In this review, we describe some of the chemical and biological properties of acridine, which is a chemotherapeutic agent that has been used for cancer treatment since 1970. In addition, we summarise the progress that has been made in the development of anticancer agents based on the clinical *in vivo/in vitro* studies that have been conducted for 13 classes of natural and synthetic acridines.

Keywords: Acridine, Anticancer, Antitumour, Chemotherapy, DNA intercalation, Topoisomerases.

INTRODUCTION

Cancer is considered one of the most challenging diseases to treat, because despite advancements in our understanding of the disease, several types still have no cure, and some tumour cells have become resistant to the drugs currently available in clinics. Thus, cancer therapy remains a challenge for all health sectors worldwide.

The likelihood of an early diagnosis in developed countries is much higher than in less developed or developing countries, which is owing to the population's general lack of access to health services. Often, a diagnosis is only made during the later stages of the cancer's progression, when the probability of a complete recovery is much lower [1].

Worldwide, cancer has the second highest mortality rate (after cardiovascular disease); however, it is one of the most preventable non communicable chronic diseases. In 2008, 7.6 million people died due to cancer, and three-quarters of them were from low- or middle-income countries. By 2015, this number is expected to rise to 9 million and increase further to 11.5 million in 2030 [2]. However, these numbers could be minimised if the government and health professionals were to collaborate to enable the development of new and better strategies for the prevention, control, and early detection of cancer.

With the aim to develop more potent and less toxic anticancer drugs, several research groups have focussed on acridine derivatives for cancer treatment, owing to their wide range of biological activity and to their ability to interact with several biological targets [3,4]. Fig. (1) shows the firsts

acridine derivatives, which were developed as antibacterial (proflavine) and anti malarial (mepacrine) compounds.

Although medical interest regarding the use of acridines as treatment compounds dates from 1888, it was not until 1913, after Browning discovered the bactericidal action of proflavine and acriflavine, that they began to be used in medical practice [5-8]. In 1930, mepacrine was discovered, which is the first synthetic anti malarial drug that is comparable to quinine in activity (Fig. 1).

The anticancer properties of acridines were first considered in the 1920s. Since then, several compounds (natural alkaloids or synthetic molecules) have been tested as anti tumour agents [3]. Currently, acridine agents are used in the clinic to treat bacterial and protozoan infections [9-12], malaria [13-18], leishmaniasis [17, 19, 20], virus infection [21-25], Chagas disease [17, 18, 26, 27], Parkinson's disease [28, 29], Alzheimer's disease [30, 31], lupus erythematosus [32], and cancer [3, 33-36]. In Table 1 we summarize acridine derivatives used for the treatment of cancer that show some clinical or preclinical benefits.

Acridine derivatives have strong activity owing to their ability to intercalate into DNA between base pairs, leading to cell cycle arrest and apoptosis [47]. In addition, they disrupt the cell cycle by inhibiting the enzymes essential for this process, (i.e., topoisomerase II [Topo II] and telomerase. Topo II is critical for cell replication because it affects the structural changes of DNA, enabling replication, transcription, and decatenation [48]. However, quinacrine- a drug that is used for the treatment of rheumatic arthritis, lupus erythematosus, malaria, tapeworm infections, Chagas disease, and epilepsy -inhibits the generation of the toxic isoform of the prionprotein in an intoxicated cell culture [49].

In 2011, Zawada *et al.* used quantum chemical modeling to enhance the future development of other biologically functional derivatives, as well as to understand the function

*Address correspondence to this author at the Núcleo de Pesquisa em Inovação Terapêutica, Universidade Federal de Pernambuco Av. Prof Moraes Rego nº 1235, Cidade Universitária CEP: 50.670-901 Recife-PE, Brasil; Tel: 55(81)2126-8947; Fax: 55(81)2126-8947; E-mail: marinapitta@gmail.com

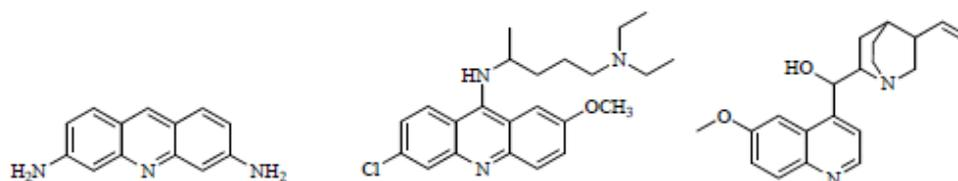


Fig. (1). Proflavine, mepacrine, and quinine.

Table 1. Class of Compound, Phase of Study, and Original Approval of some Acridine Derivatives.

Class	Compound	Phase	Original or Tentative Approval Date	Reference
9-Aminoacridine	Amsacrine, Amsidine [®]	Clinical studies - Phase III	21/11/2005	[37]
	Tacrine, Tacrinol [®]	Clinical studies - Phase II	09/09/1993	[38]
	Quinacrine, Atabrine [®]	Clinical studies - Phase II	1930	[39, 40]
	Asulacrine	Clinical studies - Phase II	-	[41]
Acridine-4-carboxamide	DACA	Clinical studies - Phase II	-	[42]
Pyrazoloacridine (PZA)	PZA + carboplatin	Clinical studies - Phase I/II	-	[43]
Natural product	Acronycine	Preclinical studies	-	[44]
Triazoloacridinone	C-1305	Preclinical studies	-	[45]
Bisamidoacridine	BRACO-19	Preclinical studies	-	[46]

Source: US FDA-Approved Drug Products, EMEA, Clinical trials.gov.

of this molecule on the atomic level. The modeling of the reactivity of acridine is relatively accurate, and confirms that aromatic nucleophilic substitution is the most probable reaction mechanism for the binding of this molecule in organisms [50].

In this context, this review summarises the progress that has been made in the development of anticancer agents based on *in vivo/in vitro* clinical studies that have researched 13 classes of natural and synthetic acridines.

CANCER THERAPIES

In addition to surgery, cancer treatment may involve procedures that are intended to kill the tumour or prevent its growth, such as hormone therapy, radiotherapy, immunotherapy, biological therapies, autophagy, photodynamic therapy, or chemotherapy [2].

Despite advances in the development of cancer therapies, surgery, radiation, and chemotherapy remain the standard treatment options. Chemotherapeutic approaches are often used for metastasized or particularly aggressive cancers. Cytocidal or cytostatic agents are most effective on cancers with rapidly dividing cells [51].

Hormone therapy is an important component of medical treatment and can result in the hormone environment being altered completely. This form of therapy requires the endocrine system of patients with hormone-sensitive cancers

to be manipulated through surgery, radiotherapy or, most commonly, hormone blockers [55].

Radiotherapy, potentially, has many benefits. It destroys cancerous cells in the body, thereby preventing recurrence and spread of the disease. In addition, this therapy can be used to treat a range of cancers, including breast, skin, and brain cancers. Approximately 52% of patients receive radiotherapy at least once during treatment. In addition to the other treatment options, such as surgery and chemotherapy, radiotherapy is an important modality for 40% of the patients who are cured of cancer [52,53]. During radiotherapy, malignant tumor cells are exposed to significant but well-localized doses of radiation, which destroys the cells. The aim is to maximize the radiation dose at the tumor location while minimizing exposure to the surrounding body tissue. The damage inflicted by radiotherapy causes cancerous cells to stop reproducing and, thus, the tumor shrinks. The therapeutic effects are dependent on intrinsic radio sensitivity differences and the abilities of the normal and malignant tissue to repair and repopulate [54].

Immunotherapy involves modulating the immune system, to try and enhance the patient's immunity [56]. Initially, the immune system is able to recognise and kill pre-cancer and cancer cells. However, surviving tumour cells are able to evade immune surveillance after immuno selection. Cancer immunotherapy develops strategies to overcome this evasion mechanism [57].

Apêndice B

Biological therapies have been explored as alternative approaches to cancer treatment, owing to their potential to specifically target and eradicate tumour cells, whilst leaving normal cells intact. By restricting cell death to malignant cells only, many of the side effects that are associated with standard therapies can be avoided. TNF-related apoptosis-inducing ligand (TRAIL) is a biological therapy that has shown great promise in pre-clinical studies owing to its ability to induce apoptotic cell death preferentially in transformed cells [58].

Autophagy is a dynamic process of protein degradation that is typically observed during nutrient deprivation. Recently, interest in autophagy has been renewed among oncologists, since after various anticancer therapies, different cancer cells types undergo autophagy. Autophagy has been found to be inhibited (either pharmacologically or genetically) in multiple studies, resulting in either cell survival or death, depending on the specific context [58].

Both surgery and radiotherapy are essentially local treatments directed at the primary tumour and any loco-regional disease. By contrast, chemotherapy is a systemic treatment and can treat distant metastases. Chemotherapy is the most frequently used anticancer treatment. Common chemotherapeutic agents include polyfunctional alkylating agents, antimetabolites, antibiotics, and mitotic inhibitors which can be used in a monotherapy regimen, or in combination with surgery and/or radiotherapy. In neoadjuvant chemotherapy, drugs are administered before the initiation of the definitive treatment (surgery or radiotherapy). It may simplify the definitive procedure and is thought to reduce the risk of micrometastatic disease. Chemotherapy has been used successfully for the management of sarcomas, in which preoperative chemotherapy improves the long-term prognosis of the disease and, by shrinking the primary tumour, may enable limb-sparing surgery. In addition, neoadjuvant chemotherapy has been considered effective for the treatment of carcinoma of the cervix [54].

However, the effects of chemotherapy depend on several factors, including the intrinsic cytotoxicity of the drug, tumour histology (type and cell differentiation), stage, volume and location (vascularisation). Despite several significant medical advancements that have been made regarding cancer in recent years, the advanced disease remains difficult to treat, and standard therapies such as chemotherapy and radiotherapy, are often associated with substantial toxicities, which can limit their application in the clinic [58].

MODE OF ACTION OF ACRIDINE DERIVATIVES

Most of the biological effects of an acridine compound can be attributed to its planar structure interacting with a DNA fraction [59]. Several substances of clinical importance, such as amsacrine, actinomycin D, and daunomycin, as well as several drugs used for the treatment of parasitic diseases, such as quinacrine and chloroquine, have the ability to bind to DNA by intercalation, inhibiting further replication and/or transcription, therefore interfering with metabolic processes [3].

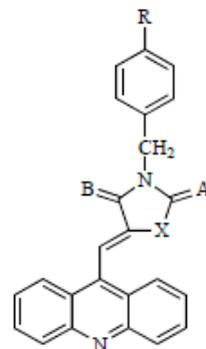
Lerman was the first researcher to propose a model for drug intercalation into DNA after examination of acridine-DNA interactions. In this model, planar aromatic molecules with 2 or 3 rings of 6 members each were inserted between adjacent double-stranded DNA base pairs. The intercalated aromatic chromophore was parallel to the nucleotide bases and perpendicular to the double-helix axis. The complex formed was then stabilised by noncovalent bonds, such as hydrophobic interactions, van der Waals force, and hydrogen bonds. These interactions are considered the most important component of intercalation. The intercalation finally generates structural deformations and changes in the physical and chemical characteristics of the DNA. Specifically, the double helix becomes rigid and stretched, causing a loss in the functionality of the DNA [60, 61].

However, the anticancer functions of acridines do not only depend on their mode of DNA intercalation; these derivatives also perform specific interactions with other nuclear receptors such as Topo and telomerase enzymes [3].

Eukaryotic Topo I and II are nuclear enzymes that are involved in numerous DNA processes, including replication and transcription. These enzymes catalyse DNA supercoil relaxation by cleavage (single- and double-strand breaks by Topo I and Topo II, respectively) and re-ligate the cleaved DNA via ATP-driven mechanisms. Acridine derivatives are able to convert the Topoenzyme into a cellular toxin, and the formation of Topo-binding agent-DNA ternary complexes are implicated by DNA scission and subsequent cell death [62].

NEW ACRIDINES WITH ANTICANCER ACTIVITY

In 2004, Pitta *et al.* synthesised thiazacridine and imidazacridine derivatives condensed at position 5 and *N*-alkylated in position 3 of the imide or thiazolering (Fig. 2), which proved to be effective in treating cancer [36].



X = S, N; A = O; B = S, O; R = Cl, F, NO₂, C₆H₅, Br

Fig. (2). General formula of thiazacridine and imidazacridine derivatives.

The method used to obtain these synthetic compounds started with the oxidation of 9-methyl-acridine, prepared from diphenylamine, which produced acridine-9-carboxaldehyde. The next stage was to obtain the ethyl ester

Apêndice B

of 2-cyano-acridin-9-ylacrylate from condensation in an alkaline medium. From an addition reaction with ethyl ester in the presence of piperidine, the thiazolidinic and imidazolidinic derivatives produced thiazacridines and imidazacridines.

To evaluate the antitumor activity of the acridines, Sarcoma 180 was implanted into mice to induce solid-tumour growth. After 10–12 days of treatment with the newly synthesised derivatives, the tumours were measured and analysed morphologically. Following low-dose administration of the compounds, tumour masses reduced significantly.

9-Aminoacridines

The development of drugs derived from 9-aminoacridine has sparked much interest among healthcare professionals owing to their ability to treat several diseases. For example, *N*4-(6-chloro-2-methoxy-9-acridinyl)-*N*1,*N*1-diethyl-1,4-pentanediamine (quinacrine [Fig. 3]) is one of the most important derivatives, as it is used for the treatment of lupus erythematosus, rheumatoid arthritis, chloroquine-resistant malaria, and Chagas disease. Tacrine, 1,2,3,4-tetrahydro-9-acridinamine, is used to treat patients with Alzheimer's disease [63].

During the early 20th century, 9-aminoacridine derivatives were used initially to treat bacteria- and protozoa-related diseases. Subsequently, they were used for the treatment of cancer and viral and prion diseases [63]. Some of its disease-targeting actions result from direct interactions (conjugation) with biomolecules, such as peptides and proteins [3].

These derivatives were originally studied as treatment agents because of their DNA intercalation ability and Topo inhibition action. Studies have showed that they can also induce *p53* and thus, generate cancer cell death by apoptosis [64].

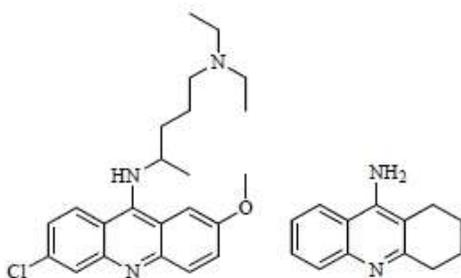


Fig. (3). Quinacrine and tacrine.

Conjugation is the joining of 2 or more molecules, which consequently share properties in the resulting compound. Peptide conjugates of 9-aminoacridine are artificial molecules that possess RNA-selective anticancer, antiviral, and antimicrobial activity. Owing to their ability to interact with DNA, these conjugated peptides may interfere with the function of the enzyme peptidyl transferase. However, the parameter that enables the peptide to distinguish between

RNA and DNA and the substituents that are required for the inhibition of peptidyl transferase remain unknown [65].

Conjugates of 2,6-diaminopurine (guanine group) with 9-aminoacridine (Fig. 4) target DNA and are potent inhibitors of L1210 and A549 cell lines. In 2007, Sebestik *et al.* observed that the growth of the chain of these compounds increased the intercalation ability and preferably alkylated the nitrogenous base adenine [63, 66].

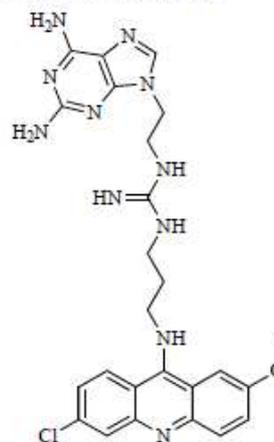


Fig. (4). Conjugate of 9-aminoacridine.

Derivatives of hydrochloride methyl ester *N*-[4-(9-acridinylamino)phenyl]-carbamic acid (AMCA) and hydrochloride methyl ester *N*-[4-(9-acridinylamino)-2-methoxyphenyl]-carbamic acid (m-AMCA) are analogues of ansacrine and inhibit TopoII β . In 1999, Turnbull *et al.* demonstrated that a mutation in the Glu522 residue caused the tumour to be resistant to these drugs. However, this mutation may simultaneously improve the anticancer potential of other drugs. Therefore, multi-target therapy for cancer treatment with this derivative may be beneficial [67].

N-[4-(9-acridinylamino)-3-methoxyphenyl]-methanesulfonamide (m-AMSA) was the first synthetic drug with intercalation ability to be used in the clinic (Fig. 5) [68, 69]. It was first commercialised in 1976 for the treatment of acute leukaemia and malignant lymphoma [68, 70], and since then, many analogues have been synthesised [59, 71–73]. In most cases, it is used in combination with cytarabine for the treatment of refractory acute leukaemia in adults.

Crystallographic studies of ansacrine showed that the phenyl ring has orthogonal orientation ($\sim 70^\circ$) in comparison to the chromophore plane. Owing to its orientation, the acridine chromophore can be accommodated parallel to a DNA groove, inducing tumour cell apoptosis by inhibiting Topo II [74].

However, asulacrine (ASL [Fig. 5]), another m-AMSA derivative, is an effective agent for the treatment lung and breast cancer [35, 40, 75]. In 1999, Su *et al.* synthesised 3-(9-acridinylamino)-5-hydroxymethyl-aniline (AHMA [Fig. 5]) analogues and evaluated their antitumor activity [76, 77].

Apêndice B

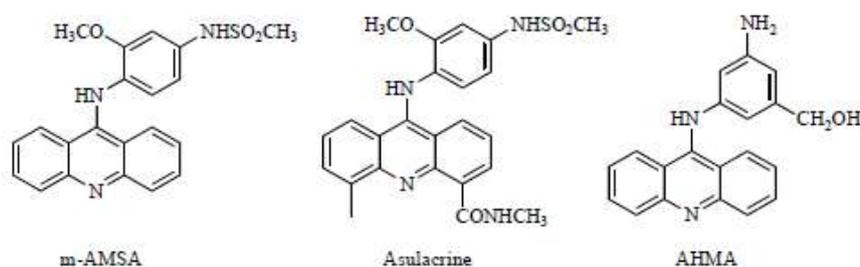


Fig. (5). Amsacrineand analogues.

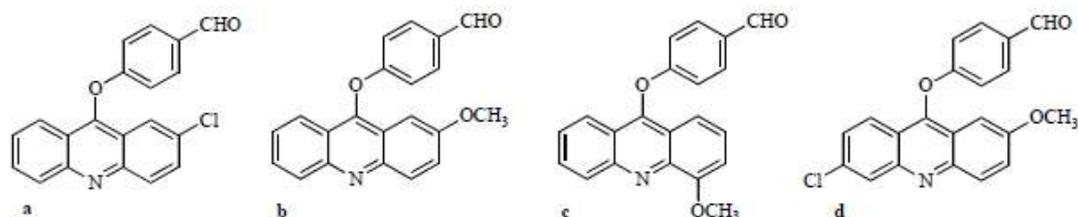


Fig. (6). Anti-inflammatory agents.

They demonstrated that some of these derivatives demonstrated potent cytotoxic action in human leukaemia cells (HL-60).

In 2000, Ferlin and colleagues synthesised C9-substituted acridines and azacridines (m-AMSA analogues). Of these, some compounds were found to induce cytotoxicity in human HL-60 and HeLa cells that were grown in culture. The DNA damage that occurred was evaluated by DNA filter elution and protein precipitation techniques. Catalytic studies with purified Topoisomerase II confirmed that these compounds can inhibit Topoisomerase II as well [78].

Chen and Sondhi demonstrated the anti-inflammatory activity of acridine derivatives in 2009 [79,80]. In 2003, Chen *et al.* synthesised 9-phenoxyacridine and 4-phenoxyfuro[2,3-*b*]quinoline derivatives [81]. Of these derivatives, 4 were shown to be more potent than the reference drug, mepacrine, for the inhibition of rat peritoneal mast cell degranulation, with IC_{50} values of 4.7, 5.9, 6.1, and 13.5 μ M (Fig. 6 A, B, C and D, respectively). These results indicate that these anti-inflammatory effects are controlled, at least in part, by the suppression of chemical mediators released by mast cells, neutrophils, and macrophages. Therefore, there is great potential for these compounds to be used as novel anti-inflammatory agents with no significant cytotoxicity.

In 2003, Giorgio *et al.* studied the *in vitro* activities of 7-substituted 9-chloro and 9-amino-2-methoxyacridines, as well as their bis- and tetra-acridine complexes, against *Leishmania infantum*. The results confirmed that several derivatives of 2-methoxyacridine, together with their corresponding dimeric and tetrameric forms, had strong antiparasitic activity *in vitro*. Anti-leishmanial activity was dependent on the type of both 7- and 9-substituted groups in monoacridines, while it varied according to the 9-substituted

group and the length of the linker in the bis- and tetra-acridines [82].

The *in vitro* cytotoxic activity of several 9-amino-nitro-acridine derivatives was performed in cell line cultures of KB and Ehrlich carcinoma cells (Fig. 7) [83]. Correlations between biological activity and chemical structure were found; the authors noted that biological activity depends on the position of the nitro group and the presence of the dialkylamino chain at the 9-position of the acridine. In addition, the introduction of new substituents, such as methyl, methoxy, and bromine in positions 4, 6, and 7 of 1-nitro-acridine, did not significantly affect biological activity, and the number of methylene groups does not affect the drug's anticancer activity.

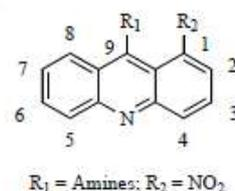
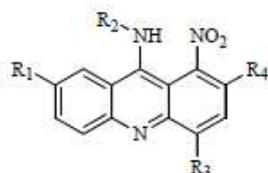


Fig. (7). General structure of 9-amino-nitro-acridine derivatives.

In 2005, Narayanan produced second-generation 1-nitroacridines that demonstrated anticancer actions in solid tumours (Fig. 8). For instance, 1-nitro-9-hydroxyethylamino acridine (C-857) presented great therapeutic efficacy against prostate and colon cancer and sarcoma cells. However, its clinical development was terminated owing to high systemic toxicity. In order to minimise this toxicity, a C-857 derivative was produced containing substitutions in the C4 and/or esterified hydroxyl groups in C9. The introduction of a methyl group on C4 led to the formation of 1-nitro-4-

methyl-9-aminoethyl-acridine (C-1748), which presented better anticancer activity (especially against prostate cancer), and produced a drastic decrease in toxicity and mutagenic potency [84].

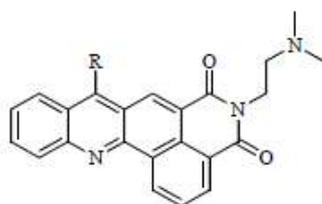


C-857: $R_1, R_3, R_4 = H; R_2 = (CH_2)_2OH$
C-1748: $R_1, R_4 = H; R_2 = (CH_2)_2OH; R_3 = CH_3$

Fig. (8). Substituted derivatives of 1-nitroacridine.

Isoquinoacridines

In 2006, Yang *et al.* designed and synthesised DNA-intercalating derivatives of isoquino[4,5-*bc*] acridine (Fig. 9) to investigate and develop molecules with antitumor, DNA-binding, and photo-damaging properties [85]. A4 ($R = O$ [Fig. 9]) exhibited the highest antitumor activities against both human lung cancer cells (A 549) and murine leukaemia cells (P388). All compounds were shown to be more cytotoxic against the P388 than A549 cell line.



$R=Cl; R=SCH_2CH_3; R=HN(CH_2CH_2)_2NCH_3; R=H; R=O$

Fig. (9). Isoquinoacridine derivatives.

Acridine-4-carboxamides

Acridine-4-carboxamides are effective anticancer agents, especially for the treatment of solid tumours and leukaemia. The tricyclic carboxamide *N*-[2-(dimethylamino)ethyl] acridine-4-carboxamide (DACA [Fig. 10]) is a DNA-intercalating agent that inhibits both TopoI and II [86]. DACA has a large spectrum of anticancer (solid tumour) mechanisms in animals and is not affected significantly by multidrug resistance (MDR) mediated by P-glycoprotein, probably owing to its high lipophilicity. Spicer *et al.* synthesised analogues of DACA with methyl, methoxy, and chlorine substitutes in the acridine ring. Several of the analogues demonstrated significant anticancer activity against solid tumours in mice [87,89]. These studies suggest that the properties of the substituent do not affect the cytotoxicity of the DACA analogue. In fact, steric bulk appears to have a greater effect on activity, with larger groups diminishing anticancer efficiency. The 7-Ph compound

and several of the 5-substituted derivatives (Fig. 10) were more cytotoxic than DACA, but were less effective in JL_A and JL_D cell lines (which had lower Topo II activity) than in wild-type JL_C , suggesting their cytotoxicity is largely mediated through interactions with Topo II [89].

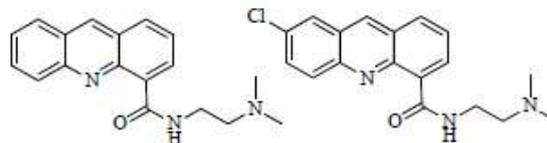
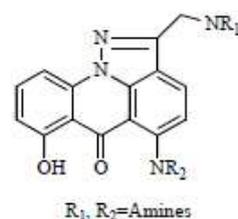


Fig. (10). DACA and its 7-chloro derivative.

The anticancer properties of acridine-2-carboxamides, acridine-3-carboxamides, and acridine-4-carboxamides are known to be significantly different. Parajuli *et al.*, in 2007, monitored the sequence-specific binding of these drugs from the intercalative binding of chromophores to DNA. In 2006, they had also monitored the sequence-specific intercalation of 9-substituted acridine-4-carboxamides in nucleic acids [90, 91].

Pyrazoloacridines/Pyrazoloacridones

Previously, Sugaya *et al.* synthesised 6H-pyrazolo-[4,5,1-*de*]acridin-6-one derivatives (Fig. 11), named pyrazoloacridones, a class of DNA-intercalating agents [92]. Biological studies conducted with pyrazoloacridones revealed that they exert antiproliferative activity *in vitro* against HeLa S₃ cells and significant antitumor activity *in vivo* against P388 leukaemia and sarcoma-180 tumours. Regarding the structure-activity relationship of pyrazoloacridones, the 7-hydroxy, (aminoalkyl)amino and (hydroxyalkyl)amino side chains at C2 and C5 have a significantly effect on the compounds' biological activity.

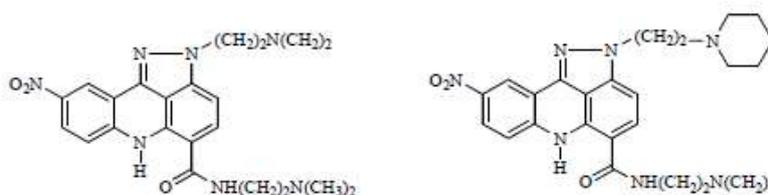
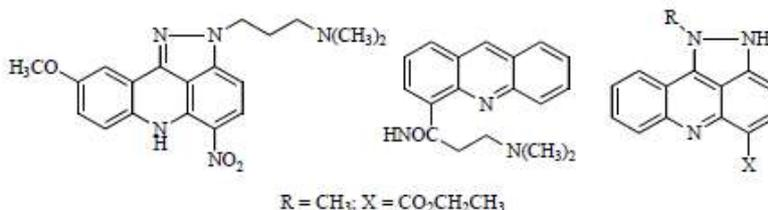


$R_1, R_2 = \text{Amines}$

Fig. (11). Pyrazoloacridone derivatives.

Derivatives of *N*-5,2-Di(ω -aminoalkyl)-2,6-dihydropyrazolo [3,4,5-*kl*]acridine-5-carboxamides are DNA-binding agents and potent cytotoxic compounds. Antonini *et al.* synthesised 25 new derivatives of pyrazolo [3,4,5-*kl*] acridine-5-carboxamide in order to determine their cytotoxic activity, the function of the pyrazole ring in DNA-binding potency, and the importance of the nitro group (presence and position) in the molecule [93]. Two of the compounds (Fig. 12) possessed cytotoxic activity in the nanomolar range against the human colon adenocarcinoma cell line HT29 and therefore, are new potential anticancer agents.

Apêndice B

Fig. (12). Pyrazolo[3,4,5-*kl*]acridine-5-carboxamide.Fig. (13). 9-methoxy derivative, acridine-4-carboxamide and pyrazolo[3,4,5-*kl*]acridine.

In an attempt to develop more potent drugs, Bu *et al.* designed derivative hybrids possessing both a pyrazole ring and 4-carboxamide chain [94]. Pyrazolo[3,4,5-*kl*]acridine derivatives were assessed for their tumour growth inhibition efficacy in Jurkat and P388 cell lines, and significant cytotoxic activity was noticed. It is noteworthy that the analogues that contained only a carboxamide group or amine chain in N-1 exhibited similar cytotoxicity to the reference compound DACA, while the hybrid compound had greater antitumor activity.

Taking into account the cytotoxic activity of acridine-4-carboxamide (Fig. 13) and pyrazolo [3,4,5-*kl*]acridine derivatives, Antonioni *et al.*, designed and synthesised 2 new classes of potential *bis* intercalating compounds: the *bis*(pyrimidoacridines) and the *bis*(pyrazoloacridine carboxamides). Of these, 1,9-*bis*{2-[2-(dimethylamino)ethyl]-2,6-dihydropyrazolo-[3,4,5-*kl*]acridine-5-carbonyl}-5-methyl-1,5,9-triazanonane 3HC has a remarkable affinity with DNA, as well as a broad spectrum of activity, excellent cytotoxic potency, and potential preliminary *in vivo* activity. Therefore, this compound is good candidate for preclinical studies on anticancer drug [95].

In 2002, Bu *et al.* obtained derivatives possessing both a pyrazole ring and 4-carboxamide chain in an attempt to obtain demonstrate the enhanced anticancer activity of the compound [94].

Natural-Product Derivatives

In addition to synthetic compounds, nature can provide an array of options to scientists. The biodiversity between various natural derivatives is great; therefore, their treatment potential should be evaluated for as many maladies as possible. Acronycine (Fig. 14) is a natural cytotoxic alkaloid from the bush *Acronychia baueri* and has exhibited high toxicity toward certain tumour cells *in vitro*. Since the 1970s, several acronycine analogues have been synthesised and evaluated for their antitumor properties [96-99]. Studies of structure-activity relationship conducted by Costes *et al.* led

to the development of acronycine derivatives with increased potencies [97]. One of the analogues, S23906-1, demonstrated promising *in vivo* activity against colon 38 adenocarcinoma in mice. Similarly, S23906-1 derived from benzoacronycine was shown to be a potent inducer of apoptosis in human promyelocytic leukaemia HL-60 and, to a lesser extent, in murine B16 melanoma cells [99, 100].

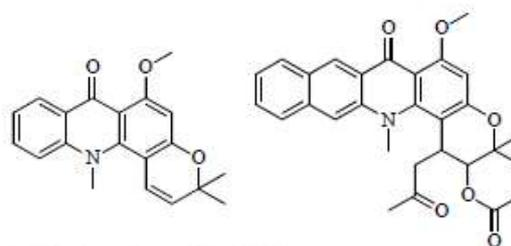
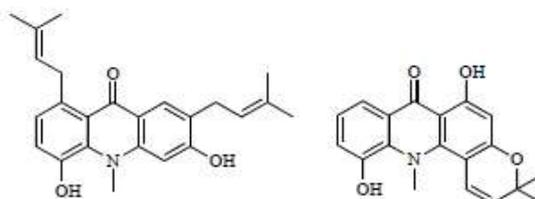


Fig. (14). Acronycine and S23906-1.

Bioactive acridone alkaloids have been isolated from *Swinglea glutinosa* Merr. (Rutaceae) and tested for antiplasmodial activity (Fig. 15). They showed promising activity against strains of chloroquine-resistant *Plasmodium falciparum* [101, 102]. Furthermore, cytotoxicity tests were performed using HeLa cells. All compounds tested exhibited good antiplasmodial activity.

Fig. (15). Acridone alkaloids active against *Plasmodium falciparum*.

Dihydroindolizino[7,6,5-*k*]acridinium chloride (Fig. 16) is a water-soluble agent that has inhibitory activity exceeding that of m-AMSA against breast tumour cell lines and the adenosquamous NCI-H647, a non-small-cell lung cancer cell line that is known to exhibit elevated levels of Topo II α [103]. The activity of this polycyclic compound is probably linked to Topo II disruption. In addition, unlike m-AMSA, this compound is not susceptible to P-glycoprotein-mediated drug efflux and retains activity in lung cells with derived resistance to etoposide, a Topo II inhibitor.

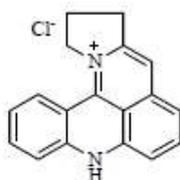
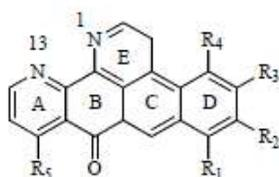


Fig. (16). Dihydroindolizino[7,6,5-*k*]acridinium chloride.

In the last few decades, several compounds with many pharmacological activities have been extracted from marine organisms, including bryostatin, dolastatin, cryptophycin, and ecteinascidin [104]. Many of these marine alkaloids are based on the pyrido[2,3,4-*k*]acridine skeleton, and ascididemin was one of the earliest discovered compounds. Some ascididemin derivatives (Fig. 17) such as bromoleptoclidone, 11-hydroxiascididemin, and neocallistactine have also been isolated from marine sources. The National Cancer Institute (USA) tested ascididemin and its natural analogues, and all exhibited anticancer activity *in vitro*. In 2000, Alvarez *et al.* studied the activity of analogues in P388D murine lymphoma cells and human lung carcinoma A549 cells [105]. In 2000, Delfourne *et al.* prepared ascididemins with D-ring modifications, and their *in vitro* results indicated that these compounds had good cytotoxic activity; in fact, some were 100times more active than the prototype [106].



Ascididemin: R₁, R₂, R₃, R₄, R₅=H
 Bromoleptoclidone: R₇=Br; R₁, R₃, R₄, R₅=H
 11-hydroxiascididemin: R₇=OH; R₁, R₂, R₃, R₄=H
 Neocallistactine: R₃=OH; R₁, R₂, R₄, R₅=H

Fig. (17). Ascididemin and derivatives.

Arnoamine A1 and B2 were the first synthesised pentacyclicpyridoacridine alkaloids that possessed a pyrrole ring fused to the pyridoacridine ring system (Fig. 18). In 2000, Delfourne *et al.* first created this compounds from 4-

chloro-8-methoxy-5-nitroquinoline [106]. The synthesis of arnoamine A and B can be accomplished in 6–7 steps, with an overall yield of 13% and 4%, respectively. In 2006, Radchenko *et al.* used an effective 7-step synthetic pathway that created to the compound ethyl 4-methoxy-1-methylpyrido-[4,3,2-*mm*]pyrrole [3,2,1-*de*]acridine-2-carboxylate (Fig. 17), with an overall yield of 41.5% [107].

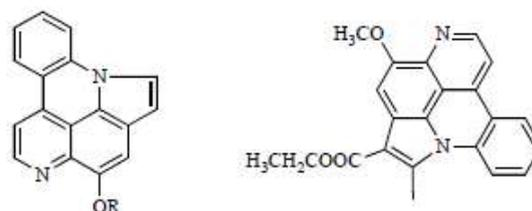


Fig. (18). Arnoamine A1 (R=H) and B2 (R=CH₃) and an analogue.

Bisamidoacridines

Telomerase prevents damage a chromosome's ends during DNA replication, and it is over expressed in tumour cells. The activation of telomerase is a crucial genetic event, as it leads to the immortality of tumour cells [108-111]. An alternative treatment approach involves the stabilization of higher-order quadruplex structures. Single-stranded guanine-rich telomeric DNA sequences can combine to form guanine quadruplex structures. After the formation of these structures by the telomere primer, the synthesis of further telomeric repeats by telomerase is inhibited. Therefore, substances that inhibit this enzyme (Fig. 19) might be promising anticancer drugs [111-115].

Qualitative molecular modeling was used to design BRACO-19, which is a 3,6,9-trisubstituted acridine ligand (Fig. 19), under the assumption that the 3 substituents would each occupy a groove in a quadruplex. BRACO-19 inhibits telomerase enzymatic activity, resulting in the shortening of telomere and also produces end-to-end chromosomal fusions in cancer cells due to quadruplex disruption of the uncapping of proteins associated with the single-strand overhang. It shows significant *in vivo* anticancer activity in tumor xenografts, which is associated with the uncapping of telomere [116].

Thiazoloacridines

Taking into account the potent anticancer activity of natural pyridothiazoloacridine alkaloids, Giorgio *et al.* synthesised 16 derivatives of thiazolo[5,4-*a*]acridine in an attempt to develop molecules that bind to and break DNA through optical activity [117]. They evaluated cytotoxic activities in *Salmonella typhimurium* and measured the effects of optical activity during the intercalation process. Only 1 compound had properties enabling DNA intercalation (Fig. 20), while 3 compounds required optical activation before intercalation into DNA could occur. The cytotoxic activity of the derivatives was performed in human stem cells from monocytic leukaemia THP1.

Apêndice B

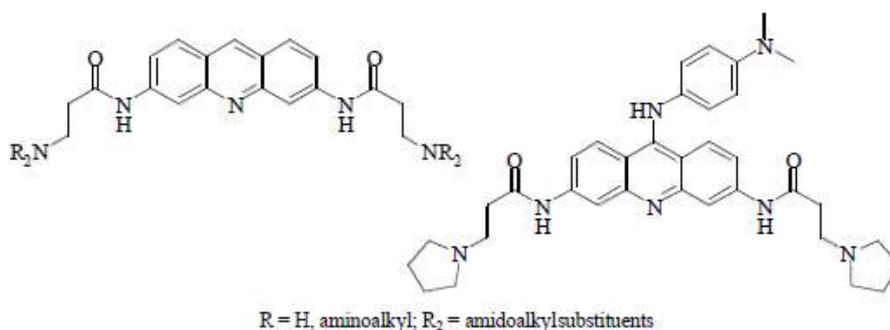


Fig. (19). Telomerase inhibitors and BRACO-19.

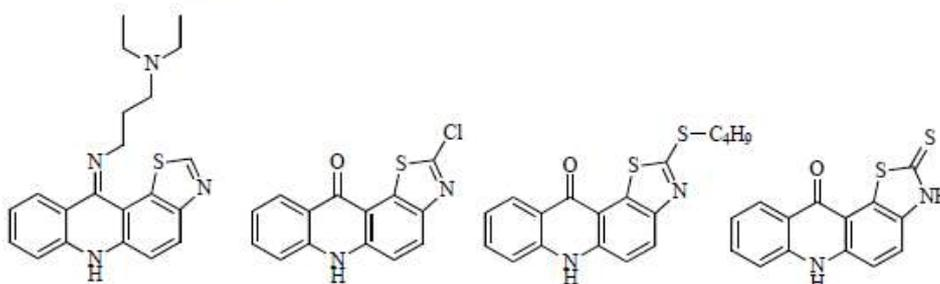


Fig. (20). Thiazolo[5,4-a]acridine derivatives.

Triazoloacridinones

In previous studies, triazoloacridinones (Fig. 21) have exhibited high cytotoxic activity against a broad spectrum of tumour cell lines *in vitro*, as well as high antitumour activity in mice against transplantable tumours, such as leukaemia P388, melanoma B16, ascites colon 26 adenocarcinoma, and colon 38 adenocarcinoma [118-120]. Research has confirmed that triazoloacridinone derivatives inhibit the DNA-Topo II complex, block the catalytic activity of Topo II, and inhibit the G2 phase of the cell cycle, leading to apoptosis.

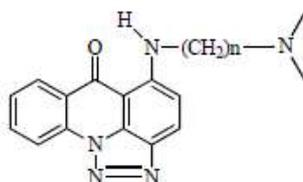


Fig. (21). Triazoloacridinones derivatives.

The most promising triazoloacridinone derivative, C-1305 (Fig. 22), has been selected for extended preclinical trials [45]. Studies have demonstrated that this compound is able to inhibit the proliferation of cells involved with poly(ADP-ribose) polymerase 1; this is of particular interest since these cells are usually resistant to Topo II inhibitors [121]. In addition, C-1305 binds to DNA by intercalation and possesses higher affinity for GC bases than AT bases [122].

However, it is known that the ability of triazoloacridinones to bind to DNA by intercalation is not crucial for their biological activity. Studies involving cell culture have revealed that C-1305, after previous metabolic activation, induces covalent crosslinks of DNA strands between some tumour cells and fibroblast cells. This binding is considered essential for the anticancer activity of C-1305.

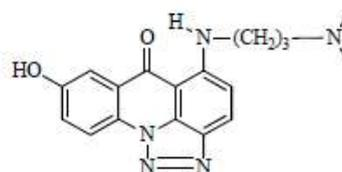
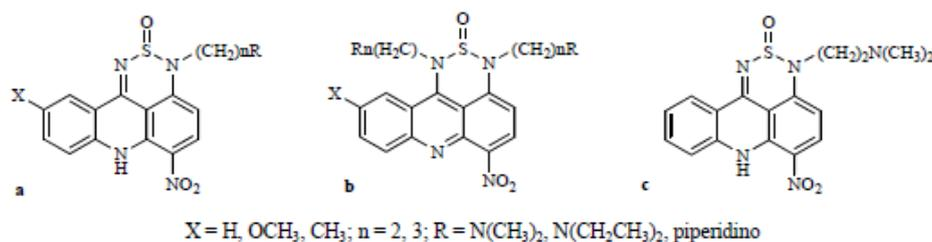


Fig. (22). C-1305.

Thiadiazinoacridines

An acridine scaffold fused to a 5- or 6-membered heterocyclic ring generates polycyclic DNA-intercalating derivatives. Antonini *et al.* synthesised 2 series of DNA-intercalating agents in 2003, namely 3-[omega-(alkylamino)alkyl]-6-nitro-thiadiazino[3,4,5-*kl*]acridines (Fig. 23A) and 1,3-di[omega-(alkylamino)alkyl]-6-nitro-thiadiazino[3,4,5-*kl*]acridines (Fig. 23B) [123]. Results indicated that 3-[2-(dimethylamino)ethyl]-6-nitro-2,7-dihydro-3H-2Δ⁴-[1,2,6]thiadiazino[3,4,5-*kl*]acridin-2-one exhibited the most potent anti tumour activity *in vivo* (Fig. 23C).

Fig. (23). Rational drug design of thiaziazino[3,4,5-*k*]acridines.

Polyacridines

In the absence of any significant steric or entropic factors, the binding constant of a symmetrical *bis*-intercalator should be approximately the squared binding constant of the monomer. Since complete dissociation of the ligand from the DNA requires both chromophores to disengage, drug dissociation rates of polyacridines are much slower than those of monomer agents [124].

When the critical distance between 2 acridine groups is reached, the compound becomes a *bis*-intercalator, and the DNA intercalation constant is increased ($>10^3$ – 10^9 M⁻¹) [125]. However, in previous studies, it has been observed that *tri*-intercalator derivatives have a lower intercalating capacity than acridine dimer compounds [64].

In 1975, Barbet *et al.* synthesised an acridine dimer (Fig. 24). They used aminoalkylated chains of spermine or spermidine to connect the 2 aromatic rings to study the dimer's affinity to DNA [126].

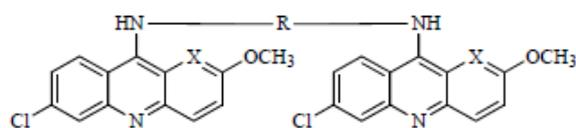
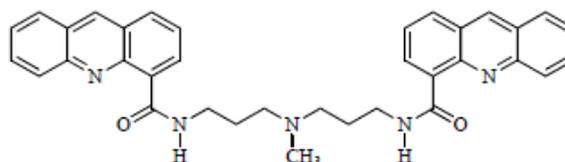


Fig. (24). Acridinedimers.

The growth inhibition effects of di-acridines, putrescine, spermidine, and spermine were evaluated in human cervical cancer cells (HeLa) and leukemic cells (L1210 and P-388) in culture and compared with the action of 9-aminoacridine [127, 128]. The results indicated that diacridines were more active than 9-aminoacridine.

Previously, 4 classes of *bis*-acridines with varying chain length, stiffness, and polarity variables at the 9-position were evaluated for antitumor properties [124]. In this study, it was found that *bis*-acridines connected by flexible chains of variable polarity had low dissociation rates and were able to make kinetics exchanges in DNA binding sites. These exchanges were reduced drastically by the inclusion of positive charges in the connection chain, but the resulting polycationic compounds were found to be inactive *in vivo*, possibly owing to their poor distribution in the human body. However, *bis*-acridines connected by the 'ideal' pyrazolic chain have strong DNA-binding affinity and good solubility in water and are active *in vivo*.

The synthesis and cytotoxicity profiles of a large number of acridine derivatives have been studied extensively [26, 88, 89, 95, 123, 129, 130]. Several derivatives of substituted *bis*(acridine-4-carboxamide) (Fig. 25) connected by a $-(\text{CH}_2)_3\text{N}(\text{Me})(\text{CH}_2)_3$ chain were prepared [130]. These dimeric analogues of DACA proved to have superior antitumor potencies compared with the corresponding monomeric DACA analogues in a board of cell lines, including wild-type (JL_C) and mutant (JL_A and JL_D) forms of human Jurkat leukaemia.

Fig. (25). *Bis*(acridine-4-carboxamide).

Bis(acridine-4-carboxamide) analogues containing small substituents at the acridine 5-position (methyl and chloro) had superior antitumor action, with an IC₅₀ in the range of 2 nM against Lewis lung carcinoma and 11 nM against JL_C [130]. Larger substituents at any position decreased potency, probably owing to a low DNA-binding affinity caused by steric hindrance. Moreover, the introduction of methyl and chlorine groups at positions 1 and 8, respectively, slightly influenced *bis*-(5-methyl-DACA) activity. All compounds were toxic against mutant and wild-type Jurkat strains and had higher selectivity for TopoI.

Sourdon *et al.* in 2001 synthesised *bis*- and *tetra*-acridines compounds linked by a short nitrogen chain, with acridinemoieties located so the self-stacking of the aromatic planes is avoided. Some derivatives showed good *in vitro* cytotoxic activity against murine cell lines. Antiproliferative activity was performed against murine L1210 leukaemia and A549 cell lines, and the derivatives (Fig. 26) presented good results against DNA repairation [131].

Several *bis*[(9-oxo-9,10-dihydroacridine-4-carbonyl) amino]alkyl) alkylamines (Fig. 27) were prepared and tested against HT-29 colon cancer cell lines [132]. Experiments suggested that the high activity of some of these compounds might be related to their strong binding affinity to DNA. Molecular dynamics simulations have shown that these compounds are able to form stable complexes with DNA through *bis*-intercalation.

Apêndice B

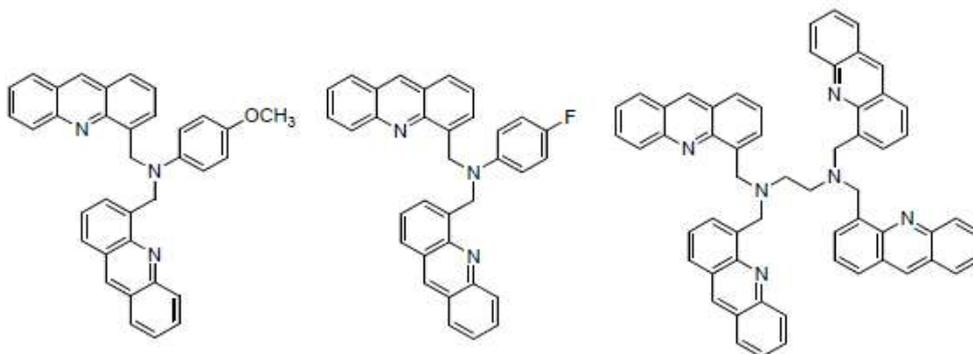


Fig. (26). Bis- and tetra-acridines derivatives.

Drugs containing platinum have been used against malignant gliomas, but to date have shown poor response rates. In 2003, Augustus *et al.* prepared bis(acridine)platinum(II) complexes (Fig. 28) and evaluated their biological activity in glioblastoma cells [133]. Cell viability assays showed that the compounds bonded strongly to double-stranded DNA and were cytotoxic in micromolar concentrations in SNB19 brain tumour cells, possibly through bis-intercalation.

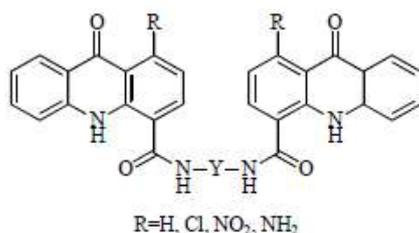


Fig. (27). Bis-(alkyl)amines derivatives.

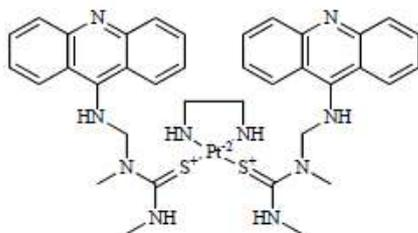


Fig. (28). Bis(acridine)platinum(II) complexes.

Antonini *et al.* in 2004 designed, synthesised, and biologically evaluated bis(pyrimido[5,6-*de*]acridines) and bis(pyrazolo[3,4-*kl*]acridine-5-carboxamides) (Fig. 29). The results indicated that these compounds are excellent DNA ligands. In addition, the bis-derivative had a higher binding affinity to DNA than the corresponding monomer, and both compound derivatives bound preferentially to AT-rich duplexes [95].

Currently, the main disadvantages of applying cancer therapies are the resulting adverse side effects. To minimise their occurrence, photodynamic therapy (PDT) is receiving increasing attention and is intended to be selective to superficial cancer [134]. Treatment involves the administration of a photosensitive drug, and the tumour is then illuminated to activate drug action. The photosensitisation that is induced by intercalating agents can cause DNA damage by 3 mechanisms. First, the electron transfer of nucleotide bases, especially guanine, to a photochemical-excited intercalating agent alters the DNA sequence. Second, the photogeneration of hydroxyl radicals can occur, which are reactive intermedia test hat can absorb the hydrogen atoms of the DNA sugar backbone. Last, an oxygen molecule that is generated from the transferring energy of an electronically excited photosensitiser preferentially oxidises guanines.

Fernandez *et al.* developed new acridine photonuclear copper complexes [135]. One compound, 2,6-bis{[(6-amino-acridin-3-yl)methoxycarbonylamino]-ethyl}methylaminomethylpyridine (Fig. 30), consisted of 2 acridinerings joined by pyridine connecting to copper. This compound split DNA by photolysis and demonstrated increased efficiency in the presence of copper II under typical bodily conditions of pH and temperature. In addition, it protects DNA through monofunctional intercalation and preferably binds to guanine and cytosine.

The proteasome is a multimeric complex possessing three endoproteolytic activities, named after their cleavage specificities on peptides, trypsin-like, post-acidic (or caspase-like, or peptidyl glutamyl peptide hydrolase), and chymotrypsin-like. This multi-protein complex is responsible for the degradation of many cell proteins, including those that regulate the cell cycle and apoptosis, and therefore, it is a potential target for treatment. Agents targeting the proteasome have gained credibility as anticancer drugs, resulting in their development and commercialisation; for example, Velcade™ (bortezomib, PS-341, Millennium Pharmaceuticals), which was approved in 2003 for the treatment of multiple myeloma. The peptide boronic acid has demonstrated antitumour activity by inhibiting chymotrypsin [136].

Apêndice B

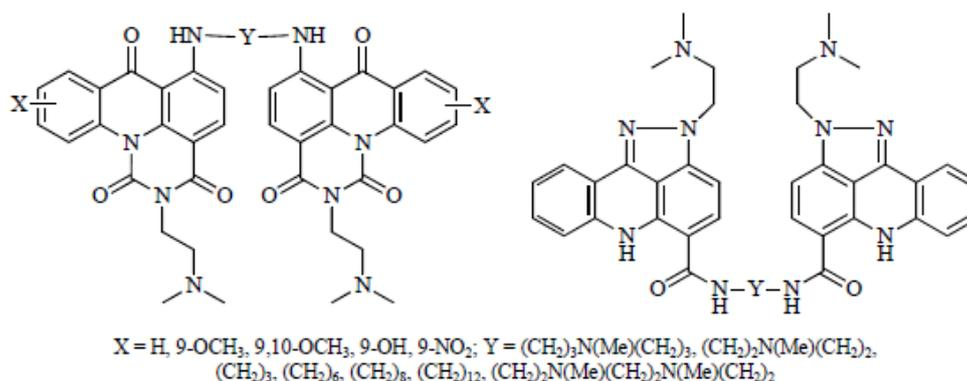


Fig. (29). Bis-pyrimido and bis-pyrazoloacridines.

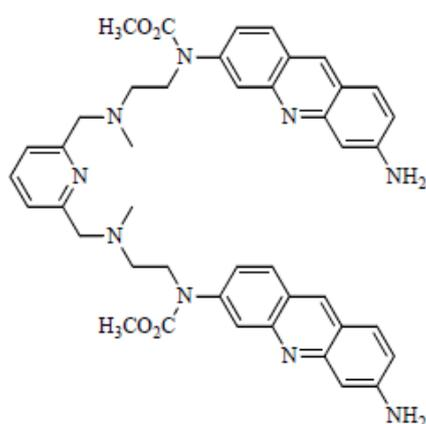


Fig. (30). Photolyase derived from bis-acridines.

Vispe *et al.* studied the action mechanisms of several of bis- and tetra-acridines (Table 2) [136]. These compounds were cytotoxic against HL-60 and demonstrated similar results when Topo II activity was low. The HL-60/MX2 cell line was resistant to mitoxantrone and amsacrine but was sensitive to the derivatives tested. This indicated that Topo II is not the only target of these compounds. When tested in proteasome targets *in vitro*, 4 of these compounds demonstrated inhibitory properties, and at least 2 compounds inhibited the entire proteasome complex.

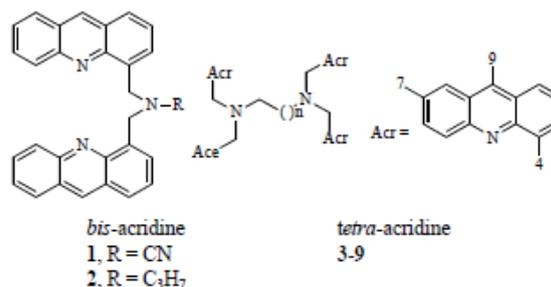
CONCLUSION

Some 59 years have passed since Watson and Crick elucidated the structure of DNA [137]. Since 1953, varied, intensive studies have been conducted, with an objective to discover compounds that will interact with DNA and result in the treatment of many diseases, including cancer.

Acridines are attractive therapeutic agents since they have a broad spectrum of biological activities such as antimicrobial, antiviral, antimalarial, antitrypanosomic, leishmanicidal, antiparkinsonian and, in particular, antineoplastic functions. They can also interact with DNA and

inhibit telomerase, Topoenzymes, and the proteasome complex. Finally, acridines have enhanced selectivity and can be used to treat multidrug-resistant tumours, which are critical limitations of current therapies in the current treatment.

Table 2. Bis- and tetra-acridine derivatives



Compound	Substituents			Bond position of the acridine
	9	7	n	
3	H	H	1	4
4	H	H	3	4
5	H	H	5	4
6	H	H	7	4
7	NH ₂	H	1	4
8	Cl	Br	3	4
9	H	H	7	2

In the last few decades, various acridine derivatives have been developed in order to modulate cell cytotoxicity, the nature of the molecule's activity, and biological targets. Thiazacridines, imidazacridines, 9-aminoacridines, isoquinoacridines, acridine-4-carboxamides, acridine-5-carboxamides, pyrazoloacridines/pyrazoloacridones, natural-product derivatives, bis-amidoacridines, thiazoloacridines,

Apêndice B

triazoloacridinones, thiaziazinoacridines, and polyacridines are several of the compounds that have been synthesised and described in this review.

Initially, acridines were used in the clinic as antimicrobial agents (proflavine and acriflavine) and then were used for the treatment of malaria (mepacrine), Parkinson's disease (tacrine), and cancer (amsacrine), among others. Several acridines have been withdrawn from the market; however, some acridines, such as asulacrine, N-(2-[dimethylamino]ethyl)acridine-4-carboxamide (DACA), and pyrazoloacridine, are under clinical trial, while others, such as C-1305 and acronycine, are undergoing preclinical study. Although the results are promising to date, the possible side effects are still a cause of concern. To minimize these concerns, a new and very important concept in drug design and development is the production of compounds with improved affinity and efficacy than those of the original drugs. Molecular hybridization should be considered during drug development. This strategy enables the development of compounds with a modified selectivity profile, different and/or dual modes of action, and reduced adverse effects based on the combination of pharmacophoric moieties of different bioactive substances.

CONFLICT OF INTEREST

The authors confirm that this article content has no conflicts of interest.

ACKNOWLEDGEMENTS

The authors are thankful to CNPq (Conselho Nacional de Desenvolvimento Científico e Tecnológico, Brasil), FACEFE (Fundação de Amparo à Ciência e Tecnologia do Estado de Pernambuco) and INCT_IF (Instituto Nacional de Ciência e Tecnologia para Inovação Farmacêutica) for financial support.

REFERENCES

- World Health Organization. Fact sheets. <http://www.who.int/mediacentre/factsheets/fs297/en/index.html> (Accessed June 11, 2011).
- World Health Organization. <http://www.who.int/topics/cancer/en/> (Accessed May 14, 2011).
- Demeunynck, M.; Charmantray, F.; Martelli, A. Interest of acridine derivatives in the anticancer chemotherapy. *Curr. Pharm. Des.*, **2001**, *7*(17), 1703-1724.
- Denny, W.A. Acridine derivatives as chemotherapeutic agents. *Curr. Med. Chem.*, **2002**, *9*(18), 1655-1665.
- Moroshkina, E.B.; Shishov, A.K.; Krivtsova, M.A.; Zhadin, N.N.; Frisman, E.V. The effect of acridine dyes on the molecular structure of DNA. *Mol. Biol. (Mosk.)*, **1975**, *9*(6), 836-844.
- Sharma, V.K.; Sahare, P.D.; Rastogi, R.C.; Ghoshal, S.K.; Mohan, D. Excited state characteristics of acridine dyes: acriflavine and acridine orange. *Spectrochim. Acta. A Mol. Biomol. Spectrosc.*, **2003**, *59*(8), 1799-1804.
- Mahmood, T.; Paul, A.; Ladame, S. Synthesis and Spectroscopic and DNA-Binding Properties of Fluorogenic Acridine-Containing Cyanine Dyes. *J. Org. Chem.*, **2010**, *75*(1), 204-207.
- Browning, C.H. 1967. Proflavine and acriflavine. *Br. Med. J.*, **1967**, *2*(5544), 111.
- Eiter, L.C.; Hall, N.W.; Day, C.S.; Saluta, G.; Kucera, G.L.; Bierbach, U. Gold(I) analogues of a platinum-acridine antitumor agent are only moderately cytotoxic but show potent activity against *Mycobacterium tuberculosis*. *J. Med. Chem.*, **2009**, *52*(21), 6519-6522.
- Wainwright, M. Acridine-a neglected antibacterial chromophore. *J. Antimicrob. Chemother.*, **2001**, *47*(1), 1-13.
- Novosad, N.V. The antimicrobial activity of thio-, thioxo- and oxo-derivatives of acridine. *Mikrobiol. Z.* **1996**, *38*(4), 55-58.
- Gaidukevich, A. N.; Bashura, G.S.; Pertsev, I.M.; Piminov, A.F.; Piatkopi, A.I. Determination of the antimicrobial activity of some acridine derivatives. *Farm. Zh.*, **1974**, *28*(6), 50-54.
- Loiseau, P.M.; Nguyen, D.X. Plasmodium berghei mouse model: antimalarial activity of new alkaloid salts and of thiosemicarbazone and acridine derivatives. *Trop. Med. Int. Health.* **1996**, *1*(3), 379-384.
- Jones, M.; Mercer, A.E.; Stocks, P.A.; La Pensée, L.J.; Cosstick, R.; Park, B.K.; Kennedy, M.E.; Piantanida, L.; Ward, S.A.; Davies, J.; Bray, P.G.; Rawe, S.L.; Baird, J.; Charidza, T.; Janneh, O.; O'Neill, P.M. Antitumor and antimalarial activity of artemisinin-acridine hybrids. *Bioorg. Med. Chem. Lett.* **2009**, *19*(7), 2033-2037.
- Shibnev, V.A.; Finogenova, M.P.; Grinberg, L.N.; Allakhverdiev, A.M. Synthesis of acridine derivatives of amino acid hydrazines and their antimalarial activity. *Bioorg. Khim.*, **1988**, *14*(11), 1565-1569.
- Muth, C.W.; Minigh, H.L.; Chookruvong, S.; Hall, L.A.; Chao, H.T. Syntheses of 9-acridine- and 2-phenanthridinemethanols as potential antimalarials. *J. Med. Chem.*, **1981**, *24*(8), 1016-1018.
- Girsault, S.; Grellier, P.; Berecibar, A.; Maes, L.; Mouray, E.; Lemièrre, P.; Debren, M.A.; Davioud-Charvet, E.; Sergheraert, C. Antimalarial, antitrypanosomal, and antileishmanial activities and cytotoxicity of bis(9-amino-6-chloro-2-methoxyacridines): influence of the linker. *J. Med. Chem.*, **2000**, *43*(14), 2646-2654.
- Figgitt, D.; Denny, W.; Chavalitshewinkoon, P.; Wilairat, P.; Ralph, R. *In vitro* study of anticancer acridines as potential antitrypanosomal and antimalarial agents. *Antimicrob. Agents. Chemother.*, **1992**, *36*(8), 1644-1647.
- Morales, N.M.; Schaefer, F.W. 3rd; Keller, S.J.; Meyer, R.R. Effects of ethidium bromide and several acridine dyes on the kinetoplast DNA of *Leishmania tropica*. *J. Protozool.*, **1972**, *19*(4), 667-672.
- Mauel, J.; Denny, W.; Gamage, S.; Ransijn, A.; Wojcik, S.; Figgitt, D.; Ralph, R. 9-Anilinoacridines as potential antileishmanial agents. *Antimicrob. Agents. Chemother.*, **1993**, *37*(5), 991-996.
- Sasvari, Z.; Bach, S.; Blondel, M.; Nagy, P.D. Inhibition of RNA recruitment and replication of an RNA virus by acridine derivatives with known anti-prion activities. *PLoS One.*, **2009**, *4*(10), e7376.
- Mucsi, I.; Molnár, J.; Tanaka, M.; Santelli-Rouvier, C.; Patelis, A.M.; Galy, J.P.; Barbe, J. Effect of acridine derivatives on the multiplication of herpes simplex virus. *Anticancer Res.*, **1998**, *18*(4C), 3011-3015.
- Zeitlenok, N.A.; Pille, E.R.; Konosh, O.V. Effect of acridine compounds on multiplication of vaccinia virus. *Vopr. Virusol.*, **1956**, *1*(2), 16-20.
- Csuk, R.; Barthel, A.; Brezesinski, T.; Raschke, C. Synthesis of dimeric acridine derived antivirals. *Bioorg. Med. Chem. Lett.*, **2004**, *14*(19), 4983-4985.
- Lyakhov, S.A.; Suveyzdis, Y.I.; Litvinova, L.A.; Andronati, S.A.; Rybalko, S.L.; Dyadyun, S.T. Biological active acridine derivatives. Part 4: Synthesis and antiviral activity of some bis-acridinylated diamides. *Pharmazie*, **2000**, *55*(10), 733-736.
- Gamage, S.A.; Figgitt, D.P.; Wojcik, S.J.; Ralph, R.K.; Ransijn, A.; Mauel, J.; Yardley, V.; Snowdon, D.; Croft, S.L.; Denny, W.A. Structure-activity relationships for the antileishmanial and antitrypanosomal activities of 1'-substituted 9-anilinoacridines. *J. Med. Chem.*, **1997**, *40*(16), 2634-2642.
- Bonse, S.; Santelli-Rouvier, C.; Barbe, J.; Krauth-Siegel, R.L. Inhibition of *Trypanosoma cruzi* trypanothione reductase by acridines: kinetic studies and structure-activity relationships. *J. Med. Chem.*, **1999**, *42*(26), 5448-5454.
- McSwain, M.L.; Forman, L.M. Severe parkinsonian symptom development on combination treatment with tacrine and haloperidol. *J. Clin. Psychopharmacol.*, **1995**, *15*(4), 284.
- Cabeza-Alvarez, C.I.; González-Rubio, M.; García-Montero, R.; Alvarez-Tejerina, A. Parkinsonian syndrome related to tacrine. *Neurologia*, **1999**, *14*(2), 96.
- Csuk, R.; Barthel, A.; Raschke, C.; Kluge, R.; Ströhl, D.; Trieschmann, L.; Böhm, G. Synthesis of monomeric and dimeric acridine compounds as potential therapeutics in Alzheimer and prion diseases. *Arch. Pharm. (Weinheim)*, **2009**, *342*(12), 699-709.

Apêndice B

- [31] Shutske, G.M.; Pierrat, F.A.; Cornfeldt, M.L.; Szwczak, M.R.; Huger, F.P.; Bores, G.M.; Harounian, V.; Davis, K.L. (+/-)-9-Amino-1,2,3,4-tetrahydroacridin-1-ol. A potential Alzheimer's disease therapeutic of low toxicity. *J. Med. Chem.*, **1988**, *31*(7), 1278-1279.
- [32] Otolenghi-Lodigiani, F. Treatment of chronic lupus erythematosus, local intradermal infiltration with an acridine preparation. *Hautarzt*, **1955**, *6*(1), 24-27.
- [33] Oppegard, L.M.; Ongolkov, A.V.; Luchini, D.N.; Schoon, R.A.; Goodell, J.R.; Kaur, H.; Billadeau, D.D.; Ferguson, D.M.; Hiasa, H. Novel acridine-based compounds that exhibit an anti-pancreatic cancer activity are catalytic inhibitors of human topoisomerase II. *Eur. J. Pharmacol.*, **2009**, *602*(2-3), 223-229.
- [34] Atwell, G.J.; Cain, B.F.; Seelye, R.N. Potential antitumour agents. 12. 9-Anilinoacridines. *J. Med. Chem.*, **1972**, *15*(6), 611-615.
- [35] Cain, B.F.; Seelye, R.N.; Atwell, G.J. Potential antitumour agents. 14. Acridylmethanesulfonanilides. *J. Med. Chem.*, **1974**, *17*(9), 922-930.
- [36] Pitta, I.R.; Lima, M.C.A.; Galdino, S.L.; Barbe, J. Molecules with Antitumour Activity and Chemical Synthesis. WO/2004/024058, March 25, 2004.
- [37] Clinical Trials.gov. Clofarabine or High-Dose Cytarabine, Pegaspargase, and Combination Chemotherapy Followed by Daunorubicin Hydrochloride or Doxorubicin Hydrochloride in Treating Young Patients With Acute Lymphoblastic Leukemia. 2010.
- [38] Clinical Trials.gov. Tacrine Effects on Cocaine Self-Administration and Pharmacokinetics. 2012.
- [39] Laufe, L.E.; Sokal, D.C.; Cole, L.P.; Shoupe, D.; Schenken, R.S. Phase I prehyostereotoxicity studies of the transcranial administration of quinacrine pellets. *Contraception*, **1996**, *54*(3), 181-186.
- [40] Gurova, K.V.; Hill, J.E.; Guo, C.; Prokvolit, A.; Burdelya, L.G.; Samoylova, E.; Khodyakova, A.V.; Ganapathi, R.; Ganapathi, M.; Tararova, N.D.; Bosykh, D.; Lvovskiy, D.; Webb, T.R.; Stark, G.R.; Gudkov, A.V. Small molecules that reactivate p53 in renal cell carcinoma reveal a NF-kappaB-dependent mechanism of p53 suppression in tumours. *Proc. Natl. Acad. Sci. U.S.A.*, **2005**, *102*(48), 17448-17453.
- [41] Sklarin, N.T.; Wiernik, P.H.; Grove, W.R.; Benson, L.; Mittelman, A.; Maroun, J.A.; Stewart, J.A.; Robert, F.; Doroshow, J.H.; Rosen, P.J. A phase II trial of CI-921 in advanced malignancies. *Invest. New Drugs*, **1992**, *10*(4), 309-312.
- [42] Dittrich, C.; Coudert, R.; Paz-Ares, L.; Caponigro, F.; Salzberg, M.; Gamucci, T.; Paoletti, X.; Hermans, C.; Lacombe, D.; Fumoleau, P. Phase II study of XR 5000 (DACA), an inhibitor of topoisomerase I and II, administered as a 120-h infusion in patients with non-small cell lung cancer. *Eur. J. Cancer*, **2003**, *39*(3), 330-334.
- [43] Galanis, E.; Buckner, J.C.; Maurer, M.J.; Reid, J.M.; Kuffel, M.J.; Ames, M.M.; Scheithauer, B.W.; Hammack, J.E.; Pipoly, G.; Kurosu, S.A. Phase I/II trial of pyrazoloacridine and carboplatin in patients with recurrent glioma: a North Central Cancer Treatment Group trial. *Invest. New Drugs*, **2005**, *23*(5), 495-503.
- [44] Su, T.L.; Chou, T.C. Experimental antitumour activity of acridone alkaloids, acronyline and glyfoline. *Chin. Pharm. J.*, **1994**, *46*(5), 371-391.
- [45] Koba, M.; Konopa, J. Interactions of antitumour triazoloacridinones with DNA. *Acta Biochim. Pol.*, **2007**, *54*(2), 297-306.
- [46] Burger, A. M.; Dai, F.; Schultes, C.M.; Reszka, A.P.; Moore, M.J.; Double, J.A.; Neidle, S. The G-quadruplex-interactive molecule BRACO-19 inhibits tumour growth, consistent with telomere targeting and interference with telomerase function. *Cancer Res.*, **2005**, *65*(4), 1489-1496.
- [47] Chabner, B.A.; Longo, D.L. In: *Cancer Chemotherapy and Biotherapy: Principles and Practice*, Lippincott William and Wilkins, Ed; Philadelphia, **2010**, pp. 451-475.
- [48] Walker, J.V.; Nitiss, J.L. DNA topoisomerase II as a target for cancer chemotherapy. *Cancer Invest.*, **2002**, *20*(4), 570-589.
- [49] Korth, C.; May, B. C. H.; Cohen, F. E.; Prusiner, S. B. Acridine and phenothiazine derivatives as pharmacotherapeutics for prion disease. *Proc. Natl. Acad. Sci. USA*, **2001**, *98*(17), 9836-9841.
- [50] Zawada, Z.; Sebestik, J.; Safarik, P.B. Dependence of the Reactivity of Acridine on Its Substituents: A Computational and Kinetic Study. *Eur. J. Org. Chem.*, **2011**, *2011*(34), 6989-6997.
- [51] Upshall, A.; Twardzik, D.R.; Sledziewski, A. Method of treatment of tumours using transforming growth factor-alpha. WO 02/24148 A2, March 28, 2002.
- [52] Department of Health. Annual Report of the chief medical officer: on the state of public health. http://www.dh.gov.uk/en/Publicationsandstatistics/Publications/AnnualReports/DH_076817 (Accessed May 23, 2012).
- [53] World Health Organization. Radiotherapy risk profile: technical manual Switzerland, 2008.
- [54] Symonds, R.P.; Foweraker, K. Principles of chemotherapy and radiotherapy. *Curr. Obstet. Gynaecol.*, **2006**, *16*, 100-106.
- [55] Pronzato, P.; Rondini, M. Hormonotherapy of advanced prostate cancer. *Ann. Oncol.*, **2005**, *16*(Suppl. 4), iv80-iv84.
- [56] Baxevasis, C.N.; Perez, S.A.; Papamichail, M. Cancer immunotherapy. *Crit. Rev. Clin. Lab. Sci.*, **2009**, *4*(4), 167-189.
- [57] Sheng, W.Y.; Huang, L. Cancer immunotherapy and nanomedicine. *Pharm. Res.*, **2011**, *28*(2), 200-214.
- [58] Lyse, A.N.; Britnie, R.J.; Thomas, S.G. Advances in Viral Vector-Based TRAIL Gene Therapy for Cancer. *Cancers*, **2011**, *3*(1), 603-620.
- [59] Chilin, A.; Marzaro, G.; Marzano, C.; Dalla, V.L.; Ferlin, M.G.; Pastorini, G.; Guiotto, A. Synthesis and antitumour activity of novel amsacrine analogs: the critical role of the acridine moiety in determining their biological activity. *Bioorg. Med. Chem.*, **2009**, *17*(2), 523-529.
- [60] Lerman, L.S. Structural considerations in the interaction of DNA and acridines. *J. Mol. Biol.*, **1961**, *3*, 18-30.
- [61] Lerman, L.S. The structure of the DNA-acridine complex. *Proc. Natl. Acad. Sci. U. S. A.*, **1963**, *49*, 94-102.
- [62] Strekowski, L.; Wilson, B. Noncovalent interactions with DNA: an overview. *Mutat. Res.*, **2007**, *623*(1-2), 3-13.
- [63] Sebestik, J.; Hlavacek, J.; Stibor, I. A role of the 9-aminoacridines and their conjugates in a life science. *Curr. Protein. Pept. Sci.*, **2007**, *8*(5), 471-483.
- [64] Wang, W.; Ho, W.C.; Dicker, D.T.; MacKinnon, C.; Winkler, J.D.; Marmorstein, R.; El-Deiry, W.S. Acridine derivatives activate p53 and induce tumour cell death through Bax. *Cancer Biol. Ther.*, **2005**, *4*(8), 893-898.
- [65] Malina, A.; Khan, S.; Carlson, C.B.; Svitkin, Y.; Harvey, I.; Sonenberg, N.; Beal, P.A.; Pelletier, J. Inhibitory properties of nucleic acid-binding ligands on protein synthesis. *FEBS Lett.*, **2005**, *579*(1), 79-89.
- [66] Alarcon, K.; Demeunynck, M.; Lhomme, J.; Carrez, D.; Croisy, A. Potentiation of BCNU cytotoxicity by molecules targeting abasic lesions in DNA. *Bioorg. Med. Chem.*, **2001**, *9*(7), 1901-1910.
- [67] Turnbull, R.M.; Meczes, E.L.; Perenna Rogers, M.; Lock, R.B.; Sullivan, D.M.; Finlay, G.J.; Baguley, B.C.; Austin, C.A. Carbamate analogues of amsacrine active against non-cycling cells: relative activity against topoisomerases IIalpha and beta. *Cancer Chemother. Pharmacol.*, **1999**, *44*(4), 275-282.
- [68] Denny, W.A. Chemotherapeutic effects of acridine derivatives. *Med. Chem. Rev.*, **2004**, *1*(3), 257-266.
- [69] Finlay, G.J.; Atwell, G.J.; Baguley, B.C. Inhibition of the action of the topoisomerase II poison amsacrine by simple aniline derivatives: evidence for drug-protein interactions. *Oncol. Res.*, **1999**, *11*(6), 249-254.
- [70] Graziano, M.J.; Courtney, C.L.; Meierhenry, E.F.; Kheoh, T.; Pegg, D.G.; Gough, A.W. Carcinogenicity of the anticancer topoisomerase inhibitor, amsacrine, in Wistar rats. *Fundam. Appl. Toxicol.*, **1996**, *32*(1), 53-65.
- [71] Baguley, B.C.; Denny, W.A.; Atwell, G.J.; Finlay, G.J.; Rewcastle, G.W.; Twigden, S.J.; Wilson, W.R. Synthesis, antitumour activity, and DNA binding properties of a new derivative of amsacrine, N-5-dimethyl-9-[(2-methoxy-4-methylsulfonylamino) phenylamino]-4-acridinecarboxamide. *Cancer Res.*, **1984**, *44*(8), 3245-3251.
- [72] Bailly, C.; Pommery, N.; Henichart, J.P. DNA-synthesis and tumour growth inhibitions by AGGA, a bleomycin-amsacrine hybrid derivative. *Cancer Lett.*, **1988**, *38*(3), 321-328.
- [73] Llana, E.; Del Campo, C.; Capo, M.; Anadon, M. Synthesis and antitumour activity of pyrido-amsacrine analogues and related compounds. *J. Pharm. Sci.*, **1993**, *82*(3), 262-265.
- [74] Figgitt, D.P.; Denny, W.A.; Gamage, S.A.; Ralph, R.K. Structure-activity relationships of 9-aminoacridines as inhibitors of human DNA topoisomerase II. *Anticancer Drug. Des.*, **1994**, *9*(3), 199-208.

Apêndice B

Novos Agentes Tiazacridínicos com Propriedades Anticâncer Marina G R Pitta

- [75] Cain, B.F.; Atwell, G.J.; Denny, W.A. Potential antitumour agents. 16,4-(Acridin-9-ylamino)methanesulfonanilides. *J. Med. Chem.*, **1975**, *18*(11), 1110-1117.
- [76] Chang, J.Y.; Lin, C.F.; Pan, W.Y.; Bacherikov, V.; Chou, T.C.; Chen, C.H.; Dong, H.; Cheng, S.Y.; Tasi, T.J.; Lin, Y.W.; Chen, K.T.; Chen, L.T. Su, T.L. New analogues of AHMA as potential antitumour agents: synthesis and biological activity. *Bioorg. Med. Chem.*, **2003**, *11*(23), 4959-4969.
- [77] Su, T.L.; Chen, C.H.; Huang, L.F.; Chen, C.H.; Bssu, M.K.; Zhang, X.G.; Chou, T.C. Synthesis and structure-activity relationships of potential anticancer agents: alkylcarbamates of 3-(9-acridinylamino)-5-hydroxymethylamine. *J. Med. Chem.*, **1999**, *42*(23), 4741-4748.
- [78] Ferlin, M.G.; Marzano, C.; Chiarello, G.; Baccichetti, F.; Bordin, F. Synthesis and antiproliferative activity of some variously substituted acridine and azacridine derivatives. *Eur. J. Med. Chem.*, **2000**, *35*(9), 827-837.
- [79] Chen, C.H.; Lin, Y.W.; Zhang, X.; Chou, T.C.; Tsai, T.J.; Kapuriya, N.; Kakadiya, R.; Su, T.L. Synthesis and *in vitro* cytotoxicity of 9-anilinoacridines bearing N-mustard residue on both anilino and acridine rings. *Eur. J. Med. Chem.*, **2009**, *44*(7), 3056-3059.
- [80] Sondhi, S.M.; Singh, J.; Rani, R.; Gupts, P.P.; Agrawal, S.K.; Saxena, A.K. Synthesis, anti-inflammatory and anticancer activity evaluation of some novel acridine derivatives. *Eur. J. Med. Chem.*, **2010**, *45*(2), 555-563.
- [81] Chen, Y.L.; Chen, L.L.; Lu, C.M.; Tzeng, C.C.; Tsao, L.T.; Wang, J.P. Synthesis and anti-inflammatory evaluation of 9-phenoxyacridine and 4-phenoxyfuro[2,3-b]quinoline derivatives. Part 2. *Bioorg. Med. Chem.*, **2003**, *11*(18), 3921-3927.
- [82] Di Giorgio, C.; Delmas, F.; Filloux, N.; Robin, M.; Seferian, L.; Azas, N.; Gasquet, M.; Costa, M.; Timon-David, P.; Galy, J.P. *In vitro* activities of 7-substituted 9-chloro and 9-amino-2-methoxyacridines and their bis- and tetra-acridine complexes against *Leishmania infantum*. *Antimicrob. Agents Chemother.*, **2003**, *47*(1), 174-180.
- [83] Konopa, J.; Pawlak, J.W.; Pawlak, K. The mode of action of cytotoxic and antitumour 1-nitroacridines. III. *In vivo* interstrand cross-linking of DNA of mammalian or bacterial cells by 1-nitroacridines. *Chem. Biol. Interact.*, **1983**, *43*(2), 175-197.
- [84] Narayanan, R.; Tiwari, P.; Inoa, D.; Ashok, B.T. Comparative analysis of mutagenic potency of 1-nitro-acridine derivatives. *Life Sciences*, **2005**, *77*(18), 2312-2323.
- [85] Yang, P.; Yang, Q.; Qian, X.; Tong, L.; Li, X. Isoquino[4,5-bc]acridines: design, synthesis and evaluation of DNA binding, anti-tumour and DNA photo-damaging ability. *J. Photochem. Photobiol. B*, **2006**, *84*(3), 221-226.
- [86] Osman, S.; Rowlinson-Busza, G.; Luthra, S.K.; Aboagye, E.O.; Brown, G.D.; Brady, F.; Myers, R.; Gamage, S.A.; Denny, W.A.; Baguley, B.C.; Price, P.M. Comparative biodistribution and metabolism of carbon-11-labeled N-[2-(dimethylamino)ethyl]acridine-4-carboxamide and DNA-intercalating analogues. *Cancer Res.*, **2001**, *61*(7), 2935-2944.
- [87] Pastwa, E.; Ciesielska, E.; Piestrzeniewicz, M.K.; Denny, W.A.; Gaizdowski, M.; Szmigiero, L. Cytotoxic and DNA-damaging properties of N-[2-(dimethylamino)ethyl]acridine-4-carboxamide (DACA) and its analogues. *Biochem. Pharmacol.*, **1998**, *56*(3), 351-359.
- [88] Bridewell, D.J.; Finlay, G.J.; Baguley, B.C. Topoisomerase I/II selectivity among derivatives of N-[2-(dimethylamino)ethyl]acridine-4-carboxamide (DACA). *Anticancer Drug Des.*, **2001**, *16*(6), 317-324.
- [89] Spicer, J.A.; Gamage, S.A.; Atwell, G.J.; Finlay, G.J.; Baguley, B.C.; Denny, W.A. Structure-activity relationships for acridine-substituted analogues of the mixed topoisomerase I/II inhibitor N-[2-(dimethylamino)ethyl]acridine-4-carboxamide. *J. Med. Chem.*, **1997**, *40*(12), 1919-1929.
- [90] Parajuli, R.; Sarma, R.L.; Das, M.L.; Medhi, C. Model study on the sequence specific stacking by chromophore of an anticancer drug, acridine carboxamide with base pairs of DNA. *IJ. Chem.*, **2007**, *46B*(9), 1483-1494.
- [91] Parajuli, R.; Medhi, C. Monitoring the sequence specific intercalation in nucleic acids by 9-substituted acridine-4-carboxamide. *I. J. Chem.*, **2006**, *45A*(1), 146-158.
- [92] Sugaya, T.; Mimura, Y.; Shida, Y.; Osawa, Y.; Matsukuma, I.; Ikeda, S.; Akinaga, S. Morimoto M, Ashizawa T, Okabe M. 6H-pyrazolo[4,5,1-de]acridin-6-ones as a novel class of antitumour agents. Synthesis and biological activity. *J. Med. Chem.*, **1994**, *37*(7), 1028-1032.
- [93] Antonini, I.; Polucci, P.; Magnano, A.; Martelli, S. Synthesis, antitumour cytotoxicity, and DNA-binding of novel N-5,2-di(omega-aminoalkyl)-2,6-dihydropyrazolo[3,4,5-k]acridine-5-carboxamides. *J. Med. Chem.*, **2001**, *44*(20), 3329-3333.
- [94] Bu, X.; Chen, J.; Deady, L.W.; Denny, W.A. Synthesis and cytotoxicity of potential anticancer derivatives of pyrazolo[3,4,5-k]acridine and indolo[2,3-a]acridine. *Tetrahedron*, **2002**, *58*(1), 175-181.
- [95] Antonini, I.; Polucci, P.; Magnano, A.; Sparapani, S.; Martelli, S. Rational design, synthesis, and biological evaluation of bis(pyrimido[5,6,1-de]acridines) and bis(pyrazolo[3,4,5-k]acridine-5-carboxamides) as new anticancer agents. *J. Med. Chem.*, **2004**, *47*(21), 5244-5250.
- [96] Liska, K.J. Preparation and antitumour properties of analogs of acronycine. *J. Med. Chem.*, **1972**, *15*(11), 1177-1179.
- [97] Costes, N.; Le Deit, H.; Michel, S.; Tillequin, F.; Koch, M.; Pfeiffer, B.; Renard, P.; Léonce, S.; Guilbaud, N.; Kraus-Berthier, L.; Pierré, A.; Atassi, G. Synthesis and cytotoxic and antitumour activity of benzo[b]pyrano[3, 2-h]acridin-7-one analogues of acronycine. **2000**, *J. Med. Chem.* *43*(12), 2395-2402.
- [98] Guilbaud, N.; Kraus-Berthier, L.; Meyer-Losic, F.; Malivet, V.; Chacun, C.; Jan, M.; Tillequin, F.; Michel, S.; Koch, M.; Pfeiffer, B.; Atassi, G.; Hickman, J.; Pierré, A. Marked antitumour activity of a new potent acronycine derivative in orthotopic models of human solid tumours. *Clin. Cancer Res.*, **2001** *7*(8), 2573-2580.
- [99] Guilbaud, N.; Léonce, S.; Tillequin, F.; Koch, M.; Hickman, J.A.; Pierré, A. Acronycine derivatives as promising antitumour agents. *Anticancer Drugs*, **2002**, *13*(5), 445-449.
- [100] David-Cordonnier, M.H.; Laine, W.; Lansiaux, A.; Kouach, M.; Briand, G.; Pierré, A.; Hickman, J.A.; Bailly, C. Alkylation of guanine in DNA by S23906-1, a novel potent antitumour compound derived from the plant alkaloid acronycine. *Biochemistry*, **2002**, *41*(31), 9911-9920.
- [101] Braga, P.A.; Dos Santos, D.A.; Da Silva, M.F.; Vieira, P.C.; Fernandes, J.B.; Houghton, P.J.; Fang, R. *In vitro* cytotoxicity activity on several cancer cell lines of acridone alkaloids and N-phenylethyl-benzamide derivatives from *Swinglea glutinosa* (Bl.) Merr. *Nat. Prod. Res.*, **2007**, *21*(1), 47-55.
- [102] Weniger, B.; Um, B.H.; Valentin, A.; Estrada, A.; Lobstein, A.; Anton, R.; Maillé, M.; Sauvain, M. Bioactive acridone alkaloids from *Swinglea glutinosa*. *J. Nat. Prod.*, **2001**, *64*(9), 1221-1223.
- [103] Stanlas, J.; Hagan, D.J.; Ellis, M.J.; Turner, C.; Carmichael, J.; Ward, W.; Hammonds, T.R.; Stevens, M.F. Antitumour polycyclic acridines. 7. Synthesis and biological properties of DNA affinic tetra- and pentacyclic acridines. *J. Med. Chem.*, **2000**, *43*(8), 1563-1572.
- [104] Rinehart, K.L.; Holt, T.G.; Fregeau, N.L.; Keifer, P.A.; Wilson, G.R.; Perun, T.J. Jr.; Sakai, R.; Thompson, A.G.; Stroh, J.G.; Shield, L.S. Bioactive compounds from aquatic and terrestrial sources. *J. Nat. Prod.*, **1990**, *53*(4), 771-792.
- [105] Alvarez, M.; Felin, L.; Ajana, W.; Joule, J.A.; Fernández-Puentes, J.L. Synthesis of Ascidiemine and an Isomer. *Eur. J. Org. Chem.*, **2000**, *2000*(5), 849-855.
- [106] Delfourne, E.; Roubin, C.; Bastide, J. The first synthesis of the pentacyclic pyridoacridine marine alkaloids: amoamines A and B. *J. Org. Chem.*, **2000**, *65*(18), 5476-5479.
- [107] Radchenko, O. S.; Balaneva, N.N.; Denisenko, V.A.; Novikov, V.L. A simple and effective approach to the synthesis of pyrido[4,3,2-mn]pyrrolo[3,2,1-de]acridine skeleton of amoamines A and B, pentacyclic marine alkaloids from the ascidian *Cystodytes* sp. *Tetrahedron Lett.*, **2006**, *47*(44), 7819-7822.
- [108] Cech, T.R. Life at the End of the Chromosome: Telomeres and Telomerase. *Angew. Chem. Int. Ed. Engl.*, **2000**, *39*(1), 34-43.
- [109] Gellert, G.C.; Jackson, S.R.; Dikmen, Z.G.; Wright, W.E.; Shay, J.W. Telomerase as a therapeutic target in cancer. *Drug Discov. Today Dis. Mech.*, **2005**, *2*(2), 159-164.
- [110] Kelland, L.R. Overcoming the immortality of tumour cells by telomere and telomerase based cancer therapeutics—current status and future prospects. *Eur. J. Cancer*, **2005**, *41*(7), 971-979.

- [111] Harrison, R.J.; Gowan, S.M.; Kelland, L.R.; Neidle, S. Human telomerase inhibition by substituted acridine derivatives. *Bioorg. Med. Chem. Lett.*, **1999**, *9*(17), 2463-2468.
- [112] Neidle, S.; Parkinson, G. Telomere maintenance as a target for anticancer drug discovery. *Nat Rev Drug Discov.*, **2002**, *1*(5), 383-393.
- [113] Harrison, R.J.; Cuesta, J.; Chessari, G.; Read, M.A.; Basra, S.K.; Reszka, A.P.; Morrell, J.; Gowan, S.M.; Incles, C.M.; Tamious, F.A.; Wilson, W.D.; Kelland, L.R.; Neidle, S. Trisubstituted acridine derivatives as potent and selective telomerase inhibitors. *J. Med. Chem.*, **2003**, *46*(21), 4463-4476.
- [114] Gunaratnam, M.; Greciano, O.; Martins, C.; Reszka, A.P.; Schultes, C.M.; Morjani, H.; Riou, J.F.; Neidle, S. Mechanism of acridine-based telomerase inhibition and telomere shortening. *Biochem. Pharmacol.*, **2007**, *74*(5), 679-689.
- [115] Zambre, V.P.; Murumkar, P.R.; Gridhar, R.; Yadav, M.R. Structural investigations of acridine derivatives by CoMFA and CoMSIA reveal novel insight into their structures toward DNA G-quadruplex mediated telomerase inhibition and offer a highly predictive 3D-model for substituted acridines. *J. Chem. Inf. Model.*, **2009**, *49*(5), 1298-1311.
- [116] Campbell, N.H.; Parkinson, G.N.; Reszka, A.P.; Neidle, S. Structural Basis of DNA Quadruplex Recognition by an Acridine Drug. *J. Am. Chem. Soc.*, **2008**, *130*(21), 6722-6724.
- [117] Di Giorgio, C.; Nikoyan, A.; Decome, L.; Botta, C.; Robin, M.; Reboul, J.P.; Sabatier, A.S.; Matta, A.; De Méo, M. DNA-damaging activity and mutagenicity of 16 newly synthesized thiazolo[5,4-a]acridine derivatives with high photo-inducible cytotoxicity. *Mutat. Res.*, **2008**, *630*(2), 104-114.
- [118] Cholody, W.M.; Martelli, S.; Konopa, J. 8-Substituted 5-[(aminoalkyl)amino]-6H-v-triazolo[4,5,1-de]acridin-6-ones as potential antineoplastic agents. Synthesis and biological activity. *J. Med. Chem.*, **1990**, *33*(10), 2852-2856.
- [119] Kuśnierczyk H, Cholody WM, Paradziej-Lukowicz J, Radzikowski C, Konopa J. Experimental antitumour activity and toxicity of the selected triazolo- and imidazoacridinones. *Arch. Immunol. Ther. Exp. (Warsz.)*, **1994**, *42*(5-6), 415-423.
- [120] Lemke, K.; Poindessous, V.; Skladanowski, A.; Larsen, A.K. The antitumour triazoloacridone C-1305 is a topoisomerase II poison with unusual properties. *Mol. Pharmacol.*, **2004**, *66*(4), 1035-1042.
- [121] Wesierska-Gadek, J.; Schloffer, D.; Gueorgieva, M.; Uhl, M.; Skladanowski, A. Increased susceptibility of poly(ADP-ribose) polymerase-1 knockout cells to antitumour triazoloacridone C-1305 is associated with permanent G2 cell cycle arrest. *Cancer Res.*, **2004**, *64*(13), 4487-4497.
- [122] Lemke, K.; Wojciechowski, M.; Laine, W.; Bailly, C.; Colson, P.; Baginski, M.; Larsen, A.K.; Skladanowski, A. Induction of unique structural changes in guanine-rich DNA regions by the triazoloacridone C-1305, a topoisomerase II inhibitor with antitumour activities. *Nucleic Acids Res.*, **2005**, *33*(18), 6034-6047.
- [123] Antonini, I.; Polucci, P.; Magnano, A.; Cacciamani, D.; Konieczny, M.T.; Paradziej-Lukowicz, J.; Martelli, S. Rational design, synthesis and biological evaluation of thiadiazinoacridines: a new class of antitumour agents. *Bioorg. Med. Chem.*, **2003**, *11*(3), 399-405.
- [124] Denny, W.A.; Atwell, G.J.; Baguley, B.C.; Wakelin, L.P. Potential antitumour agents. 44. Synthesis and antitumour activity of new classes of diacridines: importance of linker chain rigidity for DNA binding kinetics and biological activity. *J. Med. Chem.*, **1985**, *28*(11), 1568-1574.
- [125] Le Pecq, J.B.; Le Bret, M.; Barbet, J.; Roques, B. 1975. DNA polyintercalating drugs: DNA binding of diacridine derivatives. *Proc. Natl. Acad. Sci. U. S. A.*, **1975**, *72*(8), 2915-2919.
- [126] Barbet, J.; Roques, B.P.; Le Pecq, J.B. DNA-intercalating compounds. Synthesis of acridine dimers. *C. R. Acad. Sci. Hebd. Seances Acad. Sci. D*, **1975**, *281*(12), 851-853.
- [127] Wakelin, L.P.; Romanos, M.; Chen, T.K.; Glaubiger, D.; Canellakis, E.S.; Waring, M.J. Structural limitations on the bifunctional intercalation of diacridines into DNA. *Biochemistry*, **1978**, *17*(23), 5057-5063.
- [128] Chen, T.K.; Fico, R.; Canellakis, E.S. Diacridines, bifunctional intercalators. Chemistry and antitumour activity. *J. Med. Chem.*, **1978**, *21*(9), 868-874.
- [129] Spicer, J.A.; Gamage, S.A.; Finlay, G.J.; Denny, W.A. Synthesis and evaluation of unsymmetrical bis(arylcarboxamides) designed as topoisomerase-targeted anticancer drugs. *Bioorg. Med. Chem.*, **2002**, *10*(1), 19-29.
- [130] Gamage, S.A.; Spicer, J.A.; Atwell, G.J.; Finlay, G.J.; Baguley, B.C.; Denny, W.A. Structure-activity relationships for substituted bis(acridine-4-carboxamides): a new class of anticancer agents. *J. Med. Chem.*, **1999**, *42*(13), 2383-2393.
- [131] Sourdon, V.; Mazoyer, S.; Pique, V.; Galy, J.P. Synthesis of new bis- and tetra-acridines. *Molecules*, **2001**, *6*(8), 673-682.
- [132] Braña, M.F.; Casarubios, L.; Dominguez, G.; Fernández, C.; Pérez, J.M.; Quiroga, A.G.; Navarro-Ranninger, C.; de Pascual-Teresa, B. Synthesis, cytotoxic activities and proposed mode of binding of a series of bis([(9-oxo-9,10-dihydroacridine-4-carbonyl)amino]alkyl) alkylamines. *Eur. J. Med. Chem.*, **2002**, *37*(4), 301-313.
- [133] Augustus, T. M.; Anderson, J.; Hess, S.M.; Bierbach, U. Bis(acridinylthiourea)platinum(II) complexes: synthesis, DNA affinity, and biological activity in glioblastoma cells. *Bioorg. Med. Chem. Lett.*, **2003**, *13*(5), 855-858.
- [134] Triesscheijn, M.; Baas, P.; Schellens, J.H.; Stewart, F.A. Photodynamic therapy in oncology. *Oncologist*, **2006**, *11*(9), 1034-1044.
- [135] Fernandez, M.J.; Wilson, B.; Palacios, M.; Rodrigo, M.M.; Grant, K.B.; Lorente, A. Copper-activated DNA photocleavage by a pyridine-linked bis-acridine intercalator. *Bioconjug. Chem.*, **2007**, *18*(1), 121-129.
- [136] Vispé, S.; Vandenberghe, I.; Robin, M.; Annereau, J.P.; Créancier, L.; Pique, V.; Galy, J.P.; Kruczyński, A.; Barret, J.M.; Bailly, C. Novel tetra-acridine derivatives as dual inhibitors of topoisomerase II and the human proteasome. *Biochem. Pharmacol.*, **2007**, *73*(12), 1863-1872.
- [137] Watson, J.D.; Crick, F.H. Molecular structure of nucleic acids; a structure for deoxyribose nucleic acid. *Nature*, **1953**, *171*(4356), 737-738.

Apêndice B

APÊNDICE C - Artigo publicado. Synthesis and in vitro anticancer activity of novel thiazacridine derivatives

Journal: Medicinal Chemistry Research, v. 22, p. 2421-2429, 2013.

Autores: Marina Galdino da Rocha Pitta, Érika Silva Souza, Francisco Washington Araújo Barros, Manoel Odorico Moraes, Cláudia O Pessoa, Marcelo Zaldini Hernandes, Maria do Carmo Alves Lima, Suely Lins Galdino, Ivan da Rocha Pitta.

DOI 10.1007/s00044-012-0236-2

Synthesis and in vitro anticancer activity of novel thiazacridine derivatives

Marina Galdino da Rocha Pitta · Érika Silva Souza · Francisco Washington Araújo Barros · Manoel Odorico Moraes Filho · Cláudia O. Pessoa · Marcelo Zaldini Fernandes · Maria do Carmo Alves de Lima · Suely Lins Galdino · Ivan da Rocha Pitta

Received: 27 February 2012 / Accepted: 13 September 2012
© Springer Science+Business Media New York 2012

Abstract Acridine derivatives represent a well-known class of anticancer agents that generally interfere with DNA synthesis and inhibit topoisomerase II. A series of eight new 3-acridin-9-ylmethyl-thiazolidine-2,4-dione and 3-acridin-9-ylmethyl-5-arylidene-thiazolidine-2,4-dione derivatives were synthesized. All the compounds were evaluated for their cell antiproliferation activity with the 3-(4,5-dimethyl-2-thiazolyl)-2,5-diphenyl-2*H*-tetrazolium bromide, MTT assay. The antiproliferative effects of the synthesized compounds were tested against several tumoral cell lines, namely SF-295 (central nervous system), HCT-8 (colon carcinoma), and MDA-MB-435 (melanoma) cells using doxorubicin as a positive control. Among the synthesized compounds, 3-acridin-9-ylmethyl-5-acridin-9-ylmethylene-thiazolidine-2,4-dione, 3-acridin-9-ylmethyl-5-(4-methoxy-benzylidene)-thiazolidine-2,4-dione, and 3-acridin-9-ylmethyl-5-(4-bromo-benzylidene)-thiazolidine-2,4-dione exhibited the most potent anticancer activity against the HCT-8 and MDA-MB-435 cell lines. After a

detailed analysis of the structure of the thiazacridine molecules, we revealed the main possible interactions using the compound 3-acridin-9-ylmethyl-5-acridin-9-ylmethylene-thiazolidine-2,4-dione as an example. The benefits of these compounds, regardless of the pharmacological target are the presence of two aromatic rings (π systems), significant planarity (intercalating ability) and the presence of three hydrogen-bond acceptors, two of which are stronger (oxygen atoms) than the other (sulfur atom).

Keywords Thiazacridine MTT assay anticancer · Molecular modeling

Introduction

Until the early 1980s, intense research of drug discovery programs for cancer resulted in efficient medicinals, but with high toxicity due to the lack of selectivity (Brana *et al.*, 2001; Demeunynck *et al.*, 2001; Martinez and Chacon-Garcia, 2005; Cummings and Smyth, 1993; Georghiou, 1977). The design and synthesis of small molecules that bind selectively to and cleave nucleic acids are still major challenges in this field. These synthetic nucleases have important applications as tools in molecular biology and as potential therapeutic agents for the treatment of cancer (Fernandez *et al.*, 2007). Acridines and their derivatives are well-known probes for nucleic acids as well as being relevant in the field of drug development to establish new chemotherapeutic agents (Ghosh *et al.*, 2010). The acridine ring, one such nuclease, is a potential anticancer chromophore, which has a long history of treatment of human diseases, particularly parasitic infections, cancer and Alzheimer's disease (Demeunynck *et al.*, 2001; Denny, 2002; Chatellier and Lacomblez, 1990).

M. G. da Rocha Pitta · M. Z. Hernandez ·
M. do Carmo Alves de Lima · S. L. Galdino ·
I. da Rocha Pitta (✉)

Núcleo de Pesquisa em Inovação Terapêutica, Centro de
Ciências Biológicas, Universidade Federal de Pernambuco,
CEP 50670-901 Recife, Brazil
e-mail: irpitta@gmail.com

É. S. Souza
Universidade Tiradentes,
CEP 49032-490 Aracaju, Brazil

F. W. A. Barros · M. O. Moraes Filho · C. O. Pessoa
Departamento de Fisiologia e Farmacologia,
Faculdade de Medicina, Universidade Federal do Ceará,
CEP 60430-270 Fortaleza, Brazil

Published online: 28 September 2012

 Springer

Apêndice C

Novos Agentes Tiazacridínicos com Propriedades Anticâncer
Marina G R Pitta

Most acridine derivatives interact with DNA as intercalators. They represent a well-known class of multi-targeted anticancer agents that generally interfere with DNA synthesis, due to their ability to intercalate into DNA base pair and leading to cell cycle arrest and apoptosis. Treatment of human melanoma cell line (A375) with 9-phenyl acridine derivatives led to lowering of mitochondrial potential, upregulation of bax, release of cytochrome *C*, and activation of caspase 3 (Ghosh *et al.*, 2012).

Some bis-acridines bind to DNA through intercalation between consecutive nucleotides. The act of intercalation induces local structural changes to the DNA, including the unwinding of the double helix and lengthening of the DNA strand (Ferguson and Denny, 2007; Ghosh *et al.*, 2012; Sondhi *et al.*, 2010). Also, acridines are able to stabilize the DNA-topoisomerase I and II cleavable complex, and form the so-called 'ternary complex' which involves DNA, the intercalated compound, and topoisomerase (Chilin *et al.*, 2009; Vispe *et al.*, 2007). These enzymes can manipulate DNA by changing the number of topological links between two strands of the same or different DNA molecules (Champoux, 2001) and are involved in many cellular processes, such as replication, recombination, transcription, and chromosome segregation (Corbett and Osheroff, 1993; Wang, 1996; Nitiss, 1998).

The aim of this study was to evaluate the antiproliferative effect of eight novel thiazacridine derivatives against tumor cell lines.

Results and discussion

Chemistry

Thiazacridine derivatives were prepared by the method summarized in Scheme 1. Initially compound 3 was synthesized by the N-alkylation reaction of thiazolidine-2,4-dione, compound 1, with 9-bromomethyl-acridine, compound 2, in the presence of sodium hydroxide. The Michael reaction of 3-acridin-9-ylmethyl-thiazolidine-2,4-dione, compound 3, with different cyanoacrylates, compounds 4 and 6a-f, was carried out in the presence of piperidine, with ethanol as a solvent (Leite *et al.*, 2007; Mourao *et al.*, 2005; Pitta *et al.*, 2004, 2007; Pigatto *et al.*, 2011; Uchoa *et al.*, 2011). The presence of the arylidene proton peak in the synthesized derivatives, 5 and 7a-f, in proton nuclear magnetic resonance (¹H NMR) confirms completion of the nucleophilic addition reaction. It is also confirmed by MS data, which contains ions at *m/z* 193 and 235 in positive ESI-MS2 spectrum indicates the presence of the acridine and thiazolidine moiety, respectively (Fig. 1).

Biological activity

MTT assay

Compounds 3, 5, and 7a-f were tested for anticancer activity in a cell toxicity assay against three human cancer cell lines consisting of central nervous system (SF-295), colon carcinoma (HCT-8), and melanoma (MDA-MB-435), which were obtained from the National Cancer Institute (Bethesda, MD, USA).

The cells were maintained in RPMI 1640 medium supplemented with 10 % fetal bovine serum, 2 mM glutamine, 100 U/mL penicillin, and 100 µg/mL streptomycin at 37 °C with 5 % CO₂. The cells were grown in complete medium 1 day before each experiment.

The cell survival were quantified by measuring the ability of living cells to reduce the yellow dye 3-(4,5-dimethyl-2-thiazolyl)-2,5-diphenyl-2*H*-tetrazolium bromide (MTT) to a purple formazan product (Uchoa *et al.*, 2011; Denizot and Lang, 1986; Mosmann, 1983). For the experiments, cells were seeded in 96-well plates (0.7 × 10⁴ cells per well). After 24 h, when the cells reached confluence, the thiazacridine compounds (final concentration of 25 µg/mL) were dissolved in DMSO (0.1 %) and added to each well and incubated for 72 h. DMSO (0.1 %) and doxorubicin (0.3 µg/mL) were used as negative and positive controls, respectively. Thereafter, the plates were centrifuged, and the medium was replaced with fresh medium (150 µL) containing 0.5 mg/mL MTT. Three hours later, the formazan product was dissolved in 150 µL DMSO, and the absorbance was measured using a multi-plate reader (Spectra Count, Packard, Ontario, Canada) at 595 nm. The effect of the compounds was expressed as the percentage of inhibition of cellular growth (%GI), obtained from the absorbance of negative control (*A*_{NC}) and cells treated (*A*_T), according to the following formula: %GI = 100 × (1 - *A*_T/*A*_{NC}).

The potential effects on cell viability of the thiazacridine compounds are presented in Table 1. An activity scale was utilized to rank the cytotoxic potential of the tested samples against each of the cell lines: inactive samples (IS, 0–35 % inhibition), samples with low activity (LA, 36–55 % inhibition), moderate activity (MA, 56–85 % inhibition) and high activity (HA, 86–100 % inhibition).

The experiments were analyzed using the GraphPad Prism program, and the data are reported as the mean of two assays completed in triplicate.

Determination of IC₅₀

Drugs concentration that inhibited cell survival by 50 % compared with control cells (IC₅₀) were determined using

Scheme 1 Synthetic pathways of thiazacridines

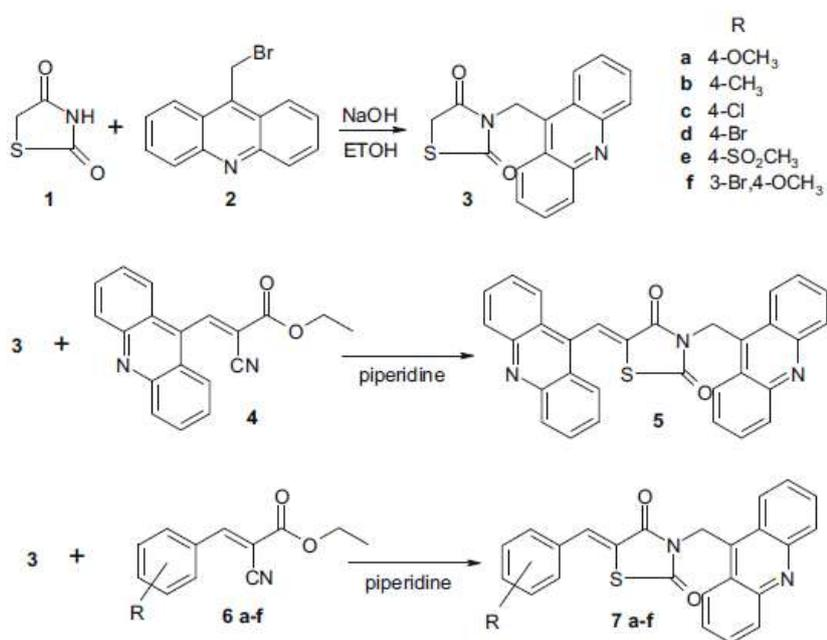


Fig. 1 Specific fragmentation in positive ESI-MS2 for 3-acridin-9-ylmethyl-5-arylidene-thiazolidine-2,4-diones

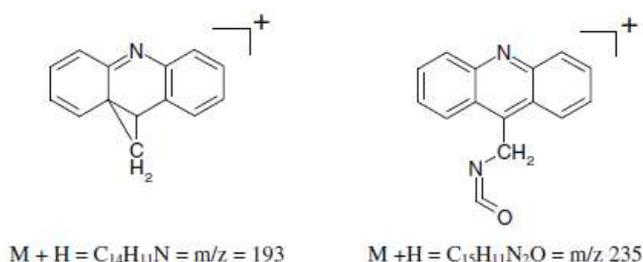


Table 1 Evaluation of cytotoxicity towards tumor cells (% cell inhibition) for the synthesized compounds 3, 5, and 7(a-f)

Compounds	SF-295	HCT-8	MDA-MB-435
3	32.8 (IS)	42.0 (LA)	0.00 (IS)
5	76.7 (MA)	92.4 (HA)	95.9 (HA)
7a	59.5 (MA)	86.7 (HA)	84.2 (MA)
7b	29.9 (IS)	51.3 (LA)	31.2 (IS)
7c	31.3 (IS)	37.8 (LA)	0.00 (IS)
7d	62.2 (MA)	96.6 (HA)	85.3 (MA)
7e	44.3 (LA)	64.3 (MA)	12.9 (IS)
7f	48.0 (LA)	72.5 (MA)	53.0 (LA)
Dox	91.1 (HA)	95.2 (HA)	93.6 (HA)

Date represent two experiments performed in triplicate. Doxorubicin (dox) was used as a positive control

Inactive samples (IS, 0–35 %), low activity (LA, 36–55 %)

Moderate activity (MA, 56–85 %) and high activity (HA, 86–100 %)

also MTT assay, as described above. The compounds were tested against four human cancer cell lines: HL-60 (promyelocytic leukemia), MDA-MB-435 (melanoma), HCT-8 (colon) and SF-295 (glioblastoma) as presented in Table 2, all obtained from the National Cancer Institute (Bethesda, MD, USA). The cells were plated in 96-well plates (0.7×10^4 cells/well for adherent cells and 0.3×10^5 cells/well for suspended cells) and compounds (0.049–25 $\mu\text{g/mL}$) dissolved in DMSO were added to each plate well.

In this report, we show the effect of eight acridine derivatives on cell survival. The structures of the synthesized compounds were confirmed by spectral data and elemental analysis and they were in full agreement with the proposed structures. The extent of inhibition of carcinoma cell lines by these compounds is schematically presented in Fig. 2. Among all the tested compounds, 3 and 7c exhibited

Table 2 Cytotoxicity activity of compounds for cancer cell lines

Compounds	Cell lines			
	HL-60	SF-295	HCT-8	MDA-MB-435
3	>25	>25	>25	>25
5	>25	4.44	4.45	7.01
7a	>25	3.37–5.85	3.57–5.55	5.50–8.92
7b	>25	>25	19.26	>25
7c	>25	>25	15.11–24.53	>25
7d	19.49	>25	20.63	>25
7e	>25	>25	18.24–23.34	>25
7f	>25	>25	>25	>25
Dox	0.02	0.48	0.04	0.24
	0.01–0.02	0.34–0.66	0.03–0.05	0.17–0.36

Data are present as IC₅₀ (µg/mL) values and 95 % confidence interval obtain by nonlinear regression. Data represent two experiments performed in triplicate. Doxorubicin (Dox) was used as positive control

the lowest inhibitory activity against the three carcinoma cell lines tested, especially against the MDA-MB-435 cell line. In addition, compounds 5, 7a, and 7d exhibited potent inhibitory activity against the MDA-MB-435 and HCT-8 cell lines, with greater than 85 % of inhibition in the HCT-8 cell line. The drugs concentrations that inhibited cell growth by 50 % compared with control cells (IC₅₀) were under 25 µg/mL for the compounds 5, 7a, and 7d. Thus, the compounds that had the best antitumor activity presented the smallest values at the IC₅₀ assays.

The biological activity of acridines is mainly attributed to the planarity of these aromatic structures, which allows

them to intercalate within the double-stranded DNA structure, thus interfering with the cellular machinery (Belmont *et al.*, 2007). In this way, connecting two planar intercalating moieties to obtain a bisacridine derivative generally increases the DNA binding affinity and the drug's residence times in the DNA-bound form (Antonini *et al.*, 2003). As expected, compound 5, which contains two acridine nucleus, showed a promising result.

In general, electronegative substituents at *para* position on the phenyl ring contributed to the biological activity. First the bromo group (7d) having a electron withdrawing inductive effect and second the methoxy group (7a) having electron donating effect

It is noteworthy that the position and the nature of the substituent on the heterocyclic core are the determinants for the biological properties observed. Therefore, it could be concluded that the cell survival of the tumor cell lines tested with the thiazacridine derivatives decreases in the presence of a methoxy group (7a), or a bromo group (7d) both at *para* position of the phenyl ring. However, the increase in the steric bulk on the phenyl ring due to the association of the bromo group (in *meta*) and methoxy group (in *para*), as in compound 7f, did not contributed to the activity.

Molecular modeling

In order to investigate the structures and properties of the thiazacridines, all optimized geometries were obtained using the AM1 semi-empirical method (Dewar *et al.*, 1985), available in the BioMedCACH software, using the internal default settings for convergence criteria. In addition, some electronic properties, such as electron affinity, ionization potential and molecular dipole moment were

Fig. 2 MTT assay for three tumor cell lines: a SF-295, b HCT-8 and c MDA-MB-435. Data represent two experiments performed in triplicate. Doxorubicin (dox) was used as the positive control. All compounds were tested at a dose 25 µg/mL. (Color figure online)

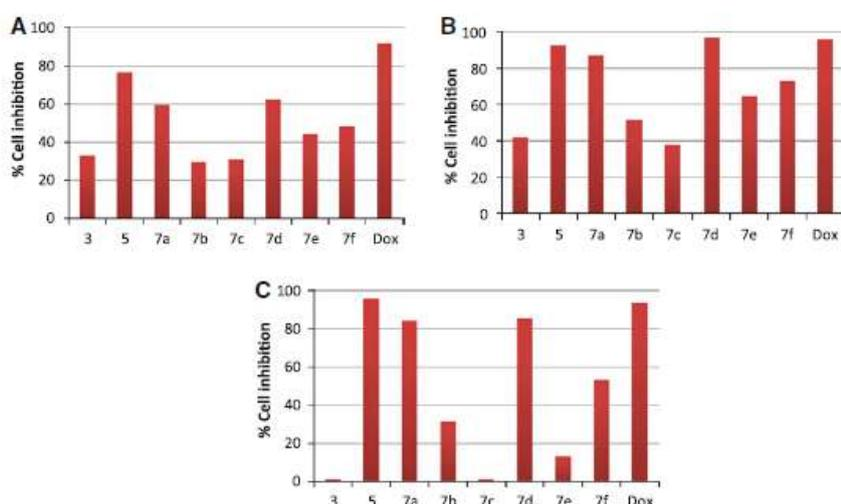


Table 3 Molecular properties and pharmacokinetic parameters, important for the good bioavailability of thiazacridine derivatives and doxorubicin (dox): number of hydrogen-bond acceptor and donor groups (nON and nOHNH, respectively), molecular weight (MW), calculated octanol/water partition coefficient (miLogP), number of

rule's violations (Nviolat), number of rotatable bonds (Nrotb), topological polar surface area (TPSA), molecular volume (Vol), the scores to judge the compound's overall potential to qualify for a drug (druglikeness and drug-score), dipole moment, electron affinity, and ionization potential energies

Compounds	Lipinski's rule of five					Nrotb ^a	TPSA ^a	Vol ^a	Druglikeness ^b	Drug-score ^b	Dipole moment (debye) ^c	Electron affinity (eV) ^c	Ionization potential (eV) ^c
	nON ^a	nOHNH ^a	MW ^a	miLogP ^a	Nviolat ^a								
3	4	0	308.36	3.07	0	2	50.27	259.51	2.15	0.42	2.48	1.21	8.56
5	5	0	497.58	6.67 ^d	1	3	64.86	425.36	4.38	0.14	2.66	1.34	8.52
7a	5	0	426.50	4.96	0	4	61.20	367.08	4.56	0.24	5.30	1.18	8.45
7b	4	0	410.50	5.35 ^d	1	3	51.97	358.10	2.97	0.22	4.72	1.22	8.46
7c	4	0	430.92	5.58 ^d	1	3	51.97	355.07	5.17	0.2	2.95	1.42	8.52
7d	4	0	475.37	5.71 ^d	1	3	51.97	359.42	2.46	0.17	2.72	1.47	8.53
7e	6	0	474.56	3.78	0	4	86.11	389.53	4.54	0.24	1.98	1.84	8.63
7f	5	0	505.39 ^d	5.7 ^d	2	4	61.20	384.97	3.52	0.17	3.89	1.32	8.50
dox	12 ^d	7 ^d	543.52 ^d	0.57	3	5	206.08	459.18	8.12	0.52	5.49	1.54	9.06

^a <http://www.molinspiration.com/cgi-bin/properties>

^b <http://www.organic-chemistry.org/prog/peo>

^c BioMedCACH software

^d Parameters that violate the Lipinski's rule of five

calculated. Then, the molecules were submitted to the classical analysis of Lipinski *et al.* (1997) using the Molinspiration online tool. Lipinski's rule of five verifies molecular features related to the optimum bioavailability of a drug. The number of rotatable bonds also seems to be an important descriptor for this purpose (Wenlock *et al.*, 2003). Other properties were also calculated, such as the topological polar surface area (TPSA), which is a very useful parameter for the prediction of drug transport properties (Ertl *et al.*, 2000), and molecular volume. In addition, we evaluated the scores to judge the compound's overall potential to qualify as a drug (druglikeness and drug-score) using the Osiris Property Explorer online system (<http://www.organic-chemistry.org/prog/peo>). All of these data are summarized in Table 3.

The TPSA is calculated at Molinspiration on-line, based on the methodology published by Ertl *et al.* (2000) as a sum of fragment contributions. Only oxygen- and nitrogen-centered polar fragments are considered. While Bytheway *et al.* (2008) applied TPSA analysis for drug design, Hou and Xu (2003) have used TPSA data for ADME evaluation. The computation of molecule volume in molinspiration website is based on group contributions and has been obtained by fitting the sum of fragment contributions to real 3D volume for a training set of about twelve thousand, mostly drug-like molecules.

From the Osiris Property Explorer online system, the druglikeness approach is based on a list of about 5,300 distinct substructure fragments with associated scores. The fragment list was created with traded drugs and commercially

available chemicals (Fluka), yielding a complete list of all available fragments. The distribution of the druglikeness values calculated for the 15000 Fluka chemicals remain in the range from -20 to 4 with the maximum occurrence around the value -1 for druglikeness score. The 3,300 traded drugs stay between -13 and 10 with the maximum around the value 2. This distribution shows that 80 % of the traded drugs have a positive druglikeness score, while the big majority of Fluka chemicals revealed negative values of druglikeness. Therefore, it is promising see that all the molecules calculated here have positive values of druglikeness ranging from 2.15 to 5.17 values (Table 2). The drug-score combines individual properties like druglikeness, cLogP, logS, molecular weight, and toxicity risks, in one value than may be used to judge the compound's overall potential to qualify for a drug. The drug-score is calculated by multiplying contributions of these individual properties, which are described as parametrized spline curves.

Thus, while the druglikeness values are based upon the occurrence frequency of each molecule's fragment in commercial drugs, the drug-score evaluates the compound's potential to qualify as a drug and is related to topological descriptors, fingerprints of druglikeness values, structural keys, and other properties such as cLogP, logs, molecular weight, and toxicity behavior. Several groups (Bernardino *et al.*, 2008; Campos *et al.*, 2009; Santos *et al.*, 2009) are using this scores (druglikeness and drug-score) to evaluate the potential of the studied molecules to become drugs.

According to Lipinski's rule, the violation of more than one of the specified criteria may decrease bioavailability. Our results demonstrated that all of the thiazacridine derivatives, except 3-acridin-9-ylmethyl-5-(3-bromo-4-methoxy-benzylidene)-thiazolidine-2,4-dione, compound **7f**, obey Lipinski's rule. It is important to stress that only the *miLogP* values, for five molecules (**5**, **7b-d**, and **7f**), slightly exceeds the value 5 preconized by Lipinski. In addition, only for molecule **7f** the molecular weight slightly passes over the limit (500). Table 2 shows that the reference drug, doxorubicin, seems to be very unlike the thiazacridine molecules, which is expected because of its peculiar molecular structure.

After a detailed analysis of the structure of thiazacridine molecules, we can see in Fig. 3 possible points of interactions of compound **5**. This derivative present high activity, at least against the HCT-8 and MDA-MB-435 cell lines (see Table 1). The benefits of these compounds, regardless of the pharmacological target, are the presence of two aromatic rings (π systems), significant planarity (intercalating ability) and the presence of three hydrogen-bond acceptors, two of which are stronger (oxygen atoms) than the other (sulfur atom).

Acridine and its derivatives are the most extensively studied DNA intercalating agents that bind reversibly but non-covalently to DNA (Hou and Xu, 2003). We evaluated the molecular properties and pharmacokinetic parameters of thiazacridine derivatives, which are considered potential drugs for anticancer treatment. Some compounds showed slightly better results when compared to the reference drug

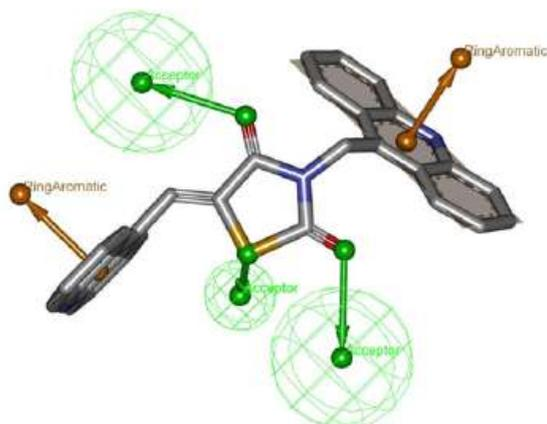


Fig. 3 Possible molecular points of interactions of thiazacridine derivatives using 3-acridin-9-ylmethyl-5-(3-bromo-4-methoxy-benzylidene)-thiazolidine-2,4-dione, compound **5**, as example. "Acceptor" corresponds to hydrogen-bond acceptor points and "Ring Aromatic" corresponds to aromatic rings. Carbon, oxygen, nitrogen and sulfur atoms are represented with gray, red, blue, and yellow colors, respectively. This figure was generated with DS visualizer software (Bytheway *et al.*, 2008) (Color figure online)

(doxorubicin), especially compounds 3-acridin-9-ylmethyl-5-(4-bromo-benzylidene)-thiazolidine-2,4-dione, compound **7d**, and 3-acridin-9-ylmethyl-5-acridin-9-ylmethylene-thiazolidine-2,4-dione, compound **5**, which were very active against the HCT-8 and MDA-MB-435 cell lines.

Materials and methods

All the synthesized compounds were analyzed with multiple analytical procedures. Melting points were determined in a capillary tube using a Quimis apparatus. Infrared spectra (IR) were recorded on a Bruker IFS66 spectrometer. ^1H NMR spectra were recorded on a Varian Plus 300 MHz spectrometer using $\text{DMSO-}d_6$ as a solvent and tetramethylsilane as an internal standard. The chemical shifts are expressed in ppm, and the following abbreviations are used: s is the singlet, d the doublet, t the triplet and m the multiplet. Mass spectra were recording using liquid chromatography/MS (LC/MS) with a HCT Ultra from Bruker Daltonics and were performed by electrospray ionization in positive or negative mode. The base peak of the MS spectrum is set to 100 (in percentage), and the height of the others peaks are measured relative to the base peak.

Experimental

Synthesis of 3-acridin-9-ylmethyl-thiazolidine-2,4-diones (**3**)

Thiazolidine-2,4-dione, compound **1**, (1.0 eq) and sodium hydroxide, previously solubilized in ethanol, were stirred for 10 min at room temperature (25 °C). 9-Bromomethyl-acridine, compound **2**, (1.0 eq) was added, and the mixture was stirred at 60 °C for 7 h. After completion of the reaction, the mixture was filtered and washed with water. The product obtained was a yellow solid. Formula: $\text{C}_{17}\text{H}_{12}\text{N}_2\text{O}_2\text{S}$. Melting point (m.p.): 196–197 °C. Yield: 51 %. IR (KBr, cm^{-1}): 2889 ($-\text{CH}_2-$), 1750 ($\text{C}=\text{O}$), 1694 ($\text{C}=\text{O}$), 750 ($\text{C}-\text{H}$). ^1H NMR (300 MHz, $\text{DMSO-}d_6$) δ 8.42 (d, 2H, $J = 8.7$ Hz, Acr-H, 4 pos.), 8.17 (d, 2H, $J = 8.4$ Hz, Acr-H, 1 pos.), 7.83–7.88 (m, 2H, Acr-H, 3 pos.), 7.65–7.70 (m, 2H, Acr-H, 2 pos.), 5.75 (s, 2H, N- CH_2), 4.23 (s, 2H, S- CH_2). MS m/z (%): (M+H) $^+$ 309.1 (100), calculated 308; +MS2 309.1 (56), 235 (100), 192 (98).

General preparation of 3-acridin-9-ylmethyl-5-arylidene-thiazolidine-2,4-dione (**5** and **7a-f**)

3-Acridin-9-ylmethyl-thiazolidine-2,4-dione, compound **3**, (1.0 eq) and either 3-acridin-9-yl-2-cyano-acrylic acid

ethyl ester, compound **4**, (1.0 eq) or one of the phenyl-substituted 2-cyano-3-phenyl-acrylic acid ethyl esters, compounds **6a–f**, were refluxed in ethanol in the presence of piperidine and heated at 50 °C for 4 h. After this period, the mixture was filtered and washed with water and ethanol (Pitta *et al.*, 2004, 2007).

3-Acridin-9-ylmethyl-5-acridin-9-ylmethylene-thiazolidine-2,4-dione (5)

Yellow solid. C₃₁H₁₉N₃O₂S. m.p.: 243–245 °C. Yield: 11 %. IR (KBr, cm⁻¹): 1759 (C=O), 1694 (C=O), 760 (C–H). H¹NMR (300 MHz, DMSO-*d*₆) δ 8.75 (s, 1H, =CH), 8.54 (d, 2H, *J* = 9.0 Hz, 3-Acr-H, 4 pos.), 8.21 (d, 2H, *J* = 8.7 Hz, 5-Acr-H, 4 pos.), 8.13 (d, 2H, *J* = 8.1 Hz, 3-Acr-H, 1 pos.), 8.04 (d, 2H, *J* = 8.4 Hz, 5-Acr-H, 1 pos.), 7.87–7.92 (m, 2H, 5-Acr-H, 3 pos.), 7.81–7.84 (m, 2H, 3-Acr-H, 3 pos.), 7.72–7.77 (m, 2H, 5-Acr-H, 2 pos.), 7.60–7.68 (m, 2H, 3-Acr-H, 2 pos.), 5.96 (s, 2H, –CH₂). MS *m/z* (%): (M+H)⁺ 498.2 (100), calculated 497; +MS2 498.2 (28), 305 (99), 236 (43), 193 (100).

3-Acridin-9-ylmethyl-5-(4-methoxy-benzylidene)-thiazolidine-2,4-dione (7a)

Yellow solid. C₂₅H₁₈N₂O₃S. m.p.: 225–226 °C. Yield: 52 %. IR (KBr, cm⁻¹): 1744 (C=O), 1679 (C=O), 1593 (C=C), 756 (C–H). H¹NMR (300 MHz, DMSO-*d*₆) δ 8.49 (d, 2H, *J* = 9.0 Hz, Acr-H, 4 pos.), 8.16 (d, 2H, *J* = 8.4 Hz, Acr-H, 1 pos.), 7.90 (s, 1H, =CH), 7.81–7.89 (m, 2H, Acr-H, 3 pos.), 7.60–7.71 (m, 2H, Acr-H, 2 pos.), 7.55 (d, 2H, *J* = 8.7 Hz, Ar-H, 2,6 pos.), 7.08 (d, 2H, *J* = 8.7 Hz, Ar-H, 3,5 pos.), 5.93 (s, 2H, N–CH₂), 3.81 (s, 3H, O–CH₃). MS *m/z* (%): (M+H)⁺ 427.2 (100), calculated 426; +MS2 427.2 (54), 235 (100), 193 (70).

3-Acridin-9-ylmethyl-5-(4-methyl-benzylidene)-thiazolidine-2,4-dione (7b)

Yellow solid. C₂₅H₁₈N₂O₂S. m.p.: 194–195 °C. Yield: 20 %. IR (KBr, cm⁻¹): 1729 (C=O), 1674 (C=O), 1604 (C=C), 760 (C–H). H¹NMR (300 MHz, DMSO-*d*₆) δ 8.46 (d, 2H, *J* = 8.7 Hz, Acr-H, 4 pos.), 8.19 (d, 2H, *J* = 8.7 Hz, Acr-H, 1 pos.), 7.90 (s, 1H, =CH), 7.81–7.86 (m, 2H, Acr-H, 3 pos.), 7.60–7.71 (m, 2H, Acr-H, 2 pos.), 7.47 (d, 2H, *J* = 8.1 Hz, Ar-H, 2,6 pos.), 7.33 (d, 2H, *J* = 8.1 Hz, Ar-H, 3,5 pos.), 5.92 (s, 2H, N–CH₂), 2.34 (s, 3H, –CH₃). MS *m/z* (%): (M+H)⁺ 411.2 (100), calculated 410; +MS2 411.2 (48), 235 (100), 193 (39).

3-Acridin-9-ylmethyl-5-(4-chloro-benzylidene)-thiazolidine-2,4-dione (7c)

Yellow solid. C₂₄H₁₅ClN₂O₂S. m.p.: 229–231 °C. Yield: 47 %. IR (KBr, cm⁻¹): 1739 (C=O), 1689 (C=O), 1608 (C=C), 750 (C–H). H¹NMR (300 MHz, DMSO-*d*₆) δ 8.45 (d, 2H, *J* = 8.7 Hz, Acr-H, 4 pos.), 8.19 (d, 2H, *J* = 8.7 Hz, Acr-H, 1 pos.), 7.93 (s, 1H, =CH), 7.83–7.88 (m, 2H, Acr-H, 3 pos.), 7.66–7.71 (m, 2H, Acr-H, 2 pos.), 7.62–7.56 (m, 4H, Ar-H), 5.93 (s, 2H, N–CH₂). MS *m/z* (%): (M+H)⁺ 431.1 (100), calculated 430; +MS2 431.1 (77), 235 (100), 193 (50).

3-Acridin-9-ylmethyl-5-(4-bromo-benzylidene)-thiazolidine-2,4-dione (7d)

Yellow solid. C₂₄H₁₅BrN₂O₂S. m.p.: 222–223 °C. Yield: 24 %. IR (KBr, cm⁻¹): 1744 (C=O), 1689 (C=O), 1608 (C=C), 750 (C–H). H¹NMR (300 MHz, DMSO-*d*₆) δ 8.45 (d, 2H, *J* = 9.0 Hz, Acr-H, 4 pos.), 8.19 (d, 2H, *J* = 8.7 Hz, Acr-H, 1 pos.), 7.90 (s, 1H, =CH), 7.84–7.89 (m, 2H, Acr-H, 3 pos.), 7.70–7.73 (d, 2H, *J* = 8.7 Hz, Ar-H, 3,5 pos.), 7.66–7.71 (m, 2H, Acr-H, 2 pos.), 7.51 (d, 2H, *J* = 8.4 Hz, Ar-H, 2,6 pos.), 5.92 (s, 2H, N–CH₂). MS *m/z* (%): (M+H)⁺ 475.1 (92), (M+2+H)⁺ 477.1 (100), calculated 474; +MS2 475.1 (100), 235 (98), 193 (50).

3-Acridin-9-ylmethyl-5-(4-methanesulfonyl-benzylidene)-thiazolidine-2,4-dione (7e)

Yellow solid. C₂₅H₁₈N₂O₄S₂. m.p.: 227–228 °C. Yield: 28 %. IR (KBr, cm⁻¹): 3440 (O=S=O), 1744 (C=O), 1689 (C=O), 1608 (C=C), 1142 (O=S=O). H¹NMR (300 MHz, DMSO-*d*₆) δ 8.46 (d, 2H, *J* = 8.4 Hz, Acr-H, 4 pos.), 8.19 (d, 2H, *J* = 8.1 Hz, Acr-H, 1 pos.), 8.03 (d, 2H, *J* = 7.2 Hz, Ar-H, 3,5 pos.), 8.02 (s, 1H, =CH), 7.85–7.90 (m, 2H, Acr-H, 3 pos.), 7.83 (d, 2H, *J* = 8.4 Hz, Ar-H, 2,6 pos.), 7.67–7.73 (m, 2H, Acr-H, 2 pos.), 5.94 (s, 2H, N–CH₂), 3.25 (s, 3H, S–CH₃). MS *m/z* (%): (M+H)⁺ 475.1 (100), 383 (99), calculated 474; +MS2 475.1 (65), 396 (100), 235 (90), 193(40), 192 (55).

3-Acridin-9-ylmethyl-5-(3-bromo-4-methoxy-benzylidene)-thiazolidine-2,4-dione (7f)

Yellow solid. C₂₅H₁₇BrN₂O₃S. m.p.: 230–232 °C. Yield: 62 %. IR (KBr, cm⁻¹): 1730 (C=O), 1684 (C=O), 1589 (C=C), 1267 (C–O), 756 (C–H). H¹NMR (300 MHz, DMSO-*d*₆) δ 8.46 (d, 2H, *J* = 8.4 Hz, Acr-H, 4 pos.), 8.19 (d, 2H, *J* = 8.1 Hz, Acr-H, 1 pos.), 7.89 (s, 1H, =CH), 7.86–7.87 (m, 2H, Acr-H, 3 pos.), 7.85 (d, 1H, *J* = 3 Hz, Ar-H, 2 pos.), 7.65–7.72 (m, 2H, Acr-H, 2 pos.), 7.58 (dd,

1H, $J = 8,7$ and $1,8$ Hz, Ar-H, 6 pos.), 7,26 (d, 1H, $J = 9,0$ Hz, Ar-H, 5 pos.), 5,92 (s, 2H, N-CH₂), 3,99 (s, 3H, O-CH₃). MS m/z (%): (M+H)⁺ 505.1 (99.5), (M+2+H)⁺ 507.1 (100), calculated 504; +MS2 505.1 (14), 490 (71), 235 (100), 192 (71), 193 (72).

Conclusion

The eight newly synthesized 3-acridin-9-ylmethyl-thiazolidine-2,4-dione and 3-acridin-9-ylmethyl-5-arylidene-thiazolidine-2,4-dione analogues were evaluated for their anticancer activity against the human cancer cell lines consisting of central nervous system (SF-295), colon carcinoma (HCT-8) and the melanoma (MDA-MB-435). We have found that the acridine dimer 3-acridin-9-ylmethyl-5-acridin-9-ylmethylene-thiazolidine-2,4-dione demonstrates potent DNA binding affinity and a significant anticancer activity against all the three cancer cell lines tested. The great majority of the molecules presented in this paper seems to obey the Lipinski's rule of five regarding the bioavailability features. In addition, the compound 3-acridin-9-ylmethyl-5-(4-methoxy-benzylidene)-thiazolidine-2,4-dione having electron donating group methoxy as substituent on phenyl ring and the compound 3-acridin-9-ylmethyl-5-(4-bromo-benzylidene)-thiazolidine-2,4-dione having a electron withdrawing inductive effect of the bromo group on the phenyl ring also exhibited strong inhibition in the same cell lines.

Acknowledgments The authors are thankful to CNPq (Conselho Nacional de Desenvolvimento Científico e Tecnológico, Brasil), the CAPES/COFECUB (Fundação Coordenação de Aperfeiçoamento de Pessoal de Ensino Superior/Comité Français d'Évaluation de la Coopération Universitaire avec le Brésil), the INCT_IF (Instituto Nacional de Ciência e Tecnologia para Inovação Farmacêutica) and the PPGIT (Programa de Pós-Graduação em Inovação Terapêutica) for their support of the joint research program.

References

- Antonini I, Polucci P, Magnano A, Gatto B, Palumbo M, Menta E, Pescalli N, Martelli S (2003) Design, synthesis, and biological properties of new bis(acridine-4-carboxamides) as anticancer agents. *J Med Chem* 46:3109–3115. doi:10.1021/jm030820x
- Belmont P, Bosson J, Godet T, Tiano M (2007) Acridine and acridone derivatives, anticancer properties and synthetic methods: where are we now? *Anticancer Agents Med Chem* 7:139–169. doi:10.2174/187152007780058669
- Bernardino AMR, Castro HC, Frugulhetti ICPP, Loureiro NIV, Azevedo AR, Pinheiro LCS, Souza TML, Giongo V, Passamani F, Magalhães UO, Albuquerque MG, Cabral LM, Rodrigues CR (2008) SAR of a series of anti-HSV-1 acridone derivatives, and a rational acridone-based design of a new anti-HSV-1 3H-benzo[b]pyrazolo[3,4-h]-1,6-naphthyridine series. *Bioorg Med Chem* 16:313–321. doi:10.1016/j.bmc.2007.09.03
- BioMedCACHe version 6.1, 2000–2003 Fujitsu Limited, <http://www.cache.fujitsu.com/biomedcache>. Accessed 25 Nov 2011
- Brana MF, Cacho M, Gradillas A, de Pascual-Teresa B, Ramos A (2001) Intercalators as anticancer drugs. *Curr Pharm Des* 7:1745–1780. doi:10.2174/1381612013397113
- Bytheway I, Darley MG, Popelier PLA (2008) The calculation of polar surface area from first principles: an application of quantum chemical topology to drug design. *Chem Med Chem* 3:445–453. doi:10.1002/cmde.200700262
- Campos VR, Abreu PA, Castro HC, Rodrigues CR, Jordão AK, Ferreira VF, Souza MCBV, Santos FC, Moura LA, Domingos TS, Carvalho C, Sanchez EF, Fuly AL, Cunha AC (2009) Synthesis, biological, and theoretical evaluations of new 1,2,3-triazoles against the hemolytic profile of the *Lachesis muta* snake venom. *Bioorg Med Chem* 17:7429–7434. doi:10.1016/j.bmc.2009.09.031
- Champoux JJ (2001) DNA topoisomerases: structure, function, and mechanism. *Annu Rev Biochem* 70:369–413. doi:10.1146/annurev.biochem.70.1.369
- Chatellier G, Lacomblez L (1990) Tacrine (tetrahydroaminoacridine; THA) and lecithin in senile dementia of the Alzheimer type: a multicentre trial. Groupe Français d'Etude de la Tetrahydroaminoacridine. *BMJ* 300:495–499. doi:10.1136/bmj.300.6723.495
- Chilin A, Marzaro G, Marzano C, Dalla Via L, Ferlin MG, Pastorini G, Guiotto A (2009) Synthesis and antitumor activity of novel amsacrine analogs: the critical role of the acridine moiety in determining their biological activity. *Bioorg Med Chem* 17:523–529. doi:10.1016/j.bmc.2008.11.072
- Corbett AH, Osheroff N (1993) When good enzymes go bad: conversion of topoisomerase II to a cellular toxin by antineoplastic drugs. *Chem Res Toxicol* 6:585–597. doi:10.1021/cr00035a001
- Cummings J, Smyth JF (1993) DNA topoisomerase I and II as targets for rational design of new anticancer drugs. *Ann Oncol* 4:533–543
- Demeunynck M, Charmantray F, Martelli A (2001) Interest of acridine derivatives in the anticancer chemotherapy. *Curr Pharm Des* 7:1703–1724. doi:10.2174/1381612013397131
- Denizot F, Lang R (1986) Rapid colorimetric assay for cell growth and survival. Modifications to the tetrazolium dye procedure giving improved sensitivity and reliability. *J Immunol Methods* 89:271–277. doi:10.1016/0022-1759(86)90368-6
- Denny WA (2002) Acridine derivatives as chemotherapeutic agents. *Curr Med Chem* 9:1655–1665. doi:10.2174/0929867023369277
- Dewar MJS, Zebisch EG, Healy EF, Stewart JJP (1985) Development and use of quantum mechanical molecular models. 76. AM1: a new general purpose quantum mechanical molecular model. *J Am Chem Soc* 107:3902–3909. doi:10.1021/ja00299a024
- Discovery Studio Visualizer v2.5.1.9167, Copyright © 2005–09. Accelrys Software Inc., San Diego
- Ertl P, Rohde B, Selzer P (2000) Fast calculation of molecular polar surface area as a sum of fragment-based contributions and its application to the prediction of drug transport properties. *J Med Chem* 43:3714–3717. doi:10.1021/jm000942e
- Ferguson LR, Denny WA (2007) Genotoxicity of non-covalent interactions: DNA intercalators. *Mutat Res* 623:14–23. doi:10.1016/j.mrfmmm.2007.03.014
- Fernandez MJ, Wilson B, Palacios M, Rodrigo MM, Grant KB, Lorente A (2007) Copper-activated DNA photocleavage by a pyridine-linked bis-acridine intercalator. *Bioconjug Chem* 18:121–129. doi:10.1021/bc0601828
- Georghiou S (1977) Interaction of acridine drugs with DNA and nucleotides. *Photochem Photobiol* 26:59–68. doi:10.1111/j.1751-1097.1977.tb07450.x
- Ghosh R, Bhowmik S, Bagchi A, Das D, Ghosh S (2010) Chemotherapeutic potential of 9-phenyl acridine: biophysical studies on its binding to DNA. *Eur Biophys J* 39:1243–1249. doi:10.1007/s00249-010-0577-z
- Ghosh R, Bhowmik S, Guha D (2012) 9-Phenyl acridine exhibits antitumor activity by inducing apoptosis in A375 cells. *Mol Cell Biochem* 361:55–66. doi:10.1007/s11010-011-1088-7

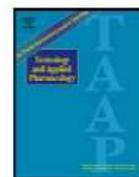
- Hou TJ, Xu XJ (2003) ADME evaluation in drug discovery. 3. Modeling blood-brain barrier partitioning using simple molecular descriptors. *J Chem Inf Model* 43:2137–2152. doi:10.1021/ci034134i
- Leite LFC, Mourao RHV, Lima MCA, Galdino SL, Hernandez MZ, Neves ARF, Vidal S, Barbe J, Pitta IR (2007) Synthesis, biological evaluation and molecular modeling studies of arylidene-thiazolidinediones with potential hypoglycemic and hypolipidemic activities. *Eur J Med Chem* 42:1263–1271. doi:10.1016/j.ejmech.2007.02.015
- Lipinski CA, Lombardo F, Dominy BW, Feeney PJ (1997) Experimental and computational approaches to estimate solubility and permeability in drug discovery and development settings. *Adv Drug Deliv Rev* 23:4–25. doi:10.1016/S0169-409X(96)00423-1
- Martínez R, Chacon-García L (2005) The search of DNA-intercalators as antitumoral drugs: what it worked and what did not work. *Curr Med Chem* 12:127–151. doi:10.2174/0929867053363414
- Molinspiration online tool. <http://www.molinspiration.com/cgi-bin/properties>. Accessed 5 Feb 2011
- Mosmann T (1983) Rapid colorimetric assay for cellular growth and survival: application to proliferation and cytotoxicity assays. *J Immunol Methods* 65:55–63. doi:10.1016/0022-1759(83)90303-4
- Mourao RH, Silva TG, Soares AL, Vieira ES, Santos JN, Lima MCA, Lima VL, Galdino SL, Barbe J, Pitta IR (2005) Synthesis and biological activity of novel acridinylidene and benzylidene thiazolidinediones. *Eur J Med Chem* 40:1129–1133. doi:10.1016/j.ejmech.2005.06.002
- Nitiss JL (1998) Investigating the biological functions of DNA topoisomerases in eukaryotic cells. *Biochim Biophys Acta* 1400:63–81. doi:10.1016/S0167-4781(98)00128-6
- Pigatto MC, Lima MCA, Galdino SL, Pitta IR, Vessecchi R, Assis MD, Santos JS, Dalla Costa T, Lopes NP (2011) Metabolism evaluation of the anticancer candidate AC04 by biomimetic oxidative model and rat liver microsomes. *Eur J Med Chem* 46:4245–4251. doi:10.1016/j.ejmech.2011.06.029
- Pitta IR, Lima MCA, Galdino SL, Barbe JF (2004). Molecules with antitumor activity and chemical. PCT/BR03/00128
- Pitta IR, Lima MCA, Galdino SL (2007) Acridine derivatives with antitumoral activity. WO 2007/109871 A2
- Santos FC, Abreu P, Castro HC, Paixão ICPP, Cirne-Santos CC, Giongo V, Barbosa JE, Simonetti BR, Garrido V, Bou-Habib DC, Silva DO, Batalha PN, Temerozo JR, Souza TM, Nogueira CM, Cunha AC, Rodrigues CR, Ferreira VF, Souza MCBV (2009) Synthesis, antiviral activity and molecular modeling of oxoquinoline derivatives. *Bioorg Med Chem* 17:5476–5481. doi:10.1016/j.bmc.2009.06.037
- Sondhi SM, Singh J, Rani R, Gupta PP, Agrawal SK, Saxena AK (2010) Synthesis, anti-inflammatory and anticancer activity evaluation of some novel acridine derivatives. *Eur J Med Chem* 45:555–563. doi:10.1016/j.ejmech.2009.10.042
- Uchoa FT, Haas SE, Junior LB, Pigatto MC, Lima MCA, Galdino SL, Pitta IR, Costa TD (2011) Development and validation of an LC-MS/MS method for the pre-clinical pharmacokinetic investigation of the anticancer candidate AC04 in rodents. *J Liq Chrom Rel Technol* 34:744–752. doi:10.1080/10826076.2011.563890
- Vispe S, Vandenberghe I, Robin M, Annereau JP, Creancier L, Pique V, Galy JP, Kruczynski A, Barret JM, Bailly C (2007) Novel tetra-acridine derivatives as dual inhibitors of topoisomerase II and the human proteasome. *Biochem Pharmacol* 73:1863–1872. doi:10.1016/j.bcp.2007.02.016
- Wang JC (1996) DNA topoisomerases. *Annu Rev Biochem* 65:635–692. doi:10.1146/annurev.bi.65.070196.003223
- Wenlock MC, Austin RP, Barton P, Davis AM, Leeson PD (2003) A comparison of physicochemical property profiles of development and marketed oral drugs. *J Med Chem* 46:1250–1256. doi:10.1021/jm021053p

APÊNDICE D - Artigo Publicado. Inhibition of DNA topoisomerase I activity and induction of apoptosis by thiazacridine derivatives.

Journal: Toxicology and Applied Pharmacology, v. 268, n. 1, p.37 - 46, 2013.

Autores: Francisco W. A. Barros, Daniel P. Bezerra, Paulo M. P. Ferreira, Bruno C. Cavalcanti, Teresinha G. Silva, Marina G. R. Pitta, Maria do C. A. de Lima, Suely L. Galdino, Ivan da R. Pitta, Letícia V. Costa-Lotufo, Manoel O. Moraes, Rommel R. Burbano, Temenouga N. Guecheva, João A. P. Henriques, Cláudia Pessoa

DOI: 10.1016/j.taap.2013.01.010



Inhibition of DNA topoisomerase I activity and induction of apoptosis by thiazacridine derivatives

Francisco W.A. Barros ^a, Daniel P. Bezerra ^{b,*}, Paulo M.P. Ferreira ^c, Bruno C. Cavalcanti ^a, Teresinha G. Silva ^d, Marina G.R. Pitta ^d, Maria do C.A. de Lima ^d, Suely L. Galdino ^d, Ivan da R. Pitta ^d, Letícia V. Costa-Lotuf ^a, Manoel O. Moraes ^a, Rommel R. Burbano ^e, Temenouga N. Guecheva ^f, João A.P. Henriques ^f, Cláudia Pessoa ^{a,*}

^a Department of Physiology and Pharmacology, School of Medicine, Federal University of Ceará, Fortaleza, Ceará, Brazil

^b Department of Physiology, Federal University of Sergipe, São Cristóvão, Sergipe, Brazil

^c Department of Biological Sciences, Federal University of Piauí, Picos, Piauí, Brazil

^d Department of Antibiotics, Federal University of Pernambuco, Recife, Pernambuco, Brazil

^e Institute of Biological Sciences, Federal University of Pará, Belém, Pará, Brazil

^f Biotechnology Center, Federal University of Rio Grande do Sul, Porto Alegre, Rio Grande do Sul, Brazil

ARTICLE INFO

Article history:

Received 28 August 2012

Revised 25 December 2012

Accepted 10 January 2013

Available online 21 January 2013

Keywords:

Acridine

Thiazolidine

Thiazacridine

DNA topoisomerase I

Apoptosis

ABSTRACT

Thiazacridine derivatives (ATZD) are a novel class of cytotoxic agents that combine an acridine and thiazolidine nucleus. In this study, the cytotoxic action of four ATZD were tested in human colon carcinoma HCT-8 cells: (5Z)-5-acridin-9-ylmethylene-3-(4-methylbenzyl)-thiazolidine-2,4-dione – AC-4; (5ZE)-5-acridin-9-ylmethylene-3-(4-bromo-benzyl)-thiazolidine-2,4-dione – AC-7; (5Z)-5-(acridin-9-ylmethylene)-3-(4-chloro-benzyl)-1,3-thiazolidine-2,4-dione – AC-10; and (5ZE)-5-(acridin-9-ylmethylene)-3-(4-fluoro-benzyl)-1,3-thiazolidine-2,4-dione – AC-23. All of the ATZD tested reduced the proliferation of HCT-8 cells in a concentration- and time-dependent manner. There were significant increases in internucleosomal DNA fragmentation without affecting membrane integrity. For morphological analyses, hematoxylin-eosin and acridine orange/ethidium bromide were used to stain HCT-8 cells treated with ATZD, which presented the typical hallmarks of apoptosis. ATZD also induced mitochondrial depolarisation and phosphatidylserine exposure and increased the activation of caspases 3/7 in HCT-8 cells, suggesting that this apoptotic cell death was caspase-dependent. In an assay using *Saccharomyces cerevisiae* mutants with defects in DNA topoisomerases 1 and 3, the ATZD showed enhanced activity, suggesting an interaction between ATZD and DNA topoisomerase enzyme activity. In addition, ATZD inhibited DNA topoisomerase I action in a cell-free system. Interestingly, these ATZD did not cause genotoxicity or inhibit the telomerase activity in human lymphocyte cultures at the experimental levels tested. In conclusion, the ATZD inhibited the DNA topoisomerase I activity and induced tumour cell death through apoptotic pathways.

© 2013 Elsevier Inc. All rights reserved.

Introduction

Topoisomerases are enzymes that regulate the overwinding or underwinding of DNA. They relax DNA supercoiling and perform catalytic functions during replication and transcription. There are two types of topoisomerases: type I enzymes that cleave one strand of DNA; and type II enzymes that cleave both strands. Both types of topoisomerases are essential for mammalian cell survival. Therefore, DNA topoisomerases are important targets for the development of cytotoxic agents (Miao et al., 2007; Moukharskaya and Verschraegen, 2012; Pommier et al., 2010; Vos et al., 2011). Topoisomerases I and II

are important anticancer targets, and topoisomerase inhibitors such as camptothecin derivatives (e.g., topotecan and irinotecan), which are used clinically to inhibit the enzymatic activity of topoisomerase I (type I enzyme), and podophyllotoxin derivatives (e.g., etoposide and teniposide), which inhibit the enzymatic activity of topoisomerase II (type II enzyme) (Hartmann and Lipp, 2006) are used to block cancer growth.

Amsacrine (*m*-AMSA), an acridine derivative, was the first synthetic topoisomerase inhibitor approved for clinical treatment. Although *m*-AMSA is an intercalator and topoisomerase II inhibitor, its metabolism has been associated with the production of free radicals, which may cause serious harm to normal tissues (Belmont et al., 2007; Blasiak et al., 2003; Ketron et al., 2012; Sebestik et al., 2007).

A number of clinical and experimental studies have demonstrated that acridine and thiazolidine derivatives are promising cytotoxic

* Corresponding authors. Fax: + 55 85 3366 8333.

E-mail addresses: danielbezerra@gmail.com (D.P. Bezerra), cpessoa@ufc.br (C. Pessoa).

agents. Recently, we described the synthesis of a novel class of cytotoxic agents, thiazacridine derivatives (ATZD), that couple the acridine and thiazolidine nucleus: (5*Z*)-5-acridin-9-ylmethylene-3-(4-methylbenzyl)-thiazolidine-2,4-dione (AC-4); (5*Z*E)-5-acridin-9-ylmethylene-3-(4-bromo-benzyl)-thiazolidine-2,4-dione (AC-7); (5*Z*)-5-(acridin-9-ylmethylene)-3-(4-chloro-benzyl)-1,3-thiazolidine-2,4-dione (AC-10); and (5*Z*E)-5-(acridin-9-ylmethylene)-3-(4-fluoro-benzyl)-1,3-thiazolidine-2,4-dione (AC-23). The chemical structures of these ATZD are illustrated in Fig. 1; their ability to interact with DNA was demonstrated using an electrochemical technique. These ATZD have demonstrated a solid tumour-selective cytotoxicity (Barros et al., 2012). Here, we study the mechanism of ATZD's selective cytotoxicity (AC-4, AC-7, AC-10 and AC-23) in human colon carcinoma HCT-8 cells.

Material and methods

The synthesis of thiazacridine derivatives. The chemical data and synthetic procedures for (5*Z*)-5-acridin-9-ylmethylene-3-(4-methylbenzyl)-thiazolidine-2,4-dione (AC-4), (5*Z*E)-5-acridin-9-ylmethylene-3-(4-bromo-benzyl)-thiazolidine-2,4-dione (AC-7), (5*Z*)-5-(acridin-9-ylmethylene)-3-(4-chloro-benzyl)-1,3-thiazolidine-2,4-dione (AC-10) and (5*Z*E)-5-(acridin-9-ylmethylene)-3-(4-fluoro-benzyl)-1,3-thiazolidine-2,4-dione (AC-23) are reported elsewhere (Barros et al., 2012; Mourão et al., 2005; Silva et al., 2001). Thiazolidine-2,4-dione was *N*-(3-alkylated) in the presence of potassium hydroxide, which enabled the thiazolidine potassium salt to react with the substituted benzylhalide in a hot alcohol medium. The thiazacridine derivatives were synthesised by the nucleophilic addition of substituted 3-benzyl-thiazolidine-diones on 3-acridin-9-yl-2-cyano-acrylic acid ethyl ester. The mechanisms of cytotoxic action for the thiazacridine derivatives were studied as single *Z* isomers for AC-4 and AC-10. The AC-7 and AC-23 compounds were studied as isomeric mixtures, but the *Z* isomer was the major stereoisomer.

Strains and media for the yeast assays. The *Saccharomyces cerevisiae* strains in this study were acquired from Euroscarf (European *Saccharomyces cerevisiae* Archive for Functional Analysis). The following *S. cerevisiae* genotypes were used in this study: BY-4741 (*MATa*; *his3Δ 1*; *leu2Δ 0*; *met15Δ 0*; *ura3Δ 0*); *Top1Δ* (YOL006c), same as BY4741 with *YOL006c::kanMX4*; *Top3Δ* (YLR234w), same as BY4741 with *YLR234w::kanMX4*. The media, solutions and buffers were prepared as previously described (Burke et al., 2000). Complete medium (YPD), containing 1% yeast extract, 2% peptone and 2% glucose was used for routine growth. The stationary-phase cultures were obtained by inoculating an isolated colony into liquid YPD medium and incubating the

culture at 28 °C for 72 h with shaking (for aeration). Cultures in the exponential phase were obtained by inoculating 5×10^6 cells/ml of the stationary-phase YPD culture into fresh YPD medium at 28 °C for 2 h. The cell concentrations were determined in a Neubauer chamber using a light microscope (LO, Laboroptik GmbH, Bad Homburg, Hessen, Germany).

Cell lines and cell culture. The cytotoxicity of ATZD was evaluated using human colon carcinoma HCT-8 cells donated by the Children's Mercy Hospital, Kansas City, MO, USA. The cells were maintained in RPMI-1640 medium supplemented with 10% foetal bovine serum, 2 mM glutamine, 100 μg/ml streptomycin and 100 U/ml penicillin. The cells were kept in tissue-culture flasks at 37 °C in a humidified atmosphere with 5% CO₂ and were harvested with a 0.15% trypsin-0.08% EDTA, phosphate-buffered saline solution (PBS).

The following experiments were performed to determine ATZD's cytotoxic mechanisms in HCT-8 cells. For all cell-based assays, the HCT-8 cells were seeded (0.7×10^5 cells/ml) and incubated overnight to allow the cells to adhere to the plate surface. Then, the cells were treated for 12- and/or 24-h at concentrations of 2.5, 5 and/or 10 μg/ml, corresponding to: 6.1, 12.2 and 24.4 μM for AC-4; 5.3, 10.6 and 21.2 μM for AC-7; 5.8, 11.6 and 23.2 μM for AC-10; 6.0, 12.1 and 24.1 μM for AC-23, respectively. The trypan blue exclusion test was performed before each experiment described below to assess cell viability. The negative control was treated with the vehicle (0.1% DMSO) used for diluting the tested substances. Amsacrine (*m*-AMSA, 0.3 μg/ml [0.8 μM], Sigma Chemical Co. St Louis, MO, USA) or doxorubicin (0.3 μg/ml [0.6 μM], Sigma Chemical Co. St Louis, MO, USA) was used as the positive control. The concentrations of ATZD used here were based on their IC₅₀ value in this cell line (3.1 μg/ml for AC-4, 5.3 μg/ml for AC-7, 3.6 μg/ml for AC-10 and 2.3 μg/ml for AC-23) as previously described (Barros et al., 2012).

Trypan blue dye exclusion test. Cell proliferation was determined using the Trypan blue dye exclusion test. After each incubation period, the cell proliferation was assessed. Cells that excluded trypan blue were counted using a Neubauer chamber.

BrdU incorporation assay. Twenty microliters of 5-bromo-20-deoxyuridine (BrdU, 10 mM) was added to each well and incubated for 3 h at 37 °C before 24-h of drug exposure. To assess the amount of BrdU incorporated into DNA, cells were harvested, transferred to cytospin slides (Shandon Southern Products Ltd., Sewickley Pennsylvania, USA) and allowed to dry for 2 h at room temperature. Cells that had incorporated BrdU were labelled by direct peroxidase immunocytochemistry using the chromogen diaminobenzidine. The slides were counterstained with hematoxylin, mounted and put under a

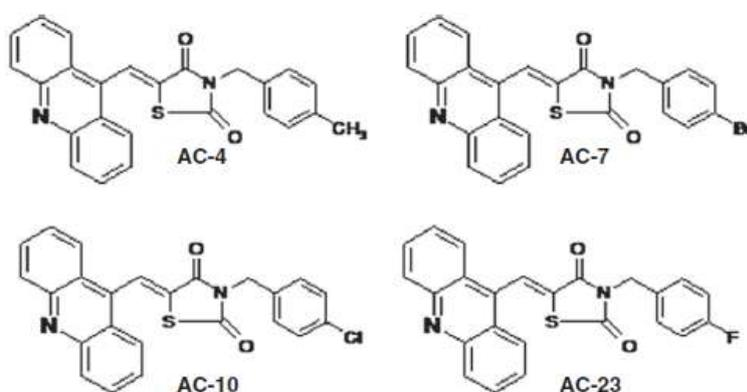


Fig. 1. The chemical structures of thiazacridine derivatives.

Apêndice D

cover slip. A light microscopy (Olympus, Tokyo, Japan) was used to determine BrdU-positivity. Two hundred cells per sample were counted to determine the percent of BrdU-positive cells.

Morphological analyses using hematoxylin–eosin staining. Untreated or ATZD-treated HCT-8 cells were examined for morphological changes under a light microscopy (Metrimplex Hungary/PZO-Labimex Model Studar lab). To evaluate any alterations in morphology, cells from the cultures were harvested, transferred to a cytospin slide, fixed with methanol for 30 s, and stained with hematoxylin–eosin.

Morphological analyses using a fluorescence microscope. Cells were pelleted and resuspended in 25 μ l of PBS. Then, 1 μ l of aqueous acridine orange/ethidium bromide solution (AO/EB, 100 μ g/ml) was added and the cells were observed under a fluorescence microscope (Olympus, Tokyo, Japan). Three hundred cells were counted per sample and classified as viable, apoptotic or necrotic (McGahon et al., 1995).

Cell membrane integrity. The integrity of the cell membrane was evaluated using the exclusion of propidium iodide (2 μ g/ml, Sigma Chemical Co. St Louis, MO, USA). Cell fluorescence was determined by flow cytometry in a Guava EasyCyte Mini System cytometer using CytoSoft 4.1 software (Guava Technologies, Hayward, California, USA). Five thousand events were evaluated per experiment and the cellular debris was omitted from the analysis.

Cell cycle distribution. The cells were harvested in a lysis solution (citrate 0.1%, triton X-100 0.1% and propidium iodide 50 μ g/ml) (Nicoletti et al., 1991), and the cell fluorescence was determined by flow cytometry, as described above.

Measurement of the mitochondrial transmembrane potential. The mitochondrial transmembrane potential was determined by the retention of rhodamine 123 dye (Gorman et al., 1997; Sureda et al., 1997). The cells were washed with PBS, incubated with rhodamine 123 (5 μ g/ml, Sigma Chemical Co. St Louis, MO, USA) at 37 °C for 15 min in the dark and washed twice. The cells were then incubated again in PBS at 37 °C for 30 min in the dark and their fluorescence was measured by flow cytometry, as described above.

Annexin assay. Phosphatidylserine externalisation was analysed by flow cytometry (Vermes et al., 1995). A Guava® Nexin Assay Kit (Guava Technologies, Hayward, CA) determined which cells were apoptotic (early apoptotic + late apoptotic). The cells were washed twice with cold PBS and then re-suspended in 135 μ l of PBS with 5 μ l of 7-amino-actinomycin D (7-AAD) and 10 μ l of Annexin V-PE. The cells were gently vortexed and incubated for 20 min at room temperature (20–25 °C) in the dark. Afterwards, the cells were analysed by flow cytometry, as described above.

Caspase 3/7 activation. Caspase 3/7 activity was analysed by flow cytometry using the Guava® EasyCyte Caspase 3/7 Kit (Guava Technologies, Hayward, CA). The cells were incubated with Fluorescent Labelled Inhibitor of Caspases (FLICATM) and maintained for 1 h at 37 °C in a CO₂ incubator. After incubation, 80 μ l of wash buffer was added and the cells were centrifuged at 2000 rpm for 5 min. The resulting pellet was resuspended in 200 μ l of wash buffer and centrifuged. The cells were then re-suspended in the working solution (propidium iodide and wash buffer) and analysed immediately using flow cytometry, as described above.

Drop test assay to determine the sensitivity of mutant *S. cerevisiae* strains with defective topoisomerases. The drop test assay determined the relative sensitivity of different *S. cerevisiae* strains to ATZD treatment. The following *S. cerevisiae* strains were used: BY-4741, *Top1Δ* and *Top3Δ*. Cells were treated with ATZD at concentrations of 50 and

100 μ g/ml and more, 4 dilutions 1:10 were performed. A suspension of 2×10^5 cells/ml of *S. cerevisiae* in the exponential phase was used. An aliquot of 3 μ l of each dilution was added to plates containing YEPD medium (YEL+ agar). After 3–4 days of growth at 28 °C, the plates were photographed. *m*-AMSA served as the positive control.

DNA relaxation assay. The inhibitory effects of ATZD on human DNA topoisomerase I were measured using a Topo I Drug Screening Kit (TopoGEN, Inc.). Supercoiled (Form I) plasmid DNA (250 ng) was incubated with human Topo I (4 units) at 37 °C for 30 min in relaxation buffer (10 mM Tris buffer pH 7.9, 1 mM EDTA, 0.15 M NaCl, 0.1% BSA, 0.1 mM spermidine and 5% glycerol) in the presence or absence of ATZD (50 and 100 μ g/ml, final 20 μ l). The concentrations used were based on the positive control indicated in this Kit. CPT (100 μ M) served as the positive control. The reaction was terminated by the addition of 10% SDS (2 μ l) and proteinase K (50 μ g/ml) and incubated at 37 °C for 30 min. The DNA samples were added to the loading dyes (2 μ l) and subjected to electrophoresis on a 1% agarose gel for 90 min at room temperature and visualised with ethidium bromide.

Assessment of the genotoxic effect in human lymphocytes. A primary culture was obtained using a standard protocol and a Ficoll gradient. In addition, phytohemagglutinin (PHA) served as a mitogen to trigger cell division in T-lymphocytes. Peripheral blood was collected from four (two women and two men) healthy donors, 19–30 years of age with no history of smoking/drinking or chronic drug use. Venous blood (10 ml) was collected from each donor into heparinised vials. Lymphocytes were isolated with a Ficoll density gradient (Histopaque-1077; Sigma Diagnostics, Inc., St. Louis). The culture medium consisted of RPMI 1640 supplemented with 20% foetal bovine serum, phytohemagglutinin (final concentration: 2%), 2 mM glutamine, 100 U/ml penicillin and 100 μ g/ml streptomycin at 37 °C with 5% CO₂ (Berthold, 1981; Brown and Lawce, 1997; Hutchins and Steel, 1983). For all of the experiments, cell viability was performed using the Trypan Blue assay. Ninety percent of the cells had to be viable before starting the experiments.

Alkaline comet assay. The alkaline (pH > 13) version of the comet assay (Single Cell Gel Electrophoresis) was performed, as described by Singh et al. (1988) with minor modifications (Hartmann and Speit, 1997). The slides were prepared in duplicate and 100 cells were screened per sample (50 cells from each duplicate slide) using a fluorescence microscope (Zeiss) equipped with a 515–560 nm excitation filter, a 590 nm barrier filter, and a 40 \times objective. The cells were visually scored and sorted into five classes according to tail length: (1) class 0: undamaged, without a tail; (2) class 1: with a tail shorter than the diameter of the head (nucleus); (3) class 2: with a tail length 1–2 \times the diameter of the head; (4) class 3: with a tail longer than 2 \times the diameter of the head; and (5) class 4: comets with no heads. A value of damage index (DI) was assigned to each comet according to its class, using the formula: $DI = (0 \times n_0) + (1 \times n_1) + (2 \times n_2) + (3 \times n_3) + (4 \times n_4)$, where n = number of cells in each class analysed. The damage index ranged from 0 (completely undamaged: 100 cells \times 0) to 400 (with maximum damage: 100 cells \times 4). DI was based on migration length and on the amount of DNA in the tail and was considered a sensitive measure of DNA (Speit and Hartmann, 1999).

Chromosome aberration assay. We used naturally synchronised human peripheral blood lymphocytes with more than 95% of the cells in the G₀ phase (Bender et al., 1988; Wojcik et al., 1996). Short-term lymphocytes cultures, at a concentration of 0.3×10^5 cells/ml, were initiated according to a standard protocol (Preston et al., 1987). ATZD were studied at different phases of the cell cycle based on the protocol described by Cavalcanti et al. (2008) with minor modifications. Doxorubicin (0.3 μ g/ml) served as a positive control. In the experimental procedures, when ATZD was added after 24-h, cells in both the G₁ and S

Apêndice D

stages were exposed, whilst it can be assumed that when ATZD was added after 69 h, only cells in the G₂ stage were exposed. When ATZD was added at the same time as the PHA stimulation (in culture start, 0 h), the cells were exposed in the G₁ stage. To obtain a sufficient number of analysable metaphases, colchicine was added at a final concentration of 0.0016%, 2 h prior to harvesting. The cells were harvested by centrifugation, treated with 0.075 M KCl at 37 °C for 20 min, centrifuged and fixed in 1:3 (v/v) acetic acid:methanol. Finally, the slides were prepared, air-dried and stained with a 3% Giemsa solution (pH 6.8) for 8 min (Moorhead et al., 1960).

The slides were analysed with a light microscope; the structural and numerical CAs were examined during metaphase in the ATZD-treated cultures and the respective controls. The frequency of CAs (in 100 metaphases per culture) and the mitotic index (MI, number of metaphases per 2,000 lymphocytes per culture) were determined.

Telomerase inhibition assay. The ability of ATZD to inhibit telomerase action was measured by determining telomere length using fluorescence in situ hybridisation with probes to telomeric sequences (TELO-FISH), as described by Lansdorp (1995) and Lansdorp et al. (1996). Short-term lymphocyte cultures were initiated according to a standard protocol (Preston et al., 1987) and were fixed (methanol:acetic acid, 3:1) on slides. The slides were hybridised with the pan telomeric Star FISH probe. The measurement of telomere length determined in each nucleus, was acquired using the image capturing software Applied Special Imaging analysis system. The images were processed using the TFL-TELO software following the protocol (Poon et al., 1999).

Statistical analysis. The data are presented as the means ± standard error of the mean of *n* experiments. The differences among experimental groups were compared using a one-way analysis of variance (ANOVA) followed by a Newman–Keuls test (*p* < 0.05). All analyses

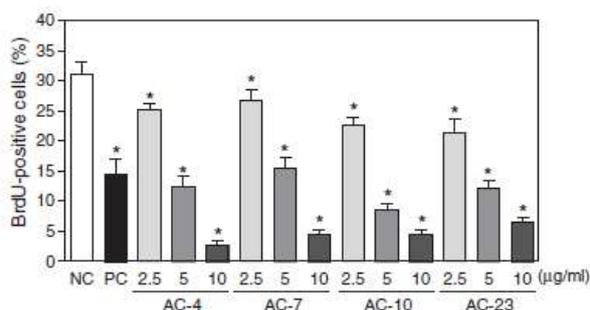


Fig. 3. The effect of thiazacridine derivatives on the proliferation of human colon carcinoma HCT-8 cells. To determine the extent of cell proliferation, inhibition BrdU incorporation was determined after a 24-h incubation. The data presented are the mean values ± S.E.M. from three independent experiments performed in duplicate. The negative control was treated with the same vehicle (NC, 0.1% DMSO) that diluted the tested substance. Amsacrine (PC, *m*-AMSA, 0.3 µg/ml) served as the positive control. *, *p* < 0.05 compared to the negative control using an ANOVA followed by a Student Newman–Keuls tests.

were carried out using the GRAPHPAD programme (Intuitive Software for Science, San Diego, California, USA).

Results

Thiazacridine derivatives inhibit the proliferation of human colon carcinoma in HCT-8 cells

Human colon carcinoma HCT-8 cells were treated with 2.5, 5 and 10 µg/ml of ATZD for 12- and/or 24-h and analysed in three different assays (trypan blue dye exclusion, propidium iodide exclusion and

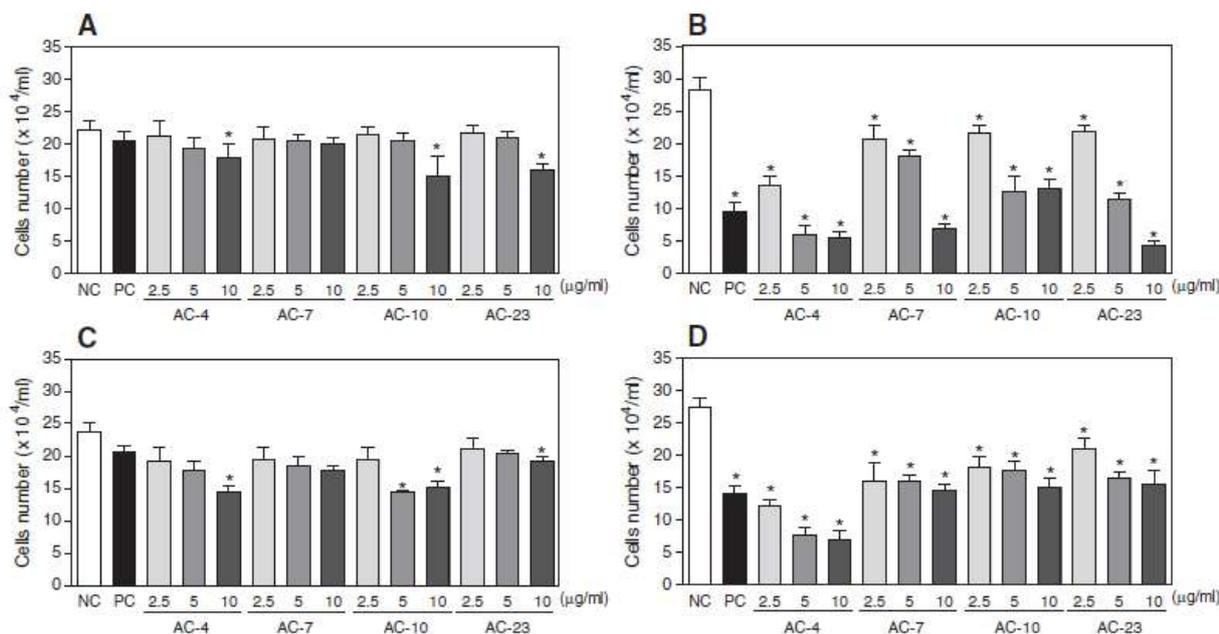


Fig. 2. The effect of thiazacridine derivatives on the proliferation of human colon carcinoma HCT-8 cells. A and B – the inhibition of cell proliferation was determined using the trypan blue dye exclusion method after 12- and 24-h incubations, respectively. C and D – the inhibition of cell proliferation was also determined using flow cytometry and propidium iodide after 12- and 24-h incubations, respectively. The data are presented as the mean values ± S.E.M. from three independent experiments performed in duplicate. The negative control was treated with the vehicle (NC, 0.1% DMSO) that diluted the test substance. Amsacrine (PC, *m*-AMSA, 0.3 µg/ml) was the positive control. For the flow cytometry analyses, 5000 events were analysed in each experiment. *, *p* < 0.05 compared to the negative control using an ANOVA followed by a Student Newman–Keuls test.

Apêndice D

Table 1
The effect of thiazacridine derivatives on the cell cycle distribution on human colon HCT-8 cells.

Drug	Concentration (µg/ml)	Cell cycle distribution (%)			
		Sub-G ₁	G ₁ /G ₀	S	G ₂ /M
<i>After 12-h incubation</i>					
NC	–	1.8 ± 0.1	62.8 ± 0.8	12.5 ± 0.3	15.7 ± 0.4
PC	0.3	1.5 ± 0.4	32.5 ± 1.7*	20.3 ± 2.4*	40.5 ± 2.1*
AC-4	2.5	3.8 ± 0.5*	58.2 ± 1.7	13.8 ± 0.9	19.7 ± 0.8*
	5	4.4 ± 0.3*	57.0 ± 1.1	15.2 ± 0.5	17.4 ± 1.3
	10	9.9 ± 1.1*	55.2 ± 2.7	14.5 ± 0.6	12.9 ± 0.9
AC-7	2.5	2.4 ± 0.4	58.3 ± 1.2	13.5 ± 0.6	19.2 ± 0.5*
	5	5.0 ± 0.6*	57.8 ± 1.3	15.3 ± 1.0	16.2 ± 0.4
	10	8.4 ± 0.9*	58.1 ± 1.6	15.3 ± 1.4	12.2 ± 0.6
AC-10	2.5	3.7 ± 0.5*	57.6 ± 1.6	14.1 ± 0.5	19.9 ± 0.5*
	5	5.3 ± 0.6*	58.2 ± 1.2	14.4 ± 0.3	17.6 ± 0.7
	10	6.9 ± 0.5*	58.4 ± 1.3	13.5 ± 0.6	16.7 ± 0.9
AC-23	2.5	3.3 ± 0.8	58.4 ± 1.0	14.7 ± 1.0	16.6 ± 0.3
	5	4.6 ± 1.0*	57.6 ± 0.7	16.6 ± 1.1	13.9 ± 0.5
	10	8.1 ± 0.8*	60.5 ± 0.3	13.0 ± 0.8	11.9 ± 0.5*
<i>After 24-h incubation</i>					
NC	–	4.7 ± 0.4	59.6 ± 0.8	14.4 ± 0.8	16.0 ± 0.3
PC	0.3	8.1 ± 1.1*	27.8 ± 1.6*	24.0 ± 2.3*	26.3 ± 1.0*
AC-4	2.5	13.9 ± 1.5*	55.2 ± 0.8	15.1 ± 1.1	17.5 ± 0.9
	5	24.7 ± 2.2*	51.8 ± 0.9*	15.1 ± 0.9	3.9 ± 0.8*
	10	43.3 ± 1.5*	44.0 ± 1.3*	10.0 ± 0.5*	3.7 ± 0.7*
AC-7	2.5	10.9 ± 0.8*	55.7 ± 1.5	14.9 ± 0.4	11.6 ± 0.4*
	5	13.7 ± 1.4*	54.9 ± 3.3*	13.6 ± 0.7	9.8 ± 0.7*
	10	26.6 ± 3.6*	54.6 ± 3.4*	8.9 ± 0.5*	5.2 ± 0.7*
AC-10	2.5	26.8 ± 0.7*	52.6 ± 2.3*	14.7 ± 0.8	10.8 ± 1.0*
	5	27.1 ± 1.0*	49.1 ± 3.1*	14.3 ± 0.6	9.7 ± 1.1*
	10	37.5 ± 1.4*	48.8 ± 1.8*	10.2 ± 0.5*	4.7 ± 0.5*
AC-23	2.5	12.1 ± 2.0*	56.3 ± 1.9	12.5 ± 0.5	10.8 ± 1.4*
	5	24.4 ± 2.1*	55.8 ± 3.3	11.1 ± 0.7	9.8 ± 1.2*
	10	28.9 ± 2.0*	52.2 ± 3.5*	6.4 ± 0.6*	4.5 ± 0.4*

The data are presented as the mean values ± S.E.M. from three independent experiments performed in duplicate. The negative control was treated with the same vehicle (NC, 0.1% DMSO) that diluted the tested substance. Amsacrine (PC, *m*-AMSA) served as the positive control. Five thousand events were analysed for the flow cytometry analysis in each experiment.

* $p < 0.05$ compared to negative control by ANOVA followed by a Student Newman-Keuls test.

BrdU incorporation). ATZD reduced the proliferation of HCT-8 cells in a concentration- and time-dependent manner.

After a 12-h incubation, cell proliferation was reduced at higher concentration tested, which was confirmed by trypan blue dye exclusion and propidium iodide exclusion ($p < 0.05$, Figs. 2A, C). After a 24-h incubation, ATZD reduced cell number ($p < 0.05$) at all concentrations tested using trypan blue dye exclusion (Fig. 2B), propidium iodide exclusion (Fig. 2D) and BrdU incorporation (Fig. 3). *m*-AMSA, the positive control, also reduced HCT-8 cell proliferation.

Thiazacridine derivatives preferentially caused human colon carcinoma HCT-8 cells to transition from the G₂/M phase to DNA fragmentation

The effects that these ATZD had on cell cycle progression were evaluated using flow cytometry after 12- and 24-h. All DNA that was sub-diploid in size (sub-G₁) was considered to be caused by internucleosomal DNA fragmentation. Table 1 indicates the cell cycle distribution obtained. After a 12-h incubation, the ATZD treated with AC-4, AC-7 and AC-10 (2.5 µg/ml) caused a small increase in the number of cells in the G₂/M phase compared with the negative control (15.7%, $p < 0.05$). For the ATZD-treated cells, the percentage of cells in the G₂/M phase were 19.7%, 19.2% and 19.9%, for AC-4, AC-7 and AC-10, respectively. After a 24-h incubation, the cells in the G₀/G₁ and S phases remained mostly unchanged; however, there were fewer cells in the G₂/M phase. Additionally, all ATZD caused significant internucleosomal DNA fragmentation at all of the concentrations tested ($p < 0.05$), which implies that ATZD preferentially caused cells from the G₂/M phase to transition into sub-G₁. Cells treated with *m*-AMSA served as the positive control, and had an increased number of cells in the G₂/M interval and a significant amount of internucleosomal DNA fragmentation.

Thiazacridine derivatives induce apoptosis in human colon carcinoma HCT-8 cells

After 12- and 24-h incubations, the effects of ATZD were evaluated based on cell morphology using hematoxylin-eosin and acridine

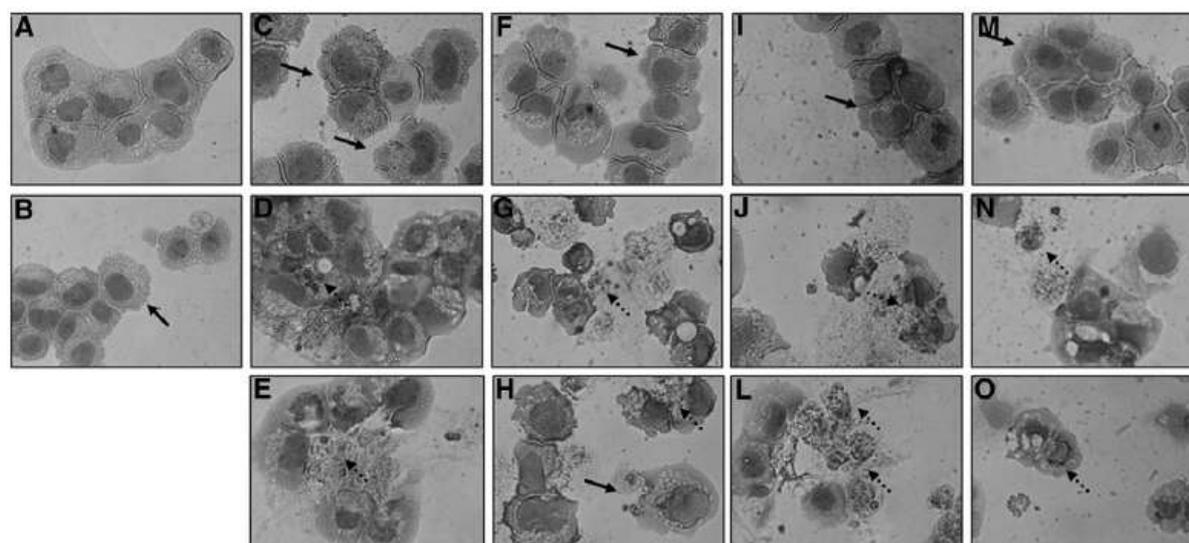


Fig. 4. The effect of thiazacridine derivatives on the cell morphology of human colon carcinoma HCT-8 cells. The cells were stained with hematoxylin-eosin and analysed by optical microscopy after a 24-h incubation with AC-4, AC-7, AC10 and AC23 at concentrations of 2.5 (C, F, I, M), 5 (D, G, J, N) and 10 µg/ml (E, H, L, O), respectively. The negative control (A) was treated with the same vehicle (0.1% DMSO) that diluted the tested substance. Amsacrine (*m*-AMSA, 0.3 µg/ml) served as the positive control (B). The continuous arrows show the apoptotic bodies and the non-continuous arrows indicate nuclear fragmentation.

Apêndice D

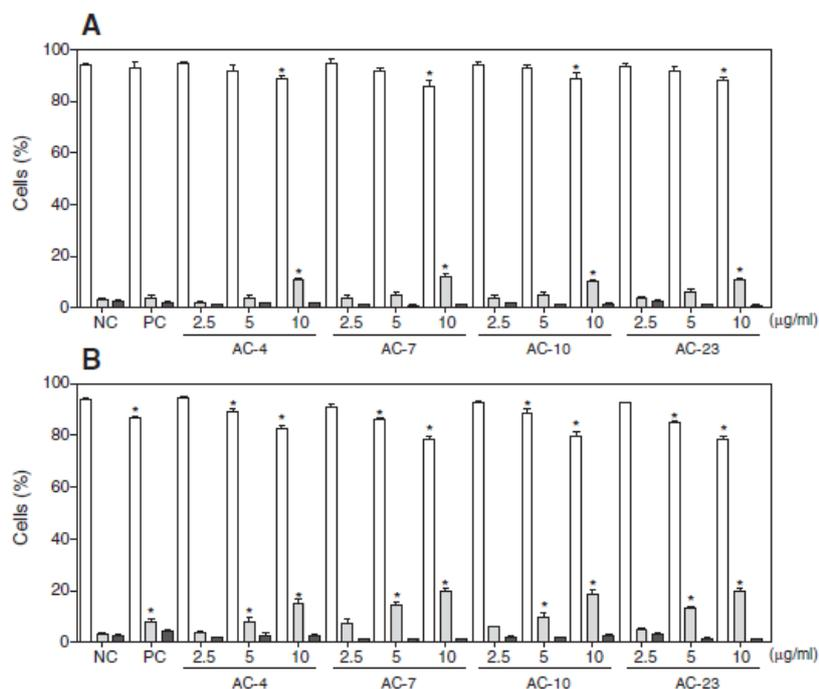


Fig. 5. The effect of thiazacridine derivatives on the viability of human colon carcinoma HCT-8 cells. A and B – cell viability (viable cells – white bar; apoptotic cells – grey bar; and necrotic cells – black bar) was determined by fluorescence microscopy using acridine orange/ethidium bromide after 12- and 24-h incubations, respectively. The data are presented as the mean values \pm S.E.M. from three independent experiments performed in duplicate. The negative control was treated with the same vehicle (NC, 0.1% DMSO) that diluted the tested substance. Amsacrine (PC, *m*-AMSA, 0.3 μ g/ml) served as the positive control. *, $p < 0.05$ compared to negative control by ANOVA followed by a Student Newman–Keuls test.

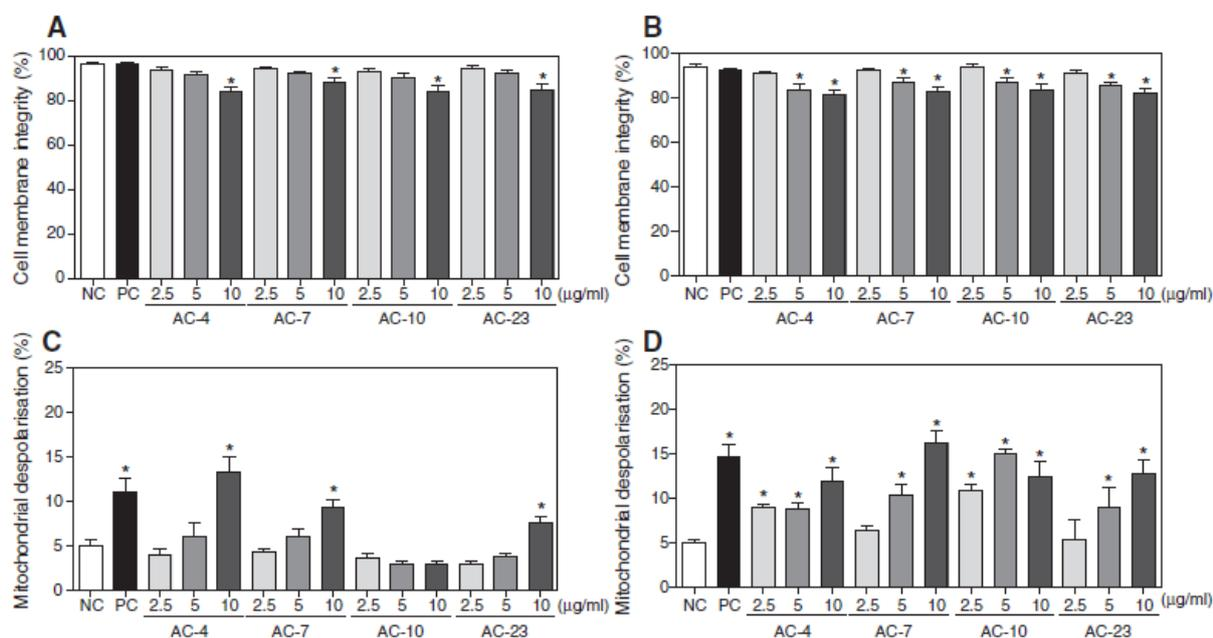


Fig. 6. The effect of thiazacridine derivatives on the viability of human colon carcinoma HCT-8 cells. A and B – the integrity of the cell membranes was determined by flow cytometry using propidium iodide after 12- and 24-h incubations, respectively. C and D – the mitochondrial membrane potential was determined by flow cytometry using rhodamine 123 after 12- and 24-h incubations, respectively. The data are presented as the mean values \pm S.E.M. from three independent experiments performed in duplicate. The negative control was treated with the same vehicle (NC, 0.1% DMSO) that diluted the tested substance. Amsacrine (PC, *m*-AMSA, 0.3 μ g/ml) served as the positive control. Five thousand events were analysed for the flow cytometry analysis in each experiment. *, $p < 0.05$ compared to the negative control using an ANOVA followed by a Student Newman–Keuls test.

Apêndice D

orange/ethidium bromide staining. The integrity of the cell membrane and the mitochondrial membrane potential were also determined by flow cytometry. Additionally, after a 24-h incubation, phosphatidylserine externalisation and caspase 3/7 activation were measured by flow cytometry.

After a 12-h incubation, HCT-8 cells either treated or untreated with ATZD, were tested at all concentrations and presented slight morphological changes (data not shown). On the other hand, after a 24-h incubation, morphological examination of HCT-8 cells showed severe drug-mediated changes. The hematoxylin–eosin stained HCT-8 cells treated with ATZD presented a morphology consistent with apoptosis, including a reduction in cell volume, chromatin condensation and nuclei fragmentation (Fig. 4). The acridine orange/ethidium bromide stained and treated cells also displayed a morphology consistent with apoptosis, in a time- and concentration-dependent manner ($p < 0.05$, Fig. 5). *m*-AMSA, served as the positive control, which also induced morphological changes consistent with apoptosis.

The integrity of the cell membrane is a parameter of cell viability that differs between apoptotic and necrotic cells. After 12- or 24-h of exposure, ATZD induced a slight disruption in the plasmatic membrane, which was only observed at the higher concentrations tested (Figs. 6A, B). As cited above, the internucleosomal DNA fragmentation was markedly increased in ATZD-treated cells ($p < 0.05$, Table 1). Both of these modifications are characteristics of apoptotic cells. In addition, ATZD induced mitochondrial depolarisation in a time- and concentration-dependent manner ($p < 0.05$, Figs. 6C, D). *m*-AMSA served as the positive control, which also induced mitochondrial depolarisation and DNA fragmentation without affecting the membrane's integrity.

In addition, phosphatidylserine externalisation (AC-4 and AC-10 at concentrations of 2.5 and 5 $\mu\text{g/ml}$) and caspase 3/7 activation (AC-4, AC-10 and AC-23 at concentrations of 5 and 10 $\mu\text{g/ml}$) were measured in ATZD-treated cells after a 24-h incubation. Phosphatidylserine exposure ($p < 0.05$, Fig. 7A) and an increase in caspase 3/7 activation ($p < 0.05$, Fig. 7B) were also observed, suggesting that a caspase-dependent apoptotic cell death had occurred. Doxorubicin served as the positive control and also induced phosphatidylserine exposure and increased caspase 3/7 activation.

Thiazacridine derivatives inhibits DNA topoisomerase I action

Because ATZD interact with DNA, they are potential topoisomerase inhibitors. The effect of ATZD on DNA topoisomerase activity was evaluated in a yeast-based assay and in a cell-free assay.

First, the effects of ATZD were evaluated using a drop test assay in a mutant strain of *S. cerevisiae* that was defective in topoisomerase type I (Fig. 8). The type IB topoisomerases (topoisomerase I in yeast) relax both positively and negatively supercoiled DNA, whereas type IA topoisomerases (topoisomerase 3 in yeast) preferentially relax negatively supercoiled DNA. At a concentration of 50 $\mu\text{g/ml}$, the ATZD were more resistant in yeast mutants that lacked topoisomerase I (*Top1 Δ*) activity compared with the wild-type strain (BY-4741), indicating that these molecules may induce lesions in topoisomerase I. In ATZD at higher concentration (100 $\mu\text{g/ml}$), the *Top1 Δ* mutant was more sensitive than the wild-type strain, which indicates that an additional cytotoxicity mechanism (i.e., interaction with topoisomerase II) may be involved. Moreover, the strain without topoisomerase 3, but with topoisomerase 1, (*Top3 Δ*), was more sensitive to the ATZD, with the exception of AC-23. *m*-AMSA served as the positive control, which showed similar effects.

In addition, the effect of ATZD on topoisomerase I activity was evaluated in a cell-free system. Purified human DNA topoisomerase I was incubated with ATZD (50 and 100 $\mu\text{g/ml}$) in the presence of supercoiled plasmid DNA; the products of this reaction were subjected to electrophoresis on agarose gels to separate the closed and open circular DNAs. Relaxation of the DNA strand was inhibited in both of the

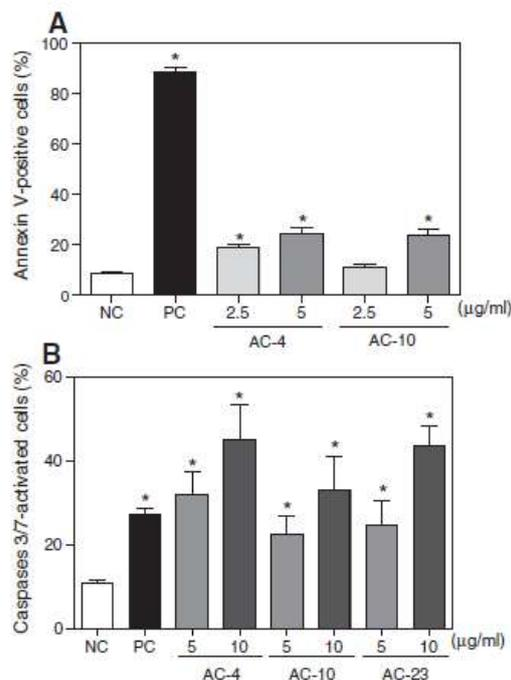


Fig. 7. The effect of thiazacridine derivatives on the viability of human colon carcinoma HCT-8 cells. A – the cell viability was determined by flow cytometry using Annexin V–PE. B – the activity of caspase 3/7 was determined by flow cytometry using propidium iodide and Flixa. The data are presented as the mean values \pm S.E.M. from three independent experiments performed in duplicate after a 24-h incubation. The negative control was treated with the same vehicle (NC, 0.1% DMSO) that diluted the tested substance. Doxorubicin (PC, 0.3 $\mu\text{g/ml}$) was the positive control. For the flow cytometry analysis, 5000 events were analysed in each experiment. *, $p < 0.05$ compared to the negative control using an ANOVA followed by a Student Newman–Keuls test.

concentrations tested (Fig. 9). CPT served as the positive control because it also inhibits DNA topoisomerase I.

Thiazacridine derivatives do not cause genotoxicity or inhibit telomerase activity in human lymphocytes

The genotoxicity of ATZD (AC-4, AC-7, AC-10 and AC-23) was evaluated in human lymphocyte cultures using an alkaline comet assay at concentrations of 2.5, 5 and 10 $\mu\text{g/ml}$. The genotoxicity of ATZD (AC-4 and AC-10) was also evaluated in human lymphocyte cultures using a chromosome aberration assay at concentrations of 2.5, 5 and 10 $\mu\text{g/ml}$. The ability of ATZD (AC-4 and AC-10) to inhibit telomerase action was performed using a pan telomeric probe at a concentration of 2.5 $\mu\text{g/ml}$. None of the ATZD showed genotoxic activity or anti-telomerase activity at any experimental concentrations tested (data not shown). Doxorubicin served as the positive control, and demonstrated potent genotoxic activity.

Discussion

The present work demonstrates the mechanism by which ATZD (AC-4, AC-7, AC-10 and AC-23) are cytotoxic in human colon carcinoma HCT-8 cells. As cited above, these agents were recently synthesised as a novel class of solid tumour-selective cytotoxic agents. These ATZD exhibit a relatively high cytotoxicity in colon carcinoma (HCT-8, HCT-15, SW-620 and COLO-205), prostate carcinoma (PC-3 and DU-145), ovarian carcinoma (OVCAR-8), melanoma (UACC-62 and MDA-MB-435) and glioblastoma (SF-295) tumour cell lines. However, these compounds were not active in leukaemia (HL-60, K-562 and

Apêndice D

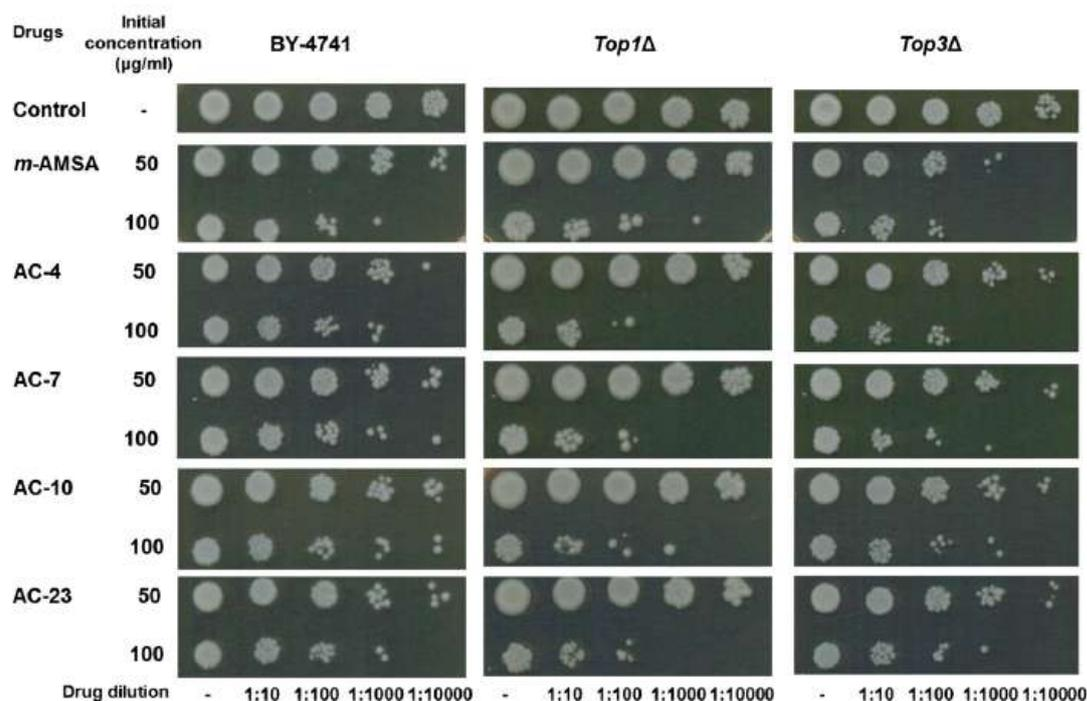


Fig. 8. The sensitivity of a wild-type strain of *Saccharomyces cerevisiae* and mutants with defective topoisomerases. The sensitivity of topoisomerases type I to thiazacridine derivatives was determined by a drop test assay. A suspension of *S. cerevisiae* cells in the exponential phase of growth was treated for 24-h in the absence or in the presence of thiazacridine derivatives at the indicated concentrations. The diluted cell cultures (10^7 – 10^3 from left to right) were spotted on YPD agar plates. Amsacrine (*m*-AMSA) served as the positive control. BY-4741: Wild-type strain; *top1Δ*: without topoisomerase I; and *top3Δ*: without topoisomerase 3.

CEM), breast carcinoma (MDA-MB-231, HS-578-T and MX-1) or normal lymphoblast (PBMC) cells (Barros et al., 2012). Here, we demonstrate the effects of ATZD on cell proliferation, cell cycle progress and apoptotic-induction using HCT-8 cells as a model. Studies in a yeast-based assay and a cell-free assay examine how ATZD interfere in topoisomerase I activity.

The ATZD inhibit human colon carcinoma HCT-8 cell proliferation in a concentration- and time-dependent manner, and their cytotoxic activity was assessed using different assays. Previously, we demonstrated that ATZD exhibited relatively high cytotoxicity against colon carcinomas and that the highlight of these ATZD was their selectivity toward solid tumours because these ATZD were not active in leukaemias or normal lymphoblasts (Barros et al., 2012). The pyrazoloacridines, bisannulated acridines, aminoderivatives of azapyranoxanthone and pyranosoflavones have also been cited as solid tumour-selective cytotoxic agents (Gao et al., 2011; Kolokythas et al., 2006; Sebolt, et al., 1987; Thale et al., 2002). Therefore, this feature is noteworthy but the mechanisms accounting for this selectivity are poorly understood.

The population of cells in the G_2/M phase was shifted to the sub- G_1 population in ATZD-treated HCT-8 cells, whilst few changes occurred in the population of cells in the G_0/G_1 or S phases. This indicates that the ATZD preferentially guide cells from the G_2/M phase into apoptosis. Manipulating the regulatory events at this checkpoint is a promising approach that will improve the efficiency of cytotoxic drugs and overcome drug resistance (Links et al., 1998). In addition, HCT-8 cells treated with ATZD presented typical hallmarks of apoptosis. Selective apoptosis, the deletion of certain cells in tissues without concomitant inflammation, is advantageous in tissue homeostasis. The induction of apoptosis is one of the main mechanisms that inhibit cancer growth and proliferation and is used by several antitumor agents (Los et al., 2003; Schultz and Harrington, 2003). Moreover, ATZD

treatment induces mitochondrial depolarisation, phosphatidylserine exposure and an increase in caspase 3/7 activation, which suggests that ATZD treatment leads to a caspase-dependent apoptotic cell death. Caspases play an essential role in apoptosis (Fan et al., 2005; Kitazumi and Tsukahara, 2011); these caspases are responsible for the cleavage of cellular proteins, such as cytoskeletal components, which leads to the morphological changes previously observed in the cells that undergo apoptosis (Kothakota et al., 1997).

The mechanism by which acridine and thiazolidine derivatives act has been continuously researched. Thiazolidine derivatives activate peroxisome proliferator-activated receptors (Barros et al., 2010). Meanwhile, acridine derivatives used in cancer chemotherapy have biological targets, such as DNA topoisomerases I and/or II, telomerase/telomeres and kinases (Castillo-González et al., 2009; Guo et al., 2009; Oppegard et al., 2009). Our understanding of ATZD's cytotoxic mechanisms have been limited to results from double stranded-DNA biosensors and single stranded-DNA solutions, which show a positive interaction with these ATZD that couple acridine and thiazolidine (Barros et al., 2012). Here, we demonstrate that ATZD inhibit DNA topoisomerase I activity.

The cytotoxicity of DNA topoisomerase I inhibitors is caused by blocking DNA topoisomerase I cleavage complexes or by inhibiting DNA topoisomerase I catalytic activity. Then, DNA topoisomerase I inhibitors work by stabilising the DNA topoisomerase I cleavage complexes, which cause DNA damage (Hsiang et al., 1989; Pommier et al., 1998; Stewart et al., 1998). Because malignant cells often contain greater amounts of DNA topoisomerase I than normal cells, tumour cells should be more sensitive to the toxic effects of these inhibitors. The malignant cells that often contain great amounts of DNA topoisomerase I include colon adenocarcinoma, several types of non-Hodgkin's lymphoma, leukaemias, melanoma and carcinomas of the

Apêndice D

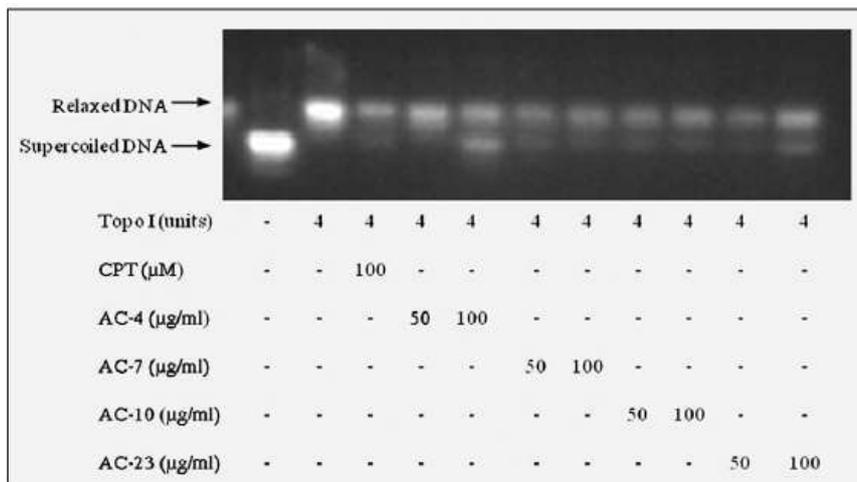


Fig. 9. The inhibition of topoisomerase I-mediated DNA supercoiling in the presence of thiazacridine derivatives. The supercoiled DNA (250 ng) was incubated with 4 units of topoisomerase I in the presence or absence of thiazacridine derivatives at the indicated concentrations. The negative control was treated with the same vehicle that diluted the tested substance. Camptothecin (CPT) served as the positive control. The DNA was analysed by electrophoresis using a 1% agarose gel. The gels were stained with ethidium bromide and photographed under UV light.

stomach, breast and lung (Potmesil, 1994). This partially explains the selective cytotoxic effects of ATZD. However, the exact mechanism of this selective antitumor activity remains to be determined.

Previous studies have reported that some acridine and thiazolidine derivatives are somatic- and germ-cell mutagenic agents capable of inducing both numerical and structural chromosome aberrations in vitro and in vivo (Attia, 2008; Attia, in press; Kao-Shan et al., 1984; Nishi et al., 1989). These compounds are highly cytotoxic/genotoxic to normal lymphocyte cells. Therefore, to improve our understanding of the ATZD's cytotoxic actions, we assessed their genotoxic effects in human peripheral lymphocytes. Previously, the cytotoxicity of these compounds was assessed against normal lymphocyte cells (Barros et al., 2012); however, the genotoxicity had not been investigated. The genotoxic effects of ATZD were determined using an alkaline comet assay and a chromosome aberration assay; the anti-telomerase activity was determined using a pan telomeric probe. In our studies, none of these ATZD agents showed genotoxicity and/or anti-telomerase activity in cultured human lymphocytes at the experimentally tested concentrations. Therefore, unlike the acridine and thiazolidine derivatives, ATZD did not cause cytotoxicity, genotoxicity and the inhibition of telomerase activity in human lymphocytes.

In this manuscript, we show that the ATZD are solid tumour-selective cytotoxic agents that inhibit DNA topoisomerase I activity and induce tumour cell death through caspase-dependent apoptosis pathways without causing genotoxicity in human lymphocytes. These data confirm that these ATZD are promising anticancer drugs.

Conflicts of interest

The authors declare no conflicts of interest.

Acknowledgments

This study was supported by the Brazilian National Research Council, National Institute of Science and Technology for Pharmaceutical Innovation (CNPq/RENORBIO/INCT-IF) and INCT-Bioanalítica. The English was edited by American Journal Experts (key#354F-6EF9-BC4F-6B4A-E706).

References

- Attia, S.M., 2008. Mutagenicity of some topoisomerase II-interactive agents. *Saudi Pharm. J.* 17, 1–24.
- Attia, S.M., in press. Molecular cytogenetic evaluation of the mechanism of genotoxic potential of amsacrine and nocodazole in mouse bone marrow cells. *J. Appl. Toxicol.* <http://dx.doi.org/10.1002/jat.1753>.
- Barros, C.D., Amato, A.A., de Oliveira, T.B., Iannini, K.B., Silva, A.L., Silva, T.G., Leite, E.S., Hernandez, M.Z., Lima, M.C.A., Galdino, S.L., Neves, F.A., Pitta, I.R., 2010. Synthesis and anti-inflammatory activity of new arylidene-thiazolidine-2,4-diones as PPAR ligands. *Bioorg. Med. Chem.* 18, 3805–3811.
- Barros, F.W., Silva, T.G., Pitta, M.G.R., Bezena, D.P., Costa-Lotufo, L.V., de Moraes, M.O., Pessoa, C., de Moura, M.A., de Abreu, F.C., de Lima, M.D., Galdino, S.L., Pitta, I.R., Goulart, M.O., 2012. Synthesis and cytotoxic activity of new acridine–thiazolidine derivatives. *Bioorg. Med. Chem.* 20, 3533–3539.
- Belmont, P., Bosson, J., Godet, T., Tiano, M., 2007. Acridine and acridone derivatives, anticancer properties and synthetic methods: where are we now? *Anticancer Agents Med. Chem.* 7, 139–169.
- Bender, M.A., Awa, A.A., Brooks, A.L., Evans, H.J., Groer, P.G., Littlefield, L.G., Pereira, C., Preston, R.J., Wachholz, B.W., 1988. Current status of cytogenetic procedures to detect and quantify previous exposures to radiation. *Mutat. Res.* 196, 103–159.
- Berthold, F., 1981. Isolation of human monocytes by ficoll density gradient centrifugation. *Blut* 3, 367–371.
- Blasiak, J., Gloc, E., Drzewoski, J., Wozniak, K., Zadrozny, M., Skórski, T., Pertyński, T., 2003. Free radical scavengers can differentially modulate the genotoxicity of amsacrine in normal and cancer cells. *Mutat. Res.* 535, 25–34.
- Brown, M.G., Lawce, H.J., 1997. Peripheral blood cytogenetic methods. In: Barch, M.J., Knutsen, T., Spurbeck, J.L. (Eds.), *The AGT Cytogenetics Laboratory Manual*. Lippincott-Raven Publishers, Philadelphia, pp. 77–171.
- Burke, D., Dawson, D., Stearns, T., 2000. *Methods in Yeast Genetics*. Cold Spring Harbor, Laboratory Press, New York.
- Castillo-González, D., Cabrera-Pérez, M.A., Pérez-González, M., Helguera, A.M., Durán-Martínez, A., 2009. Prediction of telomerase inhibitory activity for acridine derivatives based on chemical structure. *Eur. J. Med. Chem.* 44, 4826–4840.
- Cavalcanti, B.C., Sombra, C.M.L., Oliveira, J.H.H.L., Berlinck, R.G.S., Moraes, M.O., Pessoa, C., 2008. Cytotoxicity and genotoxicity of ingenamine G isolated from the Brazilian marine sponge *Pachychalina alcaloidifera*. *Comp. Biochem. Physiol. C* 147, 409–415.
- Fan, T.J., Han, L.H., Cong, R.S., Liang, J., 2005. Caspase family proteases and apoptosis. *Acta Biochim. Biophys. Sin.* 37, 719–727.
- Gao, S., Xu, Y.M., Valeriate, F.A., Gunatilaka, A.A., 2011. Pierreones A–D, solid tumour selective pyranisoflavones and other cytotoxic constituents from *Antheroporum pierreii*. *J. Nat. Prod.* 74, 852–856.
- Gorman, A.M., Samali, A., McGowan, A.J., Cotter, T.G., 1997. Use of flow cytometry techniques in studying mechanisms of apoptosis in leukemic cells. *Cytometry* 29, 97–105.
- Guo, C., Gasparian, A.V., Zhuang, Z., Borykh, D.A., Komar, A.A., Gudkov, A.V., Gurova, K.V., 2009. 9-Aminoacridine-based anticancer drugs target the PI3K/AKT/mTOR, NF-kappaB and p53 pathways. *Oncogene* 28, 1151–1161.
- Hartmann, J.T., Lipp, H.P., 2006. Camptothecin and podophyllotoxin derivatives: inhibitors of topoisomerase I and II—mechanisms of action, pharmacokinetics and toxicity profile. *Drug Saf.* 29, 209–230.

Apêndice D

- Hartmann, A., Speit, G., 1997. The contribution of cytotoxicity to DNA effects in the single cell gel test (comet assay). *Toxicol. Lett.* 90, 183–188.
- Hsiang, Y.H., Lihou, M.G., Liu, L.F., 1989. Arrest of replication forks by drug-stabilized topoisomerase I-DNA cleavable complexes as a mechanism of cell killing by camptothecin. *Cancer Res.* 49, 5077–5082.
- Hutchins, D., Steel, C.M., 1983. Phytohaemagglutinin-induced proliferation of human T lymphocytes: differences between neonate and adults in accessory cell requirements. *Clin. Exp. Immunol.* 52, 355–364.
- Kao-Shan, C.S., Micetich, K., Zwelling, L.A., Whang-Peng, J., 1984. Cytogenetic effects of amsacrine on human lymphocytes *in vivo* and *in vitro*. *Cancer Treat. Rep.* 68, 989–997.
- Ketron, A.C., Denny, W.A., Graves, D.E., Osheroff, N., 2012. Amsacrine as a topoisomerase II poison: importance of drug-DNA interactions. *Biochemistry* 51, 1730–1739.
- Kitazumi, I., Tsukahara, M., 2011. Regulation of DNA fragmentation: the role of caspases and phosphorylation. *FEBS J.* 278, 427–441.
- Kolokythas, G., Poulis, N., Marakos, P., Pratsinis, H., Kletsas, D., 2006. Design, synthesis and antiproliferative activity of some new azapyranoxanthone aminoderivatives. *Eur. J. Med. Chem.* 41, 71–79.
- Kothakota, S., Azuma, T., Reinhard, C., Klippel, A., Tang, J., Chu, K., McGarry, T.J., Kirschner, M.W., Koths, K., Kwiatkowski, D.J., Williams, L.T., 1997. Caspase-3-generated fragment of gelsolin: effector of morphological change in apoptosis. *Science* 278, 294–298.
- Lansdorp, P.M., 1995. Telomere length and proliferation potential of hematopoietic stem cells. *J. Cell Sci.* 108, 1–6.
- Lansdorp, P.M., Verwoerd, N.P., van de Rijke, F.M., Dragowska, V., Little, M.T., Dirks, R.W., Raap, H.J., 1996. Heterogeneity in telomere length of human chromosomes. *Hum. Mol. Genet.* 5, 685–691.
- Links, M., Ribeiro, J., Jackson, P., Friedlander, M., Russell, P.J., 1998. Regulation and deregulation of G₂ checkpoint proteins with cisplatin. *Anticancer Res.* 18, 4057–4066.
- Los, M., Burek, C.J., Stroh, C., Benedyk, K., Hug, H., Mackiewicz, A., 2003. Anticancer drugs of tomorrow: apoptotic pathways as target for drug design. *Drug Discov. Today* 8, 67–77.
- McGahan, A.J., Martin, S.J., Bissonnette, R.P., Mahboubi, A., Shi, Y., Mogil, R.J., Nishioka, W.K., Green, D.R., 1995. The end of the (cell) line: methods for the study of apoptosis *in vitro*. *Methods Cell Biol.* 46, 153–185.
- Miao, Z.H., Player, A., Shankavaram, U., Wang, Y.H., Zimonjic, D.B., Lorenzi, P.L., Liao, Z.Y., Liu, H., Shimura, T., Zhang, H.L., Meng, L.H., Zhang, Y.W., Kawasaki, E.S., Popescu, N.C., Aladjem, M.L., Goldstein, D.J., Weinstein, J.N., Pommier, Y., 2007. Nondissociating functions of human topoisomerase I: genome-wide and pharmacologic analyses. *Cancer Res.* 67, 8752–8761.
- Moorhead, P.S., Nomell, P.C., Mellman, W.J., Battips, D.M., Hungerford, D.A., 1960. Chromosome preparations of leukocytes cultured from human peripheral blood. *Exp. Cell Res.* 20, 613–616.
- Moukharskaya, J., Verschraegen, C., 2012. Topoisomerase I inhibitors and cancer therapy. *Hematol. Oncol. Clin. North Am.* 26, 507–525.
- Mourão, R.H., Silva, T.G., Soares, A.L., Vieira, E.S., Santos, J.N., Lima, M.C., Lima, V.L., Galdino, S.L., Barbe, J., Pitta, I.R., 2005. Synthesis and biological activity of novel acridinylidene and benzylidene thiazolidinediones. *Eur. J. Med. Chem.* 40, 1129–1133.
- Nicoletti, I., Magliorati, G., Pagliacci, M.C., Grignani, F., Riccardi, C., 1991. A rapid and simple method for measuring thymocyte apoptosis by propidium iodide staining and flow cytometry. *J. Immunol. Methods* 139, 271–279.
- Nishi, Y., Miyakawa, Y., Kato, K., 1989. Chromosome aberrations induced by pyrolysates of carbohydrates in Chinese hamster V79 cells. *Mutat. Res.* 227, 117–123.
- Oppegard, L.M., Ougolkov, A.V., Luchini, D.N., Schoon, R.A., Goodell, J.R., Kaur, H., Billadeau, D.D., Ferguson, D.M., Hiasa, H., 2009. Novel acridine-based compounds that exhibit an anti-pancreatic cancer activity are catalytic inhibitors of human topoisomerase II. *Eur. J. Pharmacol.* 602, 223–229.
- Pommier, Y., Pourquier, P., Fan, Y., Strumberg, D., 1998. Mechanism of action of eukaryotic DNA topoisomerase I and drugs targeted to the enzyme. *Biochim. Biophys. Acta* 1400, 83–105.
- Pommier, Y., Leo, E., Zhang, H., Marchand, C., 2010. DNA topoisomerases and their poisoning by anticancer and antibacterial drugs. *Chem. Biol.* 17, 421–433.
- Poon, S.S., Martens, U.M., Ward, R.K., Lansdorp, P.M., 1999. Telomere length measurements using digital fluorescence microscopy. *Cytometry* 36, 267–278.
- Potmesil, M., 1994. Camptothecins: from bench research to hospital wards. *Cancer Res.* 54, 1431–1439.
- Preston, R.J., San Sebastian, J.R., McFee, A.F., 1987. The *in vitro* human lymphocyte assay for assessing the clastogenicity of chemical agents. *Mutat. Res.* 189, 175–183.
- Schultz, D.R., Harrington, W.J., 2003. Apoptosis: programmed cell death at molecular level. *Semin. Arthritis Rheum.* 32, 345–369.
- Sebestik, J., Hlavacek, J., Stibor, I., 2007. A role of the 9-aminoacridines and their conjugates in a life science. *Curr. Protein Pept. Sci.* 8, 471–483.
- Sebolt, J.S., Scavone, S.V., Pinter, C.D., Hamelehl, K.L., Von Hoff, D.D., Jackson, R.C., 1987. Pyrazoloacridines, a new class of anticancer agents with selectivity against solid tumours *in vitro*. *Cancer Res.* 47, 4299–4304.
- Silva, T.G., Barbosa, F.S.V., Brandão, S.S.F., Lima, M.C.A., Galdino, S.L., Pitta, I.R., Barbe, J., 2001. Synthesis and structural elucidation of new benzylidene imidazolidines and acridinylidene thiazolidines. *Heterocycl. Commun.* 7, 523–528.
- Singh, N.P., McCoy, M.T., Tice, R.R., Schneider, E.L.A., 1988. Single technique for quantitation of low levels of DNA damage in individual cells. *Exp. Cell Res.* 175, 184–191.
- Speit, G., Hartmann, A., 1999. The comet assay (single-cell gel test). A sensitive genotoxicity test for the detection of DNA damage and repair. *Methods Mol. Biol.* 113, 203–212.
- Stewart, L., Redinbo, M.R., Qiu, X., Hol, W.G., Champoux, J.J., 1998. A model for the mechanism of human topoisomerase I. *Science* 279, 1534–1541.
- Sureda, F.X., Escubedo, E., Gabriel, C., Comas, J., Camarasa, J., Camins, A., 1997. Mitochondrial membrane potential measurement in rat cerebellar neurons by flow cytometry. *Cytometry* 28, 74–80.
- Thale, Z., Johnson, T., Tenney, K., Wenzel, P.J., Lobkovsky, E., Clardy, J., Media, J., Pietraszkiewicz, H., Valeriote, F.A., Crews, P., 2002. Structures and cytotoxic properties of sponge-derived bisannulated acridines. *J. Org. Chem.* 67, 9384–9391.
- Vermes, L., Haanen, C., Steffens-Nakken, H., Reutelingsperger, C., 1995. A novel assay for apoptosis. Flow cytometric detection of phosphatidylserine expression on early apoptotic cells using fluorescein labeled Annexin V. *J. Immunol. Methods* 184, 39–51.
- Vos, S.M., Tretter, E.M., Schmidt, B.H., Berger, J.M., 2011. All tangled up: how cells direct, manage and exploit topoisomerase function. *Nat. Rev. Mol. Cell Biol.* 12, 827–841.
- Wojcik, A., Sauer, K., Zolzer, F., Bauch, T., Muller, W.U., 1996. Analysis of DNA damage recovery processes in the adaptive response to ionizing radiation in human lymphocytes. *Mutagenesis* 11, 291–297.

Apêndice D

APÊNDICE E - Patente depositada. Tiazacridinas utilizadas na terapia anticâncer

Depósito internacional N^o: PCT/BR2012/000421

UNIVERSIDADE FEDERAL DE PERNAMBUCO

Inventores: Suely Lins Galdino, Ivan da Rocha Pitta, Marina Galdino da Rocha Pitta, Francisco Washington Araújo Barros, Claudia Do Ó Pessoa, Manoel Odorico de Moraes Filho, Maira Galdino da Rocha Pitta.

7. Declaração na forma do item 3.2 do Ato Normativo nº 127/97:

7.1 Declaro que os dados fornecidos no presente formulário são idênticos ao da certidão de depósito ou documento equivalente do pedido cuja prioridade está sendo reivindicada.

em anexo

8. Declaração de divulgação anterior não prejudicial: (Período de Graça):
(art. 12 da LPI e item 2 do AN nº 127/97)

em anexo

9. Procurador (74)

9.1 Nome:

9.2 CNPJ/CPF:

9.3 API/OAB:

9.4 Endereço completo

9.5 CEP:

9.6 Telefone:

9.7 Fax:

9.8 E-Mail:

10. Listagem de seqüências Biológicas (documentos anexados) (se houver):

- Listagem de seqüências em arquivo eletrônico: nº de CDs ou DVDs (original e cópia),
- Código de controle alfanumérico no formato de código de barras: fl.
- Listagem de seqüências em formato impresso: fls.
- Declaração de acordo com o artigo da Resolução INPI nº 228/09: fls.

11. Documentos anexados (assinale e indique também o número de folhas):
(Deverá ser indicado o nº total de somente uma das vias de cada documento)

<input checked="" type="checkbox"/>	11.1 Guia de Recolhimento	01 fls.	<input checked="" type="checkbox"/>	11.5 Relatório descritivo	05 fls.
<input type="checkbox"/>	11.2 Procuração	fls.	<input checked="" type="checkbox"/>	11.6 Reivindicações	03 fls.
<input type="checkbox"/>	11.3 Documentos de Prioridade	fls.	<input checked="" type="checkbox"/>	11.7 Desenhos	02 fls.
<input type="checkbox"/>	11.4 Doc. de contrato de trabalho	fls.	<input checked="" type="checkbox"/>	11.8 Resumo	01 fls.
<input checked="" type="checkbox"/>	11.9 Outros que não aqueles definidos no campo 11 (especificar) Anexo Titulares, Anexo Inventores, declaração de poderes.				04 fls.

12. Total de folhas anexadas (referentes aos campos 10 e 11): 14 fls.

13. Declaro, sob penas da Lei, que todas as informações acima prestadas são completas e verdadeiras.

Recife, 10 de outubro, 2013

Local e Data

Assinatura e Carimbo

ANEXO 1

ANEXO DE TITULARES

Título: "Tiazacridinas Utilizadas na Terapia Anticâncer"

-
- 5 **Nome:** Universidade Federal de Pernambuco - UFPE
Qualificação: Autarquia Federal – Instituição de Ensino Superior
CNPJ/CPF: 24.134.488/0001-08
Endereço: Av. Professor Moraes Rego, 1235
Bairro: Cidade Universitária **Cidade:** Recife
CEP: 50670-901 **Estado:** Pernambuco **País:** Brasil
10 **Telefone:** (81)2126-8959 **Fax:** (81) 2126-8600
-
- 15 **Nome:** Universidade Federal do Ceará - UFC
Qualificação: Autarquia Federal – Ensino, Investigação Científica e Extensão.
CNPJ/CPF: 07.272.636/0001-31.
Endereço: Avenida da Universidade, nº 2853
Bairro: Benfica **Cidade:** Fortaleza
CEP: 60020-181 **Estado:** Ceará **País:** Brasil
Telefone: (85) 3366 7301 / 3366 7302. **Fax:** (85) 3366 7303.
-
- 20

ANEXO 2**INVENTORES:**

(1) **Nome:** Suely Lins Galdino

Qualificação: Brasileira, Casada, Professor Associado I

5 **RG:** 218413 - SSP/PB **CPF:** 202.821.254-34

Endereço: Avenida Boa Viagem 5554 Ap 202

Bairro/Cidade/UF: Boa Viagem – Recife – PE

CEP: 51030-000

Telefone: (81) 8739-1954

10

(2) **Nome:** Ivan Da Rocha Pitta

Qualificação: Brasileiro, Casado, Prof. Titular e Coordenador Inct-If.

RG: 146088 - MAER, **CPF:** 075.127.244-20

Endereço: Avenida Boa Viagem 5554 Ap 202

15 **Bairro/Cidade/UF:** Boa Viagem – Recife – PE

CEP 51030-000

Telefone: (81) 8838-1944

(3) **Nome:** Maria Do Carmo Alves De Lima

20 **Qualificação:** Brasileira, Solteira, Professor Associado I

RG: 2141596 - SSP/PE **CPF:** 280.819.514-15

Endereço: Rua Beta Nº 55

Bairro/Cidade/UF: Sucupira – Jaboatão dos Guararapes – PE

CEP: 54280-550

25 **Telefone:** (81) 3257-3838

(4) **Nome:** Marina Galdino Da Rocha Pitta

Qualificação: Brasileira, Solteira, Mestre, Doutoranda

RG: 7328302 - SDS/PE **CPF:** 060.883.204-94

30 **Endereço:** Avenida Boa Viagem 5554 Ap 202

Bairro/Cidade/UF: Boa Viagem – Recife – PE

CEP: 51030-000

Telefone: (81) 8838-1986

- 5
5
(5) Nome: Francisco Washington Araújo Barros
Qualificação: Brasileiro, Casado, Mestre, Doutorando
RG: 424460955- SSP/MA **CPF:** 853.481.983-15
Endereço: R. Gustavo Sampaio, Nº 372
Bairro/Cidade/UF: Parque Araxá – Fortaleza – CE
CEP: 60450-635
Telefone: (85) 8709-7350
- 10
10
(6) Nome: Claudia Do Ó Pessoa
Qualificação: Brasileira, Solteira, Doutorado, Professor Assoc. II
RG: 1827177- SSP/ **CPF:** 520.891.184-15
Endereço: Rua Eduardo Garcia, 888 Apt 901
Bairro/Cidade/UF: Aldeota – Fortaleza – CE
15
CEP: 60150-100
Telefone: (85) 3264-5775
- 20
20
(7) Nome: Manoel Odorico De Moraes Filho
Qualificação: Brasileira, Casado, Doutorado, Professor
RG: 357360- SSP/CE **CPF:** 048.545.433-53
Endereço: Rua República Do Libano, 881/500
Bairro/Cidade/UF: Meireles – Fortaleza - CE
CEP: 60160-140
25
Telefone: (85) 9989-3459
- 30
30
(8) Nome: Maira Galdino Da Rocha Pitta
Qualificação: Brasileira, Solteira, Doutorada, Professor Adjunto
RG: 6304255- SSP/PE **CPF:** 039.972.064-22
Endereço: Avenida Boa Viagem 5554 Ap 202
Bairro/Cidade/UF: Boa Viagem – Recife – PE
CEP: 51030-000
Telefone: (81) 3459-1136

Apêndice E

APÊNDICE F - Espectros de NMR¹H e IR de tiazacridinas

Acridin-9-il-metil-tiazolidina-2,4-diona (LPSF AA-1A)

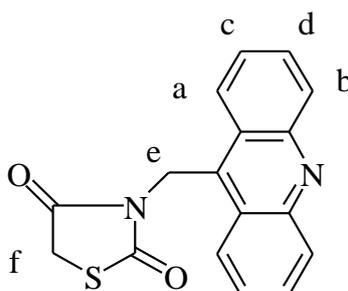
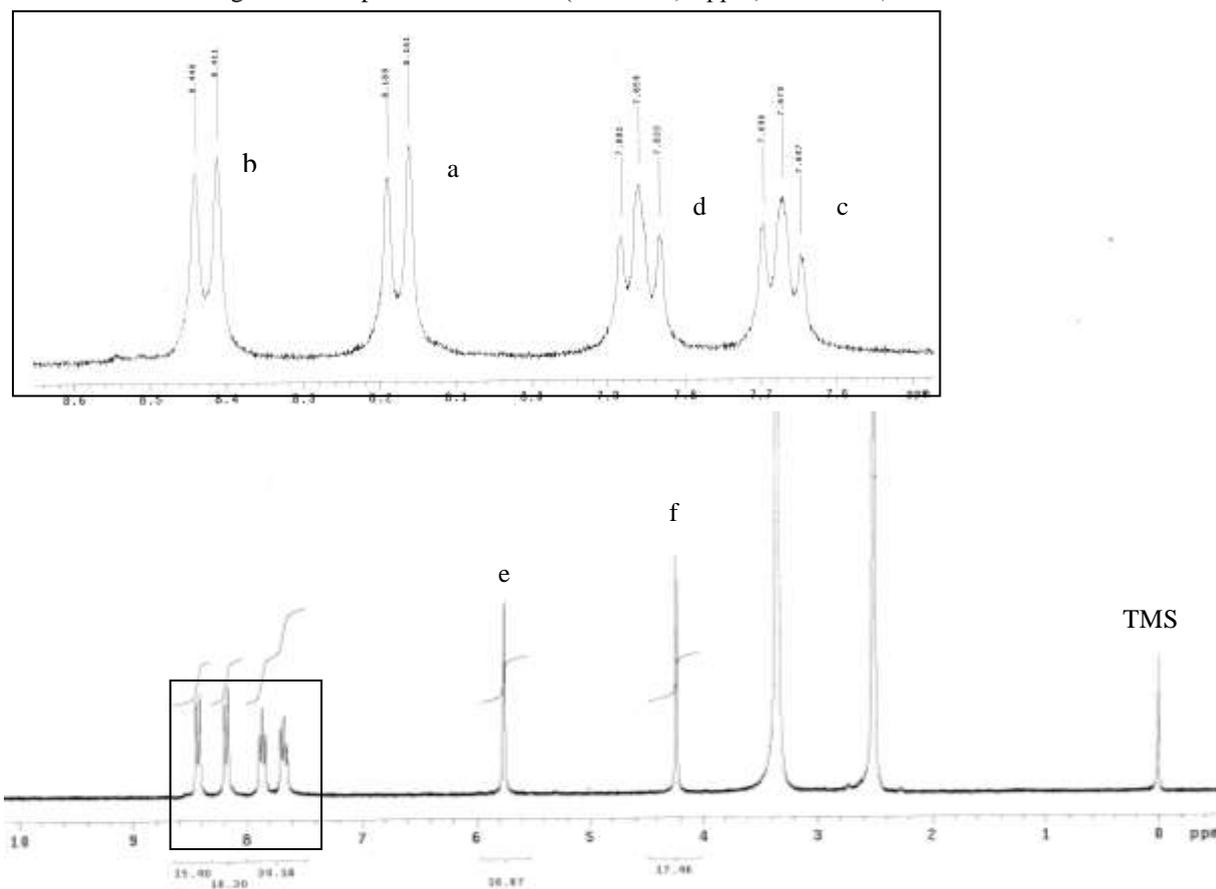


Figura 24 - Espectro de NMR¹H (400 MHz, δ ppm, DMSO-d₆) do LPSF AA-1A



Fonte: Autora, 2012

Apêndice F

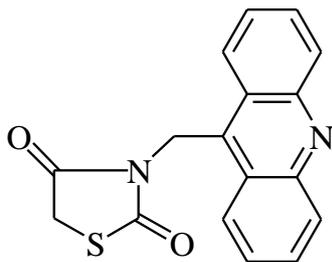
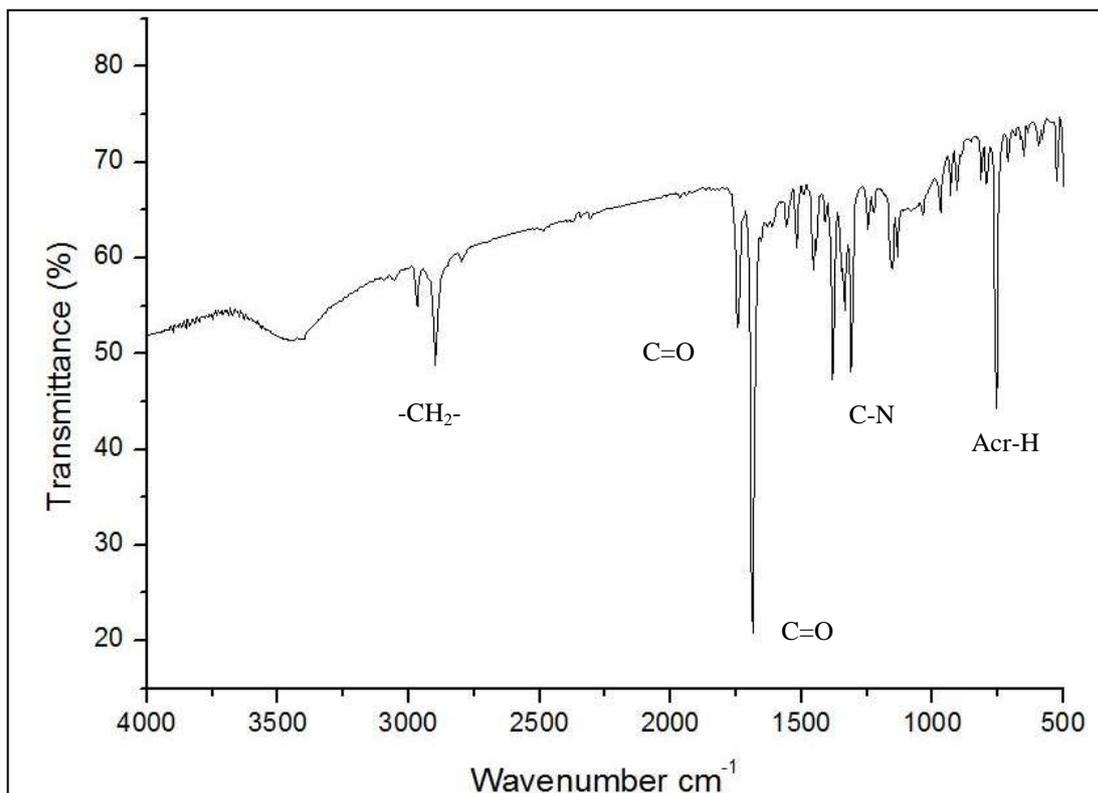


Figura 25 - Espectro de IR do LPSF AA-1A



Fonte: Autora, 2012

Apêndice FNovos Agentes Tiazacridínicos com Propriedades Anticâncer
Marina G R Pitta

3-Acridin-9-ilmetil-5-(5-bromo-2-metoxi-benzilideno)-tiazolidina-2,4-diona (LPSF AA-10)

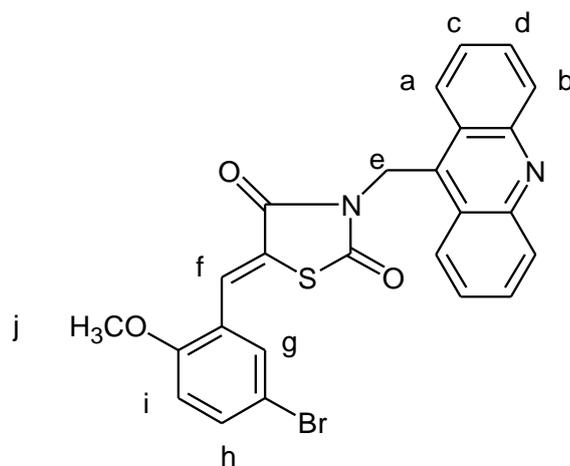
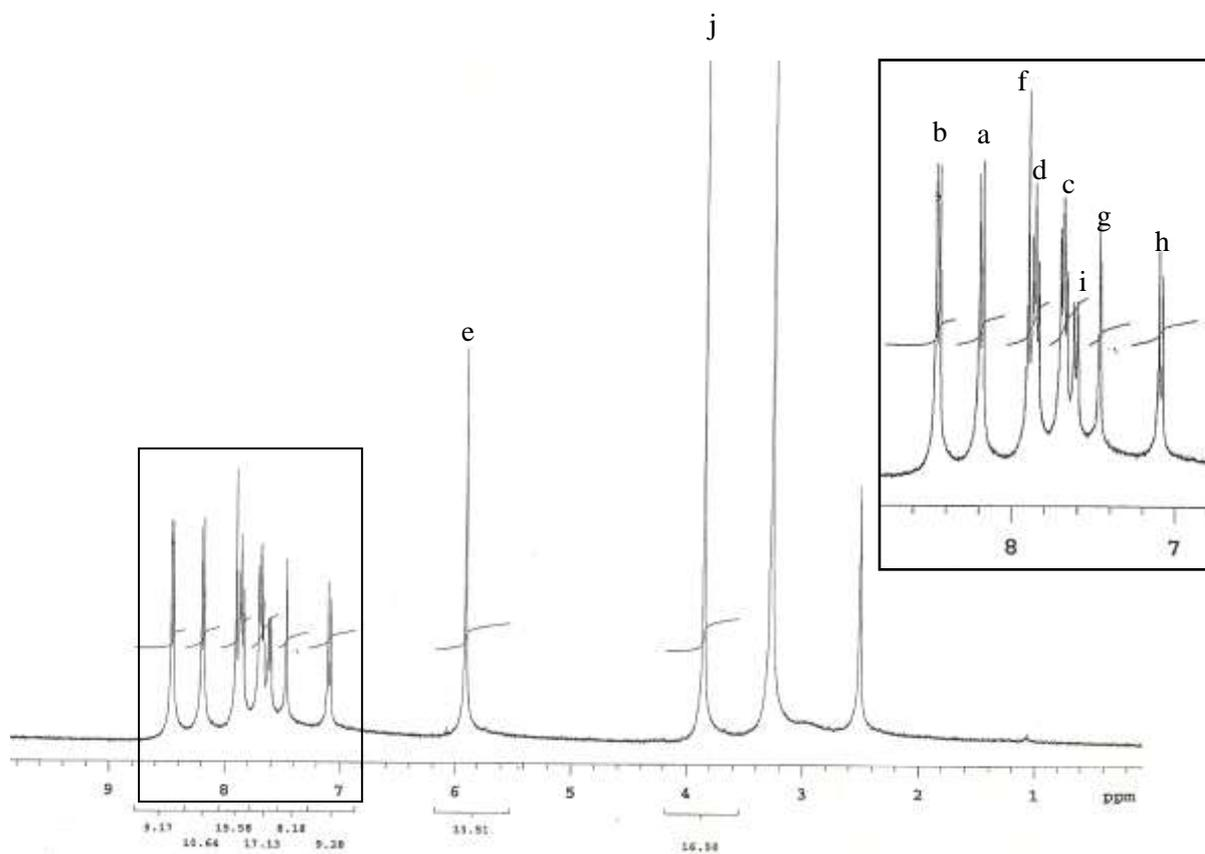


Figura 26 - Espectro de NMR¹H do LPSF AA-10



Fonte: Autora, 2012

Apêndice F

Novos Agentes Tiazacridínicos com Propriedades Anticâncer
Marina G R Pitta

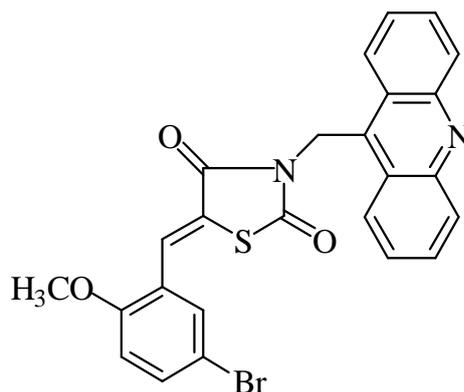
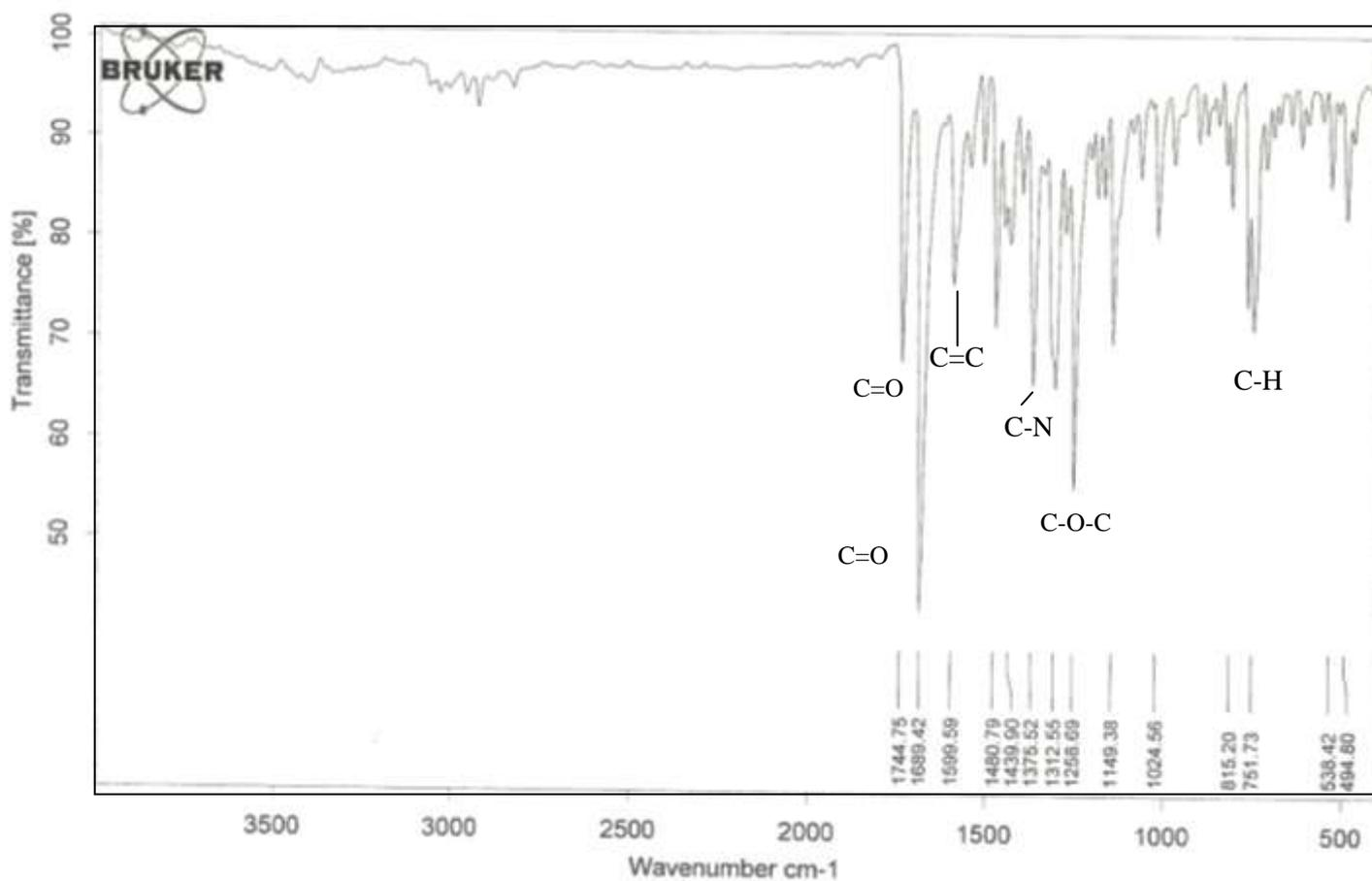


Figura 27 - Espectro de IR do LPSF AA-10. Deformação axial normal de C=O, 1744 cm^{-1} , 1689 cm^{-1} . Deformação axial das ligações C=C do anel, 1599 cm^{-1} . Deformação axial de C-N, 1375 cm^{-1} . Deformação axial simétrica de C-O-C, 1258 cm^{-1} . Deformação angular fora do plano de C-H de aromático, 751 cm^{-1}



Fonte: Autora, 2012

Apêndice F

Novos Agentes Tiazacridínicos com Propriedades Anticâncer
Marina G R Pitta

3-Acridin-9-ilmetil-5-bifenil-4-ilmetileno-tiazolidina-2,4-diona (LPSF AA-11)

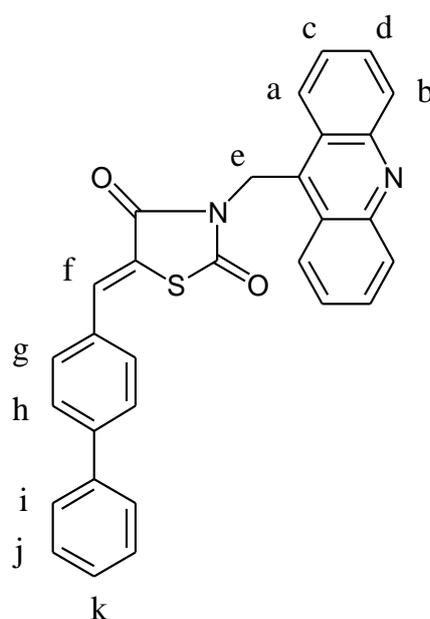
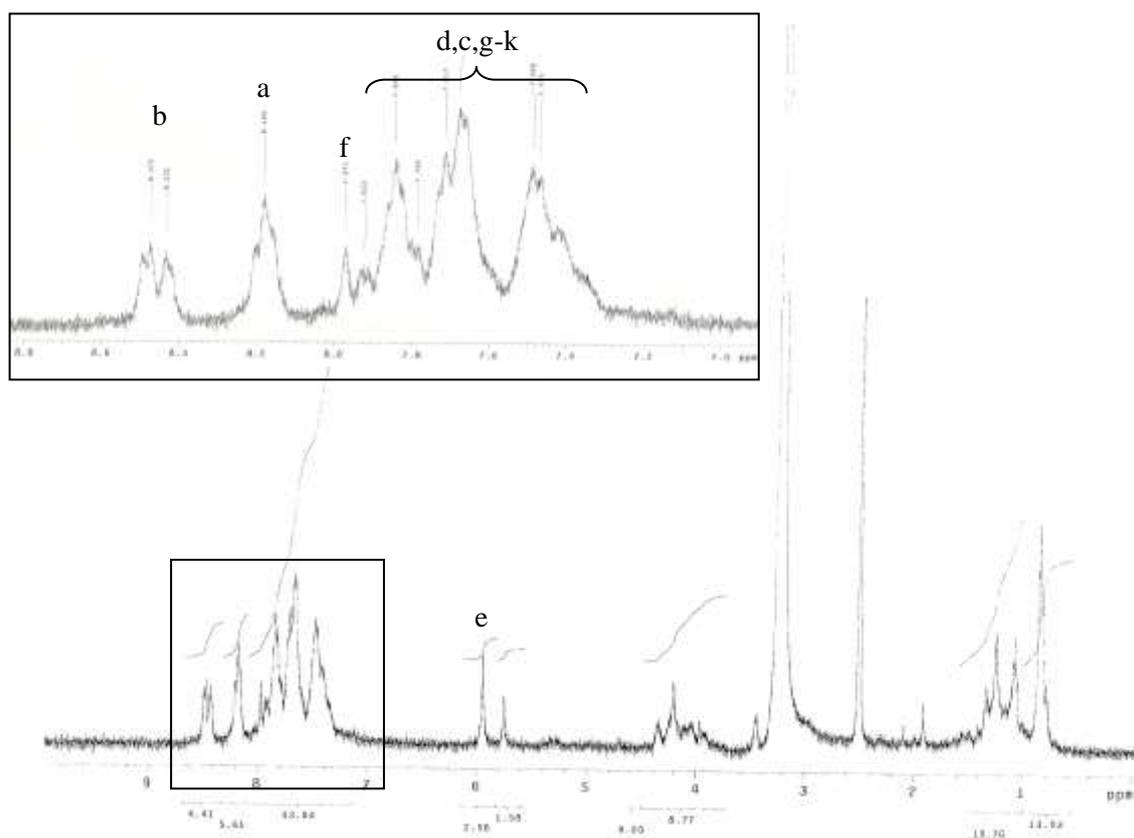


Figura 28 - Espectro de NMR¹H do LPSF AA-11



Fonte: Autora, 2012

Apêndice F

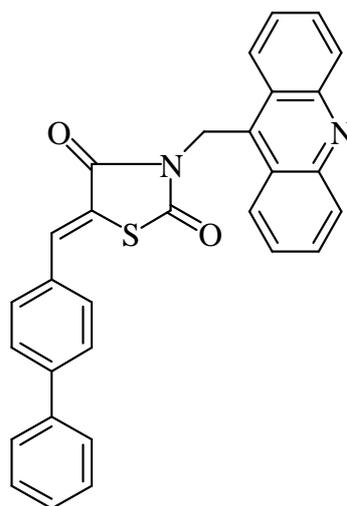
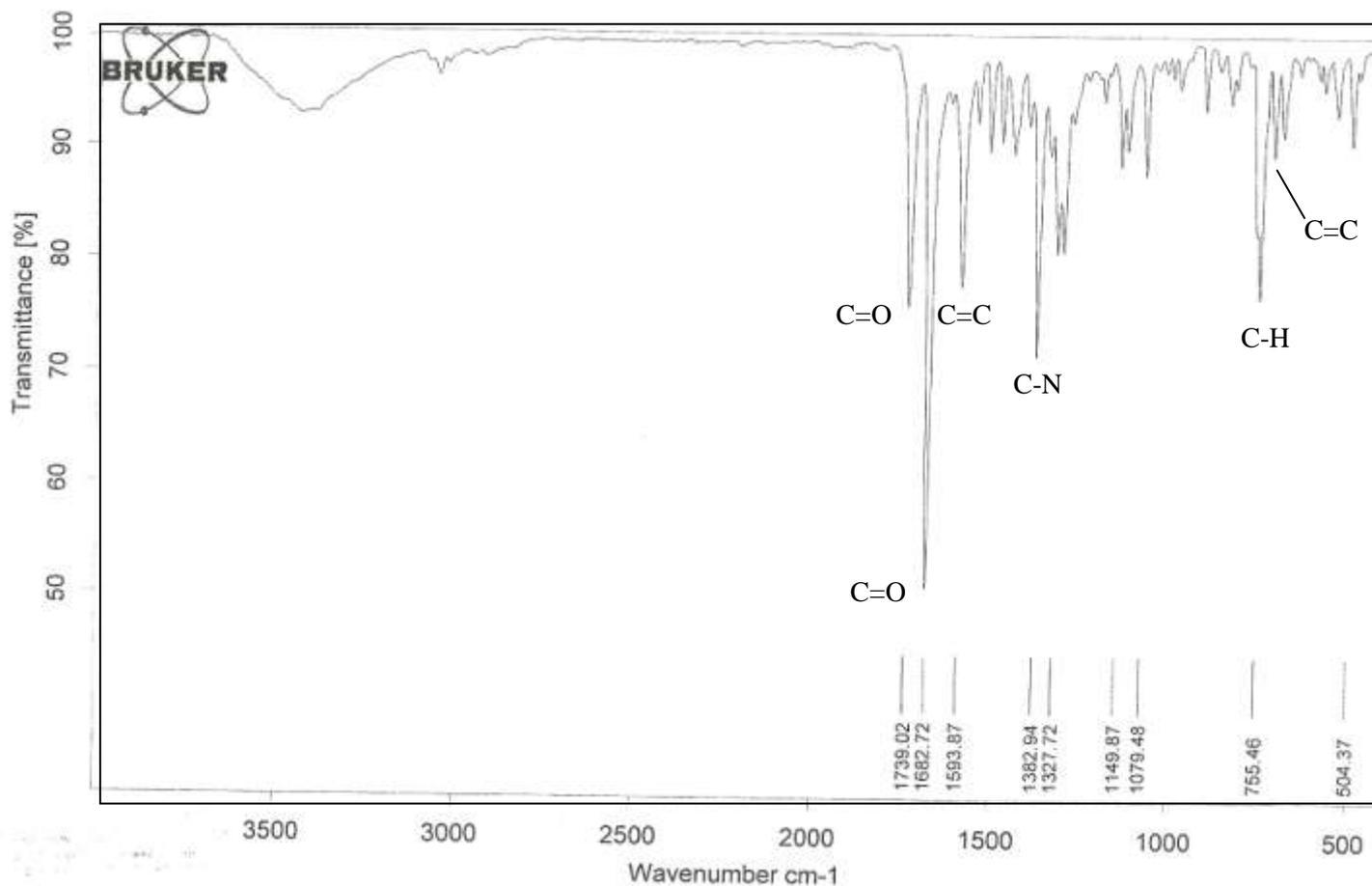


Figura 29 - Espectro de IR do LPSF AA-11. Deformação axial normal de C=O, 1739 cm^{-1} , 1682 cm^{-1} . Deformação axial das ligações C=C do anel, 1593 cm^{-1} . Deformação axial de C-N, 1382 cm^{-1} . Deformação angular fora do plano de C-H de aromático, 755 cm^{-1} . Deformação angular de C=C, 707 cm^{-1}



Fonte: Autora, 2012

Apêndice F

Novos Agentes Tiazacridínicos com Propriedades Anticâncer
Marina G R Pitta

3-Acridin-9-ilmetil-5-(3,5-dimetoxi-benzilideno)-tiazolidina-2,4-diona (LPSF AA-12)

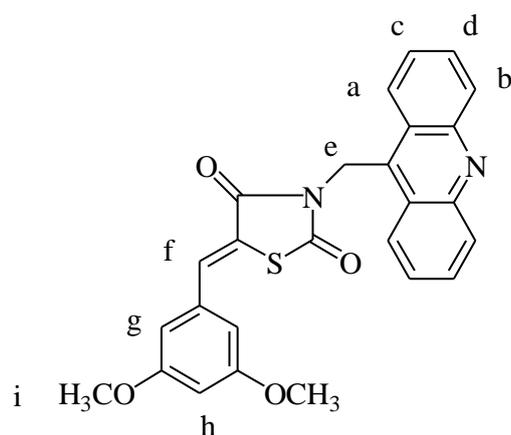
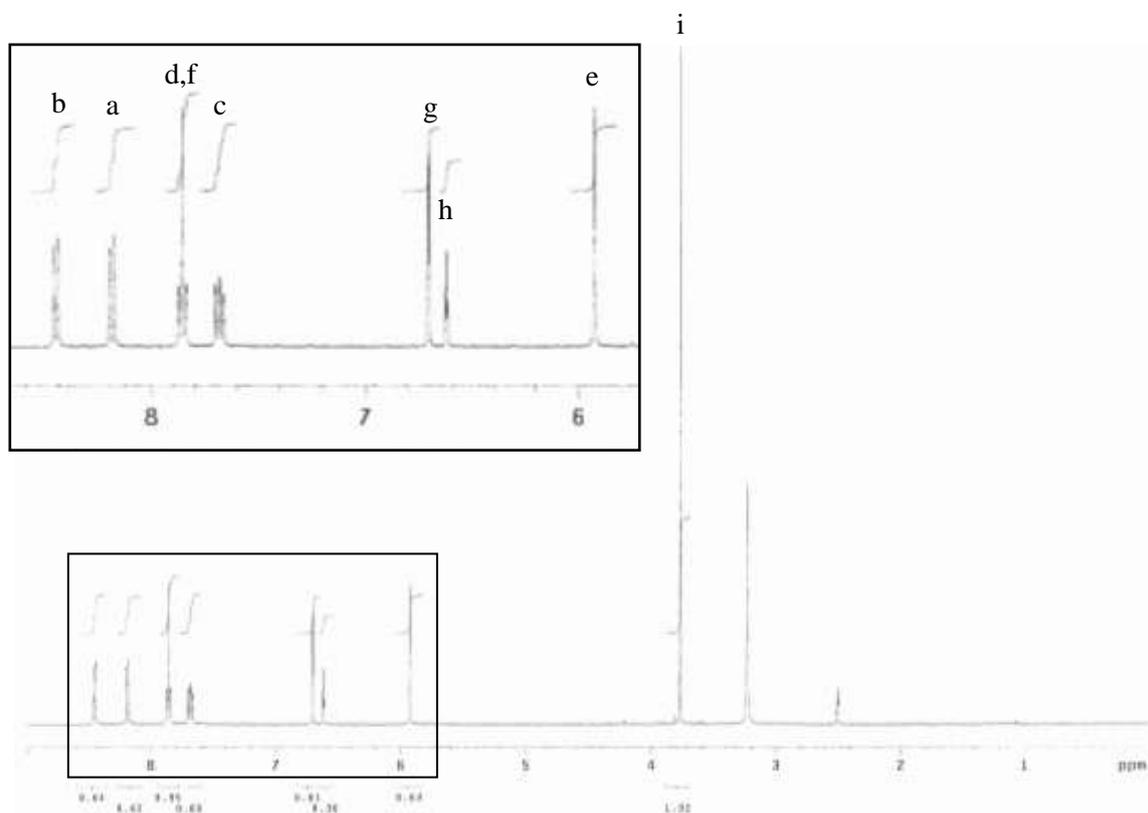


Figura 30 - Espectro de NMR¹H do LPSF AA-12



Fonte: Autora, 2012

Apêndice F

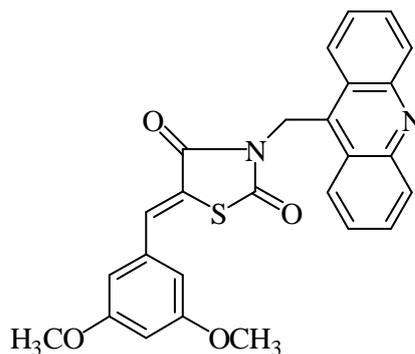
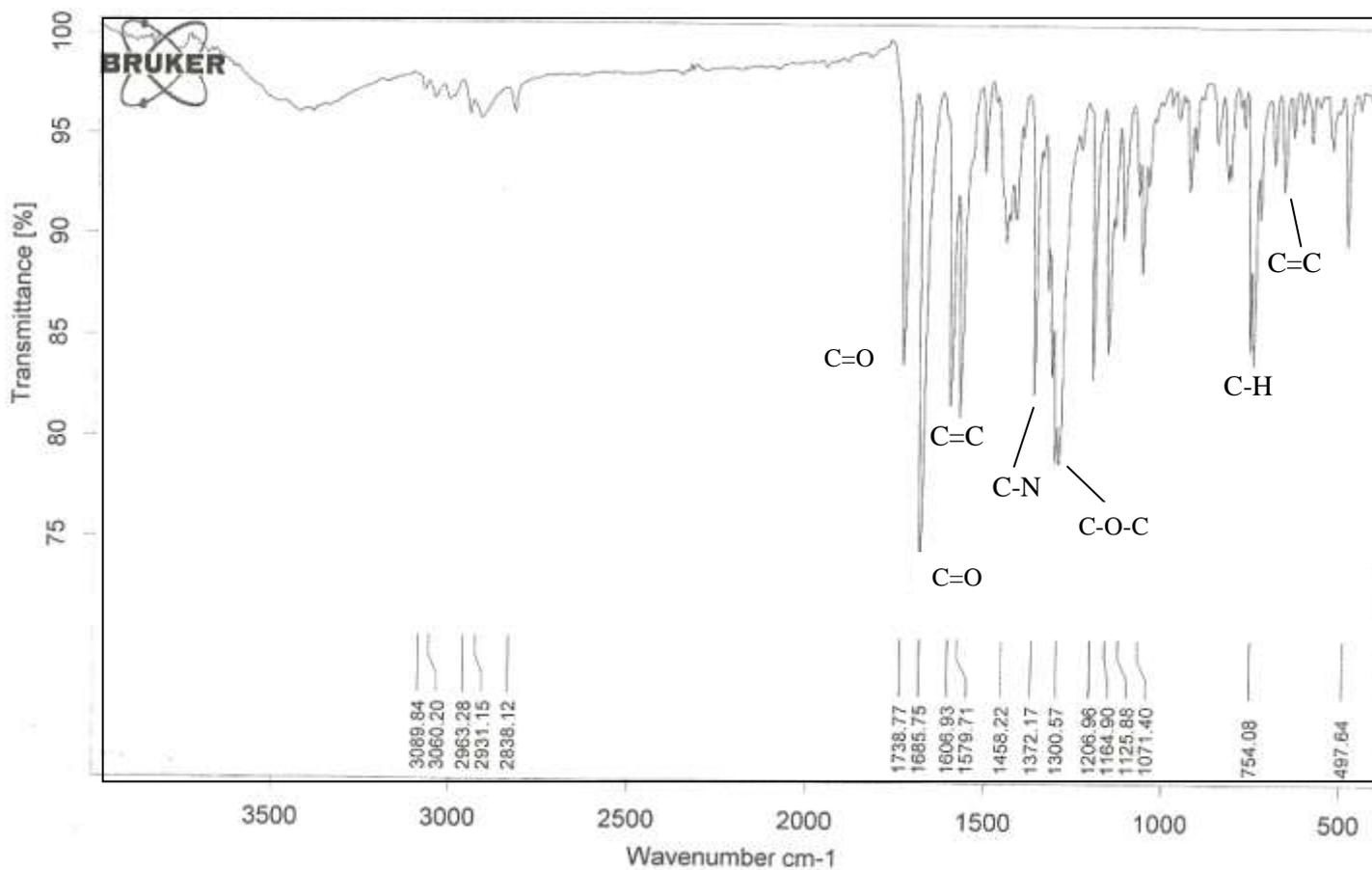


Figura 31 - Espectro de IR do LPSF AA-12. Deformação axial normal de C=O, 1738 cm^{-1} , 1685 cm^{-1} . Deformação axial das ligações C=C do anel, 1606 cm^{-1} . Deformação axial de C-N, 1372 cm^{-1} . Deformação axial simétrica de C-O-C, 1300 cm^{-1} . Deformação angular fora do plano de C-H de aromático, 754 cm^{-1} . Deformação angular de C=C, 707 cm^{-1}



Fonte: Autora, 2012

Apêndice F

3-Acridin-9-ilmetil-5-(2,3-dicloro-benzilideno)-tiazolidina-2,4-diona (LPSF AA-13)

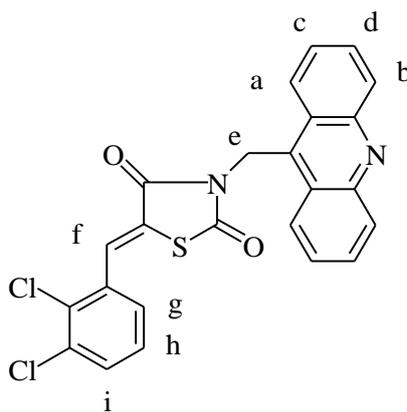
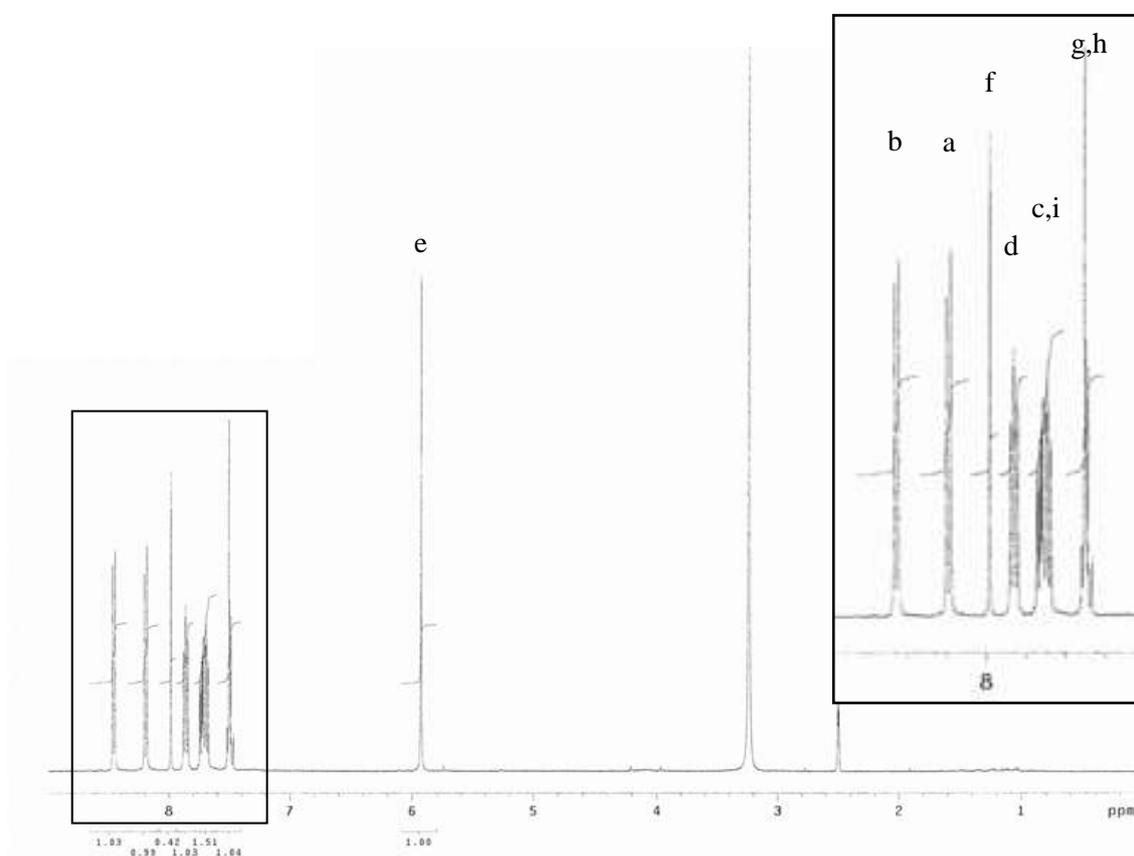


Figura 32 - Espectro de NMR¹H do LPSF AA-13



Fonte: Autora, 2012

Apêndice F

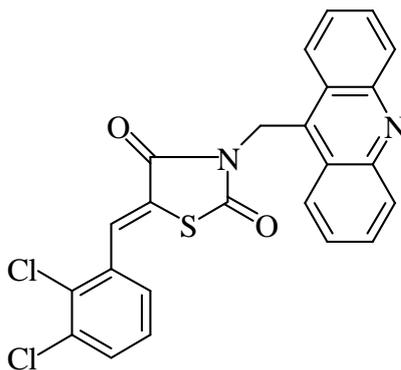
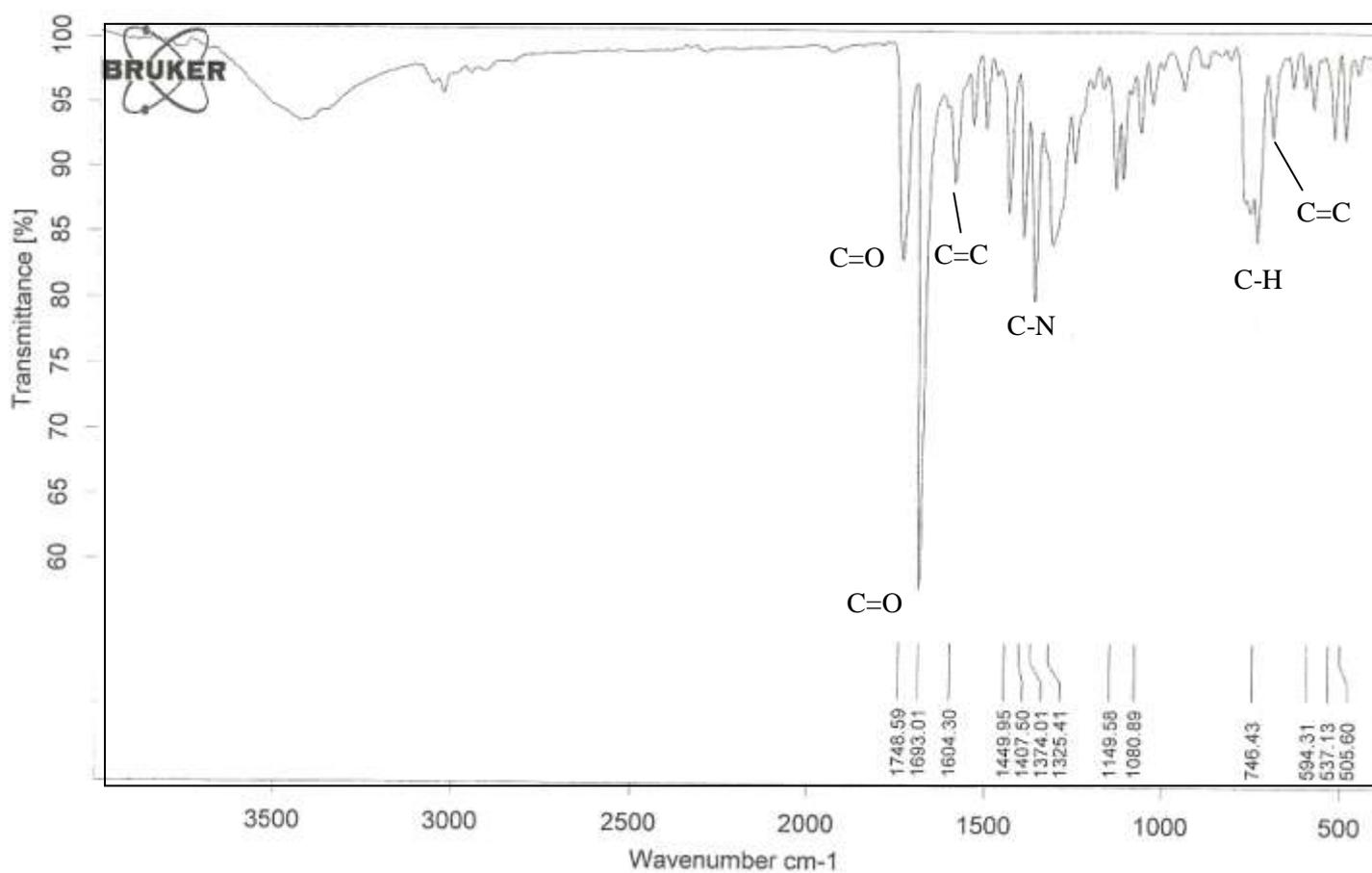


Figura 33 - Espectro de IR do LPSF AA-13. Deformação axial normal de C=O, 1748 cm⁻¹, 1693 cm⁻¹. Deformação axial das ligações C=C do anel, 1604 cm⁻¹. Deformação axial de C-N, 1374 cm⁻¹. Deformação angular fora do plano de C-H de aromático, 746 cm⁻¹. Deformação angular de C=C, 740 cm⁻¹



Fonte: Autora, 2012

Apêndice F

Acridin-9-ilmetil-5-(3-bromo-benzilideno)-tiazolidina-2,4-diona (LPSF AA-14)

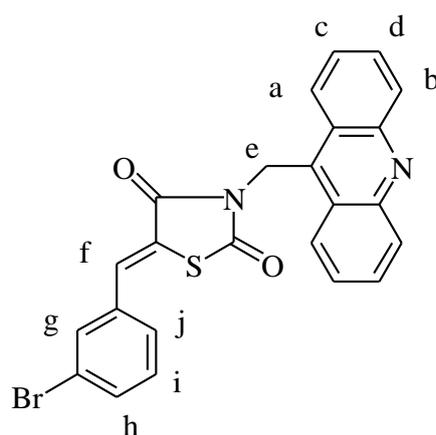
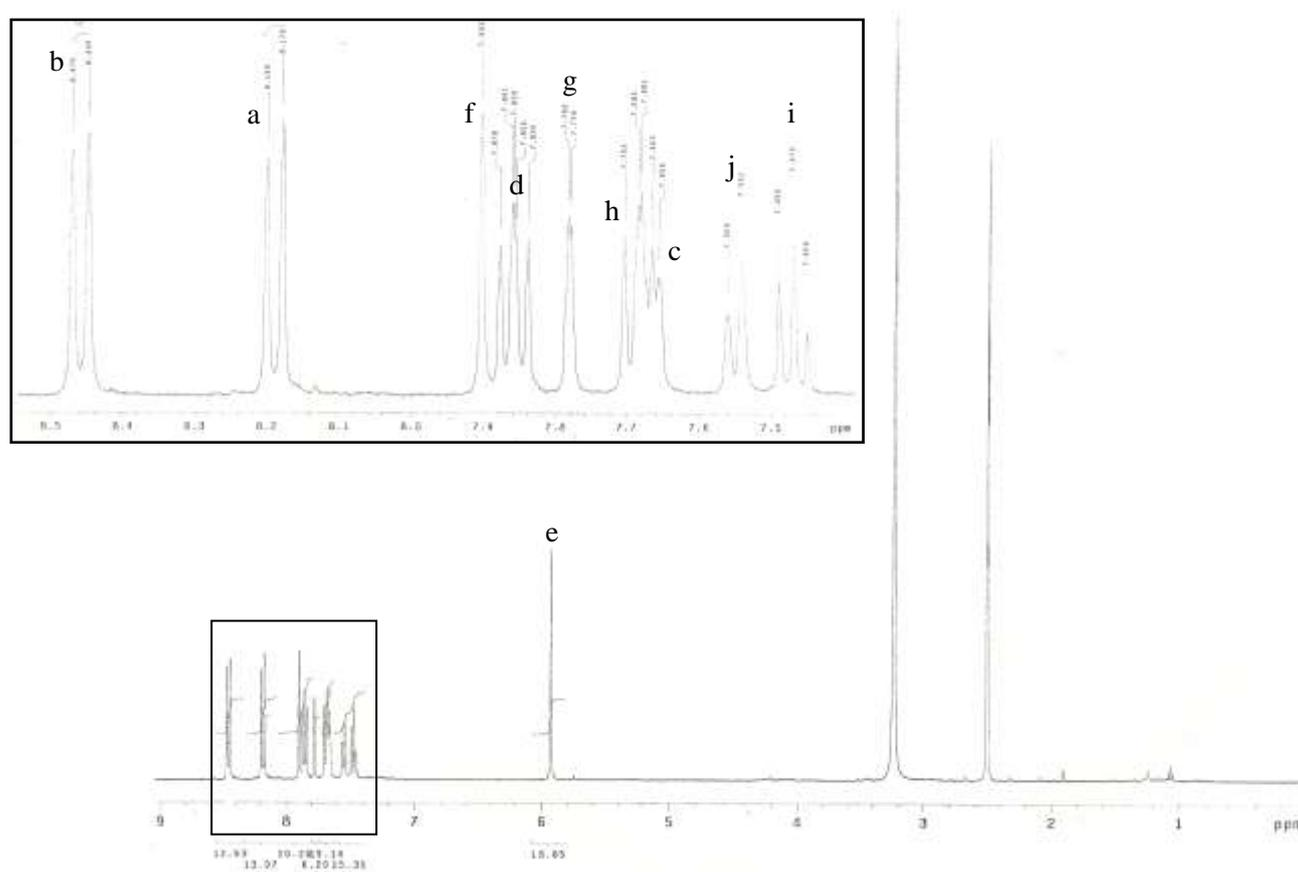


Figura 34 - Espectro de NMR¹H do LPSF AA-14



Fonte: Autora, 2012

Apêndice F

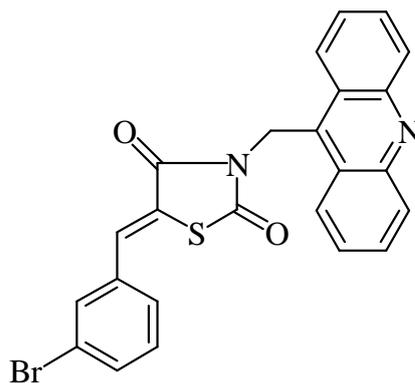
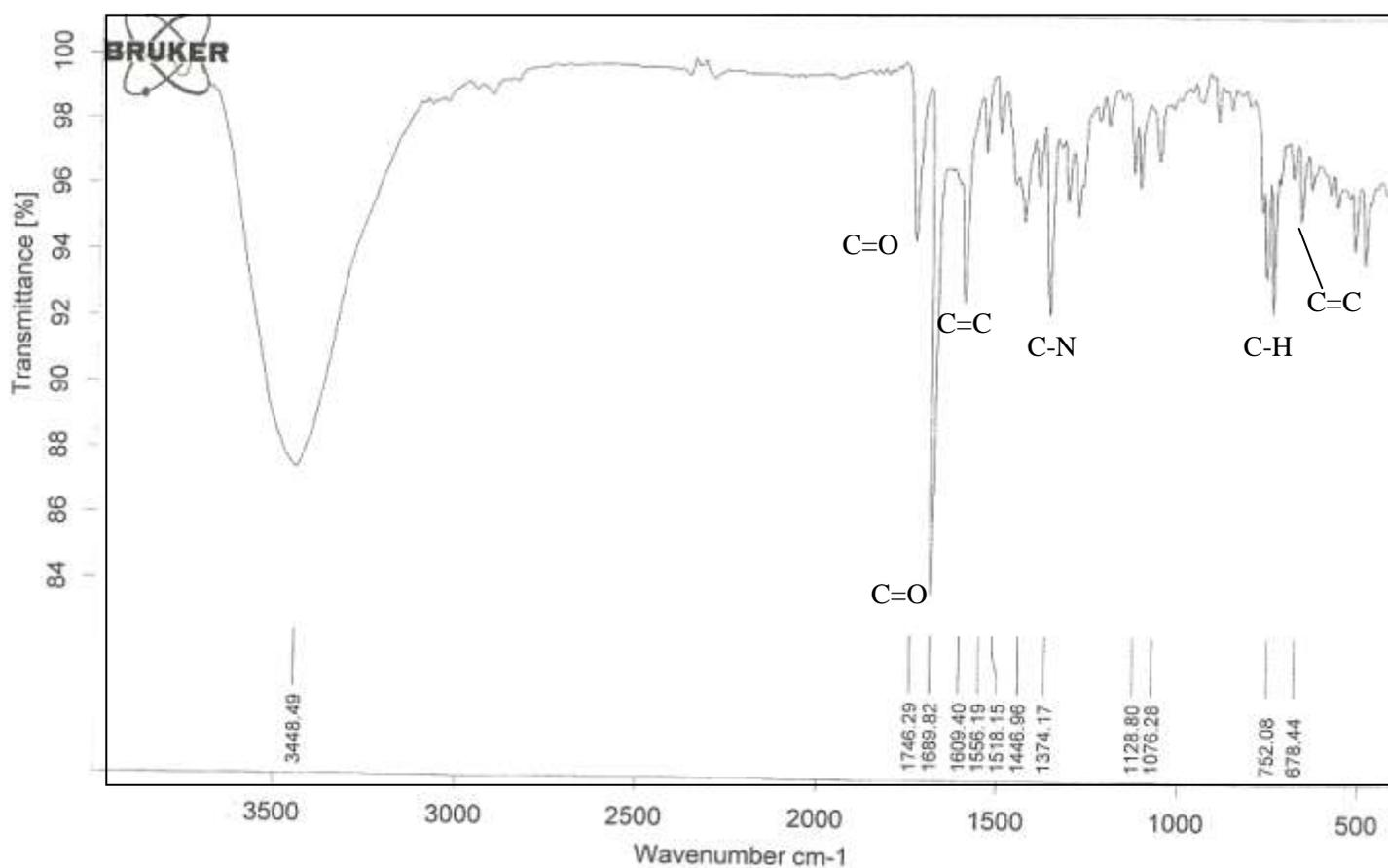


Figura 35 - Espectro de IR do LPSF AA-14. Deformação axial normal de C=O, 1746 cm^{-1} , 1689 cm^{-1} . Deformação axial das ligações C=C do anel, 1609 cm^{-1} . Deformação axial de C-N, 1374 cm^{-1} . Deformação angular fora do plano de C-H de aromático, 752 cm^{-1} . Deformação angular de C=C, 678 cm^{-1}



Fonte: Autora, 2012

Apêndice F

3-Acridin-9-ilmetil-5-(1H-indol-3-ilmetileno)-tiazolidina-2,4-diona (LPSF AA-15)

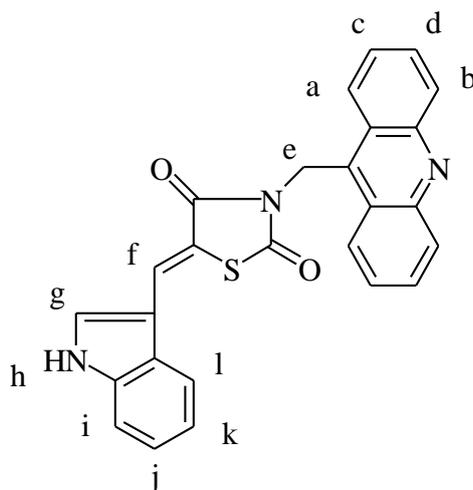
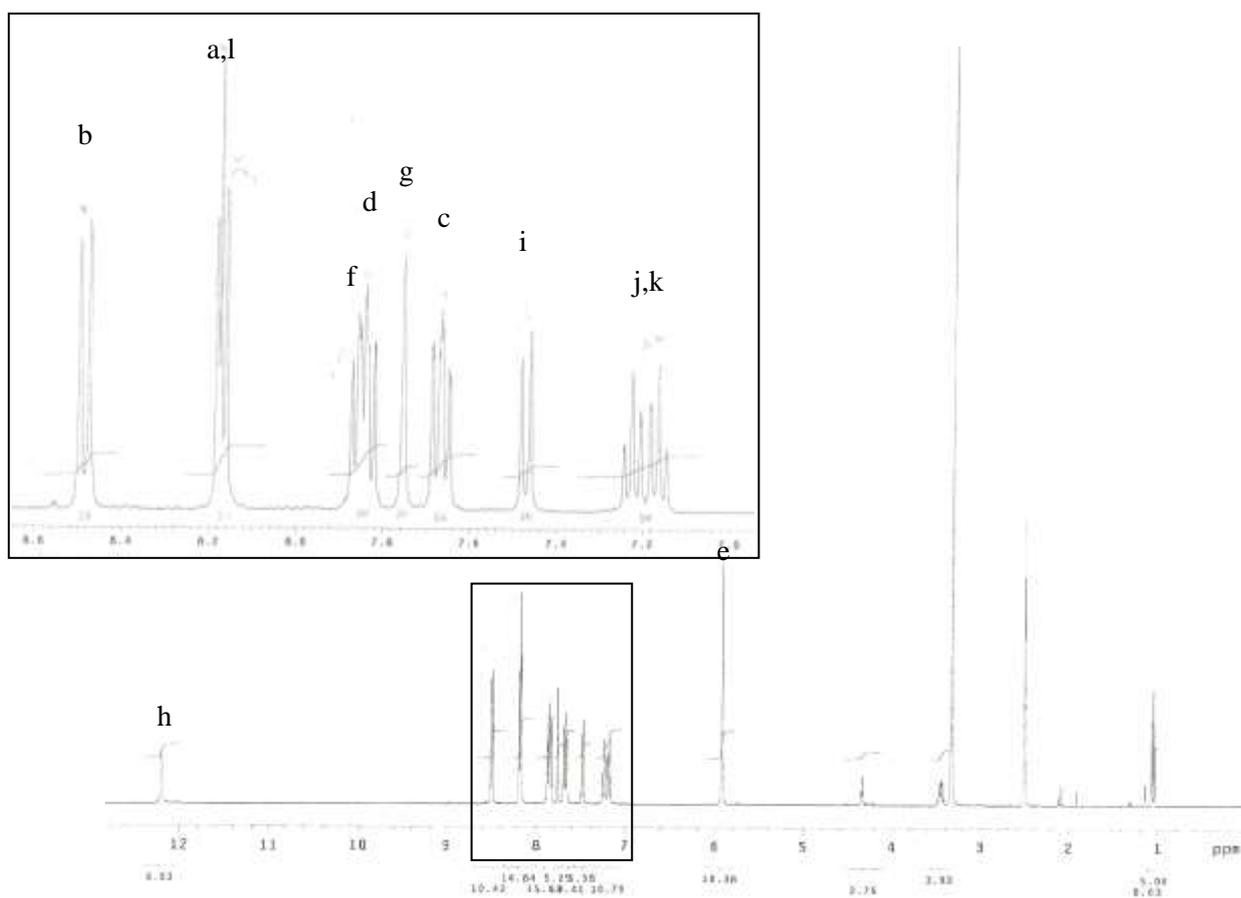


Figura 36 - Espectro de NMR¹H do LPSF AA-15



Fonte: Autora, 2012

Apêndice F

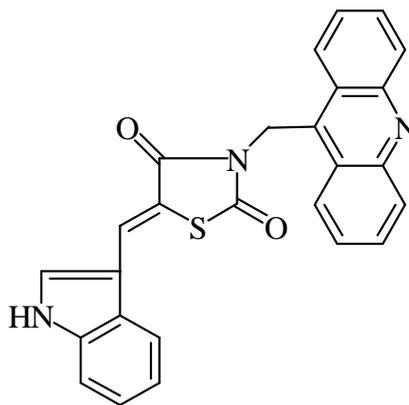
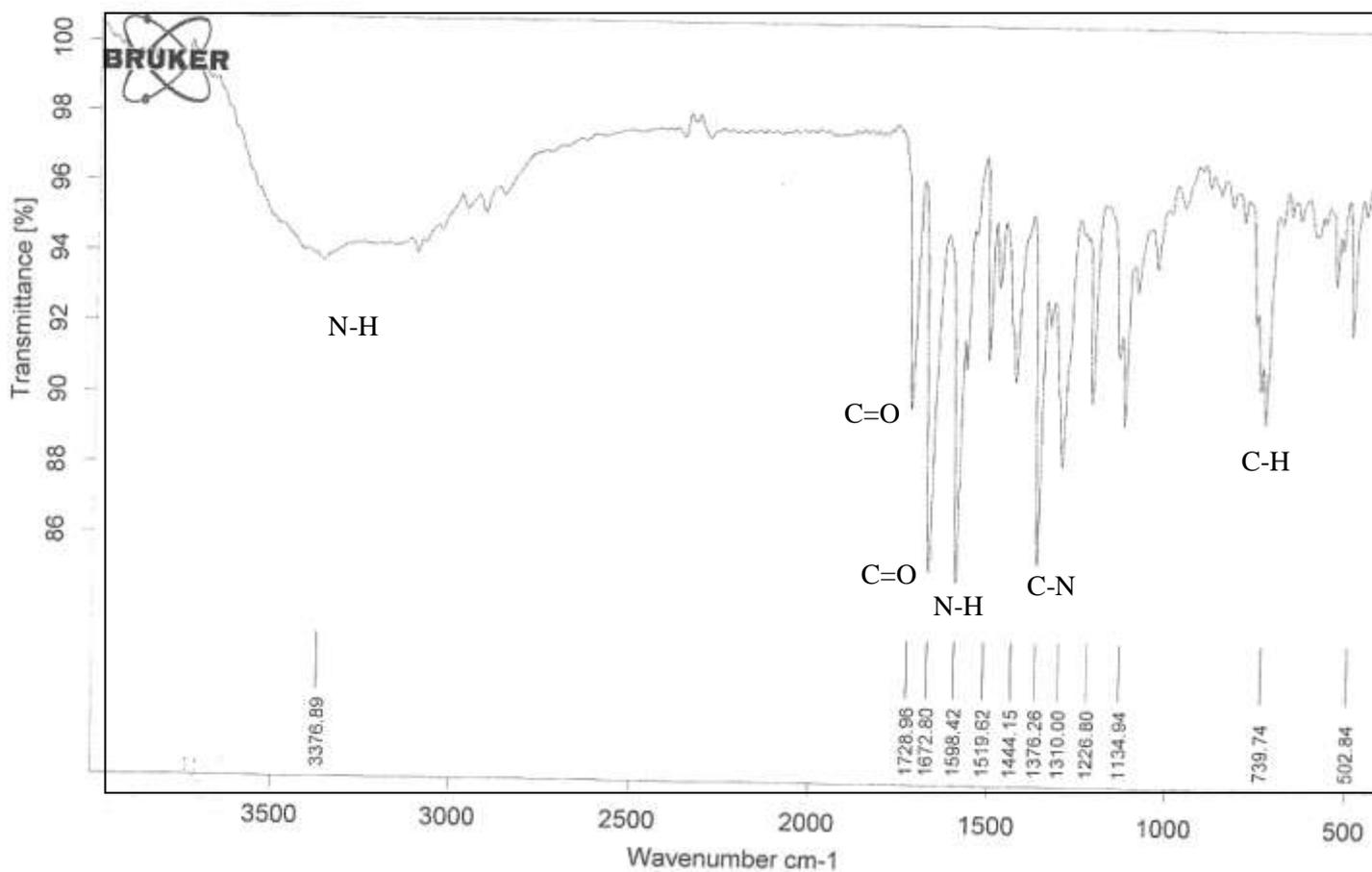


Figura 37 - Espectro de IR do LPSF AA-15. Deformação axial de N-H, 3376 cm^{-1} . Deformação axial normal de C=O, 1728 cm^{-1} , 1672 cm^{-1} . Deformação angular de N-H, 1598 cm^{-1} . Deformação axial de C-N, 1376 cm^{-1} . Deformação angular fora do plano de C-H de aromático, 739 cm^{-1}



Fonte: Autora, 2012

Apêndice F

Novos Agentes Tiazacridínicos com Propriedades Anticâncer
Marina G R Pitta

3-Acridin-9-ilmetil-5-(4-fluoro-benzilideno)-tiazolidina-2,4-diona (LPSF AA-16)

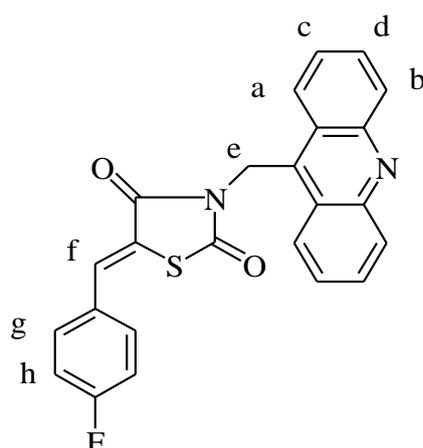
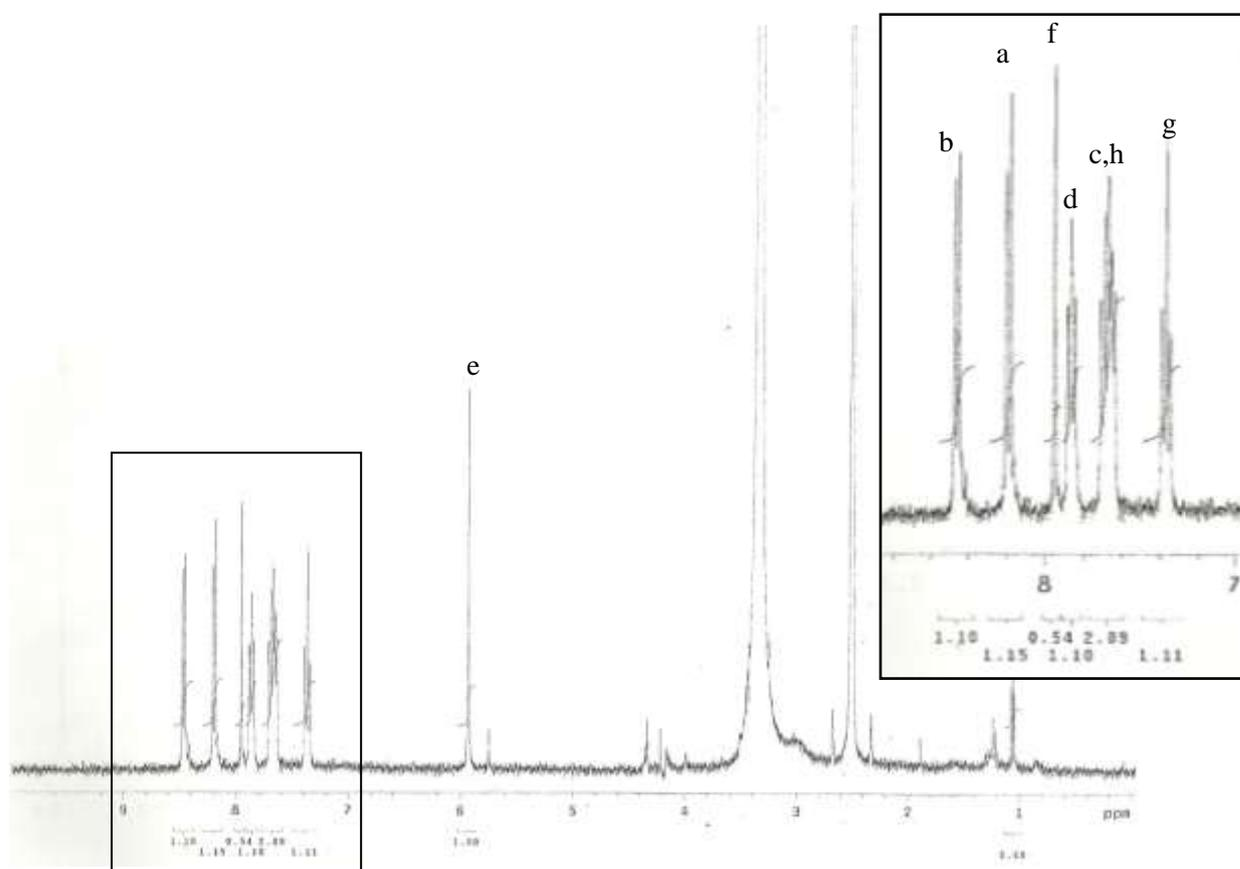


Figura 38 - Espectro de NMR¹H do LPSF AA-16



Fonte: Autora, 2012

Apêndice F

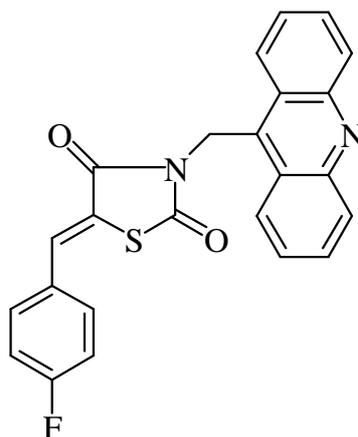
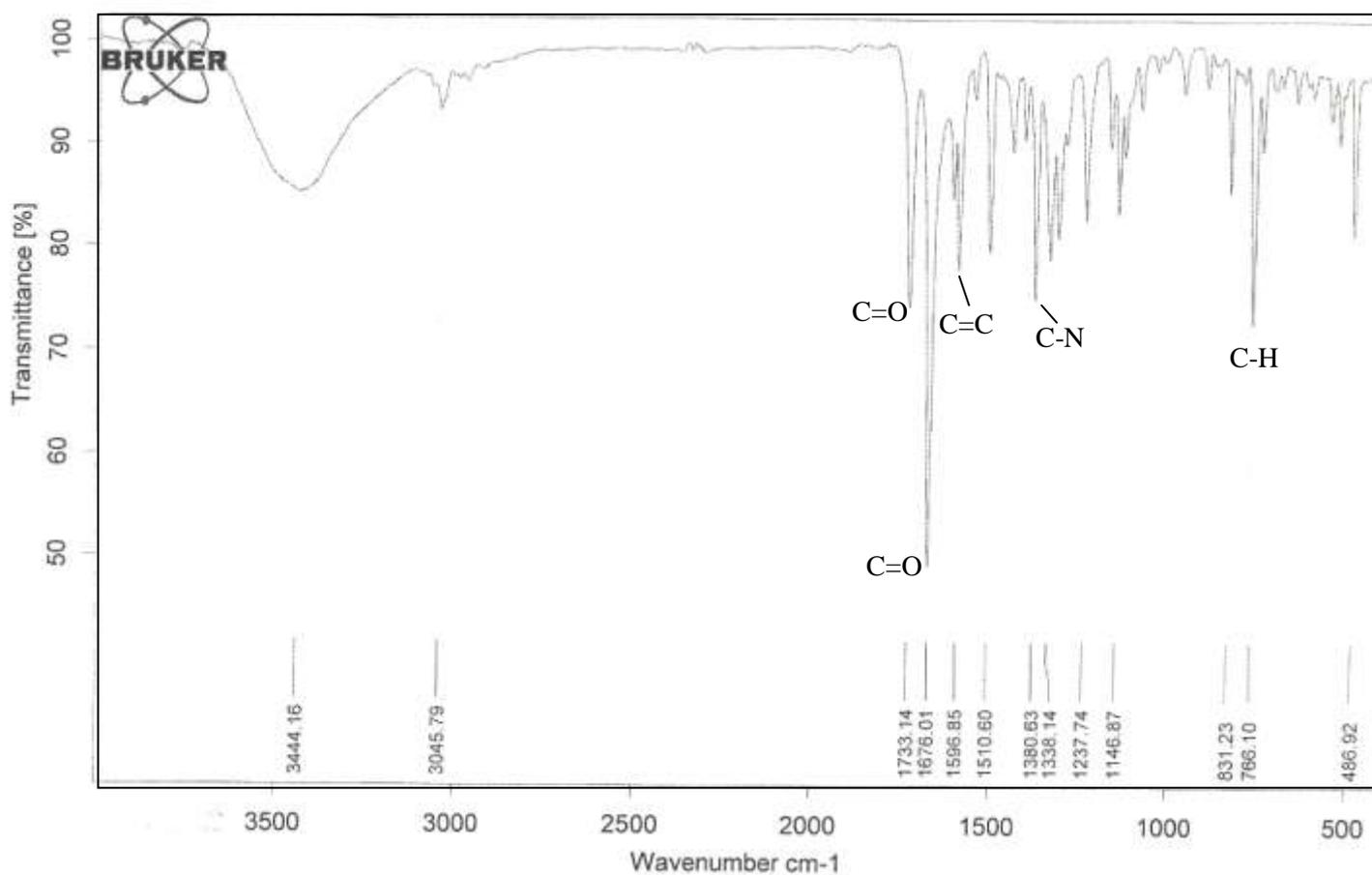


Figura 39 - Espectro de IR do LPSF AA-16. Deformação axial normal de C=O, 1733 cm^{-1} , 1676 cm^{-1} . Deformação axial das ligações C=C do anel, 1596 cm^{-1} . Deformação axial de C-N, 1380 cm^{-1} . Deformação angular fora do plano de C-H de aromático, 766 cm^{-1}



Fonte: Autora, 2012

Apêndice F

Novos Agentes Tiazacridínicos com Propriedades Anticâncer
Marina G R Pitta

3-Acridin-9-ilmetil-5-(3,4,5-trimetoxi-benzilideno)-tiazolidina-2,4-diona (LPSF AA-17)

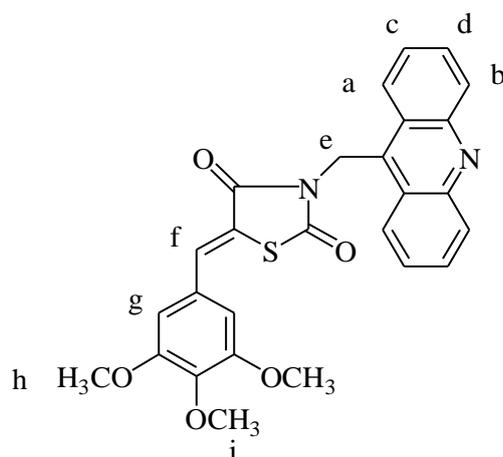
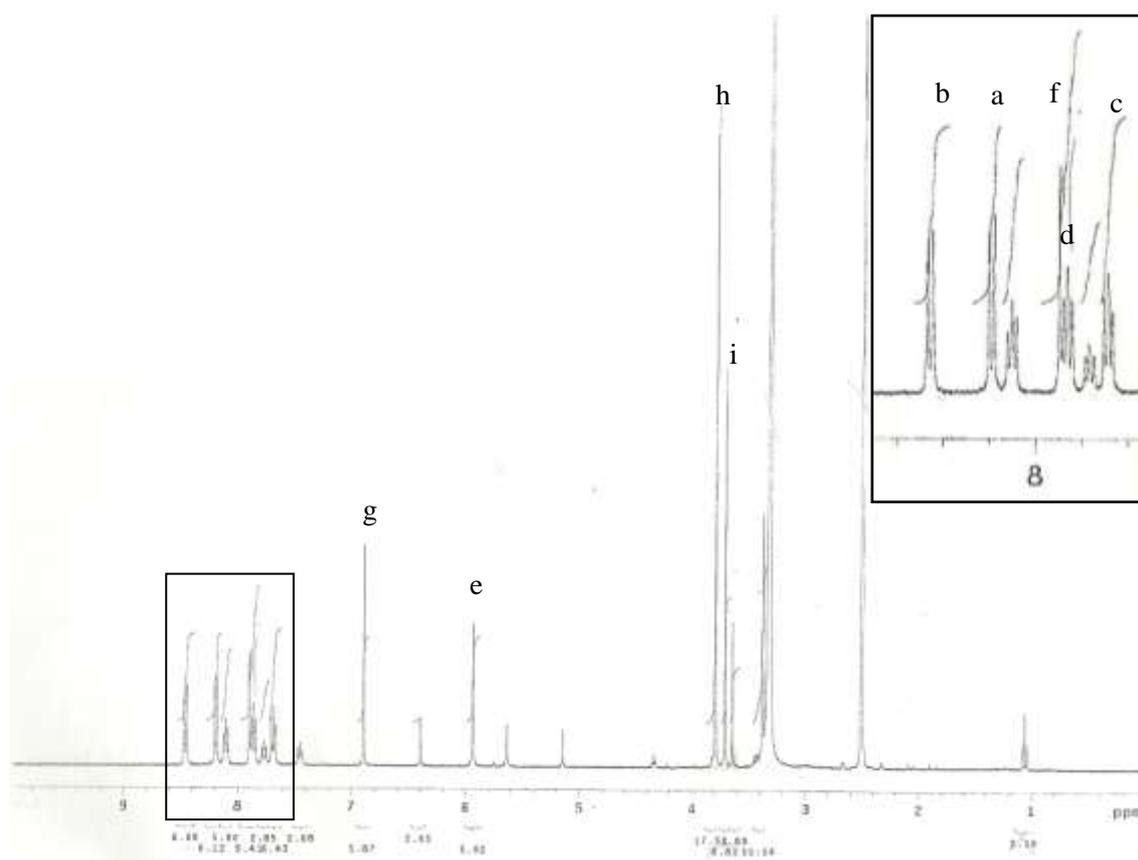


Figura 40 - Espectro de NMR¹H do LPSF AA-17



Fonte: Autora, 2012

Apêndice F

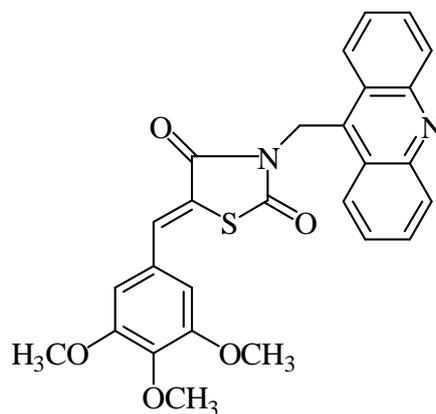
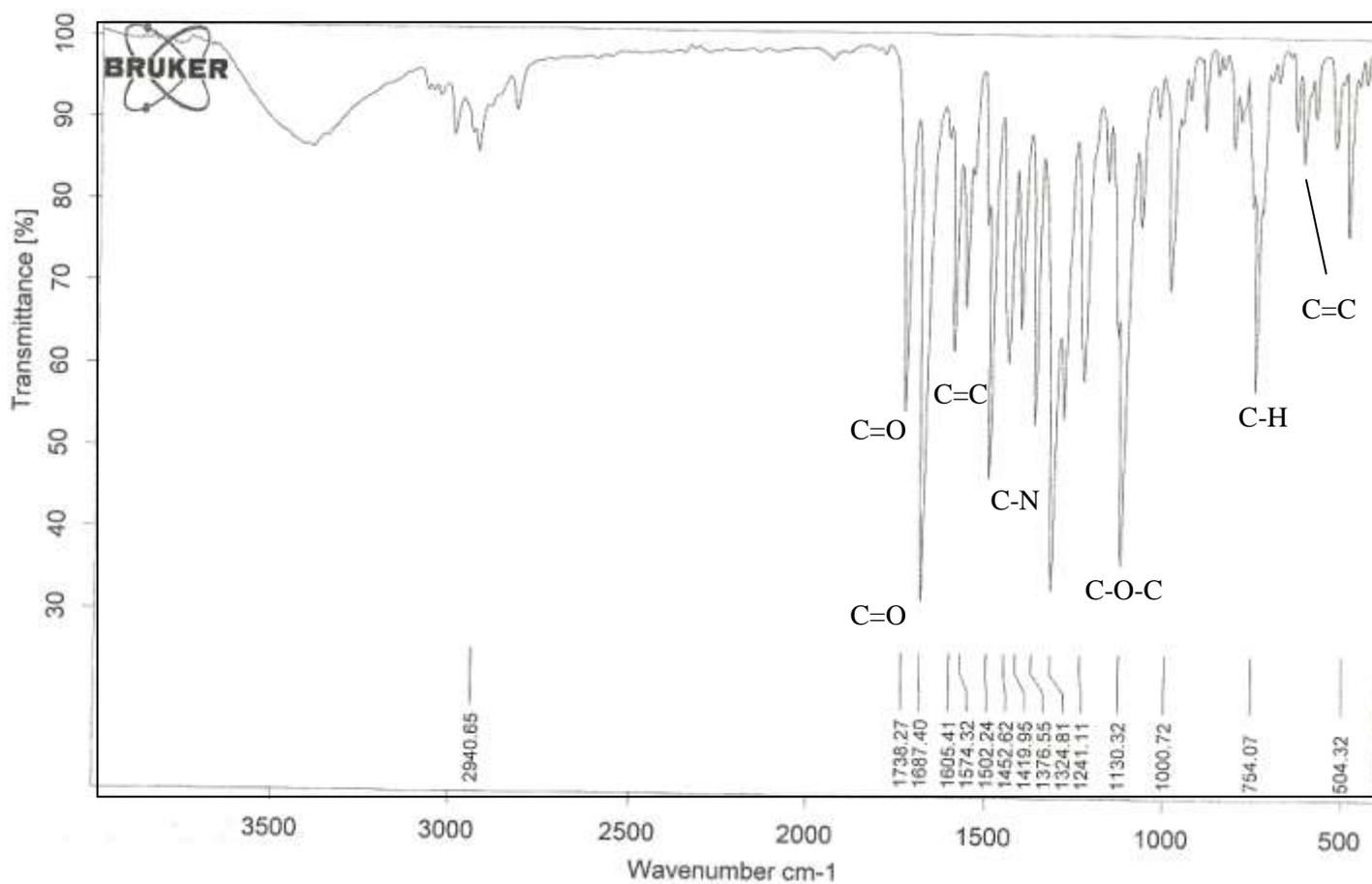


Figura 41 - Espectro de IR do LPSF AA-17. Deformação axial normal de C=O, 1738 cm^{-1} , 1687 cm^{-1} . Deformação axial das ligações C=C do anel, 1605 cm^{-1} . Deformação axial de C-N, 1382 cm^{-1} . Deformação axial assimétrica C-O-C, 1130 cm^{-1} . Deformação angular fora do plano de C-H de aromático, 754 cm^{-1} . Deformação angular de C=C, 707 cm^{-1}



Fonte: Autora, 2012

Apêndice F

3-Acridin-9-ilmetil-5-(3,4-dicloro-benzilideno)-tiazolidina-2,4-diona (LPSF AA-18)

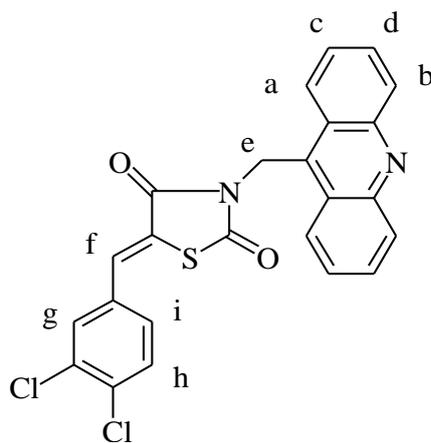
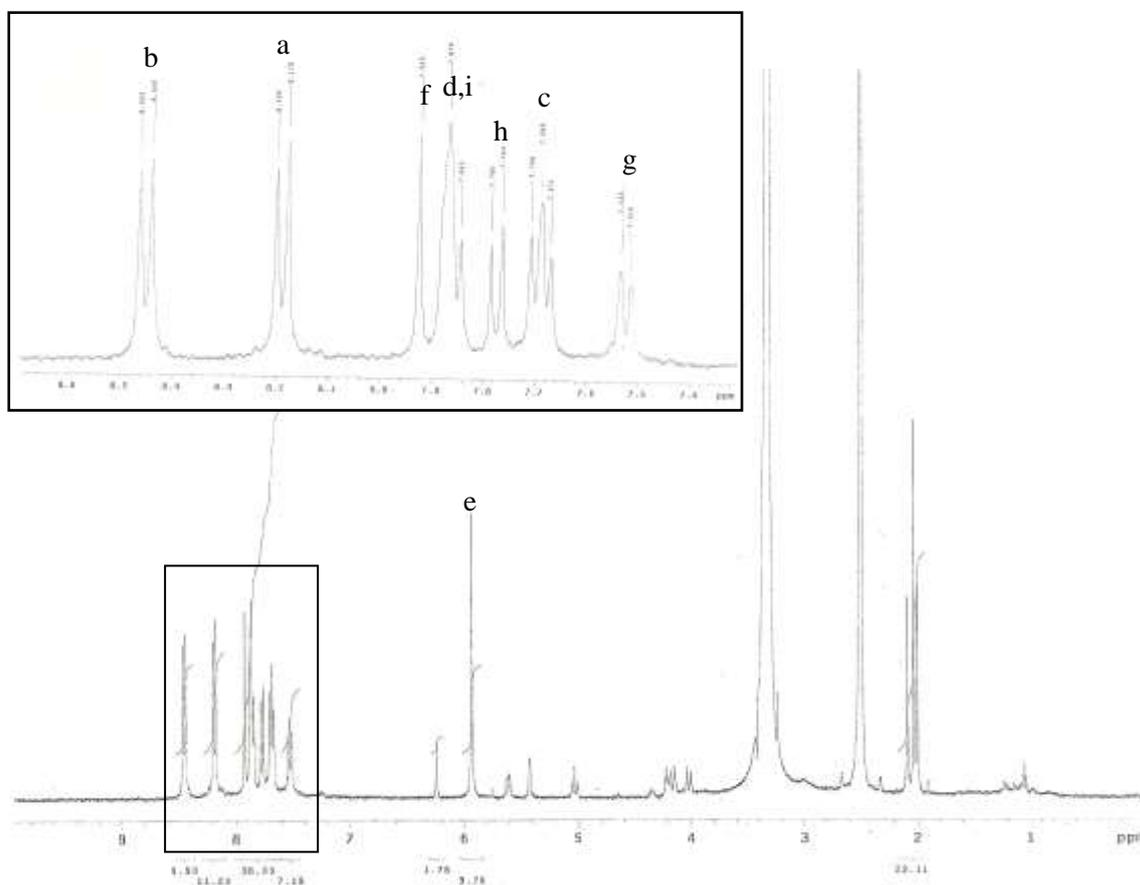


Figura 42 - Espectro de NMR¹H do LPSF AA-18



Fonte: Autora, 2012

Apêndice F

Novos Agentes Tiazacridínicos com Propriedades Anticâncer
Marina G R Pitta

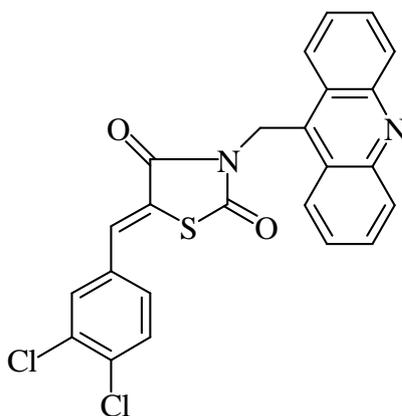
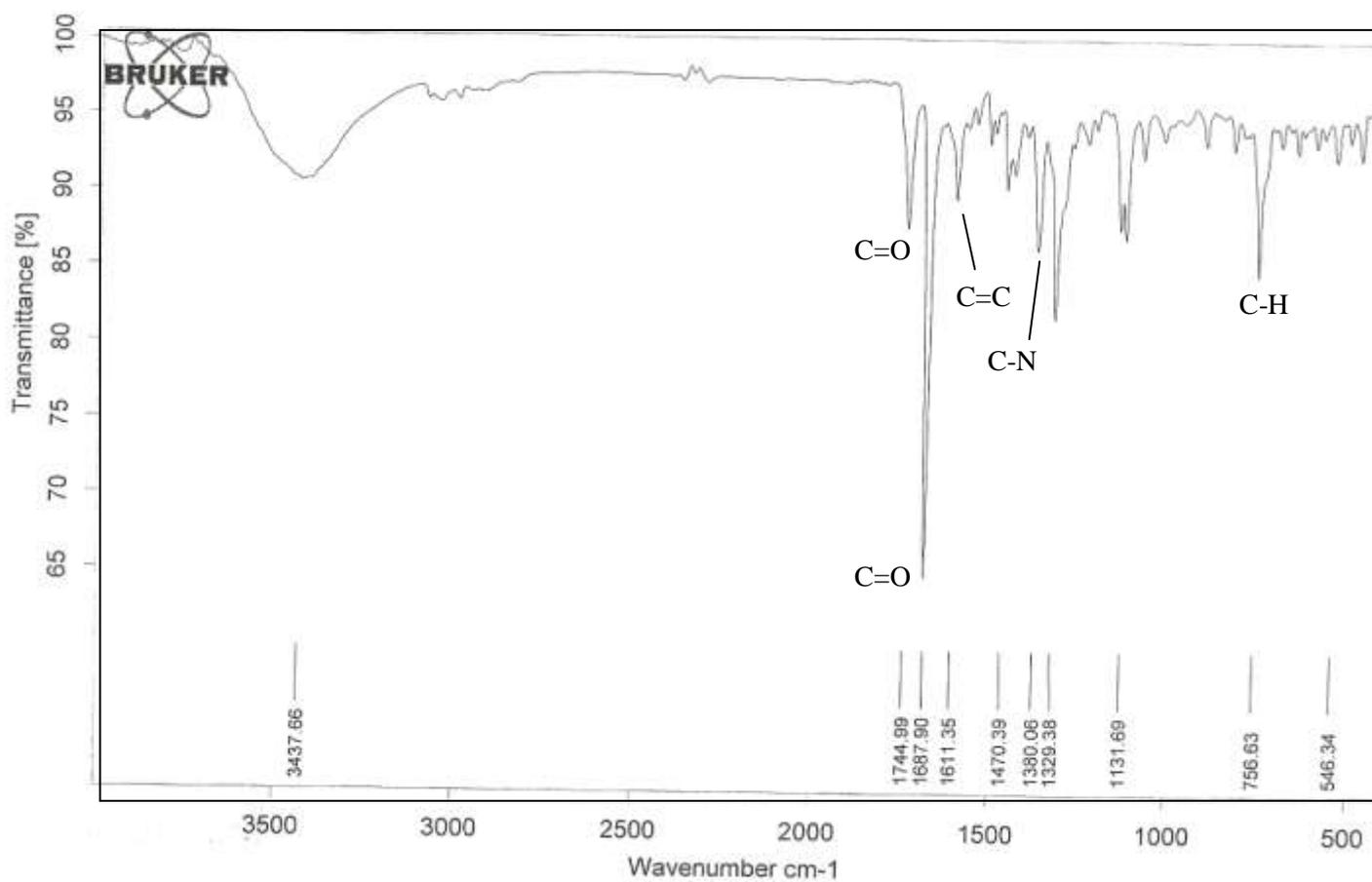


Figura 43 - Espectro de IR do LPSF AA-18. Deformação axial normal de C=O, 1744 cm^{-1} , 1687 cm^{-1} . Deformação axial das ligações C=C do anel, 1611 cm^{-1} . Deformação axial de C-N, 1380 cm^{-1} . Deformação angular fora do plano de C-H de aromático, 756 cm^{-1}



Fonte: Autora, 2012

Apêndice F

3-Acridin-9-ilmetil-5-(2,4-dicloro-benzilideno)-tiazolidina-2,4-diona (LPSF AA-19)

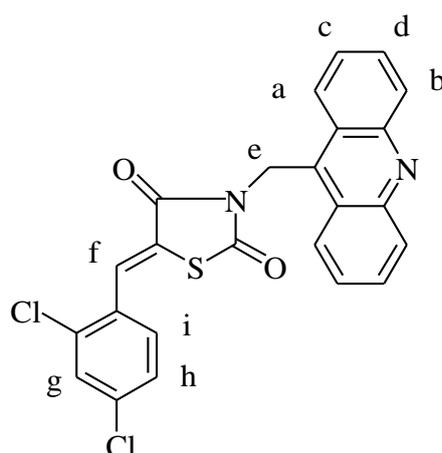
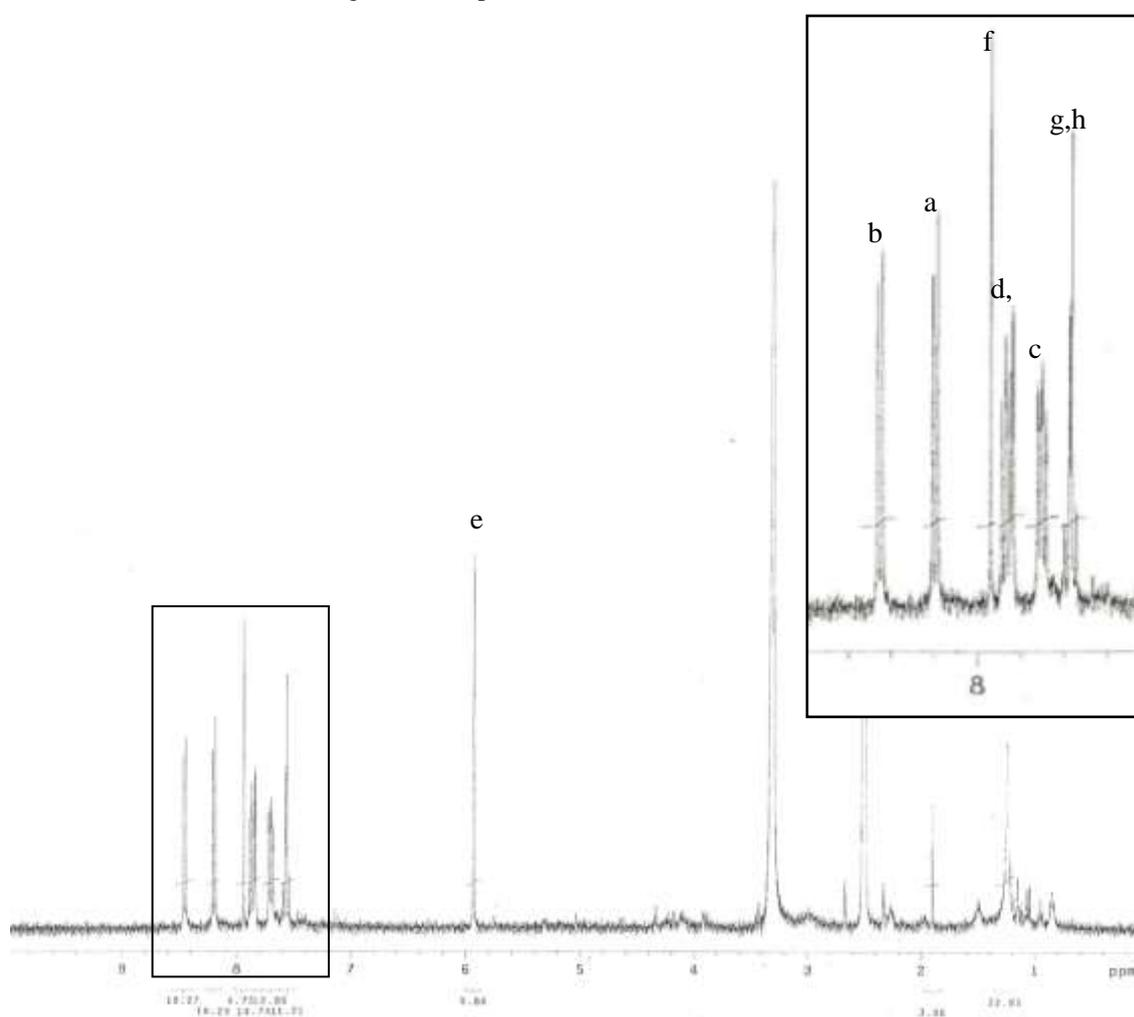


Figura 44 - Espectro de NMR¹H do LPSF AA-19



Fonte: Autora, 2012

Apêndice F

Novos Agentes Tiazacridínicos com Propriedades Anticâncer
Marina G R Pitta

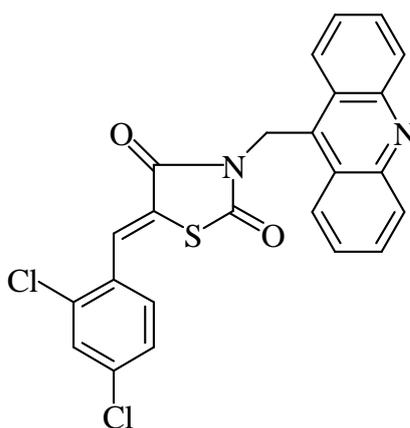
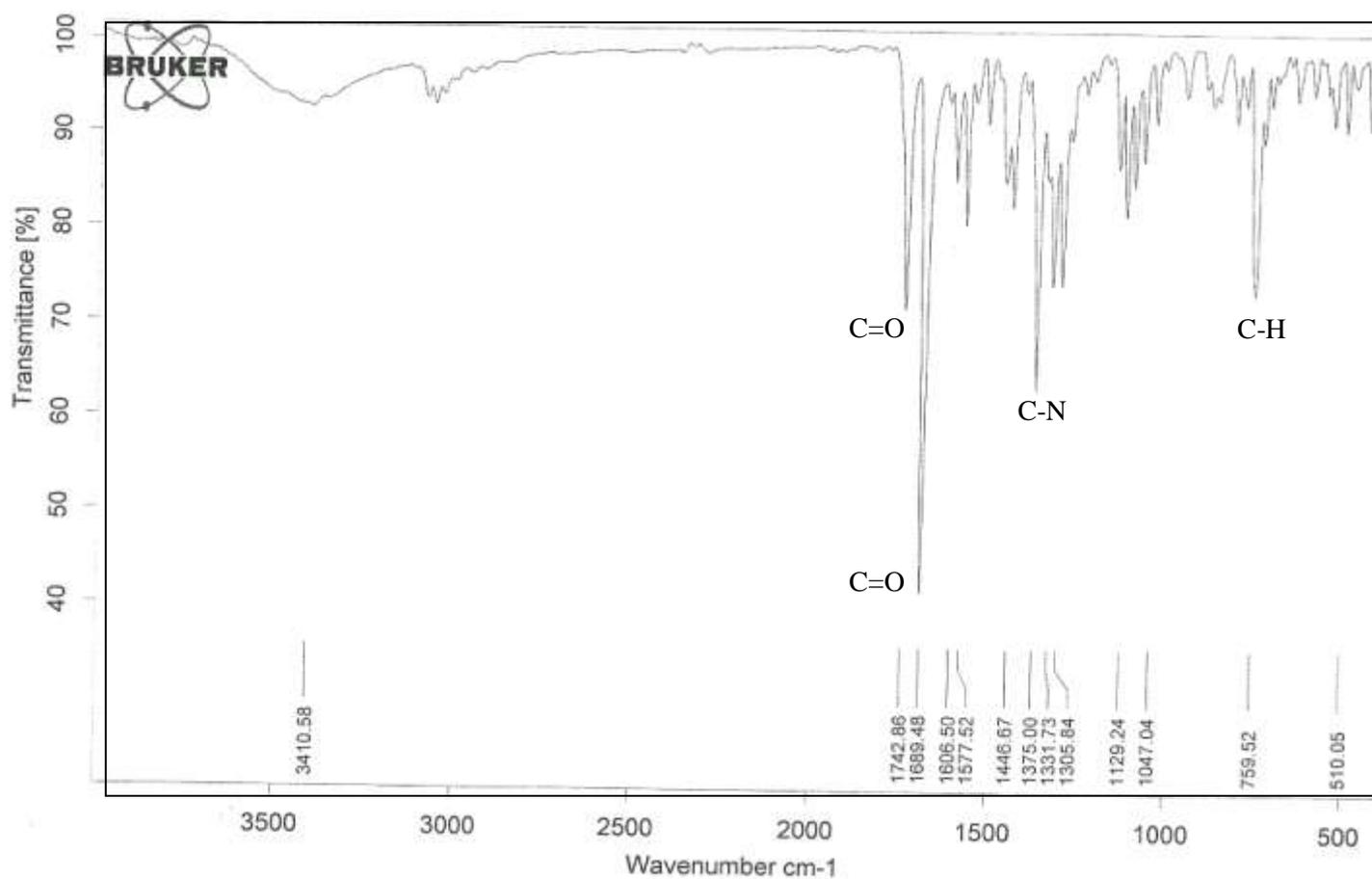


Figura 45 - Espectro de IR do LPSF AA-19. Deformação axial normal de C=O, 1742 cm^{-1} , 1689 cm^{-1} . Deformação axial de C-N, 1375 cm^{-1} . Deformação angular fora do plano de C-H de aromático, 759 cm^{-1}



Fonte: Autora, 2012

Apêndice F

Novos Agentes Tiazacridínicos com Propriedades Anticâncer
Marina G R Pitta

3-Acridin-9-ilmetil-5-(2-cloro-5-nitro-benzilideno)-tiazolidina-2,4-diona (LPSF AA-20)

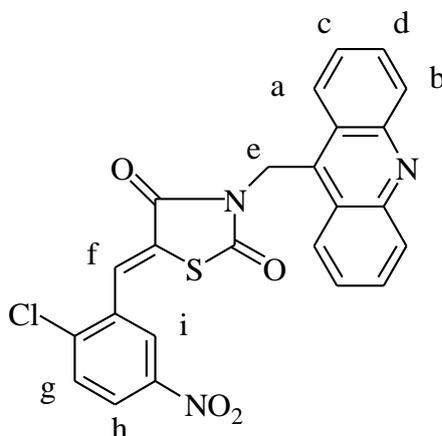
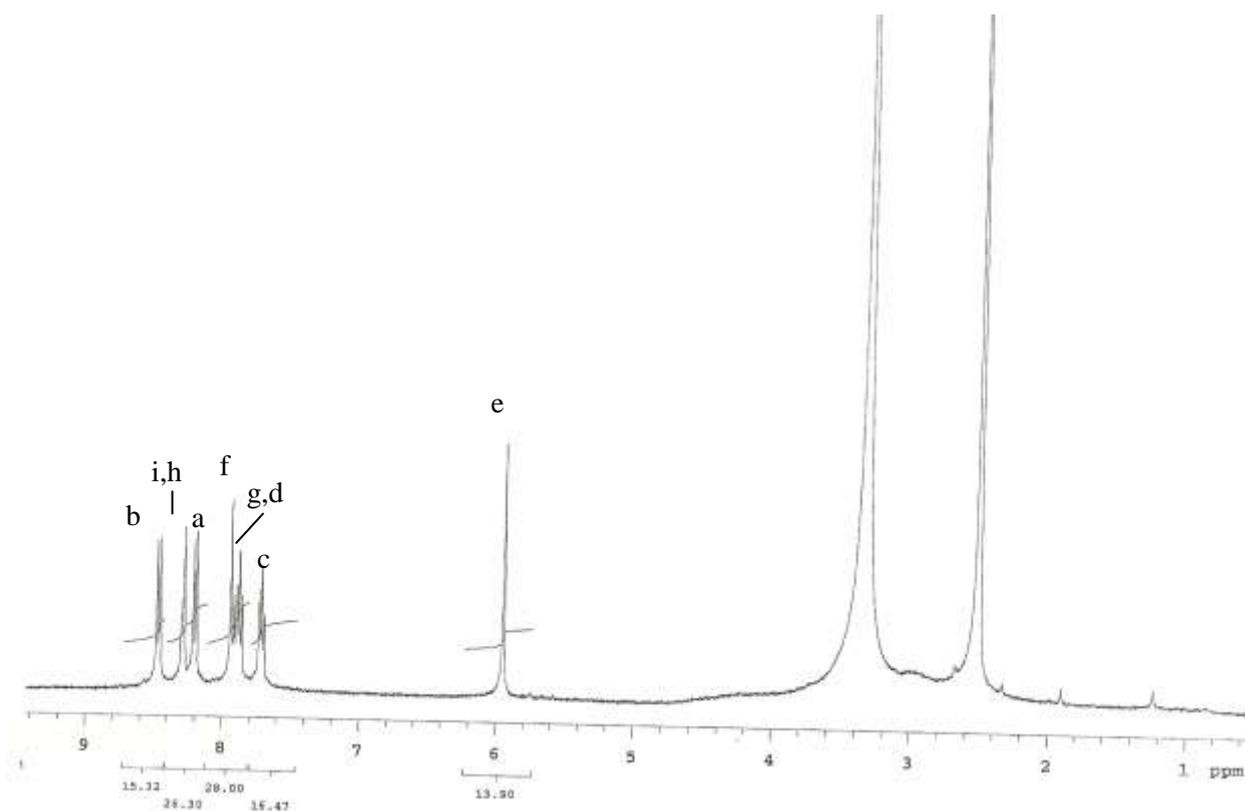


Figura 46 - Espectro de NMR¹H do LPSF AA-20



Fonte: Autora, 2012

Apêndice F

Novos Agentes Tiazacridínicos com Propriedades Anticâncer
Marina G R Pitta

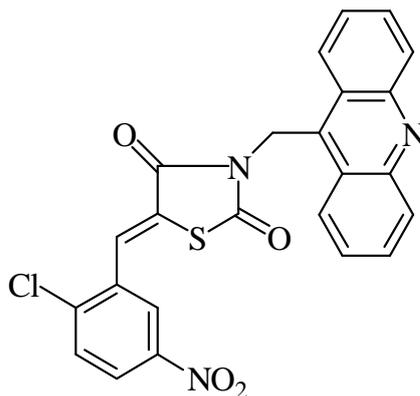
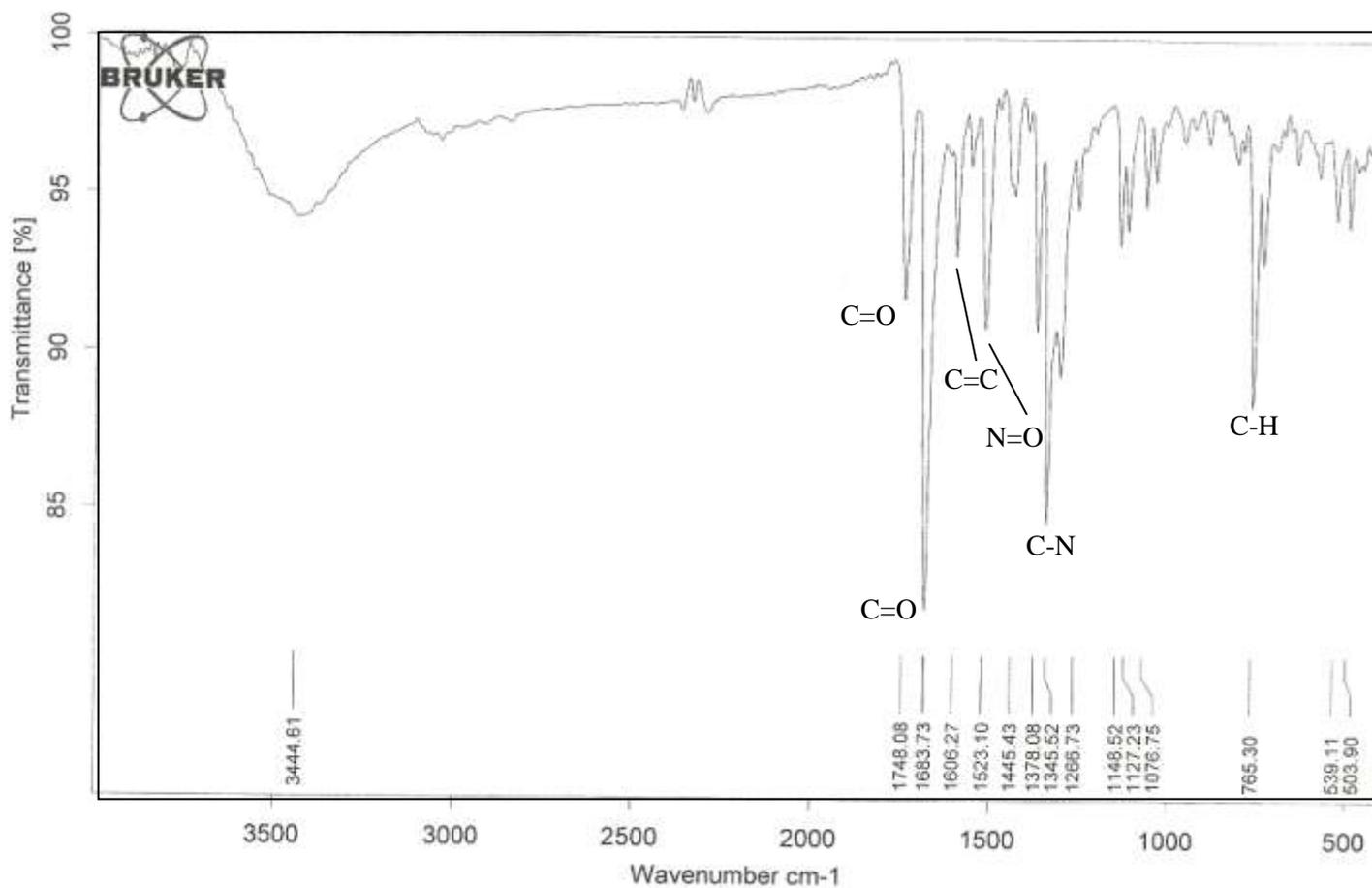


Figura 47 - Espectro de IR do LPSF AA-20. Deformação axial normal de C=O, 1748 cm^{-1} , 1683 cm^{-1} . Deformação axial das ligações C=C do anel, 1606 cm^{-1} . Deformação axial simétrica de N=O, 1523 cm^{-1} . Deformação axial de C-N, 1345 cm^{-1} . Deformação angular fora do plano de C-H de aromático, 765 cm^{-1}



Fonte: Autora, 2012

Apêndice F

3-Acridin-9-ilmetil-5-(4-benziloxi-benzilideno)-tiazolidina-2,4-diona (LPSF AA-22)

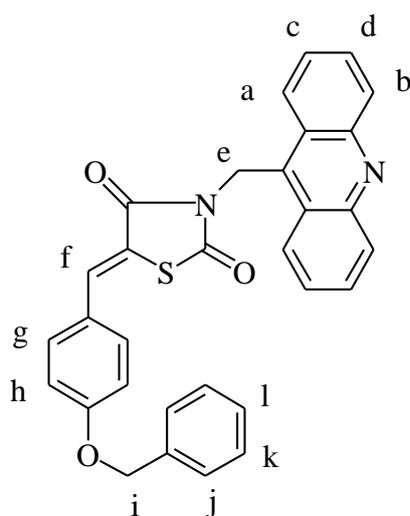
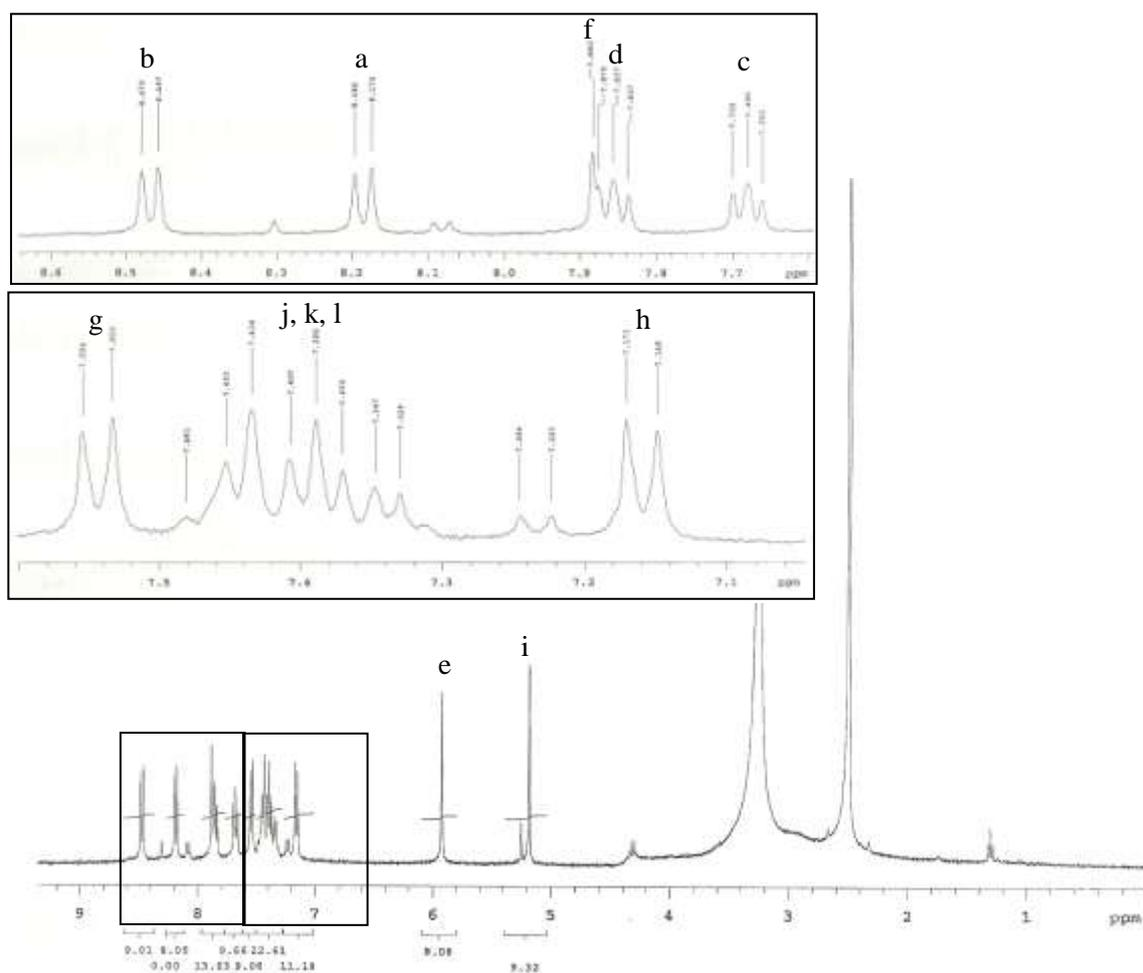


Figura 48 - Espectro de NMR¹H do LPSF AA-22



Fonte: Autora, 2012

Apêndice F

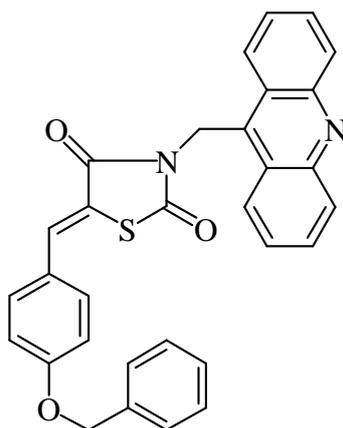
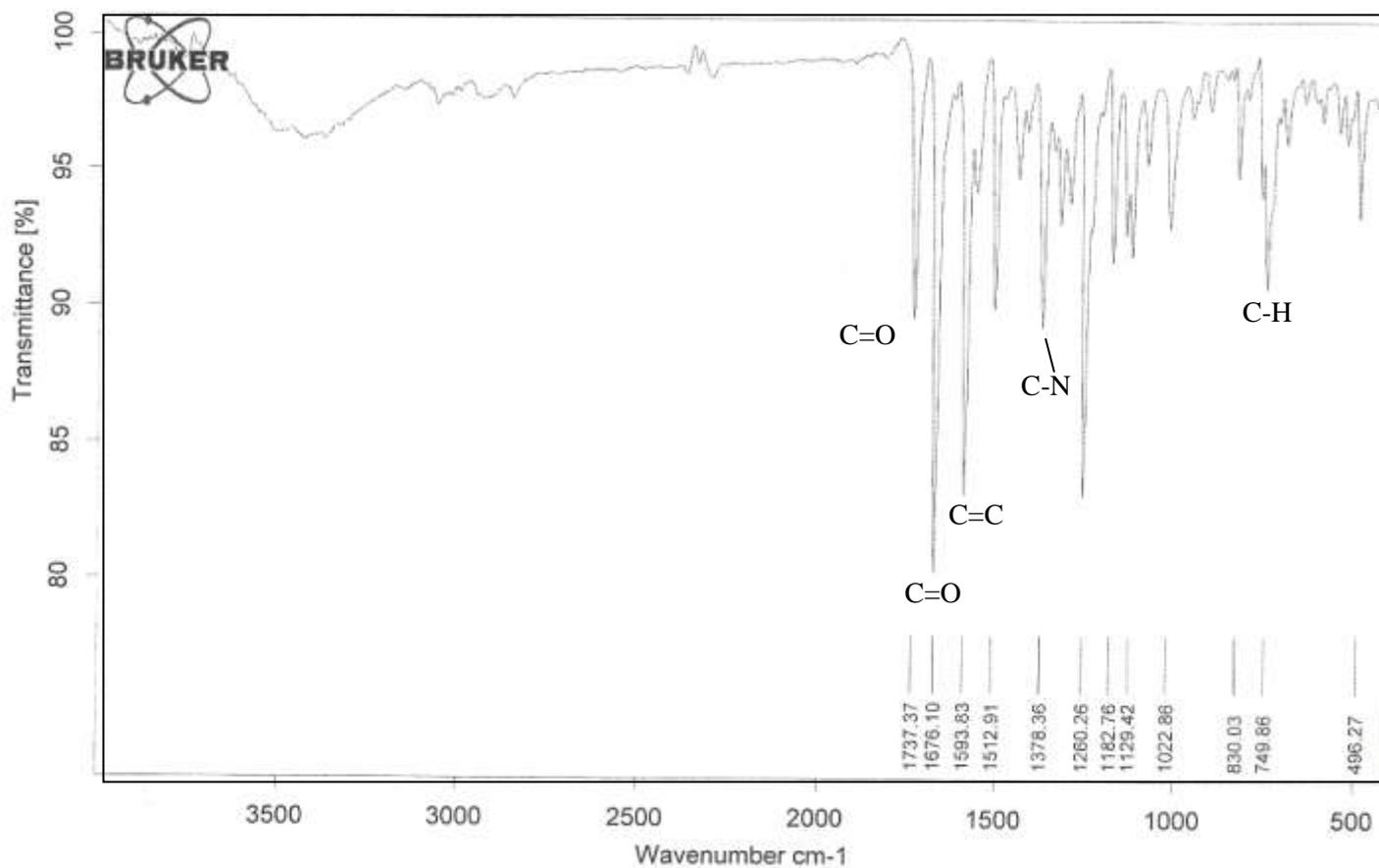


Figura 49 - Espectro de IR do LPSF AA-22. Deformação axial normal de C=O, 1737 cm^{-1} , 1676 cm^{-1} . Deformação axial das ligações C=C do anel, 1593 cm^{-1} . Deformação axial de C-N, 1378 cm^{-1} . Deformação angular fora do plano de C-H de aromático, 749 cm^{-1}



Fonte: Autora, 2012

Apêndice F

3-Acridin-9-ilmetil-5-(4-nitro-benzilideno)-tiazolidina-2,4-diona (LPSF AA-23)

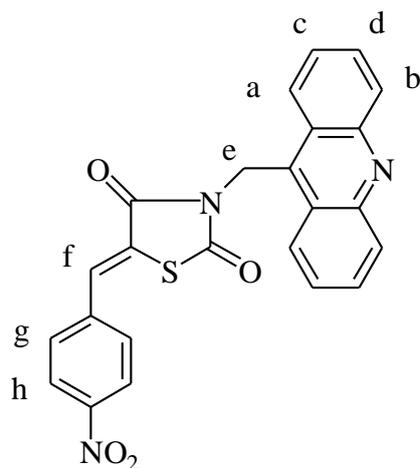
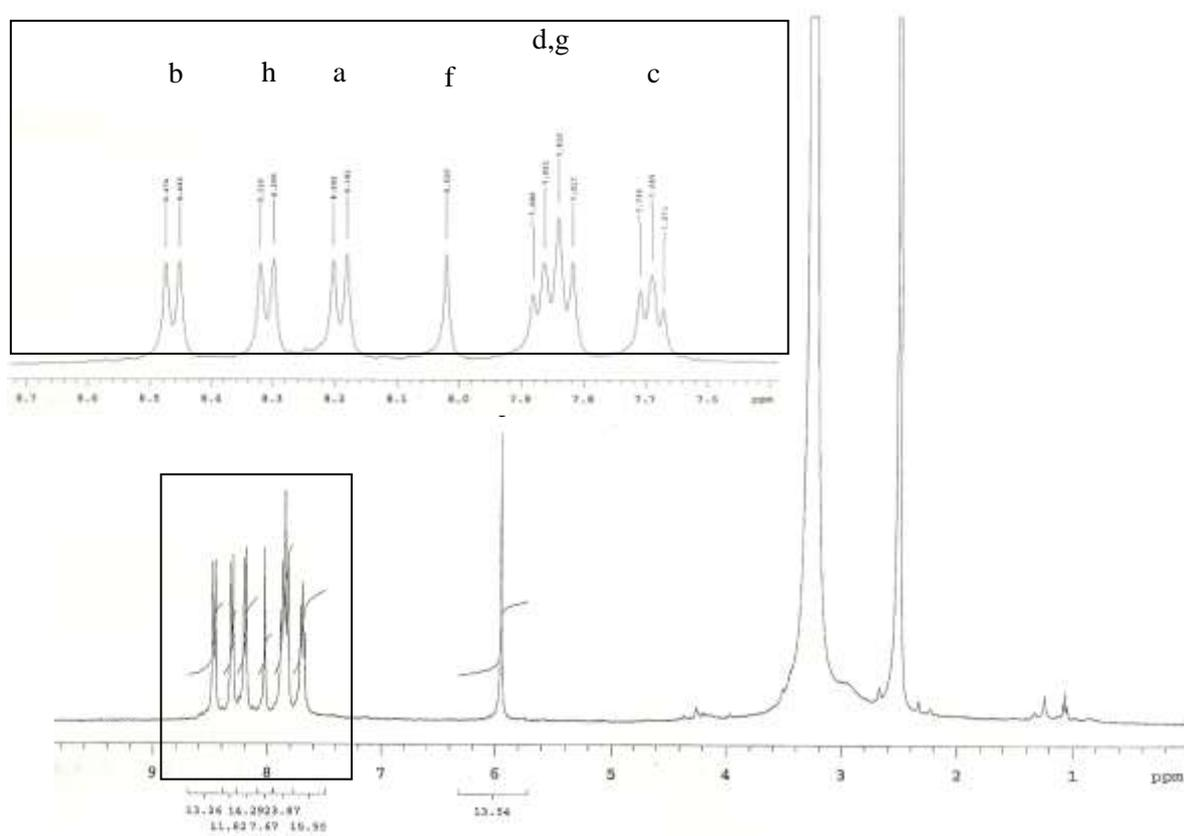


Figura 50 - Espectro de NMR¹H do LPSF AA-23



Fonte: Autora, 2012

Apêndice F

Novos Agentes Tiazacridínicos com Propriedades Anticâncer
Marina G R Pitta

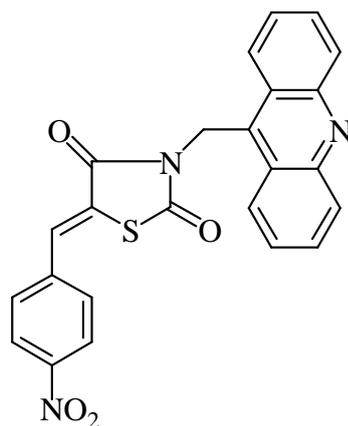
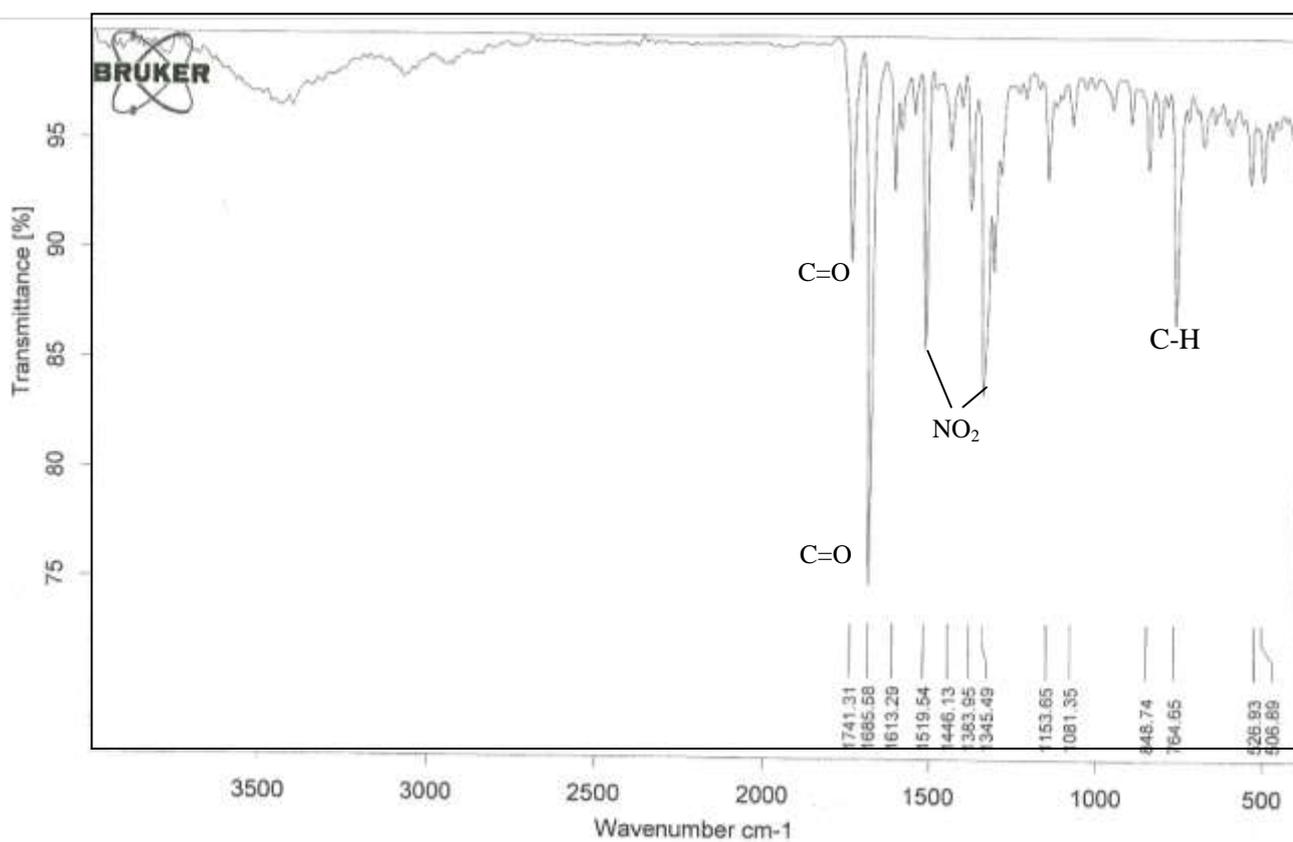


Figura 51 - Espectro de IR do LPSF AA-23. Deformação axial normal de C=O, 1741 cm^{-1} , 1685 cm^{-1} .
 Deformação axial assimétrica de N=O, 1519 cm^{-1} . Deformação axial simétrica de N=O, 1345 cm^{-1} .
 Deformação angular fora do plano de C-H de aromático, 764 cm^{-1}



Fonte: Autora, 2012

Apêndice F

3-Acridin-9-ilmetil-5-(9H-fluoren-3-ilmetileno)-tiazolidina-2,4-diona (LPSF AA-26)

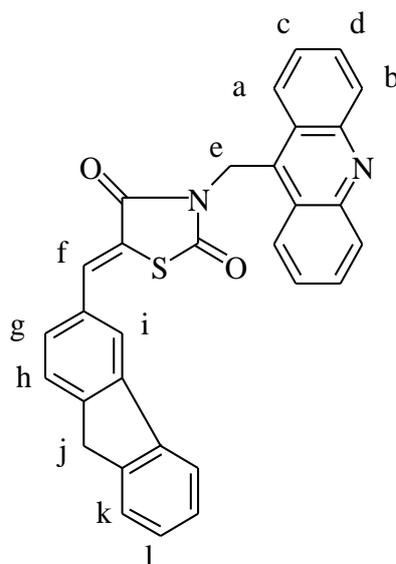
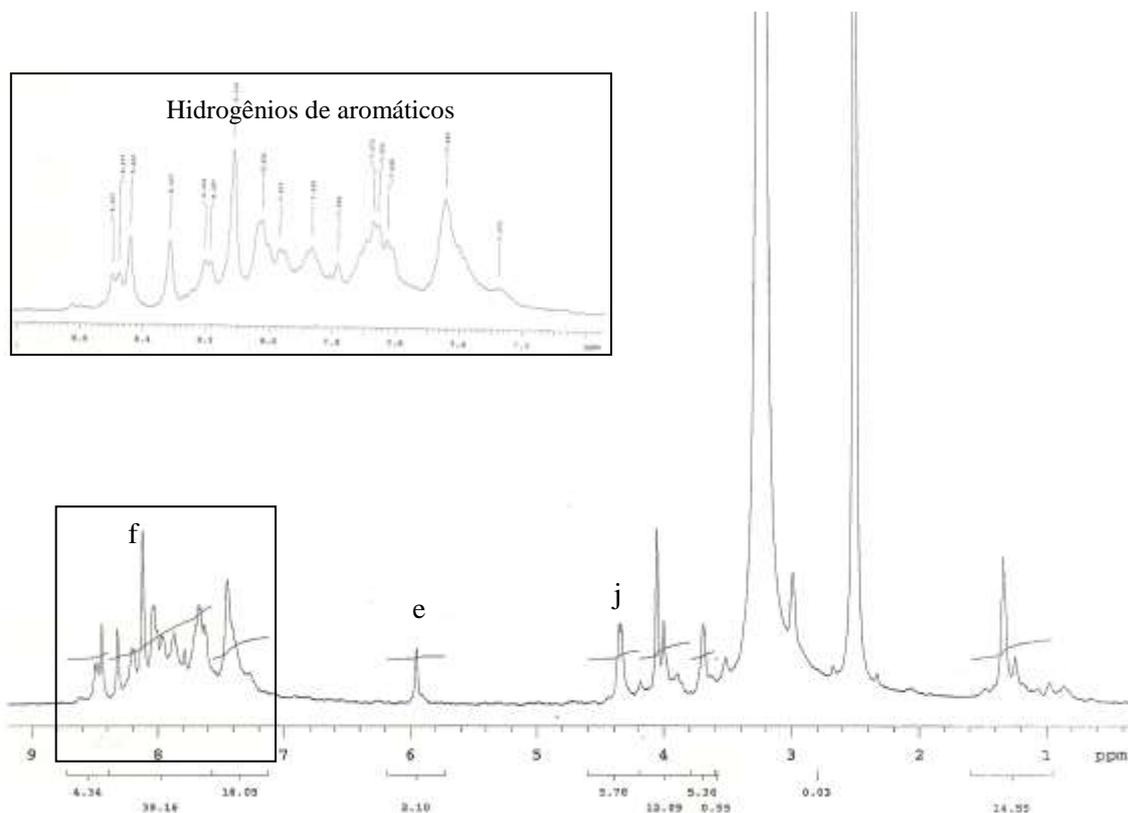


Figura 52 - Espectro de NMR¹H do LPSF AA-26



Fonte: Autora, 2012

Apêndice F

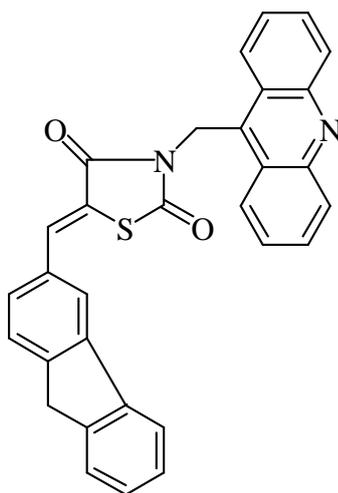
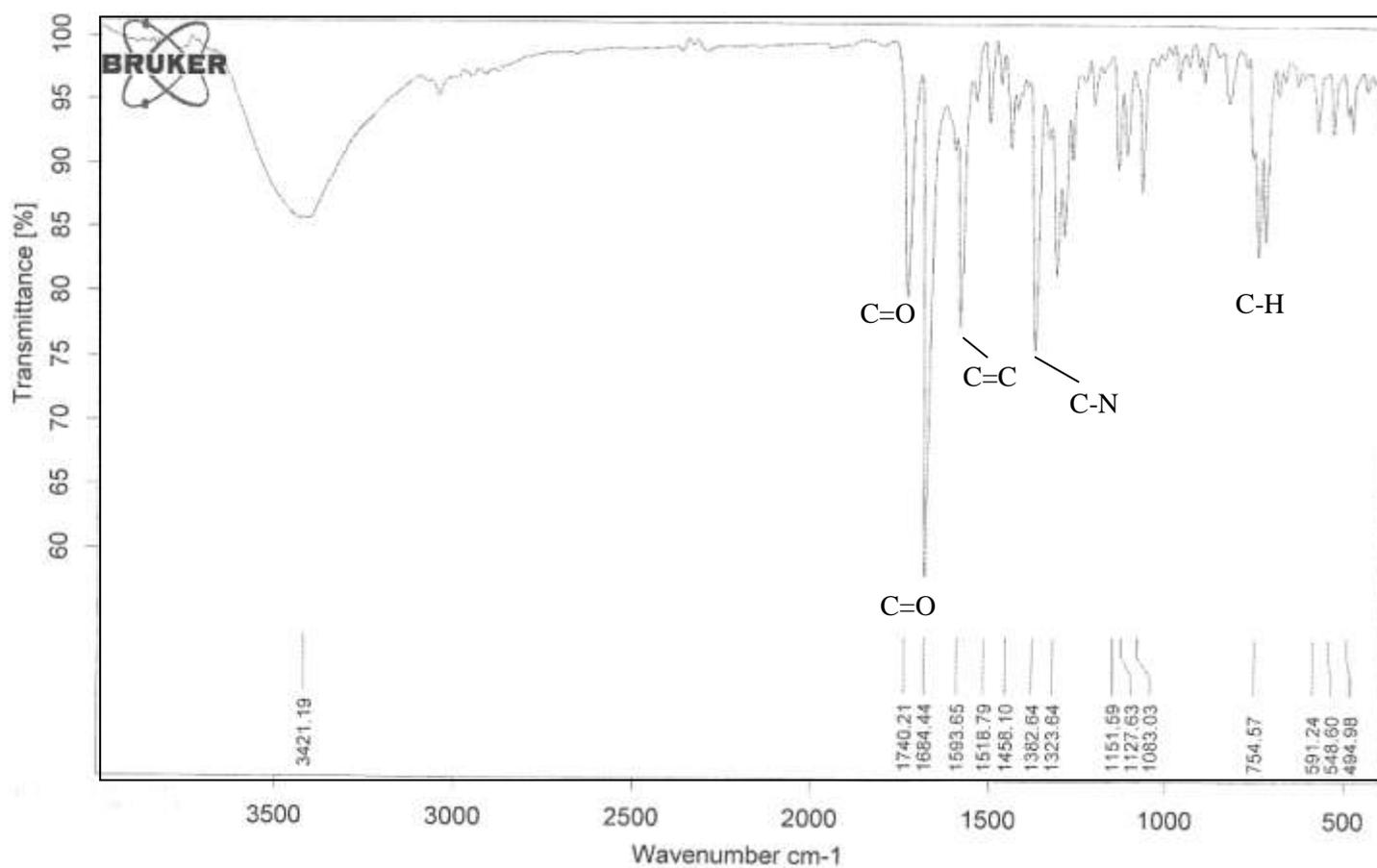


Figura 53 - Espectro de IR do LPSF AA-26. Deformação axial normal de C=O, 1740 cm^{-1} , 1684 cm^{-1} . Deformação axial das ligações C=C do anel, 1593 cm^{-1} . Deformação axial de C-N, 1382 cm^{-1} . Deformação angular fora do plano de C-H de aromático, 754 cm^{-1}



Fonte: Autora, 2012

Apêndice F

Novos Agentes Tiazacridínicos com Propriedades Anticâncer
Marina G R Pitta

3-Acridin-9-ilmetil-5-(3-cloro-benzilideno)-tiazolidina-2,4-diona (LPSF AA-30)

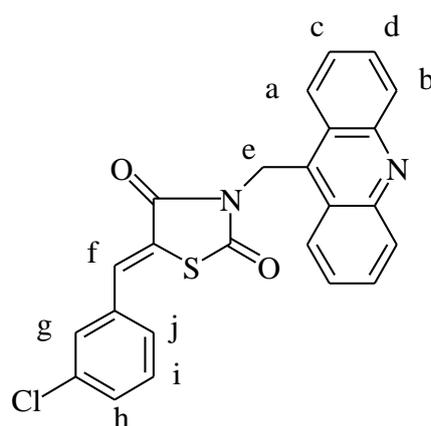
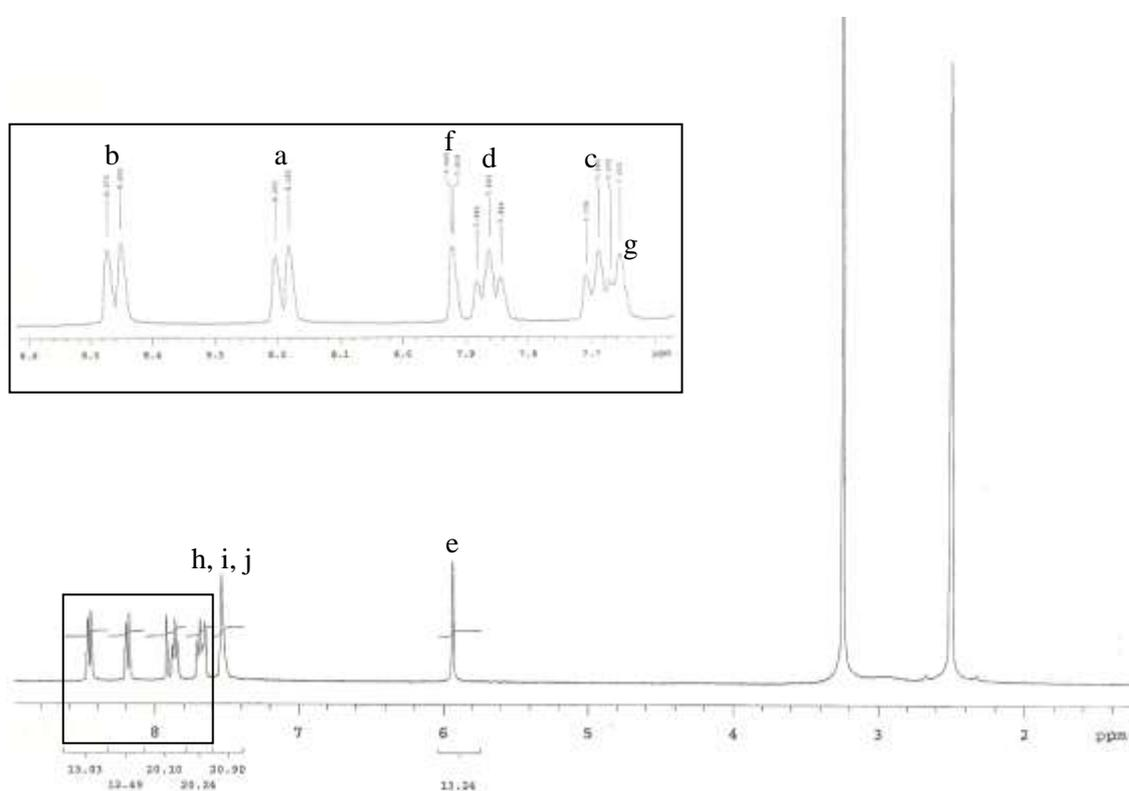


Figura 54 - Espectro de NMR¹H do LPSF AA-30



Fonte: Autora, 2012

Apêndice F

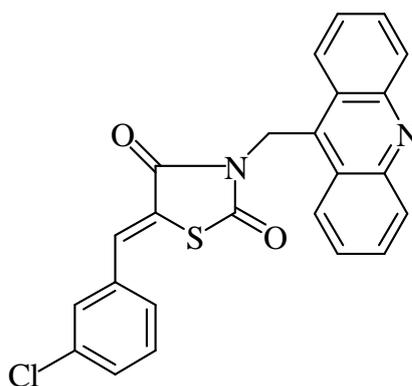
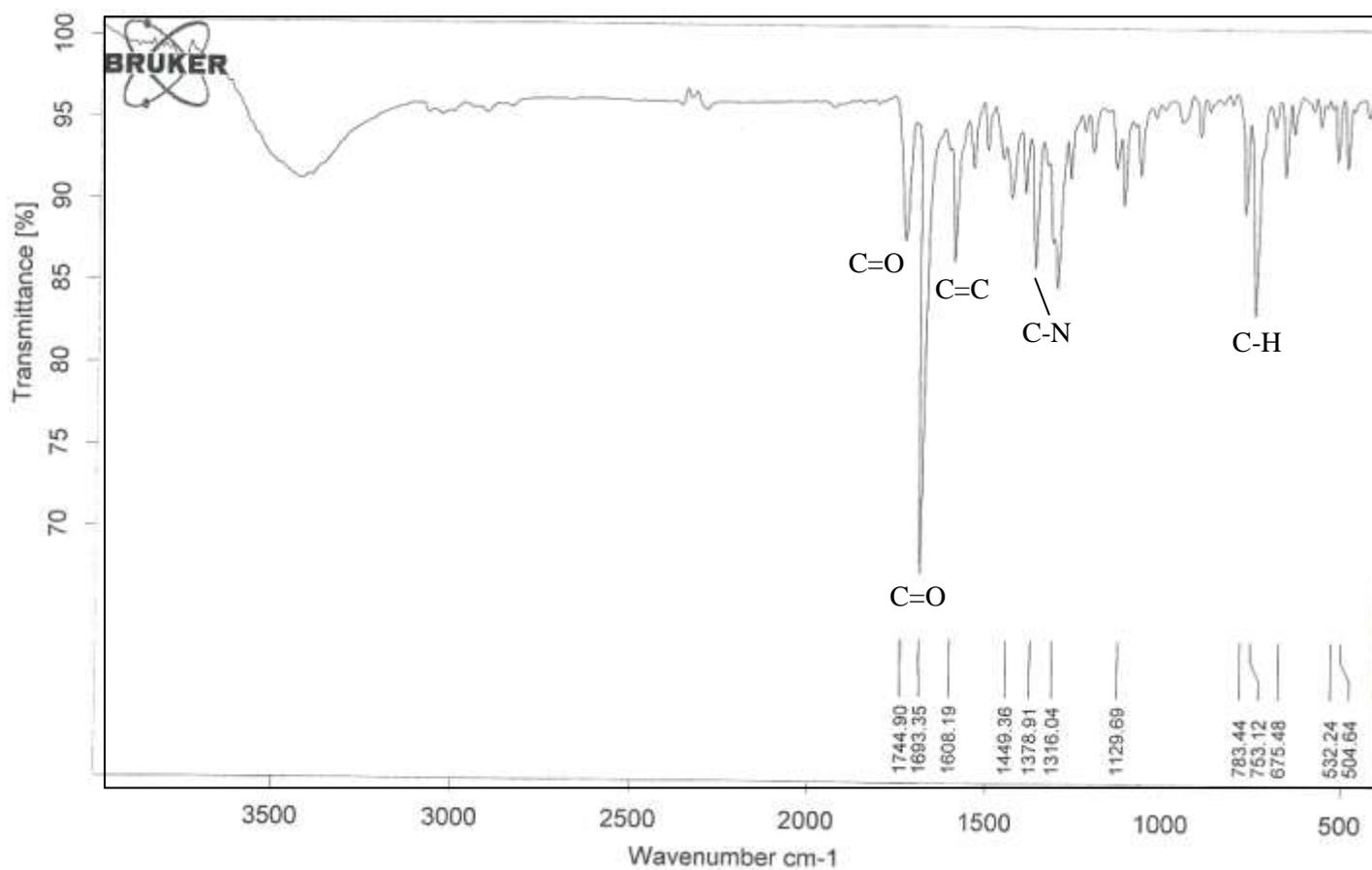


Figura 55 - Espectro de IR do LPSF AA-30. Deformação axial normal de C=O, 1744 cm^{-1} , 1693 cm^{-1} . Deformação axial das ligações C=C do anel, 1608 cm^{-1} . Deformação axial de C-N, 1378 cm^{-1} . Deformação angular fora do plano de C-H de aromático, 753 cm^{-1}



Fonte: Autora, 2012

Apêndice F

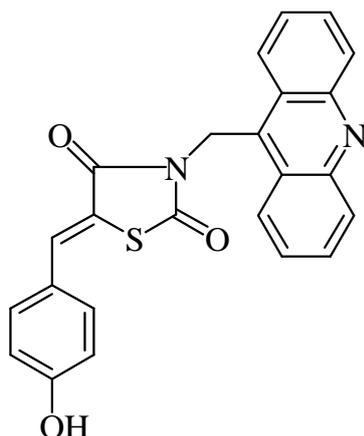
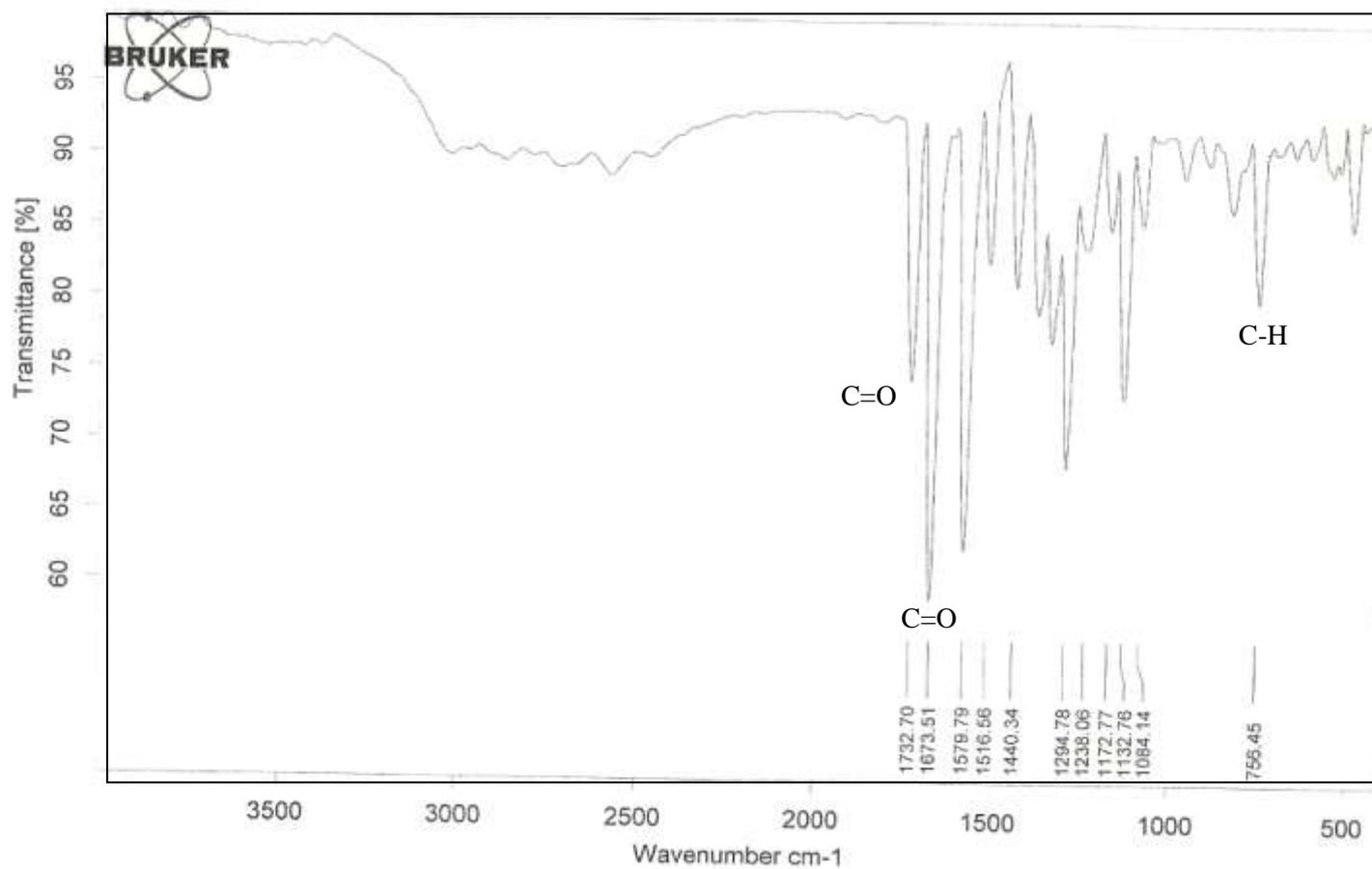


Figura 57 - Espectro de IR do LPSF AA-31. Deformação axial de O-H, larga, $3300\text{-}2500\text{ cm}^{-1}$. Deformação axial normal de C=O, 1732 cm^{-1} , 1673 cm^{-1} . Deformação angular fora do plano de C-H de aromático, 756 cm^{-1}



Fonte: Autora, 2012

Apêndice F

Novos Agentes Tiazacridínicos com Propriedades Anticâncer
Marina G R Pitta